REPORT NO. UMTA-NY-06-0006-78-1

ENERGY STORAGE PROPULSION SYSTEM FOR RAPID TRANSIT CARS

Test Results and System Evaluation

AiResearch Manufacturing Company

Metropolitan Transportation Authority

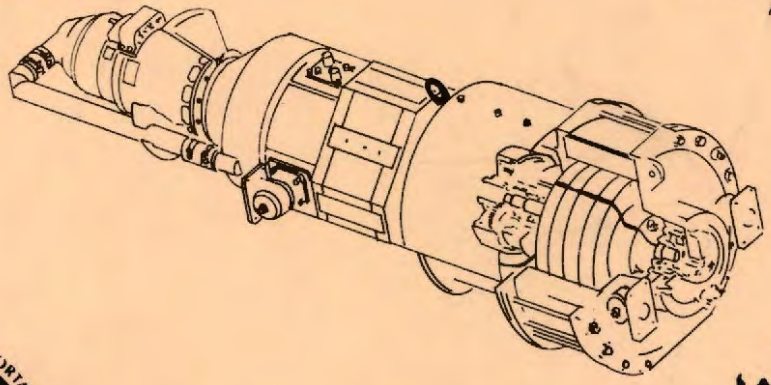

Urban Mass Transportation Administration

New York State Department of Transportation

FINAL REPORT
OCTOBER 1978

Prepared By
Metropolitan Transportation Authority
1700 Broadway
New York, N.Y. 10019

Prepared For

U.S. Department of Transportation
Urban Mass Transportation Administration
Office of Technology Development and Deployment
Washington, D.C. 20590

N.Y. State Department of Transportation
Development Division
1220 Washington Ave.
Albany, N.Y. 12232

The preparation of this report has been financed in part through a grant from the United States Department of Transportation, Urban Mass Transportation Administration, under the Urban Mass Transportation Act of 1964, as amended.

Technical Report Documentation Page

1. Report No.	2. Government Accession No.	3. Recipient's Catalog No.
UMTA-NY-06-0006-78-1		

4. Title and Subtitle	5. Report Date
Energy Storage Propulsion System for Rapid Transit Cars: Test Results and System Evaluation	October 1978
	6. Performing Organization Code
	8. Performing Organization Report No.
7. Author(s) Donald Raskin	
9. Performing Organization Name and Address Metropolitan Transportation Authority 1700 Broadway New York, New York 10019	10. Work Unit No. (TRAIS) NY-06-0006
	11. Contract or Grant No.
12. Sponsoring Agency Name and Address U.S. Department of Transportation Urban Mass Transportation Administration 2100 Second Street, S.W. Washington, D.C. 20590	13. Type of Report and Period Covered Final Report
	14. Sponsoring Agency Code

15. Supplementary Notes Also sponsored by:
N.Y. State Department of Transportation
1220 Washington Avenue
Albany, New York 12232

and

AiResearch Manufacturing Co.
The Garrett Corporation
2525 West 190th Street
Torrance, California 90509

16. Abstract

When a rail transit vehicle accelerates, it draws energy from a wayside electric power source; when it decelerates, the car must rid itself of this energy. Conventional rail cars dissipate this energy in the form of heat. This report describes the testing and evaluation of a transit car propulsion system which was designed to save much of this presently wasted energy by storing the car's kinetic energy in flywheels which are mounted below the car floor. The stored energy is then available for the subsequent acceleration of the car. Two New York City rapid transit cars were outfitted with the Energy Storage Propulsion System and were tested under a variety of conditions on a range of New York City Transit System routes. Overall propulsion energy reductions of 14-26%, as compared with conventional equipment, were measured in revenue service operations. Further reductions should be attainable by this system, if improvements derived from this test program were to be incorporated into the equipment and control configuration. Tunnel heating effects, power reduction, gyroscopic forces and other characteristics of the system were investigated and evaluated.

17. Key Words	18. Distribution Statement
Energy Storage, Flywheel, Rapid Transit, Electric Propulsion, Energy Conservation	Available to the Public through the National Technical Information Service, Springfield, Virginia 22161.

19. Security Classif. (of this report)	20. Security Classif. (of this page)	21. No. of Pages	22. Price
Unclassified	Unclassified	87	

Form DOT F 1700.7 (8-72) Reproduction of completed page authorized

Energy Storage Train Undergoing Test Operations on New York's Sea Beach Test Track, January 1976

PREFACE

When a rail transit vehicle accelerates, it draws its kinetic energy from a wayside electric power source; when it decelerates, the car must dissipate this energy in some manner. Conventional rail cars transform this energy into heat. This report describes the testing and evaluation of a transit car propulsion system which was designed to save much of this lost energy by storing the car's kinetic energy in flywheels mounted below the car floor. The stored energy is then available for the subsequent acceleration of the car.

Two New York City rapid transit cars were retrofitted with an Energy Storage Propulsion System and were tested under a variety of conditions on a range of New York City Transit System routes. Overall propulsion energy reductions of 14-26%, as compared with conventional equipment, were measured in revenue service operations. Further reductions should be attainable by this system, if improvements from this test program were to be incorporated into the equipment and control configuration. Tunnel heating effects, power reduction, gyroscopic forces and other characteristics of the system were investigated and evaluated.

The Energy Storage system was developed by The Garrett Corporation, under a contract with the New York State Metropolitan Transportation Authority (MTA). The development and test program was sponsored by the U.S. Department of Transportation's Urban Mass Transportation Administration, the New York State Department of Transportation, Garrett and MTA.

ACKNOWLEDGEMENT

The success of the test program which is reported herein was dependent on the skills, integrity and dedication of the people listed below. The project sponsors owe a great debt of gratitude to these engineers, technicians and operating personnel.

For The Garrett Corporation

R. Couvillion
J. Gardner
C. Huggett
R. Lewis
P. McCarty
R. McCommon
R. McConnell
G. Prewitt
J. Puzzo
G. Sessions
C. Weinstein

For New York City Transit Authority

S. Adams
C. Bordeaux
S. Cagne
D. Eisenstein
N. Ghaly
W. Jehle
M. Johnson
A. Rafail
E. Schaeffer

For Metropolitan Transportation Authority

R. Yutko

CONTENTS

FIGURES

TABLES

EXECUTIVE SUMMARY

This report presents the results and the conclusions drawn from the testing of a prototype flywheel energy storage propulsion system which was installed under two New York City subway cars and tested on representative lines of the New York subway system. *The testing established that the use of on-board flywheel energy storage leads to substantial energy savings.* Further improvements in energy economy should be achievable, based on observations resulting from the testing. However, significant increases in equipment reliability and maintainability beyond that demonstrated by the prototype equipment would be required to make the hardware practical for daily operation on a metropolitan transit sytem.

The principal objectives of the test program were to evaluate the ability of the Energy Storage (ES) system to:

- Reduce propulsion energy usage
- Reduce propulsion power demands
- Reduce tunnel heating caused by propulsion energy use.

Further goals of the program were the investigation of:

- Ability of the ES cars to operate on their own stored energy, in the absence of third rail power
- Compatibility of the ES system with the New York subway system with regard to performance, operations and safety considerations
- Reliability of the equipment
- Maintainability of the propulsion components.

The energy measurements were performed primarily in revenue (passenger-carrying) service with the two ES cars permanently coupled to two standard control cars of the same class (R-32). The acceleration and braking performance of the ES pair was carefully matched to that of the standard pair, as determined by a strain gauge link bar between the pairs, so that each pair would be expending an equal effort throughout the test program.

Overall propulsion energy savings of 14 to 26% were obtained by the ES cars. On the A-line, considered to be typical of New York's Division B lines, the overall propulsion energy saving was 23%. The underlying operational factors affecting the savings within this range were investigated and made explicit, so that the results could be applied to other transit systems.

As a result of the testing of the ES system in the "real world", the need for certain improvements in the equipment and controls became apparent. A conservative estimate of the energy effectiveness of such potential modifications, based on measurements of ES system parameters, would be an increase in the energy savings on the A-line to 29% of the standard car propulsion usage.

Adding the effect of reduced losses in the third rail distribution system, the A-line savings could become 32%, estimated conservatively, for the improved ES equipment.

Power level reductions for 15-second and 60-second ratings were 18% and 28%, respectively in sample measurements on the A-line. Power reductions over longer rating periods would be in the same percentages as the energy savings.

Underfloor temperature reductions could not be verified by test, but should be in proportion to energy savings.

Operation without 3rd rail power was demonstrated as enabling ES cars, with flywheels charged to 85% of top rotational speed, to travel approximately one-half mile from a standing start, while carrying a crush load. However, the importance of moving the car *immediately* after the loss of third rail power was emphasized by the fact that the internal energy drain of the ES cars would have caused the loss of all of the available on-board energy within a 3-minute waiting period.

Gyroscopic effects were found to have been essentially negligible in comparison to the forces ordinarily encountered in routine car operations.

Noise levels for the flywheel-equipped cars were not grossly higher than the standard R-32's. However, these levels were significantly higher than the most modern cars on the New York system.

No significant problems were encountered regarding *carborne vibrations, signal system interference,* or *capacitor discharge considerations.*

Reliability and maintainability for this "first generation" flywheel propulsion equipment were poor, with the MTBF maturing to no better than 120-hours.

Future directions. Gross equipment simplifications and design improvements are possible, based upon the experience gained in the present program and in UMTA's ACT-1 program. With such a re-design, significant increases in both energy efficiency and equipment reliability could be expected. A medium-scale demonstration and test program to prove the effectiveness of these improvements and to establish the reliability and maintainability of the equipment is required before production orders for flywheel propulsion systems can be placed.

PART I—INTRODUCTION

BACKGROUND

This report describes the test and evaluation of the Energy Storage propulsion system for rapid transit cars. The characteristics of the system were investigated in the "real world" by installing the novel equipment under two New York City subway cars and operating the cars both under test track conditions and in revenue service on several lines of the New York City Transit System.

The principal benefit of the Energy Storage system is to reduce the energy required to propel transit cars. This reduction is achieved by mounting flywheel energy storage devices under the cars, providing a means for the cars' braking energy to be stored in the flywheels as the train decelerates, and then re-using this energy on the next acceleration of the cars. The re-use of this braking energy, rather than casting it off as heat as is done on conventional vehicles, has the side benefit of lessening the heating of subway tunnels. This latter feature is of particular importance on lines for which car air conditioning and station cooling are being considered.

The Metropolitan Transportation Authority of New York and the New York City Transit Authority, operators of the largest rail rapid transit system in North America, with support from the United States Department of Transportation's Urban Mass Transportation Administration and from the New York State Department of Transportation, undertook the investigation of this propulsion system because of a need, as perceived in 1970, to reduce peak power demands on the local utility. This concern resulted from the fact that the New York subway system, alone, accounted for approximately 10% of the peak load on the utility, which at the time was experiencing difficulties in meeting demand. The concern about *power* shortages in 1970 was replaced during the course of the Energy Storage development and test program by a nationwide awareness of shortages in *energy*. As is now all too familiar, the developing energy shortage has brought with it a sharp rise in energy costs, thus adding urgency to the broad range of efforts toward reducing energy usage.

The Energy Storage propulsion system was designed and manufactured by AiResearch Manufacturing Co. of California, a division of The Garrett Corporation.

REPORT ORGANIZATION

The format of this report is such that it can be read on three levels of increasing technical detail. The principal observations and conclusions are listed in the preceding Executive Summary. Part I describes the equipment and the test program and discusses the most notable test results. In Parts II and III, considerable detail is given regarding the test and in-service performance. In addition, Part II describes the methods for applying the energy conservation data to rapid transit systems other than New York's. Appendices are provided which give specific information on the New York subway routes and on the instrumentation used in the test program.

ENERGY STORAGE SYSTEM OPERATION

This section of the report will discuss the operation of the Energy Storage (ES) system, making reference to equipment performance characteristic curves which were recorded during the test program.

This description will be brief since the design and operation of the ES equipment has been reported in detail in Reference 1. Since it is felt that a fuller appreciation for the design and operation of this equipment can be obtained by reference to that report, a copy of Reference 1 is included at the back of the present report. The present section will concentrate on operational differences between the originally conceived equipment and the "as-built" hardware.

The ES propulsion system is composed of two energy storage units (ESU's), four separately-excited traction motors, and a chopper with input and output filters, along with electrical switchgear and controls. Each ESU is made up of a flywheel unit in vacuum casing, a speed-reducing gearbox and a separately-excited motor. One of the two ESU's for each car has an alternator mounted on the motor shaft, as well, which provides power for the fields of all of the motors.

This equipment is interconnected as shown in Figure 1, so that power can flow from the flywheels during acceleration (in the form of electricity generated in the ESU motor) and back to the flywheels from the traction motors (now acting as generators, being turned by the car's wheels) during braking. Power can also enter the system through the chopper from the third rail to make up for system losses and to allow the initial flywheel start-up. At all times the flow of power is under the direction of the low voltage solid state logic circuits which compromise the Electronic Control Unit (ECU).

Figures 2 and 3 describe the system function in test operation under one of the two ES cars.

The four chart segments in Figure 2 portray eight parameters under the three conventional modes of acceleration command for New York subway cars. "Switching" is a limited performance mode, intended primarily for yard operations. In conventional cars, the series mode configures the traction power circuit such that all four motors in the car are in series. The parallel mode connects the two trucks in parallel (with two series-connected motors in each parallel branch) and provides for weakening of motor field strengths. As

measured on a 0.1% upgrade, the three modes give initial acceleration rates of 0.9, 2.7, and 2.3 MPH/sec, respectively. In the test recorded in Figure 2, each acceleration command was held for a distance of approximately 1000-ft, at which point a full service brake application was made.

Referring to chart #1401 on Figure 2, certain of the performance characteristics of the ES system can be noted in an acceleration from a standing start. Notice in curve D that the voltage across a pair of traction motors rises smoothly until it reaches line voltage at a speed of 17MPH (curve G). At the start, the traction motor armature current (curve C) rises steeply to approximately 400 Amps before leveling off. The third rail current in curve B, however, does not rise immediately. Rather, it remains at the steady auxiliary load level until the car is moving at approximately 8MPH, since the propulsion current is being generated by the flywheel (curve E). Curve F shows the flywheel speed decreasing from 86% of full speed down to about 75% before braking is initiated.

When braking is commanded, the third rail (B) drops to the auxiliary level. The traction motor voltage (D) is forced up (by increasing the motor field strength) and the current flows from the traction motor (C) to the ESU (E). Accordingly the flywheel is accelerated to 87% (F) as energy is stored and the car comes to a stop (G).

The charts is Figure 3 give additional details of the system function in braking. With the car travelling at 45MPH, a full service brake is applied, resulting in an average deceleration rate of 3.5 MPH/sec. The onset of the braking cycle can be detected by the rise of brake cylinder pressure to the "inshot" level of 8 psi (curve E). Traction motor voltage (C) increases, sending current from the motors (B) to the ESU (D) and the flywheel speed (F) increases from 77% to 91% of full speed. Notice in curve E that the friction brakes do not apply until the car speed is down to approximately 7MPH.

Two significant differences in the "as-built" equipment, as compared with the somewhat idealized system described in Reference 1, are as follows: First the characteristics in the chopper current curve (B in Figure 2) are not the simple step-function described in Reference 1. This difference is due to the final design's attempt to sacrifice a small degree of power averaging in order to save an additional amount of energy. (This trade-off is discussed on page 14 of Reference 1). The change in performance was brought about by a modification to the flywheel speed "schedule" — the relationship between flywheel speed and car speed which is built into the system's electronic controls. The particular schedule used in the "as-built" controls consisted of two straight-line segments which were an approximation to the parabolic curve shown in Figure 4 of Reference 1. This choice had the additional attribute of simplifying the control logic.

The second item of variance between anticipated and actual hardware was in the total system weight. Each "as-built" ES car weighed approximately 6.4 tons more than the corresponding unmodified R-32 class car. This is an additional one ton above the 5.4 ton differential predicted in Reference 1. This additional weight resulted from heavier-than-anticipated supports for the ESU's and a heavier alternator along with ESU blower ducting, which were installed after the initial testing.

The car weights are summarized in Table 1.

TABLE 1
Car Weights

	even car	odd car
Energy Storage Cars	41.1 Ton*	41.4 Ton
Conventional R-32 cars	34.7	35.1
Difference in car weight	6.4	6.3

* Test instrumentation and recorders weighing 1.4 Tons not included.

TEST PROGRAM

The objectives of the test program can be divided into three groups. The most important goals in the program were to establish and evaluate quantitatively the reduction of propulsion energy and power usage, to verify a reduction in waste heat generation under the cars, to assess the reliability of the ES equipment and to estimate the probable costs of maintaining this equipment.

Of secondary importance was the demonstration of two particular features of the ES cars. The first feature was the ability of the car to move in the total absence of a third rail power, using energy which was stored in the flywheel. The second attribute, which was relatively novel at the time of inception of the program, was the use of a chopper for control of the current from the third rail.

Following in significance were a range of specialized tests to establish either that the equipment was compatible with the New York system or that its performance levels met generally held acceptance standards. Additionally, two sets of tests were performed: one as part of UMTA's baseline test program and the other as an effort to gather additional information about conventional R-32 cars.

The test and evaluation work performed under this program was in conformance with the Project Experimental Design, which had been prepared by the UMTA for the Energy Storage Project.

The test objectives are listed in Table 2. Also in the Table are cross-references indicating the particular phase of the test program during which each objective was investigated.

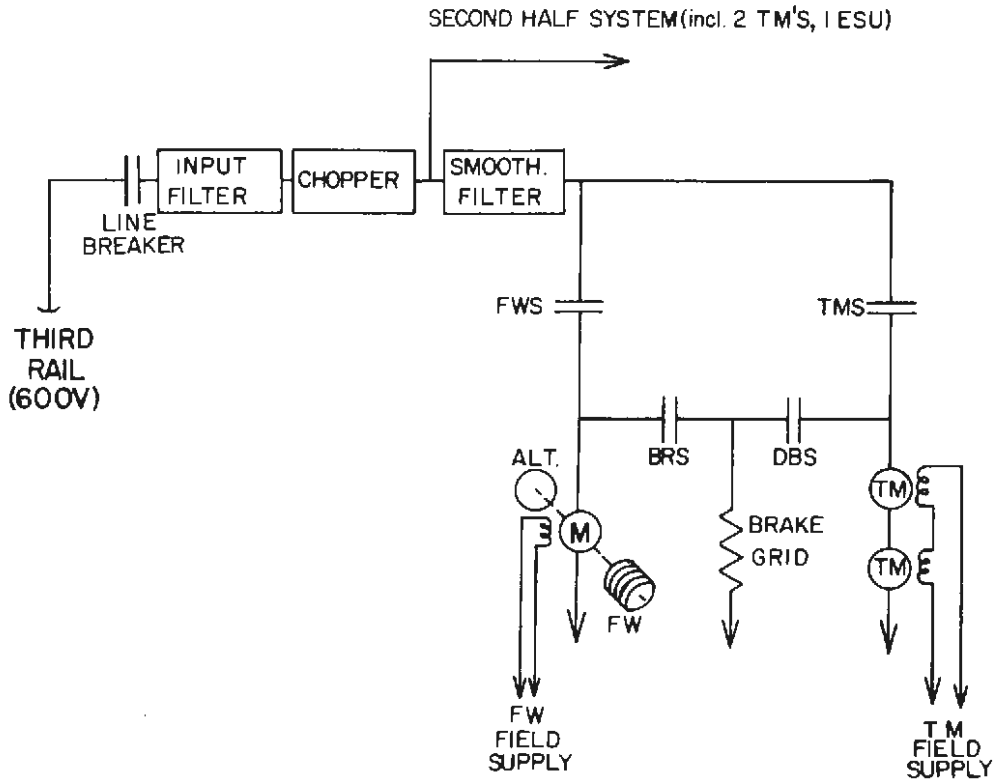

Figure 1. Power Distribution Diagram

TABLE 2
Summary of Energy Storage Car Test Program

	Torrance		Pueblo		New York		
	Lab	On-car	Check out	Track tests	2-car tests	4-car tests	Revenue service
Primary Objectives							
Energy and power reduction	X			X		X	X
Underfloor temperature reduction				X		X	
Reliability				X	X	X	X
Maintenance costs						X	X
Secondary Objectives							
Operation on dead third rail		X		X	X		
Observe chopper operation				X	X		
Ancillary Tests							
Compatibility with R-32	X	X		X		X	
Signal interference	X			X	X		
Noise levels				X		X	
Vibration levels				X		X	
Failure modes	X		X	X	X		
Capacitor discharge	X	X		X	X		
Static stresses				X			
Dynamic stresses				X		X	
UMTA Baseline Tests				X			
R-32 starting grid energy							X

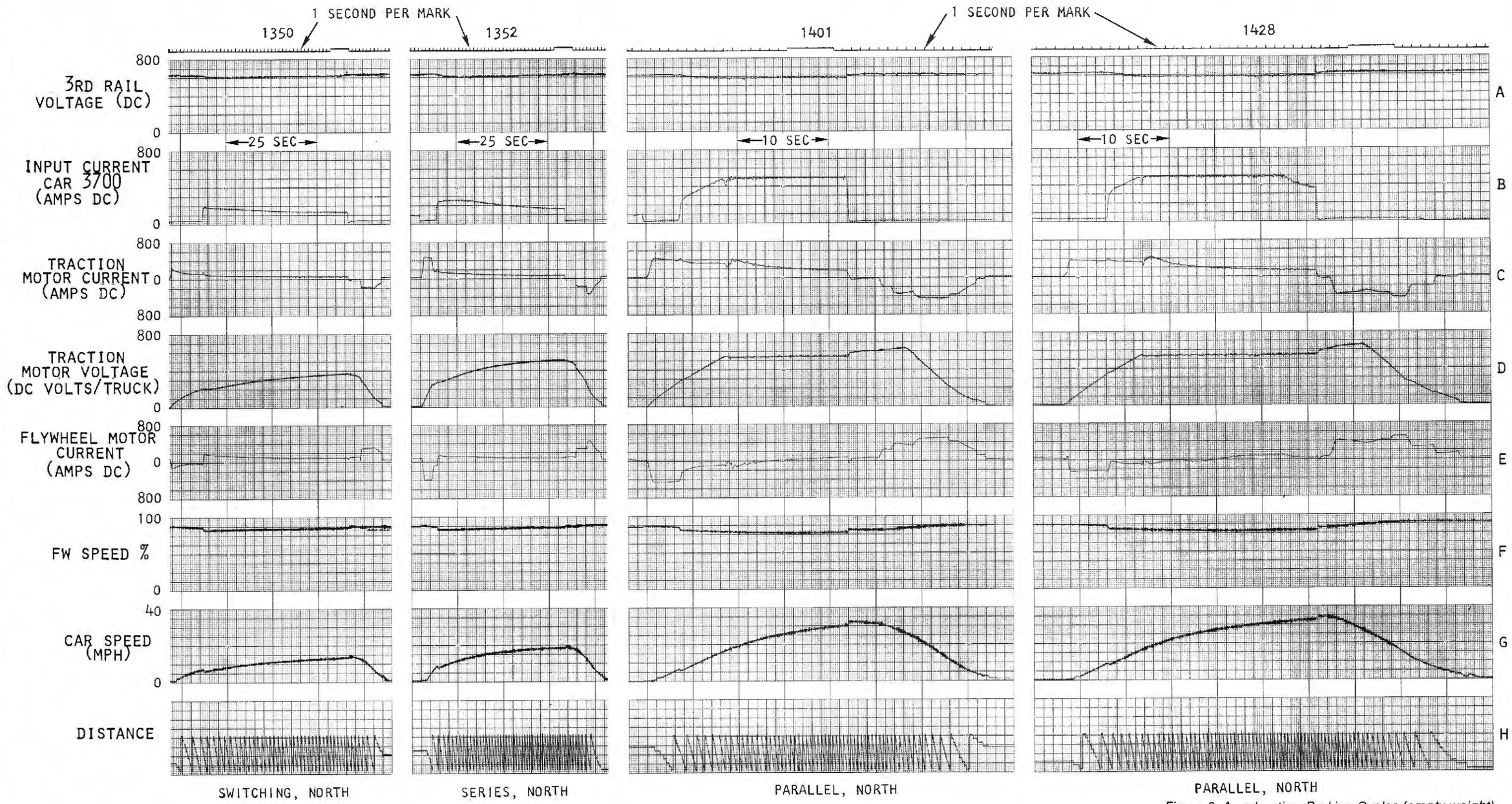

Figure 2. Acceleration-Braking Cycles (empty weight)

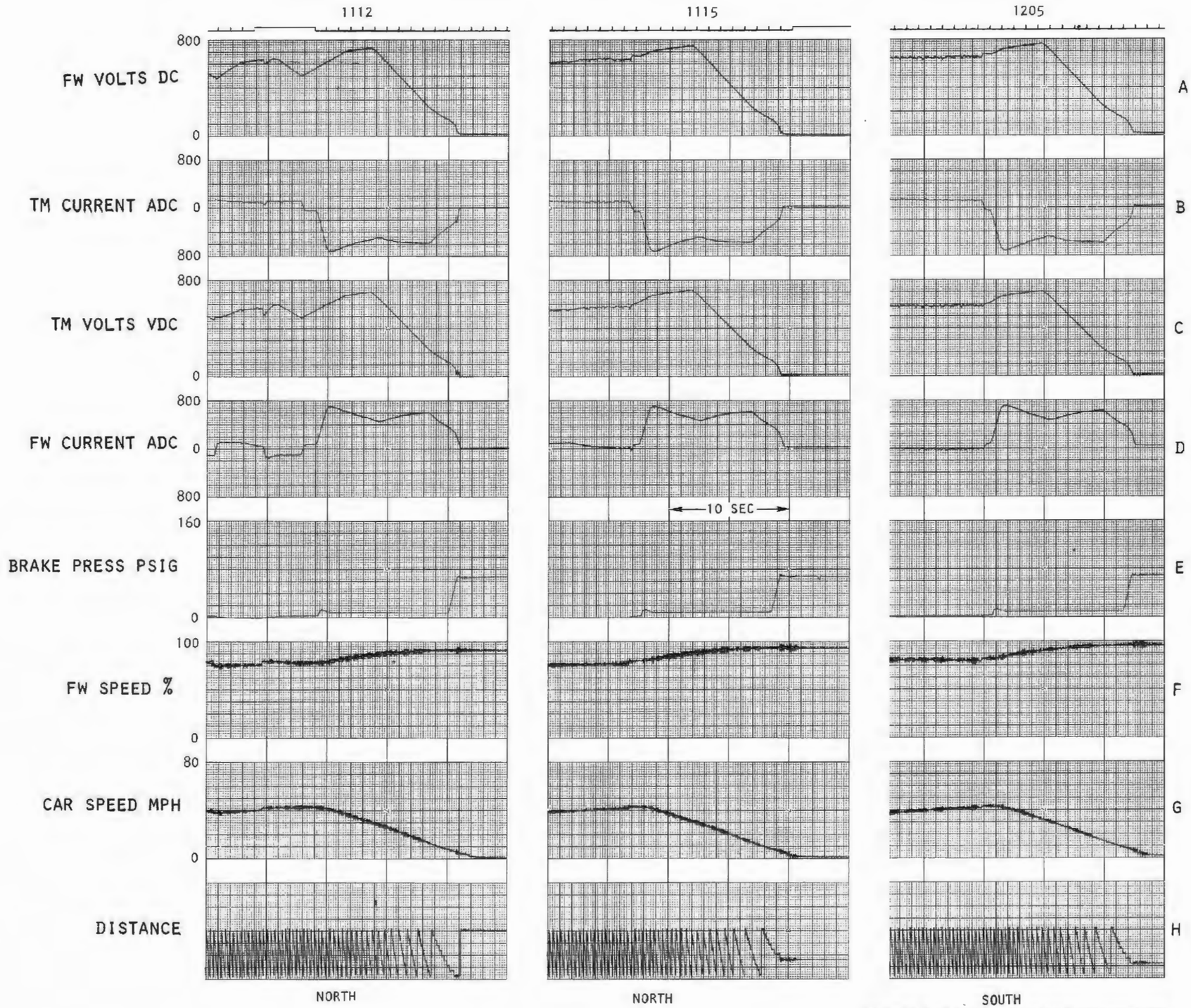

Figure 3. Full Service Braking (empty weight)

The test program was, in fact, divided into three stages which paralleled the development of the hardware and the increasing confidence level of the project participants for that equipment.

Initially the testing took place at the facilities of the equipment manufacturer, AiResearch Manufacturing Co. of California (a division of The Garrett Corporation) in Torrance, California. This work included component and half-car system tests in the lab, initial checkout after installation under the cars, and the demonstration of the cars' ability to propel themselves from fully-charged flywheels with no attachment to wayside power sources.

The principal goal of the testing at the U.S. Department of Transportation Test Center in Pueblo, Colorado was to enable Garrett technicians to check-out the ES system in operation on a third rail and to make modifications as problems were uncovered. While at Pueblo, two additional efforts were completed. First the investigation of stress levels in the ESU mounts under a variety of static loading conditions was completed. Second, the series of data gathering procedures referred to as the UMTA Baseline Tests were carried out. The results of the latter testing are reported in Reference 2; the test procedures, themselves, are contained in Reference 3.

As soon as the two ES cars arrived in New York, they were put through a series of checkout trials. These tests were aimed at (1) establishing compatibility with the NYCTA signal system, (2) confirming the fail-safety of various protective circuits, and (3) generally upgrading the ES system to operate reliably on the NYCTA third rail electrification. These tests were performed with the two-car unit on yard tracks at 207th Street and Coney Island Car Shops of the NYCTA.

The next major step was to adjust the performance of the two ES cars in acceleration and braking to match as closely as possible the performance of typical class R-32 cars. This effort was of critical importance to the remainder of the test program, because the basic foundation of the evaluation of the ES concept was to compare energy consumption of the two ES cars with a pair of similar, but conventionally propelled cars. It was believed that the most credible method for making such a comparison was to do so directly, with the conventional and ES cars coupled together in train with each other. Furthermore, to ensure that each type of car was expending equal effort in both acceleration and braking, a device was installed on the inter-pair drawbar to monitor any pulling or pushing forces between the pairs. To the greatest extent possible, all comparative testing was performed with the two pairs linked together.

In view of the UMTA participation in the project, a second basic criterion for the testing was to ensure that the results could be interpreted in general terms, for use by any existing or planned rail transit system. Thus, the initial comparison of energy usage, performed on the NYCTA Sea Beach test track, was a determination of relative energy consumption under a variety of operational conditions. This testing, referred to as the "Duty Cycle Tests", recorded energy consumption by each of the two pairs as a function of station spacing distance, top speed, car loading and station dwell time.

This testing was followed by operation of the four-car train in simulated service on ten NYCTA lines, observing service schedules for running time but not carrying passengers.

During the Sea Beach and simulated service testing phases, determinations of relative noise and vibration levels were performed. Additionally, the recording of stress levels in the ESU support structure during car operations was completed. Measurements of electrical and mechanical losses in the ESU were gathered at this time, as well, along with an investigation into the energy losses in the conventional cars' starting grids.

All of the testing which has been described above was preliminary to a six-month trial period for the cars in revenue passenger-carrying service on a variety of lines of the New York City Transit System. At all times during this revenue service testing, the two pairs of cars were linked together (sometimes operating as a four-car train, sometimes as a part of trains up to ten cars in length) with continuous monitoring of energy consumption in each pair.

Prior to placing the cars into revenue service, a press demonstration run was performed, which included operation of the four-car train into the terminal station with third-rail power shut off and the ESU's in the two ES cars propelling the four cars. As an added effort to obtain community involvement in the program, special posters describing the propulsion system and the ES program were installed in the two ES cars (Figures 4 and 5). One of the posters surrounded a continuously-reading digital display of the energy consumed by each of the two pairs. A telephone number where citizens could obtain daily schedules of ES car operations was publicized. On the average, one or two calls per day were received.

As had been anticipated at the start of the program, the ES equipment was removed from the two cars at the conclusion of the six-month revenue service trial and the cars were restored to their original configuration.

A chronology of the major events in the ES program is listed in Table 3.

TABLE 3
Energy storage project chronology

MILESTONE	DATE ACHIEVED		MONTHS AFTER GRANT
Grant Award	July	1971	—
Garrett Contract Award	January	1972	6
Design Complete (Note 1)	August		13
Component Fabrication (Note 2)	February	1973	19
Lab Verification of System Performance	April		21
Car Modification Begins (Note 3)	May		22
First Alternator Retrofit Complete	September		26
Weld Deficiency Correction	December		29
Installation Complete	January	1974	30
Torrance Testing Complete	February		31
Pueblo Testing Begins	February		31
Alternator & Bearing Retrofit Complete	November		40
UMTA Tests Complete	January	1975	42
All Pueblo Testing Complete	February		43
Ship to New York	March		44
Shake-down Testing (207th Street) Complete	June		47
Analytical Runs (Sea Beach Track) Complete	November		52
Simulated Service Test Complete	January	1976	54
Revenue Service Begins	February		55
Revenue Service Ends	September		62
Test Data Summary Report	February	1977	67
Draft Final Project Report	March	1978	80
Final Project Report	October		87

Note 1: Initial design complete in May 1972; two additional weeks required for weight reduction program.

Note 2: Delays included late delivery of castings to Garrett, oil-vacuum pump redesign, bearing redesign to reduce rotational losses, and oil seal redesign.

Note 3: The start of the car modifications was held up because of the need for Garrett to perform a more extensive structural analysis than had been intended originally.

OVERVIEW OF PRINCIPAL RESULTS

Energy reduction

The equipment tested under the two R-32 cars demonstrated that on-board flywheel energy storage is an impressive means for achieving major savings in transit car propulsion energy. As expected, fast local runs were most conducive to energy conservation by on-board storage, but fast express runs showed significant savings by this method, as well. Steady-state losses in the equipment and low available kinetic energy made slow runs (those with extended speed restriction areas or with such frequent stops that inter-station speeds are low) less effective applications, but these runs use relatively less energy in the first place.

The levels of energy savings actually achieved were made more impressive by the observation of three critically significant deficiencies in the design of the ES hardware, each of which caused the measured savings to be lower than what should have been achievable.

1. The mechanical and electrical power losses in the energy storage units (ESU's) were unnecessarily high.
2. There was a very apparent need for a means to reduce energy consumption by the ES equipment while the cars were stationary, i.e., during turnaround layovers at terminals and during extended yard moves.
3. The two ESU's under each car provided more energy storage capacity than was actually needed, thereby adding unnecessarily to the car weight and to the system energy losses.

The effect of the lay-over and yarding periods was dramatic in reducing the potential savings in energy. Thus, a 32% saving in propulsion energy consumption, as measured in runs from terminal to terminal on the NYCTA A-line, was reduced to a net savings of 23% when lay-overs and yard movements were included.

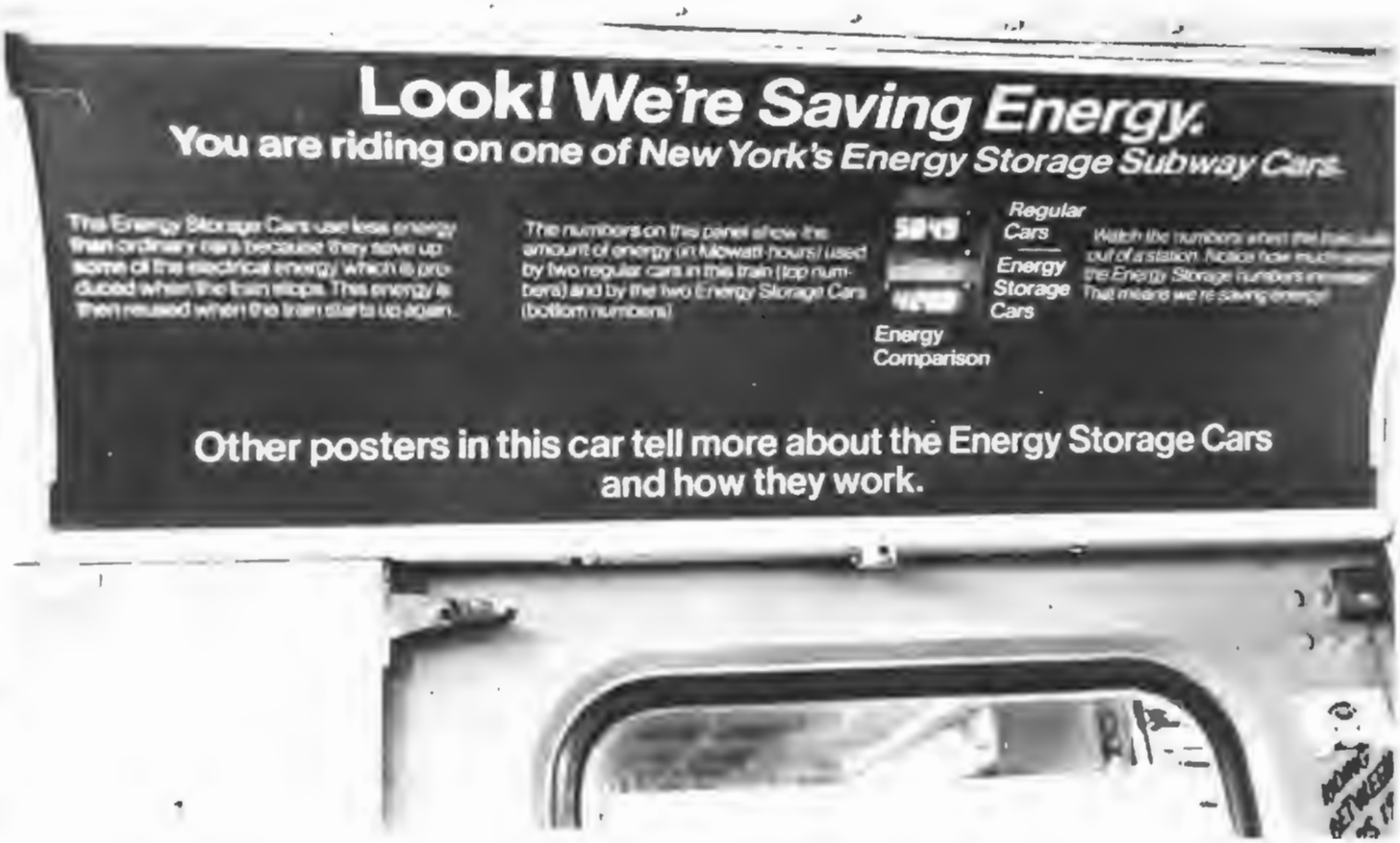

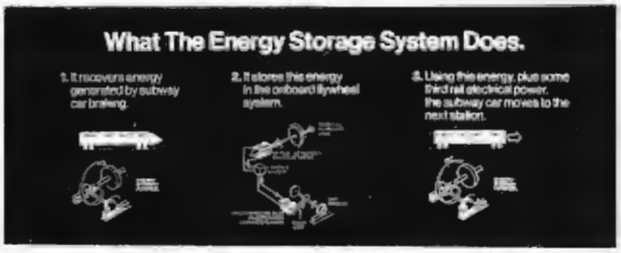

Figures 4 and 5. Posters Informing Public of ES Operation

Terminal-to-terminal savings ranged between 20 and 40%, for the NYCTA lines over which the four-car unit operated but total overall savings (including the non-productive time) amounted to only 14 to 26%.

Of course the basic cause of this reduction in energy savings potential was the high level of losses in the ESU's, coupled with a control system which called for the flywheels to maintain a speed of 9800 RPM under car idle conditions. Moreover, the high loss levels had a very significant effect in reducing the potential for savings during terminal-to-terminal runs, as well, since these losses acted as a constant drain of energy whenever the ESU's were in operation.

The over-design in energy storage capacity amplified the effect of the losses, since the losses depend to some extent on the magnitude of the design capacity. The storage capacity was based on the perceived need to store the kinetic energy of a crush-loaded car traveling at maximum speed (50MPH), as explained in Reference 1. As observed during the test program, the coincidence of these two conditions of load and speed does not occur with any significant frequency, since crush loads are often associated with less than highest speeds, and vice versa.

Thus it appears quite clearly that a reduction in ESU running losses, which would be aided by a reduction in designed storage level, combined with an automated removal of input power from the ESU under idle conditions should lead to a substantial further improvement in energy savings beyond those actually measured with the "first generation" hardware used in the present program. Quantitatve estimates of the benefits of a reduction in ESU losses and of a provision for ESU coasting during layover are given in Part II.

Two additional observations can be made from the propulsion energy measurements performed during this test program. First, the energy consumed by both the ES-equipped and conventional cars in simulated service was 10 to 20% higher than the energy recorded during the revenue sevice runs. Furthermore, the simulated service energy agrees with calculations based on the full performance duty cycle tests. Thus, both the duty cycle and simulated service tests overestimate the propulsion energy actually used in normal service, despite all efforts to make these tests as realistic as possible. The most likely explanation for this disparity is based upon the fact, which has been observed in a variety of transit energy calculations, that the station-to-station running time is not strongly dependent upon propulsion energy expended. Thus the adherence to the schedule during simulated service testing did not guarantee that the energy expended would agree with that which is used in normal service. In fact, the simulated service and duty cycle test tended to be run with full acceleration and braking rates more frequently than is experienced normally.

Interestingly enough, however, the *percentage* energy savings by the ES cars as compared with the conventional pair for any given route were approximately the same in revenue service and in simulated service. Thus the difference in performance between the two tests changed only the absolute amounts of energy, not the *relative* consumption of the two types of propulsion equipment.

Later in the report, the measured revenue service energy consumption by the standard cars will be shown to agree quite well with the numbers derived by an NYCTA Consultant who used a computer-based train performance simulation.

The second point drawn from the energy measurements is that for a given route, the daily variations in propulsion energy consumption per trip were quite small. At first thought, one might consider that differences in individual motormen or in traffic disruptions would make the accurate determination of line-haul energy a difficult matter. In fact, the measurements in this test program showed that by recording energy consumption by one pair of cars running on a line for no more than ten days, a mean energy value can be determined for that type of car on that line with a standard deviation of only 1 to 2%.

Operation on dead third rail

The tests which were performed demonstrated that, given a reasonable "charge" in the ESU (flywheel at 85% of top speed), distances of 2000 ft or greater can be covered on level track in the absence of third rail power, even with the cars carrying a crush load. It is hoped that in the future this capability would enable flywheel-equipped trains to proceed to the next station during a power outage.

However, the performance of the ES equipment under such emergency conditions must be viewed against the ES losses which were demonstrated, as well. The 85% flywheel speed represents about 1.5 kwh of usable energy for each car, but this energy would be used up by the losses in the ESU in barely three minutes. Thus any delay in getting clearance to proceed under emergency conditions would diminish or defeat the ES cars' potential ability to propel themselves. Again, any improvement in reducing ESU losses would ameliorate this situation.

R-32 car grid energy

The final energy-related item was a subsidiary effort to measure the loss of propulsion energy in the starting grids of standard R-32's during car acceleration. This investigation arose because of the attention that was

being given to solid-state propulsion controls (e.g., choppers) and their potential for energy savings through the avoidance of starting resistances. The present tests determined that the magnitude of this energy loss in the R-32's accounted for approximately 8 to 12% of the total propulsion energy consumed.

In view of the fact that solid state controls have losses on the order of 5%, this particular advantage of the chopper does not appear to be of primary significance.

Gyroscopic forces

Of particular concern in any application of flywheel devices to moving vehicles is the potential problem of gyroscopic action, which could affect steering of the vehicle around curves. For this reason, as well as for reasons related to particular structural concerns, measurements were made of the dynamic loading on the supports of the ESU under extreme conditions of track curvature and authorized speed.

It was found that the stresses generated by gyroscopic action were unmeasurably small. This was in accordance with theoretical estimates which put the loading in the range of a few hundred pounds per flywheel mount. This is negligibly small compared with the loading due to the dead weght of the ESU, itself.

Noise and vibrations

Tests of internal and external noise and of carborne vibrations demonstrated that the levels generated in each category by the ES cars were acceptable when compared with the standard R-32's. For example, the air compressor on the cars could be heard above the noise level emitted by the ESU's. Operation of the ES cars within the reverberant environment of a concrete subway station was acceptable as well, when compared with conventional equipment.

This is not to say, however, that noise levels which were acceptable in 1964, when the R-32's were built, are still acceptable in 1978. The equipment installed under the two ES test cars would not meet the sound levels specified in the latest NYCTA car contract, nor would they compare favorably with the modern R-46 cars recently placed in service in New York.

Signal interference

The use of a chopper to control the flow of current from the third rail gives rise to a concern that the chopper frequency and its harmonics should not generate "false clear" signals that could cause an unsafe operational condition. Tests performed on the ES cars in the lab in Torrance, at Pueblo and on various track circuits on the NYCTA system indicated an absence of such unsafe emissions.

Underfloor temperatures

Since the ES cars demonstrated reductions in energy usage, it is clear that they generated less waste heat than did the standard R-32's. This is because the ES car conserves energy by the re-use of energy which conventional cars throw off as heat (either in dynamic braking grids or in friction brake shoes on the wheel treads).

Unfortunately with no more than two ES cars, it was not possible to demonstrate directly the waste heat reduction. An attempt was made during the simulated service testing to measure underfloor temperatures in representative locations under both the ES and standard cars. These measurements did not demonstrate significant differences. This fact can be explained by the smallness of the effects caused by two cars traveling in so massive a heat sink as a subway tunnel.

Brake shoe wear

One of the original objectives of the test program was to have been a comparison of the relative consumption of materal in the brake shoes as used on ES cars versus standard cars. The thought behind this hypothesis was that with greater "dynamic braking" in the ES cars, friction brake wear would be reduced.

It must be realized, however, that under normal operating conditions, even a conventional dynamic braking system (which applies friction brakes at approximately 8 MPH) uses its brake shoes very sparingly. In a stop from 40 MPH, for instance, only 4% of the car's kinetic energy must be absorbed by the friction brakes. In fact, during the Revenue Service Test, the brake shoe wear on the two standard cars was only approximately 5% in the 13,900 miles travelled.

This amount of wear extrapolates to a full shoe life of approximately 170,000 miles or over three years of normal service. The actual fleet service life experience is, of course, very much less than that, being approximately 44,000 miles for cast iron shoes. Thus it is clear that the rate of shoe wear is not a linear function of car mileage and that it must actually increase as the shoe thickness decreases, with the shoe becoming less effective as a heat "sink".

In any case, the attempt to investigate differences in brake shoe life as a part of the ES Revenue Service Test was nullified by the relatively low car mileage during the six-month period, as discussed in the following section, and the resultant low amount of brake shoe consumption.

Reliability and maintainability

The reliability performance of the ES equipment can best be summarized by an overall assessment of the revenue service testing. This phase of the testing

came after four years of development, test and redesign including eleven months of testing on the NYCTA system and yet the cars accumulated less than half the average mileage of the NYCTA fleet during the six-month period.

Clearly, the equipment under test represented a "first generation" flywheel propulsion system for transit cars and the above observation can be explained to a large degree on that basis. To a certain extent, the lack of availability of the ES cars was due to slow turnaround of problems that did occur. The slowness of correction can be attributed to (1) small spare parts stock, (2) poor maintainability design of the ESU's and (3) lack of maintenance experience.

In fact, one must take the realistic viewpoint that this equipment had all of the shortcomings that appear to be typical of the early stages in an advancing technology. Nevertheless, the equipment *was* capable of being operated in passenger-carrying service on the busiest transit system in North America.

Details of the failure and in-service records are presented in Part III of this report.

FUTURE DIRECTIONS

Under UMTA's sponsorship, the Energy Storage propulsion system has been advanced to a more refined stage of development as part of the ACT-1 car program. The ACT-1 propulsion system, also designed and manufactured by The Garrett Corporation, has several features which take advantage of the experience gained in the ES program. Principal among these are control simplifications, ESU loss reduction, and ESU maintainability improvements.

Most fundamentally, the control simplification consists of the elimination of the chopper. The reduction in ESU losses results from improvements in the bearings, seals and pumps. The maintainability of the ESU is improved by relocating the vacuum and oil pumps so that they can be accessed without disassembling the entire ESU.

It is clear to all of the participants in these flywheel propulsion development programs that the present hardware is not yet ready for immediate fleet-wide application to rapid transit cars. The ACT-1 hardware appears to represent a significant improvement beyond that which was tested in the ES program. However, the reliability of the ACT-1 equipment under the wide range of conditions normally encountered in rapid transit service has yet to be determined. Reliability is, of course, critical to any passenger-carrying operation. Of equal importance for the hardware development is the evaluation of equipment maintenance costs under service conditions, since unfavorable maintenance costs could possibly outweigh the financial gains to be achieved by energy savings.

In order to properly evaluate reliability and maintenance questions, a more extensive demonstration program would be needed. To be meaningful, such a program would need to utilize propulsion equipment that would represent *production* hardware to the greatest extent possible.

Preliminary investigations of a medium-scale retrofit program for NYCTA subway cars are underway. These investigations have centered around the thought of applying the ACT-1 propulsion system—with only one ACT-1 Energy Storage Unit per car—to a 50 or 60-ft New York car. An automatic coasting mode for the ESU during idling periods would be incorporated.

Such a system offers promise for countering all of the problems uncovered in the original ES program.

At the same time, transit operators continue an interest in AC induction motor propulsion. This propulsion system should save braking energy through regeneration of the dynamic braking currents back into the third rail system. The use of induction motors should give rise to significant purchase and maintenance cost savings, as well.

In a shorter time-frame, it should be noted that low-technology-content measures for propulsion energy conservation exist, as well. These include the increased use of vehicle coasting and the application of performance-limiting modifications to conventional propulsion equipment. Both of these short-term approaches are under investigation by the NYCTA.

PART II — TEST DATA REPORT

ENERGY

This unit of the data report is composed of five sections. The results of the revenue service test are presented first, since they are of the greatest significance. These results are then compared with the simulated service data, followed by the duty cycle test results. A section presenting various measurements of the parasitic losses on the ES propulsion system, including flywheel start-up, ensues. The unit concludes with a discussion of standard R-32 starting grid energy losses.

Revenue service test

As has been stated before, the two Energy Storage cars were placed in passenger-carrying service on the New York subway system along with a pair of unmodified R-32 cars. The four-car unit composed of ES cars 3700-3701, linked to standard cars 3702-3703 carried a meter which measured the propulsion energy consumed by each pair (including "propulsion auxiliaries" such as equipment blowers and power supplies). *Note that the energy consumed by the car auxiliaries (e.g. car heating, ventilation and lighting) was not included in the data collected.* The characteristics of the NYCTA lines upon which the cars saw service are listed in Table 4; more detailed information on the routes is contained in Appendix A.

The most straightforward manner in which the relative energy consumption data can be presented is to list the total energy consumed by each pair while in service on each line. This is done in Table 5. It is important to make clear that in Table 5 and in all other energy summaries to follow, *all* of the meaningful measurements are included in the tabulations. The only data which are *not* shown are those readings collected when one of the four cars was not propelling properly or when the instruments were not recording correctly. The tables *do* include data collected during train operations that were subject to delays or disruptions, since these events will occur at times in any transportation system.

Table 5 shows quite readily the good and the bad features of the ES equipment. The first energy column, which reports the energy consumed in moving the cars in passenger-carrying service, lists very substantial energy savings. These savings are undermined to some degree, however, by the consumption listed for layover and for movements into and out of the yards. Nevertheless, net savings of 14 to 26% *were* achieved, with an overall average of a 19.2% reduction from the standard cars' propulsion energy. The latter figure is biased to the low side by the fact that the ES cars spent a disproportionate number of days on the least favorable run.

TABLE 4
NYCTA routes covered in revenue service

Line	Terminals N	Terminals S	Route Length (Miles)	Number of Station Stops	Average Station Spacing (feet)	Average run time (min.)	Schedule speed (MPH)
A (Brooklyn Exp)	207 St.	Lefferts	23.6	29	4290	67	21.1
(Brooklyn Local)	207 St.	Lefferts	23.6	38	3270	71	19.9
AA	168 St.	Hudson Term.	9.8	22	2360	32	18.4
B	168 St.	Stillwell	21.0	35	3160	72	17.5
	57 St.	Stillwell	15.0	24	3300	51	17.7
D	205 St.	Brighton Beach	24.6	29	4480	71	20.8
E*	179 St.	Hudson Term.	16.2	22	3890	47	20.7
	179 St.	Euclid	25.0	28	4720	76	19.8
N*	57 St.	Stillwell	15.4	18	4500	48	19.2
RR	Ditmars	95 St.	17.6	38	2450	66	16.0

* Subsequent to completion of revenue service testing, the N route was extended to Queens and the E route to Euclid Ave. was replaced by a CC route from Bedford Park Blvd. to Euclid Ave.

The information in Table 5 is most useful for preliminary consideration of applications in New York. For more wide-spread applications and for a better understanding of the assets and liabilities of the ES equipment, it is necessary to refine these gross data, as is done in Table 6. This breakdown separates out the individual runs and shows, among other things, the remarkably low daily variation of energy usage on any particular run (the "±" listing is the standard deviation of the average energy value for each run). With the running energy further summarized in Table 7, one is in a position to appreciate more fully the potential for energy saving by energy storage.

- In terminal-to-terminal running, the ES cars used an average of 2.98 kwh of propulsion energy per car-mile as compared with 4.37 kwh/car-mile for the standard cars. The saving of 1.39 kwh/car-mile represents a 31.8% propulsion energy reduction for the lines served by the test cars.
- The running energy reduction on the AA local was 40%. However, the extensive terminal layovers caused the ESU's to use up 6.5 of the 21 kwh which were saved during a terminal-to-terminal run, on the average, thus lowering the net saving to approximately 25%.
- The propulsion energy per station stop for each type of equipment on each line, when plotted against station spacing distance (Fig. 6), is remarkably linear. This observation leads to a simple method for predicting the relative energy consumption for similar cars on any given transit line as a function of the average station spacing for that line. Least-squares-fit straight lines are drawn through the data points in Figure 6. From these two lines an absolute energy savings and a percent energy saving can be calculated. The predicted curve is drawn in Figure 7 and the actual percent savings for the service lines are plotted, as well. The scatter of the test results about the predicted curve merely indicates that the prediction, which is based solely upon station spacing and not on other route characteristics such as running speed, is too simple. Nonetheless, it can be used to make "first guess" approximations.
- A more reliable estimate of percentage propulsion energy saving can be based on a double regression of the energy data in terms of both station spacing and schedule speed. The propulsion energy for each type of equipment on a given route can be expressed as:

$$E = C_0 + C_1 n + C_2 t,$$

where E = propulsion energy per car-mile
n = number of stops per mile on the route
t = scheduled running time per mile on the route

The constants C_0, C_1 and C_2 derived from the revenue service test data are given in Table 8 for the two types of propulsion equipment. The values of the coefficients are consistent with expectation in that the standard cars' propulsion energy is strongly dependent upon the number of stops, whereas the ES cars depend upon the time consumed during the run. The standard car consumed less energy for propulsion on slow trips (C_2 negative) while the ES system was most effective

TABLE 5
Total Energy Consumed in Revenue Service Testing

Line	No. of one-way trips		Kilowatt-hours consumed by each pair: Running	Layover	Yard Moves	Total	Difference St'd–ES	Percent Saving
A	72	St'd	14,022.1	3.3	167.8	14,193.2	3,232.6	22.8%
		ES	9,458.3	1017.5	484.8	10,960.6		
B & AA	92	St'd	12,706.3	213.8	91.5	13,011.6	2,420.1	18.6
		ES	8,740.3	1625.1	226.1	10,591.5		
D	85	St'd	16,047.6	161.8	114.7	16,324.1	3,276.4	20.1
		ES	11,653.5	1032.0	362.2	13,047.7		
E	12	St'd	2,025.5	37.0	47.6	2,110.1	552.6	26.2
		ES	1,323.8	179.8	53.9	1,557.5		
N	201	St'd	23,824.7	9.5	299.8	24,134.0	3,427.3	14.2
		ES	18,522.2	1437.1	747.4	20,706.7		
RR	67	St'd	10,676.8	14.2	732.8	11,423.8	2,694.8	23.6
		ES	7,052.9	691.7	984.4	8,729.0		
		6-Month Total St'd				81,196.8	15,603.8	19.2%
		ES				65,593.0		

TABLE 6
Average Energy Consumption in Revenue Service

Line	Revenue Running				Layover		Yard Operations	
	No. of one-way trips		kwh/car one-way	±	No. of layovers	kwh/car per layover	Number	kwh/car per move
A (Bklyn Express)	36	St'd	91.6	2.3	91	0.0	24	3.5
		ES	65.0	2.5		5.6		10.1
			26.6			−5.6		6.6
A (Bklyn Local)	36	St'd	103.2	1.3				
		ES	66.4	2.0				
			36.8					
B (168 St.)	34	St'd	91.7	2.5	103	1.1	11	4.2
		ES	66.1	2.8		7.6		10.3
			25.6			−6.5		−6.1
B (57 St.)	17	St'd	65.3	1.3				
		ES	50.1	0.6				
			15.2					
AA	41	St'd	51.9	1.1				
		ES	31.1	0.3				
			20.8					
D	85	St'd	94.4	1.7	93	0.8	14	4.1
		ES	68.6	1.1		5.5		13.0
			25.8			−4.7		−8.9
E (Hudson Term'l)	8	St'd	67.8	2.6	14	1.3	3	8.0
		ES	44.2	3.0		6.4		9.0
			23.6			−5.1		1.0
E (Euclid)	4	St'd	117.6	5.7				
		ES	77.2	6.5				
			40.4					
N (57 St.)	201	St'd	59.3	0.7	225	0.0	45	3.4
		ES	47.6	1.0		3.2		8.3
			11.7			−3.2		−4.9
RR	67	St'd	79.7	1.2	75	0.1	15	24.5
		ES	52.7	1.2	75	4.6		32.8
			27.0			−4.5		−8.3

when there were many stops (C_1 negative).

From the two energy values computed by the regression formulas, a prediction can be made for the savings in energy on the route. The formulas have been applied to the test lines and the results are listed in Table 9 with comparisons to the actual energy measurements. The agreement between calculated and measured energy savings is within the standard deviation of the measurements.

• By way of confirmation of the energy measurements, it is noteworthy that the measured propulsion energy consumption for the standard cars is in remarkably close agreement with the values predicted by a computer simulation performed by Gibbs & Hill for NYCTA (Reference 4). The comparison of measured versus simulated energy consumption for those lines which are common to the two studies is listed in Table 10. The high degree of agreement between the measurements and the calculations is reassuring because the Gibbs & Hill simulation was calibrated to give an energy consumption which was consistent with total energy usage at a given period on the New York subway system.

TABLE 7
Energy consumption during running time in revenue service

Line	kwh consumed by st'd car per one-way	per car-mi	per stop	kwh consumed by ES car per one-way	per car-mi	per stop	% saving
A (Bklyn Exp)	91.6	3.89	3.16	65.0	2.76	2.24	29.1%
(Bklyn Local)	103.2	4.38	2.72	66.4	2.82	1.75	35.7
AA	51.8	5.27	2.35	31.0	3.16	1.41	40.0
B (168 St)	91.6	4.37	2.62	66.0	3.15	1.89	27.9
(57 St)	65.3	4.35	2.72	50.1	3.34	2.09	23.2
D	94.4	3.84	3.26	68.6	2.79	2.37	27.1
E (H Term)	67.8	4.19	3.08	44.2	2.73	2.01	34.7
(Euclid)	117.6	4.70	4.20	77.2	3.08	2.76	34.3
N (57 St)	59.2	3.85	3.29	47.6	3.10	2.64	19.8
RR	79.7	4.52	2.10	52.6	2.98	1.38	34.3

TABLE 8
Multiple regression coefficients

Propulsion energy/car-mile =
$C_0 + C_1 \times$ (stops/mile) $+ C_2 \times$ (minutes/mile)

	Standard R-32	Energy Storage Car
C_0	3.41	1.14
C_1	0.864	−0.171
C_2	−0.138	0.664

TABLE 9
Energy predictions based on multiple regression formulas

Line	Stops per mile	Minutes per mile	Standard car kwh/car-mile Meas'd	Calc'd	ES car kwh/car-mile Meas'd	Calc'd	% Saving Meas'd	Calc'd
A (Exp.)	1.23	2.85	3.89	4.08	2.76	2.82	29.1	30.9
A (Local)	1.61	3.01	4.38	4.39	2.82	2.86	35.7	34.9
AA	2.24	3.26	5.27	4.90	3.16	2.92	40.0	40.4
B (168 St.)	1.67	3.43	4.37	4.38	3.15	3.13	27.9	28.5
B (57 St.)	1.60	3.40	4.35	4.33	3.34	3.12	23.2	27.9
D	1.18	2.89	3.84	4.03	2.79	2.86	27.1	29.1
E (H. Terminal)	1.36	2.90	4.19	4.19	2.73	2.83	34.7	32.5
E (Euclid)	1.12	3.04	4.70	3.96	3.08	2.97	34.3	25.0
N	1.17	3.13	3.85	3.99	3.10	3.02	19.8	24.3
RR	2.15	3.74	4.52	4.75	2.98	3.25	34.3	31.6

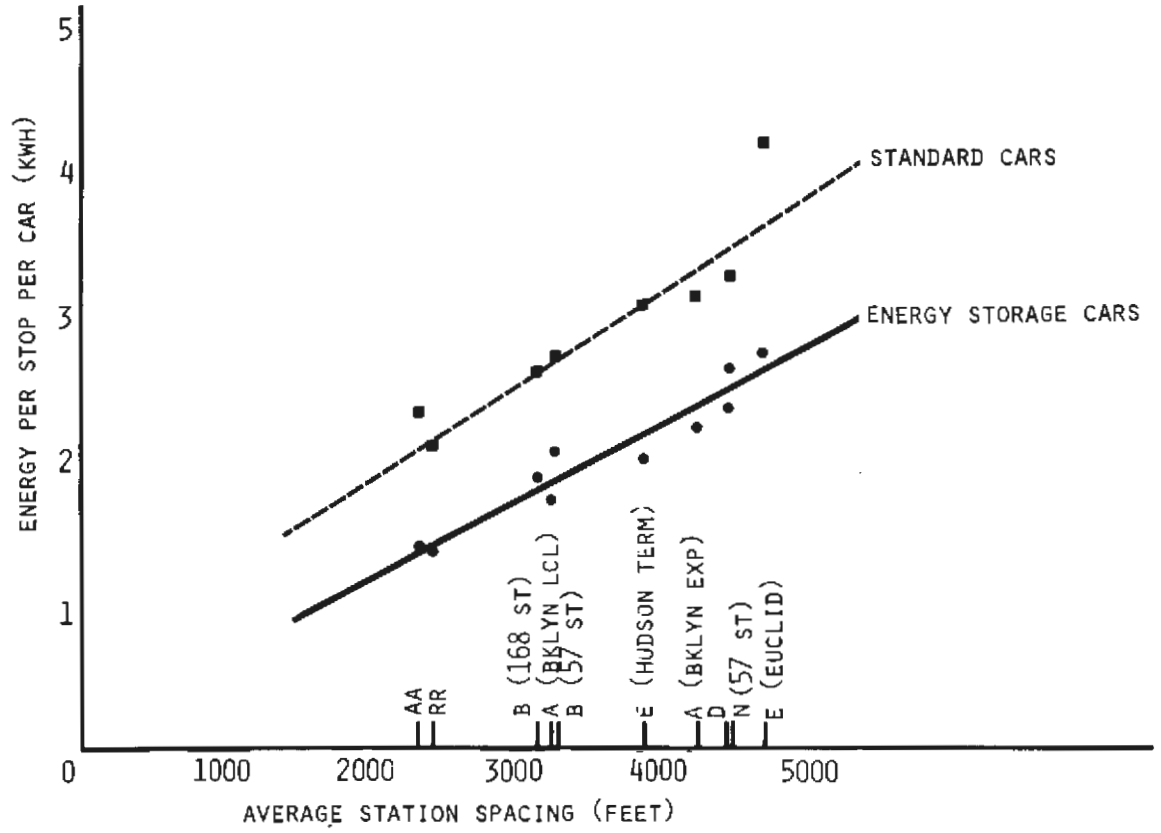

Figure 6. Average Propulsion Energy per Station Stop in Revenue Service

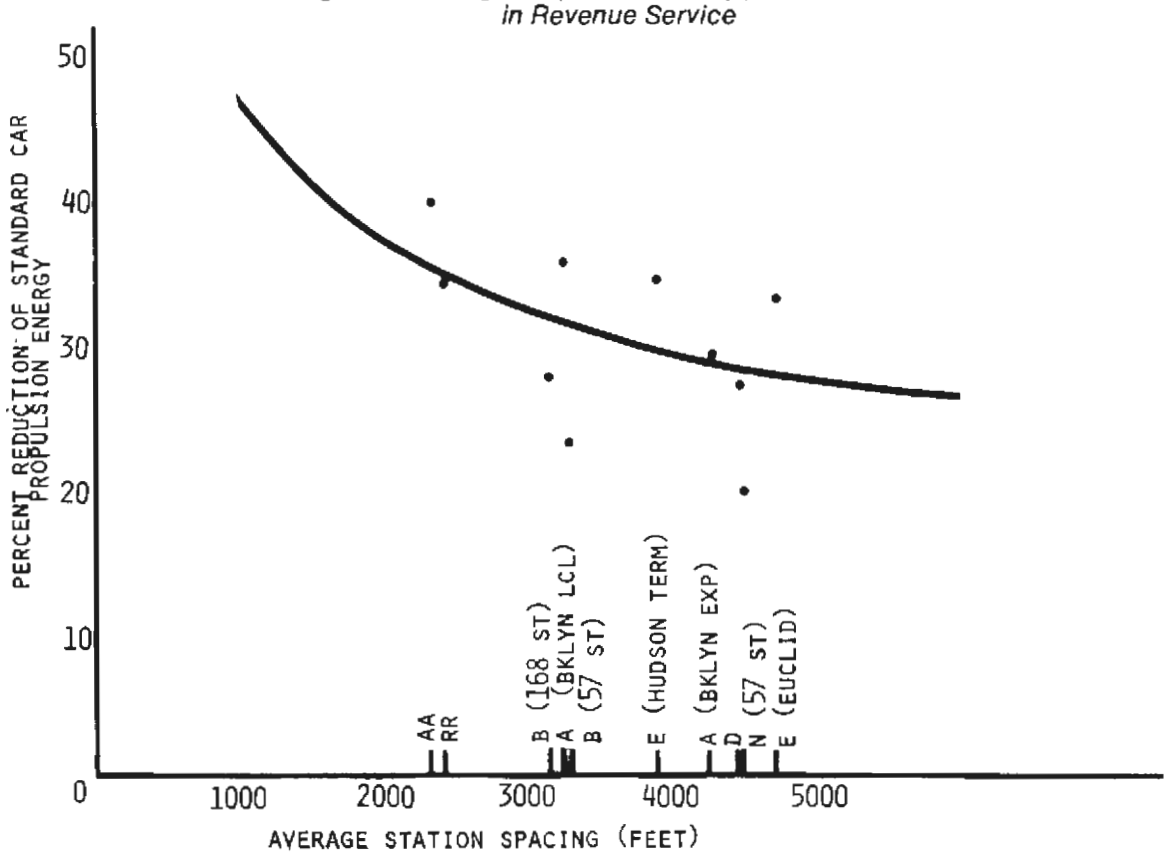

Figure 7. Prediction of Energy Savings Based on Station Spacing Model

TABLE 10
Comparison of computer simulation with standard R-32 propulsion energy consumption in revenue service

NYCTA Line	Propulsion energy/car in one-way run	
	Simulation*	Actual
A (Brooklyn exp.)	111.1 kwh	91.6 kwh
B (168th St.)	93.1	91.6
D	93.8	94.4
E (Euclid Ave)	119.2	117.6
N	68.4	59.2
RR	79.2	79.7

*derived from Table III-3 in Optimization of Power Resources (NYCTA); Parsons, Brinckerhoff-Gibbs & Hill, May 1976.

TABLE 11
Examples of propulsion energy consumption by assignment on NYCTA A-line

Assignment	kwh/car St'd	kwh/car ES	kwh Savings	% Savings
4 *Local—4 Express				
Running	779.0	525.4		
9 Layovers	0.0	50.4		
2 Yard moves	7.0	20.2		
1 FW start-up	—	5.8		
	786.0	601.8	184.2	23.4
10 Local—4 Express**				
Running	1397.9	923.8		
15 Layovers	0.0	84.0		
1 Yard moves	3.5	10.1		
1 FW start-up	—	5.8		
	1401.4	1023.7	377.7	27.0
6 Local—4 Express***				
Running	985.3	658.2		
12 Layovers	0.0	67.2		
4 Yard moves	14.0	40.4		
2 FW start-up	—	11.6		
	999.3	777.4	221.9	22.2
2 Express***				
Running	183.2	129.9		
4 Layovers	0.0	22.4		
4 Yard moves	14.0	40.4		
2 FW start-up	—	11.6		
	197.2	204.3	−7.1	3.6% loss

*Number of one-way trips
**part of two-day cycle
***with yard layover in mid-day

• Highly reliable evaluations of total propulsion energy consumption for both ES and standard cars can be made for any assignment of the cars on those routes in New York upon which the test cars saw service. These estimates can be performed by determining the number of one-way trips, layovers and yard moves in the assignment and adding up the energy associated with each, as listed in Table 6. The amount of energy required for starting the flywheels before leaving the yard (5.8 kwh/car) must be added for each yard departure, as well.

Illustrative examples of this type of calculation, based on actual assignments on the A-line of the NYCTA appear in Table 11. The examples cover a wide variety of assignments and result in energy consumption ranging from a 27% saving to a 3.6% loss. Using this sort of calculation one could establish the most favorable assignments for a limited fleet of ES cars.

Simulated service test

As mentioned previously, the four-car test train was operated in simulated service over a representative sample of NYCTA routes (Division B). The operation occurred at night, stopping at all scheduled stations but not boarding passengers. Every effort was made to ensure that the simulated operation be as close to normal as possible by continually checking the progress of the train against the scheduled running time. The cars were at their empty weight except that one of the ES cars (3700) carried approximately 3000 lb. of instrumentation. Each route was traversed for three round trips; the total distance covered was 1016 miles.

The results of this test phase are listed in Table 12, along with comparative data from the revenue service testing. Since the intent of the simulated runs was to investigate the propulsion energy consumed while

TABLE 12
Simulated service energy consumption

	SIMULATED SERVICE kwh/car one-way (kwh/car-mile)			REVENUE SERVICE kwh/car one-way (kwh/car-mile)		
Line	St'd	ES	% Saving	St'd	ES	% Saving
A (Brooklyn Local)	109.5 (4.65)	76.9 (3.27)	29.8%	103.2 (4.38)	66.4 (2.82)	35.7%
AA	57.3 (5.84)	35.4 (3.60)	38.1	51.8 (5.27)	31.0 (3.16)	40.0
B (168 St.)	104.0 (4.96)	78.6 (3.75)	24.5	91.6 (4.37)	66.0 (3.15)	27.9
D	122.9 (4.96)	93.1 (3.78)	24.2	94.4 (3.84)	68.6 (2.79)	27.1
E (H Terminal)	68.4 (4.22)	48.5 (2.99)	29.2	67.8 (4.19)	44.2 (2.73)	34.7
EE (Cont'l-W'hall)	72.5 (5.32)	53.2 (3.90)	26.7			
F	127.8 (4.74)	94.1 (3.49)	26.4			
N	68.6 (4.47)	51.0 (3.32)	25.6	59.2 (3.85)	47.6 (3.10)	19.8
RJ*	106.1 (4.86)	82.4 (3.78)	22.3			
RR	85.2 (4.83)	63.5 (3.60)	25.5	79.7 (4.52)	52.6 (2.98)	34.3

*Synthetic route combining RR with J from 95th St., Brooklyn to 168th St., Jamaica.

traversing the various routes, no layover or yarding energy is included.

The most important conclusion to be drawn from Table 12 is the fact that the simulated service energy measurements are in general 5 to 15% higher than the corresponding values for revenue service operations. Clearly the adherence to timetable did not ensure that the normal performance levels would be observed in the simulation of service. The fact that both the standard car and the ES car energy were higher in simulated service points to this conclusion. This explanation is further confirmed by the duty cycle test results to be presented in the following section.

With regard to the *percent* energy saving results, there is a fairly good correlation between simulated and revenue service. In particular, the relative ranking of the seven routes covered in both test phases is identical except that the order of the N-line and the D-line is interchanged, with the N-line appearing more favorable in the simulation ranking. It was observed during the revenue service period that there appeared normally to be a good deal of coasting on the N-line, thus reducing the energy consumption. Since coasting is itself a form of energy storage, its benefit detracts from the capabilities of flywheel storage. This is one of the reasons why the N-line was the least favorable ES route during the revenue service tests. It is considered likely that there was significantly less coasting on the N-line during the simulated service test, hence the disparity in the rankings.

For reasons which are stated in Appendix A, the A-line was determined to be "typical" of the NYCTA Division B lines for energy storage considerations. Considerable effort, therefore, was applied by Garrett to modeling this line on a computer, and a corresponding effort was expended during the simulated service test to acquire operational data for comparison with the computer model. Thus, a complete record was obtained of the important performance parameters during the A-line simulated service runs. Selected data traces from one of the A-line round trips are presented in Figure 8. (The cars were in numerical order, with 3703 leading from 207th St. to Lefferts Blvd. and 3700 leading on the return.)

The functioning of the four cars can be reconstructed in Figure 8 by correlating the car speed trace with the four third rail current traces at the bottom of the chart. (Recall that cars 3700-3701 were ES cars and 3702-3703 were unmodified R-32's.) Of particular note is the observation that certain accelerations require no third rail current for the ES cars — all of the acceleration energy being drawn from the flywheels. An example of this performance is displayed on chart #4, in the acceleration from 42nd Street to 34th Street.

The onset of third rail current draw by the ES cars consistently lags that of the standard cars and the peak currents are uniformly lower.

The output of the strain gage which was attached to the link-bar between the two pairs of cars is also displayed in Figure 8 ("SG Coupler" trace). Details of the strain gage and its calibration are given in Appendix B; its operation, however, can best be seen in Figure 8. The strain gage signal naturally corresponds to tensions and compressions in the link-bar. It can be seen from Figure 8 that the two pairs of cars are not perfectly matched in performance profile — this is impossible with two such fundamentally different propulsion systems. In fact, the ES cars tended to begin accelerating slightly before the cam controlled cars. Furthermore, the deceleration of the two pairs differed to a small degree because of dissimilarities in friction brake hold-off characteristics. Nevertheless, the strain gage output traces indicate a very high degree of performance matching. Note that the strain gage signal level when the cars are stationary is not significant, since this indicates merely the forces "locked into" the drawbar when the two pairs come to rest at slightly different instants in time.

Station-by-station energy consumption data for typical A-line runs for both pairs of cars in Revenue Service are listed in Appendix C.

The computer energy model of the ES car operating on the A-line, performed by Garrett, predicts a propulsion energy of 3.34 kwh/car-mile when corrected for total trip time and passenger load. This compares favorably with the measured value of 3.19 kwh/car-mile (a 0.08 kwh/car-mile correction was made to the measured energy value to account for the energy consumed by the instrumentation which was in operation during the simulated service runs). Thus the Garrett computer model is well-keyed to the type of performance observed in the simulated service test. As has been mentioned above, however, the actual revenue service propulsion energy (2.82 kwh/car-mile) was significantly lower. Therefore, the computer model does not accurately predict actual energy consumption in revenue service. Undoubtedly the accuracy of the model would be improved by adding constraints to each segment of the simulated run to reflect the maximum speed level actually attained in revenue service operations.

Duty cycle tests

This portion of the Energy Storage propulsion system evaluation consisted of a series of tests run on the NYCTA Sea Beach test track to determine the dependence of energy saving capabilities upon such variables as car loading, station spacing, top speed between stations, and station dwell time. For each combination of the parameters, a series of starts and stops was made for a distance of approximately 19

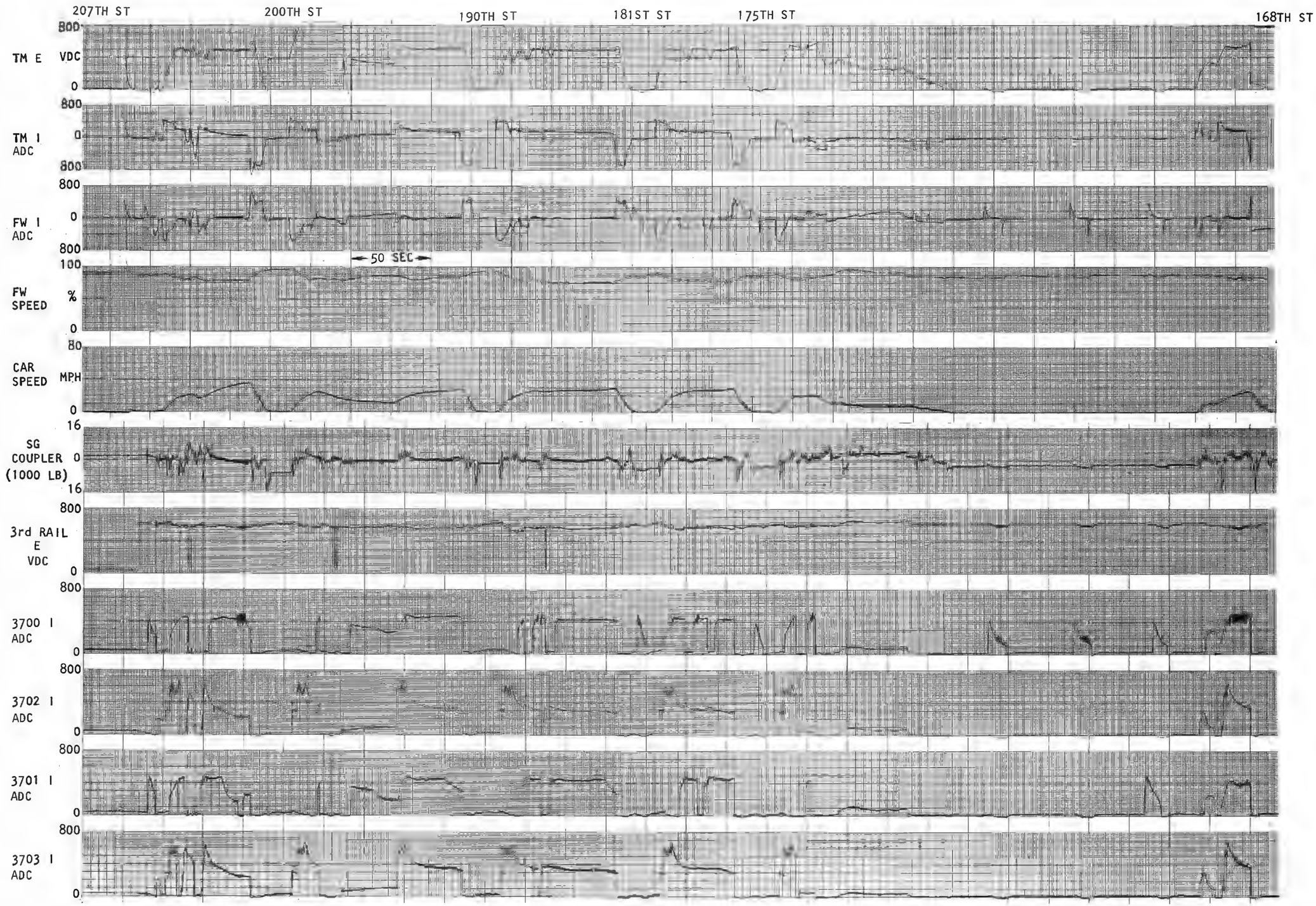

Figure 8. A-Line Simulated Service, Sheet 1 of 14

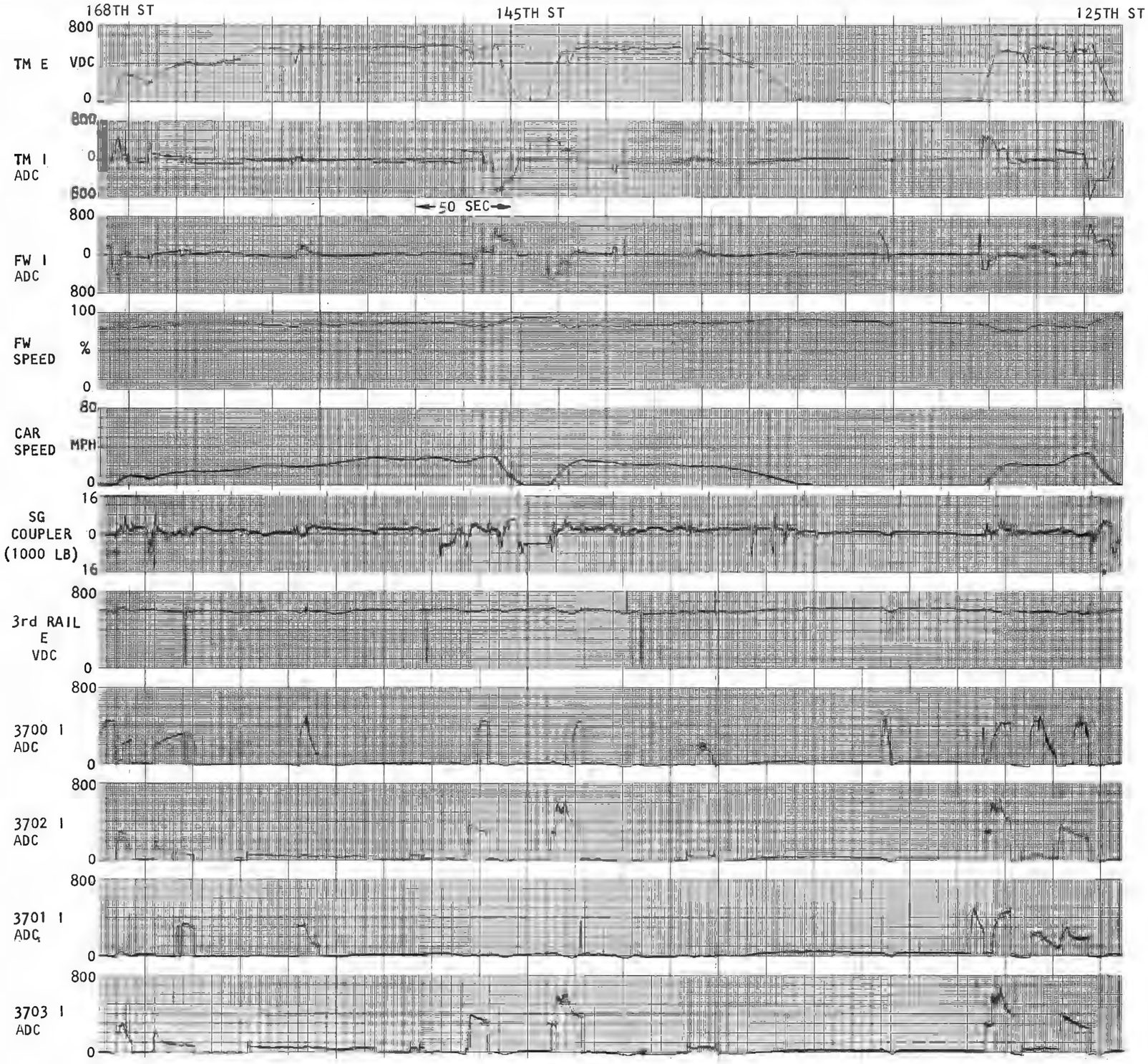

Figure 8 Continued, Sheet 2 of 14

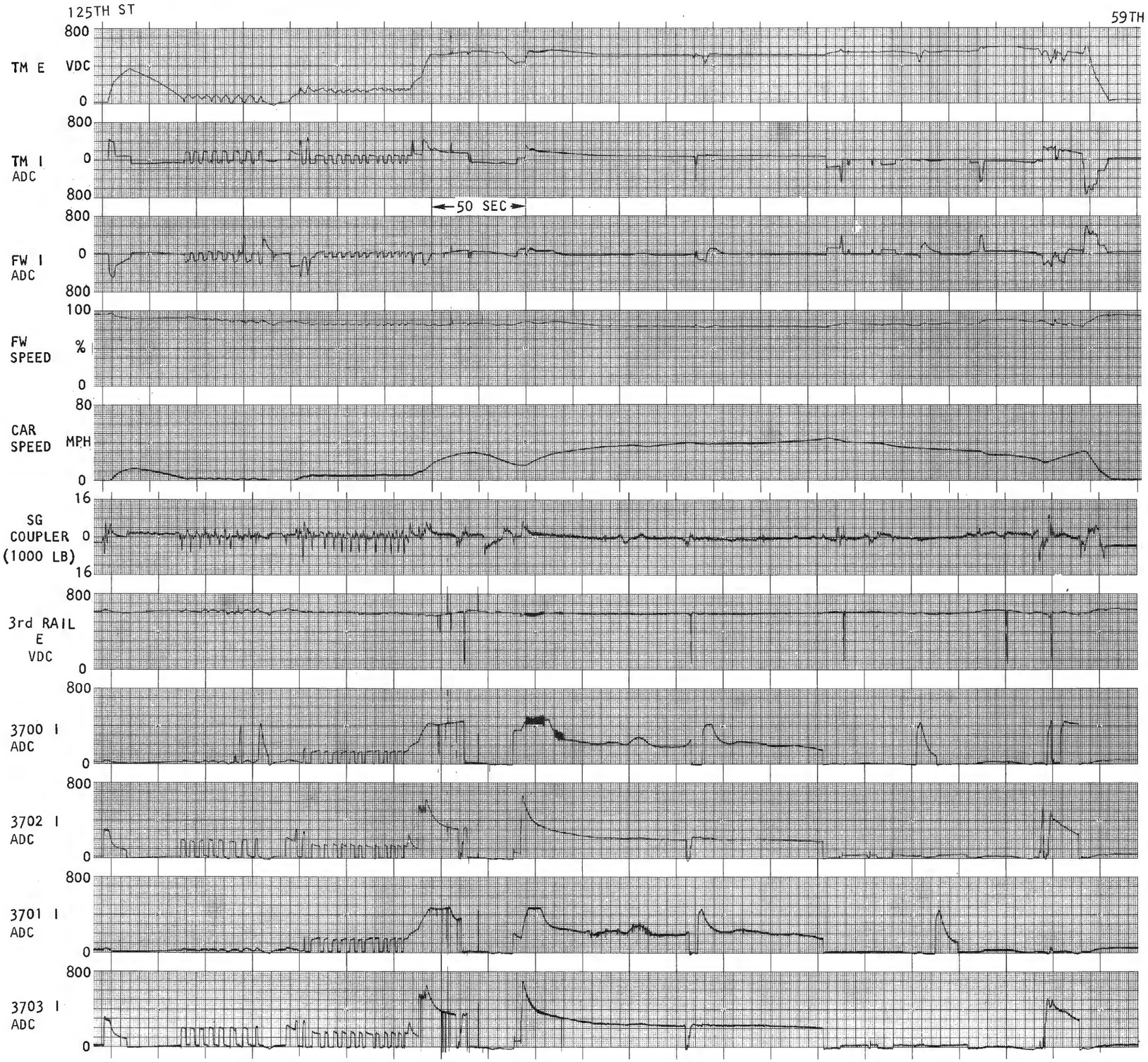

Figure 8 Continued, Sheet 3 of 14

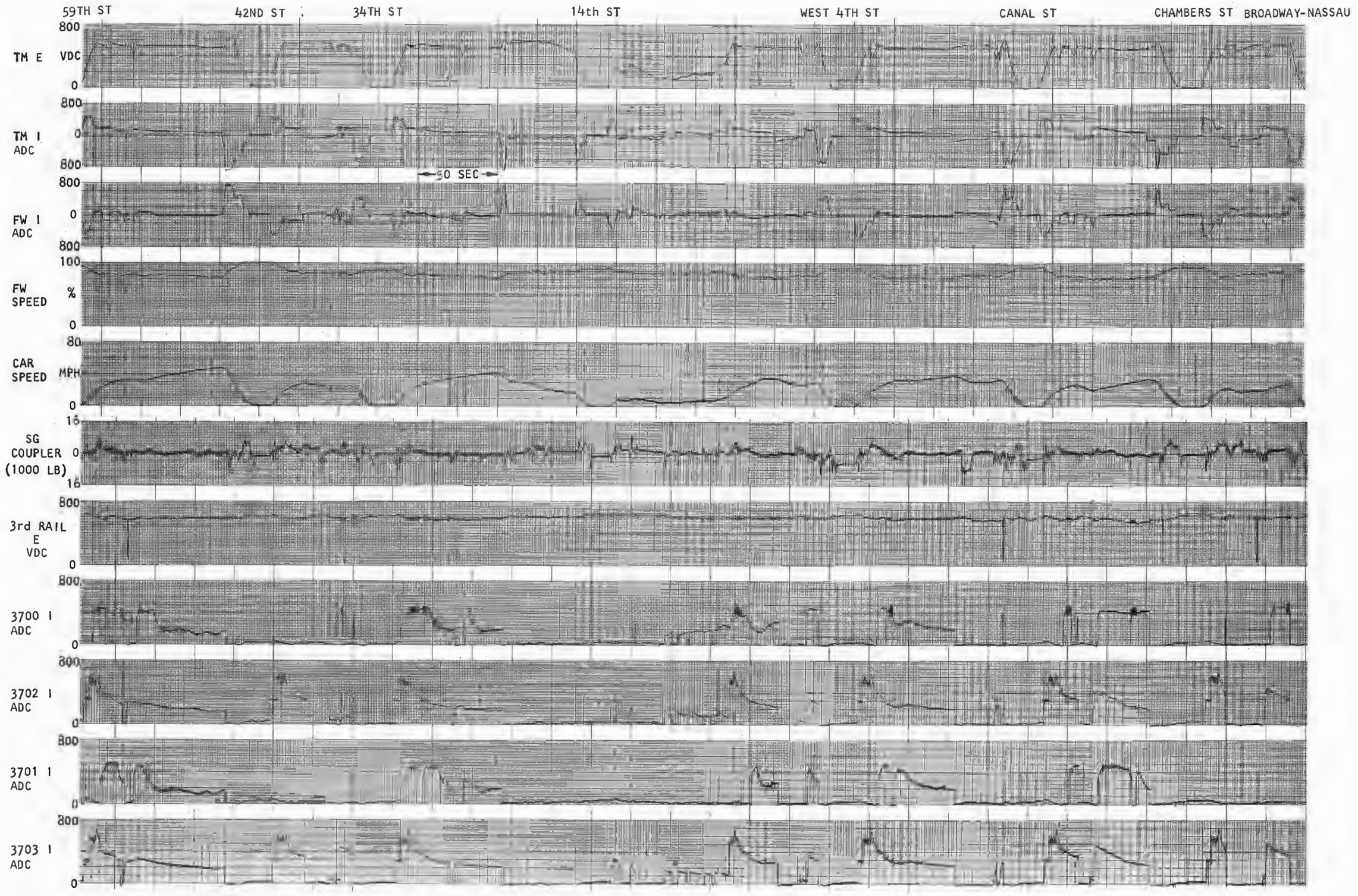

Figure 8 Continued, Sheet 4 of 14

BROADWAY-NASSAU HIGH ST JAY ST.-BORO HALL HOYT-SCHERMERHORN STS. LAFAYETTE AVE. CLINTON-WASHINGTON AVES. FRANKLIN AVE NORSTRAND AVE. KINGSTON AVE

TM E VDC 800 0

TM I ADC 800 0 800

FW I ADC 800 0 800

50 SEC

FW SPEED % 100 0

CAR SPEED MPH 80 0

SG COUPLER (1000 LB) 16 0 15

3rd RAIL E VDC 800 0

3700 I ADC 800 0

3702 I ADC 800 0

3701 I ADC 800 0

3703 I ADC 800 0

Figure 8 Continued, Sheet 5 of 14

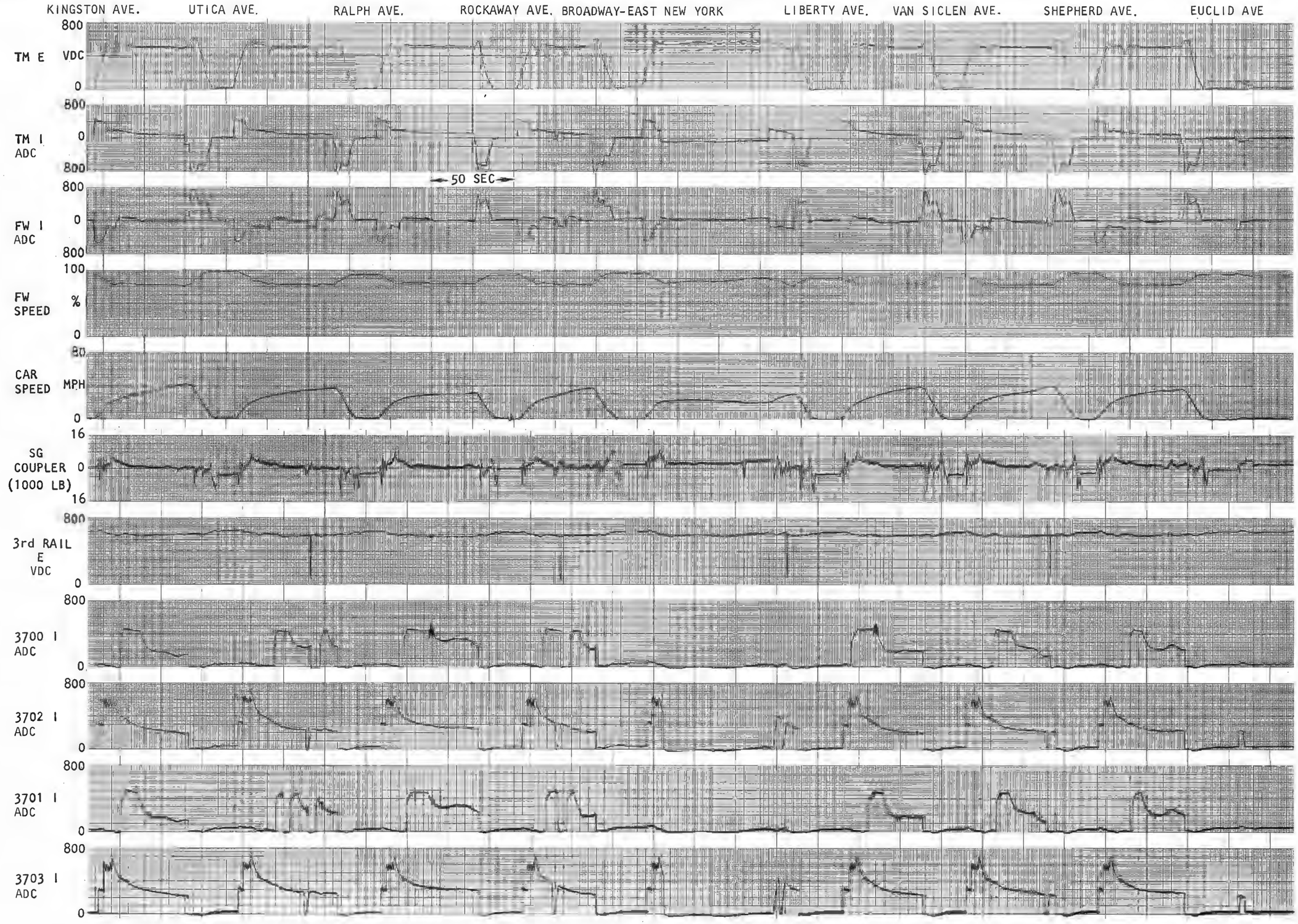

Figure 8 Continued, Sheet 6 of 14

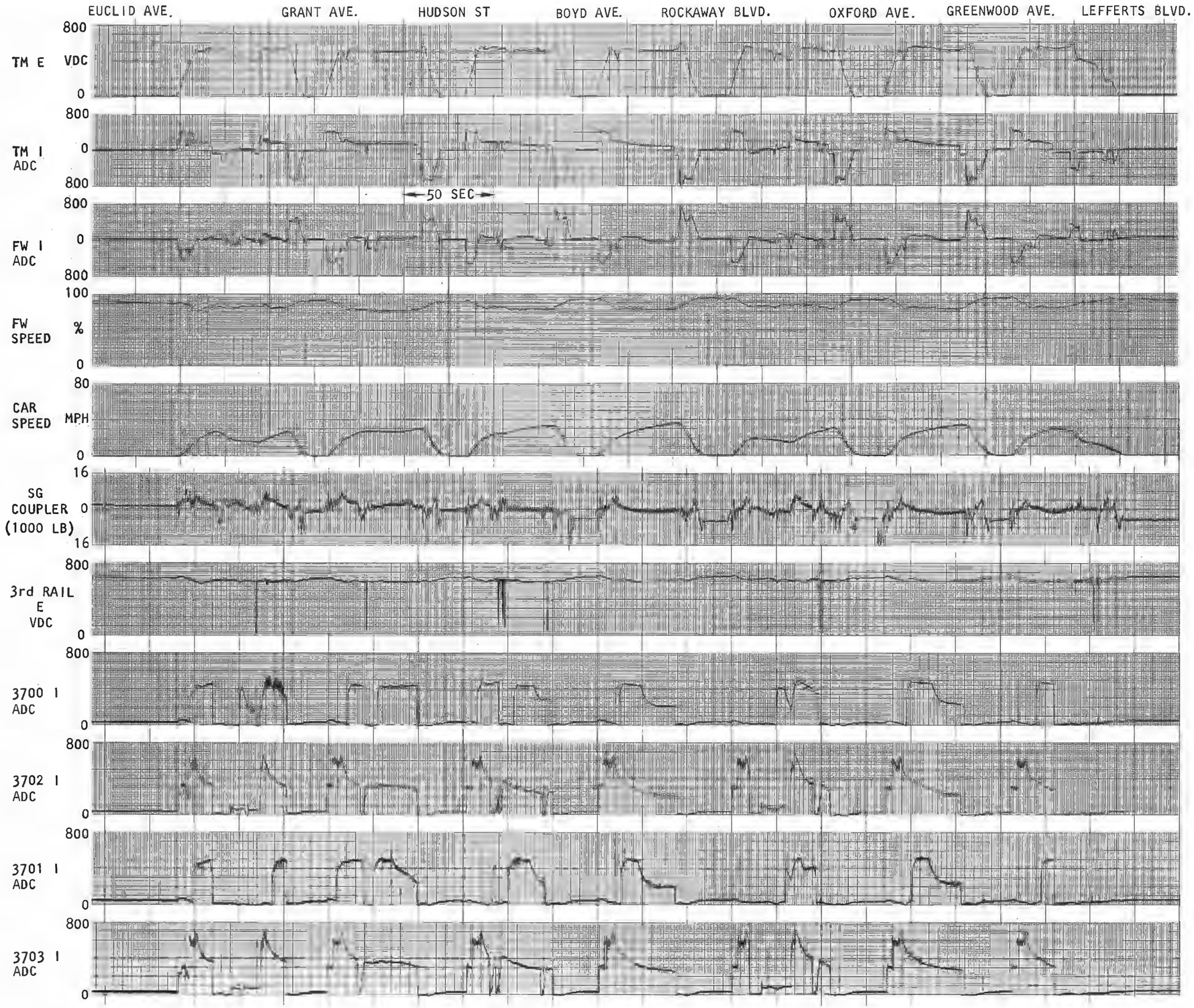

Figure 8 Continued, Sheet 7 of 14

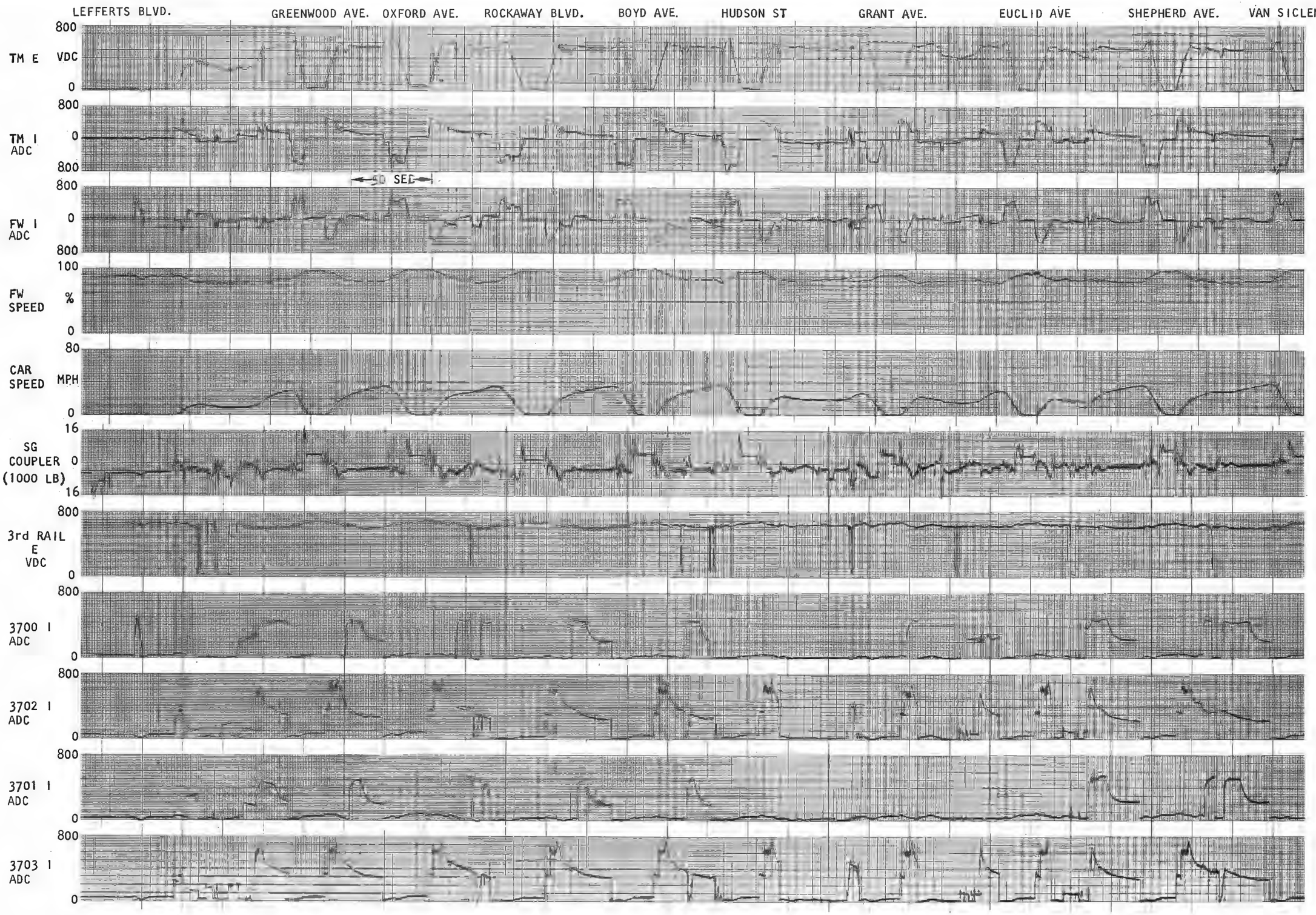

Figure 8 Continued, Sheet 8 of 14

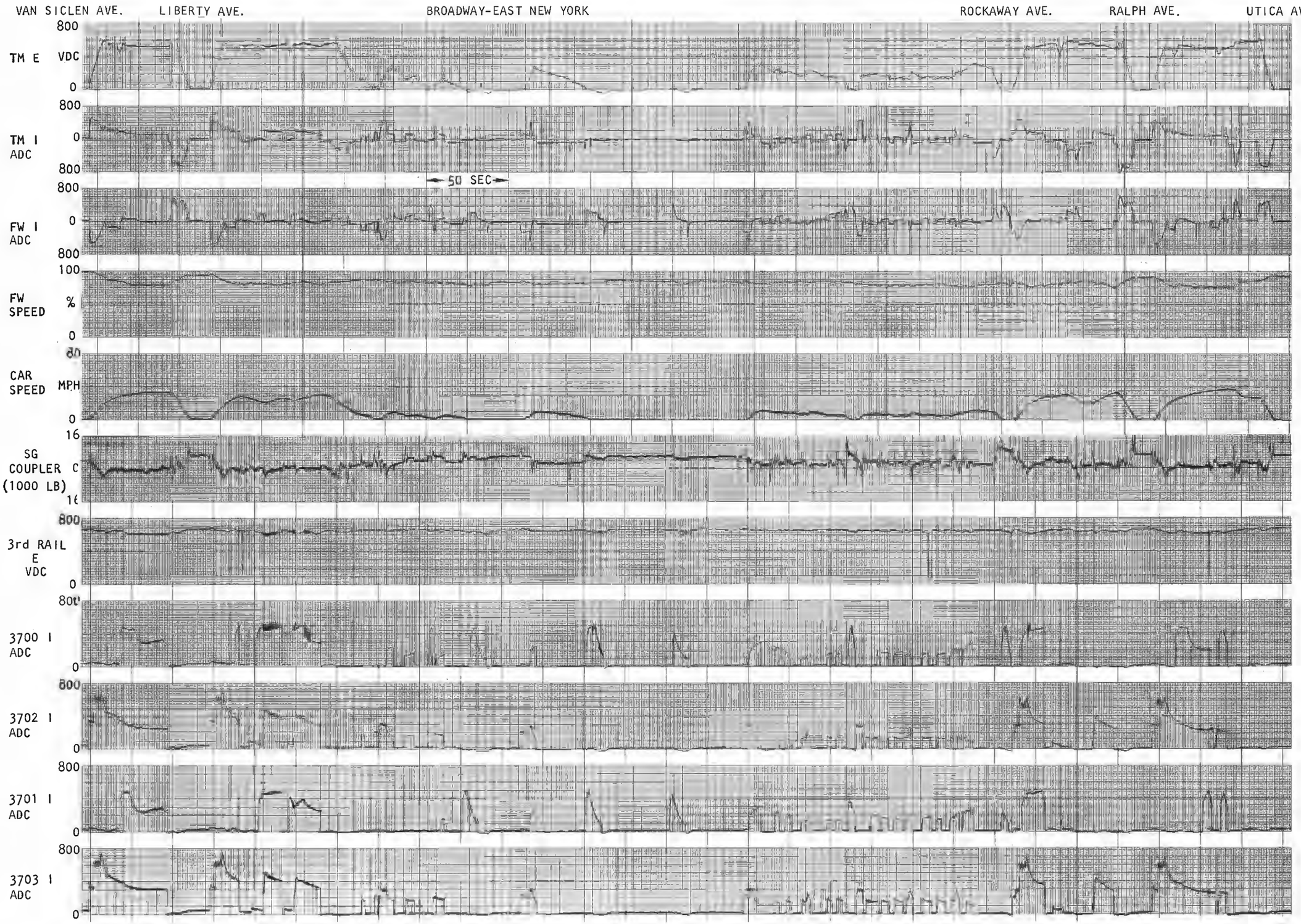

Figure 8 Continued, Sheet 9 of 14

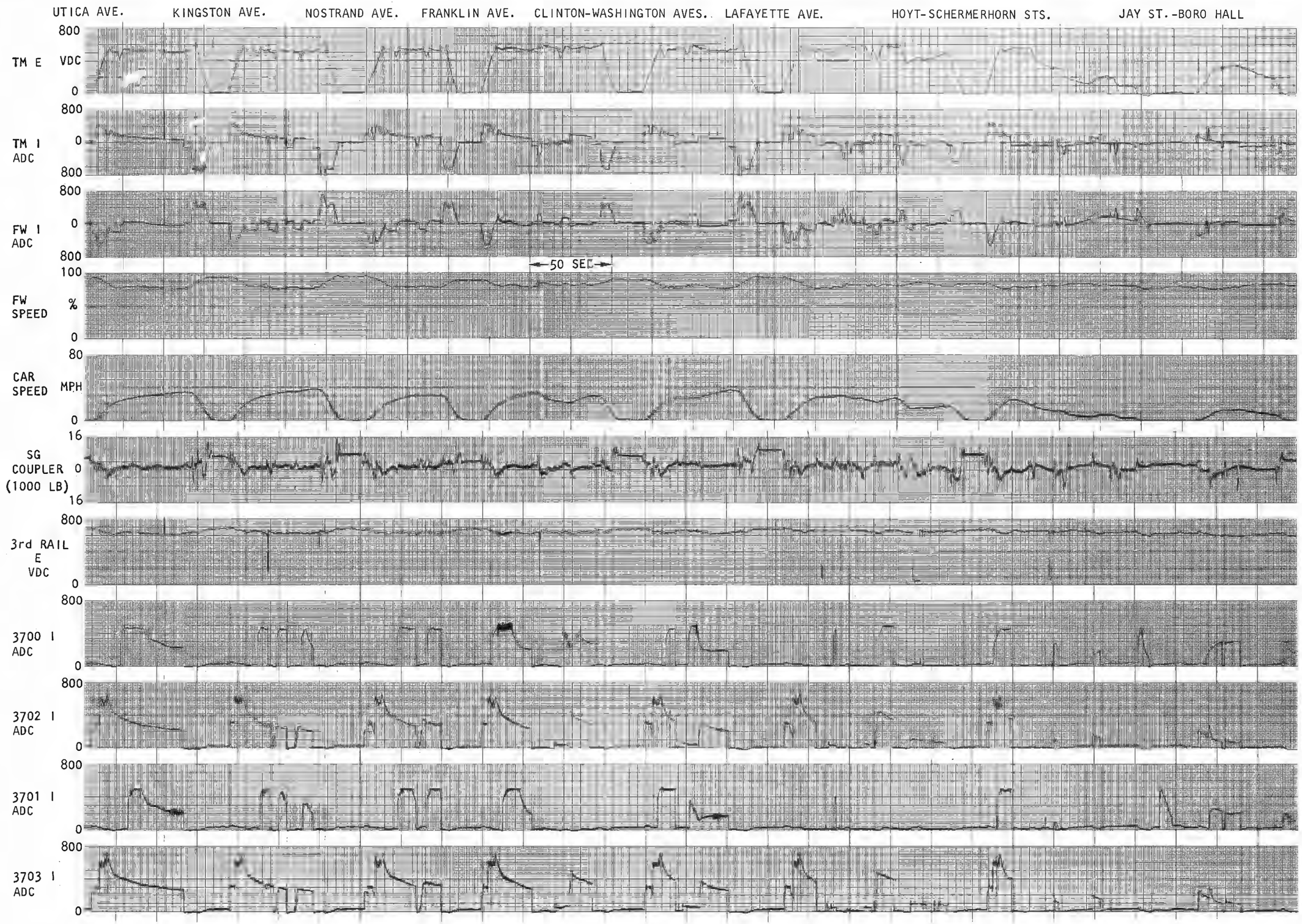

Figure 8 Continued, Sheet 10 of 14

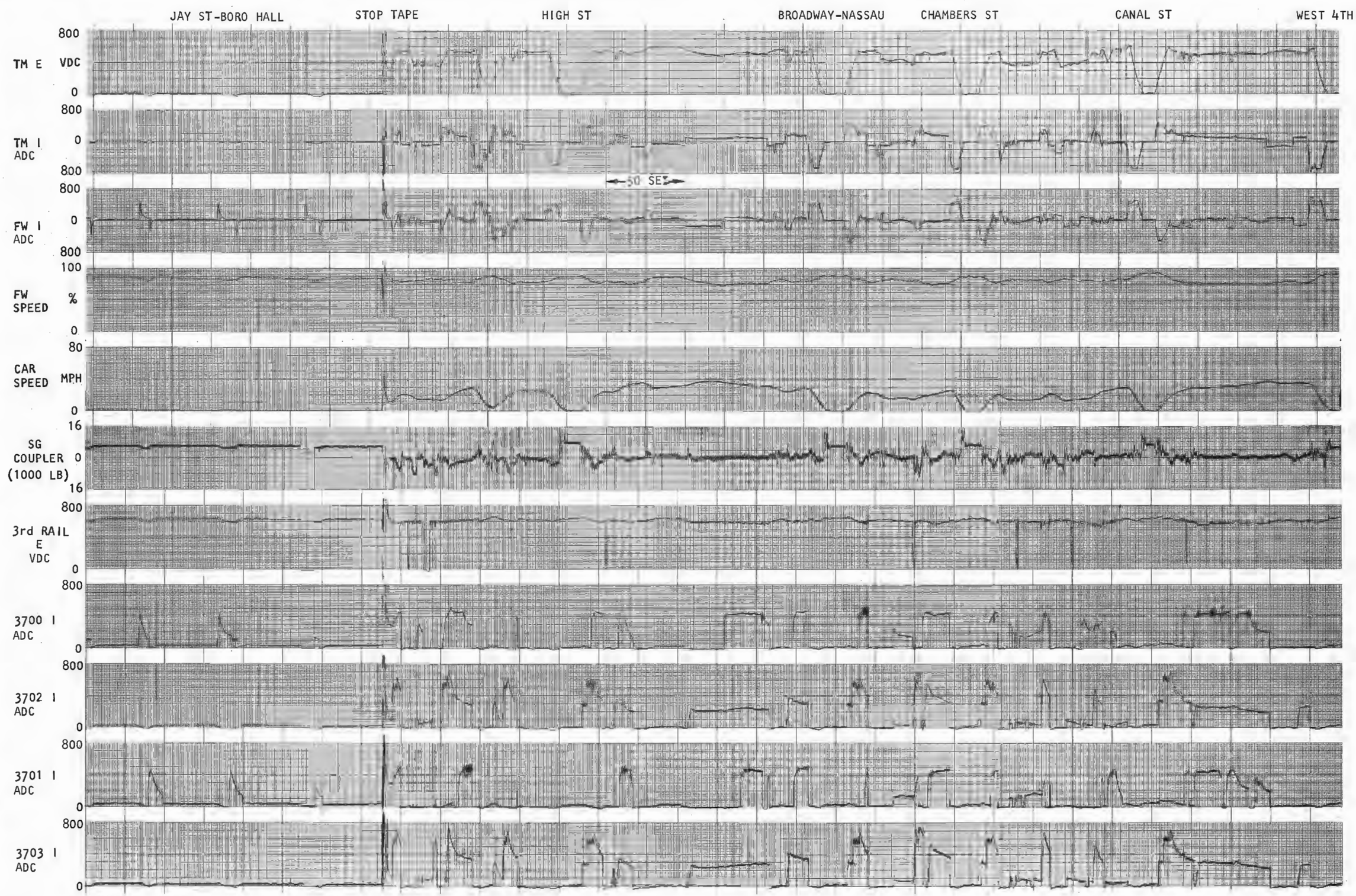

Figure 8 Continued, Sheet 11 of 14

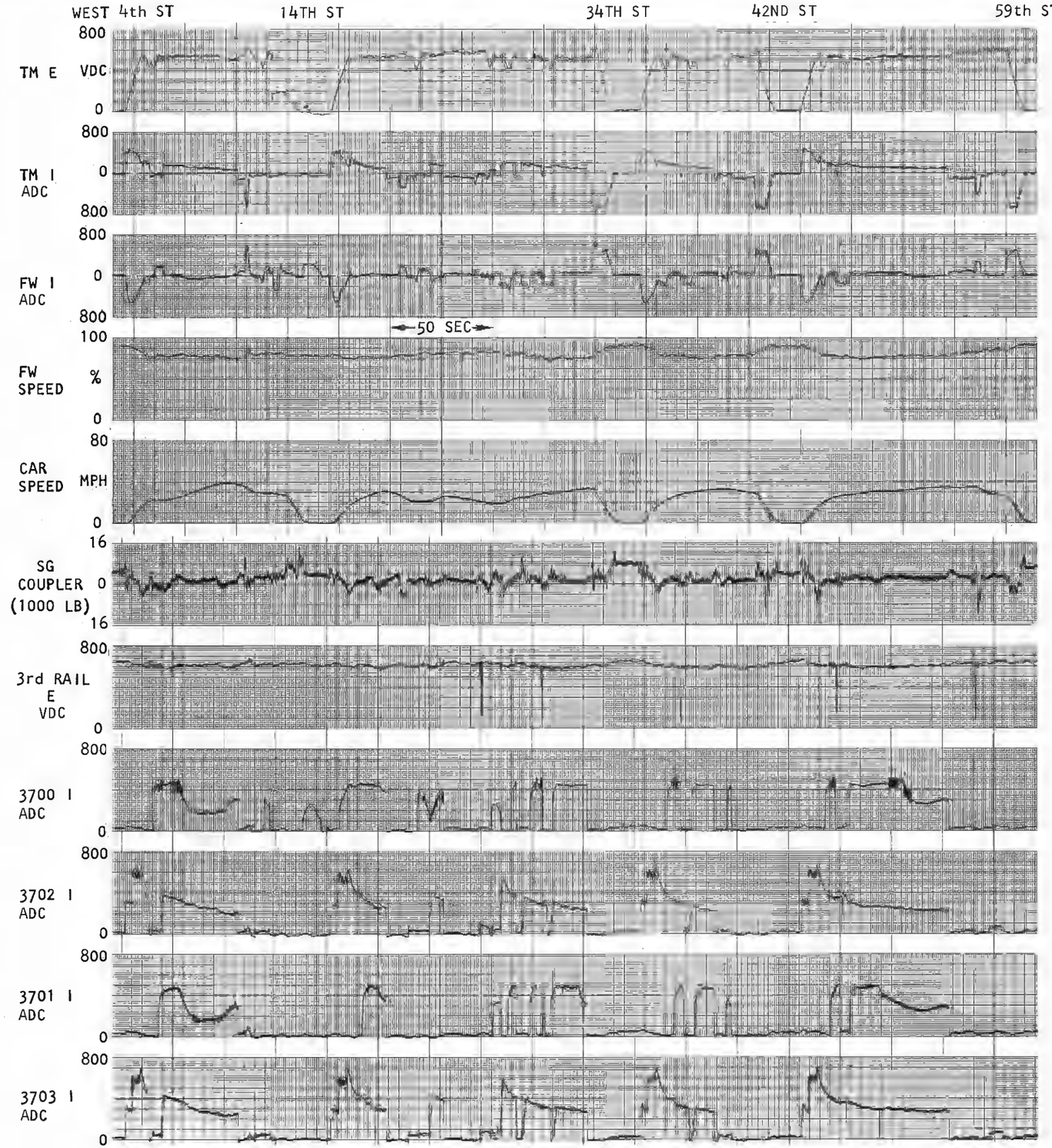

Figure 8 Continued, Sheet 12 of 14

miles. The profile of the Sea Beach track over which these tests were run is provided in Appendix A.

The mode of operation of the four-car train was to command full acceleration (up to the prescribed maximum speed, if any) and then apply full service braking to stop at the appointed distance markers. While this mode of operation may not be completely representative of the normal operation on the New York subway system (and the subsequent discussion will indicate that there is a lack of correspondence), it is the only mode which is easily reproduced from run to run. This makes it possible to compare the energy consumption for various combinations of the parameters, which was of primary importance. The consistency and repeatability can be seen in the tabulation of the duty cycle data (Tables 13 and 14, on next page) by noting the agreement between standard car energy consumption measurements for runs varying only in station dwell time (which variation has no effect on standard car propulsion energy consumption).

Selected data from Tables 13 and 14 are plotted in Figures 9 through 12. One of the most interesting observations which can be made from Figures 11 and 12 is that for a series of stops at a given spacing there appears to be a speed which gives a minimum in energy consumption for the ES cars. This is quite different from the behavior of the standard cam controlled equipment, whose energy continually increases with speed until a maximum achievable speed is attained.

Another noteable result is the fact that the *percentage* energy saving by the ES propulsion system is essentially independent of car loading, as shown in Table 15. The explanation of this observation follows from the fact that the flywheels are able to store additional braking energy for a more heavily-loaded car. This added stored energy is in approximate proportion with the additional energy required to accelerate the heavy car.

The information listed in Table 16 is of more widespread interest. At each of the stop spacings listed, the energy consumption *for either type of car* rose by approximately 16% when the car was crush loaded. Note, however, that this increase is much less than the fractional increase in car weight. Thus one can make a general conclusion that propulsion energy consumption increases only approximately one-quarter to one-third of one percent for each one percent increase in car weight.

Using the lines fitted to the data in Figure 9 and 10, one could, in principle, make general predictions of energy consumption for the two types of propulsion equipment. One simply needs to divide a given route into individual station spacing segments and read from the appropriate graph the energy that is consumed in traversing each segment. Unfortunately, this method does not appear to give accurate predictions for actual operations on the New York City Transit System, for reasons which have been discussed earlier.

Calculations based on this method are demonstrated in Table 17. For the AA and N lines two calculations were performed: one using the 45 MPH duty cycle curves and one using the 30 MPH curves. It can be seen that the actual revenue service measurements fall in-between the 45 MPH and 30 MPH calculations. This latter fact is consistent with the previously-stated observation that scheduled performance on the New York subway system is generally somewhat less than the maximum of car capability — a fact that is, in turn, consistent with prudent scheduling for reliable operations.

Samples of the performance charts for the Duty Cycle Testing are given in Figures 13 and 14.

TABLE 15
Comparison of energy savings at empty and crush loading

Stop Spacing	% energy saving* empty	crush
2000 ft	35.0%	35.2%
2440 (N average)	34.8	34.9
3000	33.9	32.3
5000	28.2	24.2

*45 MPH maximum speed, 30 second stops

TABLE 16
Increase in energy consumption with car load

Stop spacing	Ratio of crush-load energy to empty-load energy* Standard	ES
2000 ft	1.18	1.18
2440 (N average)	1.15	1.15
3000	1.14	1.16
5000	1.13	1.20
Ratio of crush weight to empty car weight:	1.60	1.51

*45 MPH maximum speed

TABLE 13
Duty cycle tests—Empty Weight

Station spacing (ft)	Speed limit (MPH)	Dwell time (sec)	No. stops	Total distance (miles)	Total time (min.)	Propulsion Energy Consumed kwh/pair St'd	kwh/pair ES	kwh/car-mile St'd	kwh/car-mile ES	kwh/car-stop St'd	kwh/car-stop ES	% reduction
2000	15	30	50	18.9	99.4	126.0	175.4	3.33	4.63	1.26	1.75	−39.2
	20	15	48	18.2	72.2	135.4	128.0	3.72	3.52	1.41	1.33	5.5
		30	50	18.9	83.7	136.4	145.1	3.60	3.83	1.36	1.45	−6.4
	30	17.4	50	18.9	60.3	202.5	137.7	5.35	3.64	2.03	1.38	32.0
		30	48	18.2	67.4	185.6	135.1	4.90	3.57	1.86	1.35	27.2
	45	17.4	50	18.9	58.0	247.8	157.4	6.54	4.16	2.48	1.57	36.5
		30	50	18.9	67.8	251.3	163.3	6.63	4.31	2.51	1.63	35.0
3000	15	30	30	17.0	81.2	100.9	148.5	2.96	4.35	1.68	2.48	−47.2
	20	30	30	17.0	67.0	109.7	119.5	3.22	3.51	1.83	1.99	−8.9
	30	19	30	17.0	47.3	138.9	107.3	4.07	3.15	2.32	1.79	22.8
		30	30	17.0	52.7	138.9	112.4	4.07	3.30	3.23	1.87	19.0
	45	19	30	17.0	43.5	190.8	123.6	5.60	3.63	3.18	2.06	35.2
		30	30	17.0	48.9	193.1	127.7	5.66	3.75	3.22	2.13	33.9
5000	30	21	20	18.9	47.1	118.9	106.4	3.14	2.81	2.97	2.66	10.5
		30	20	18.9	50.1	119.8	110.6	3.16	2.92	3.00	2.77	7.7
	45	21	20	18.9	40.2	173.1	125.3	4.57	3.31	4.33	3.13	27.6
		30	20	18.9	43.0	178.2	127.9	4.70	3.38	4.46	3.20	28.2
N-line segment	30	18	40	18.6	54.8	164.2	126.0	4.41	3.39	2.05	1.58	23.3
		30	40	18.6	62.4	164.4	129.8	4.42	3.49	2.06	1.62	21.1
	45	17	40	18.6	51.6	229.0	136.7	6.16	3.67	2.86	1.71	40.3
		30	40	18.6	60.3	229.9	150.2	6.18	4.03	2.87	1.88	34.8

TABLE 14
Duty cycle tests—crush-loaded cars (21 tons added weight)

Station spacing (ft)	Speed limit (MPH)	Dwell time (sec)	No. stops	Total distance (miles)	Total time (min.)	Propulsion Energy Consumed kwh/pair St'd	kwh/pair ES	kwh/car-mile St'd	kwh/car-mile ES	kwh/car-stop St'd	kwh/car-stop ES	% reduction
2000	15	30	48	18.2	96.4	127.6	199.2	3.51	5.48	1.33	2.08	−56.1
	20	30	48	18.2	82.0	169.1	158.4	4.65	4.36	1.76	1.65	6.3
	30	17	48	18.2	59.6	249.3	161.6	6.86	4.44	2.60	1.68	35.2
		30	48	18.2	68.8	248.8	164.9	6.84	4.53	2.59	1.72	33.7
	45	17	48	18.2	59.0	283.8	183.3	7.81	5.04	2.96	1.91	35.4
		30	48	18.2	68.2	284.4	184.3	7.82	5.07	2.96	1.92	35.2
3000	15	30	32	18.2	87.6	125.7	164.7	3.46	4.53	1.96	2.57	−31.0
	20	30	32	18.2	72.0	137.2	143.7	3.77	3.95	2.14	2.25	−4.7
	30	18	32	18.2	53.0	183.8	138.0	5.06	3.80	2.87	2.16	24.9
		30	32	18.2	60.7	178.5	143.6	4.90	3.95	2.79	2.24	19.6
	45	18	32	18.2	49.5	236.4	156.5	6.50	4.30	3.69	2.45	33.8
		30	32	18.2	55.3	234.5	158.7	6.45	4.36	3.66	2.48	32.3
5000	30	21	20	18.9	49.7	152.2	124.1	4.02	3.28	3.81	3.10	18.5
		30	20	18.9	51.7	151.7	128.8	4.00	3.40	3.79	3.22	15.1
	45	21	20	18.9	44.8	209.2	149.5	5.53	3.96	5.23	3.74	28.5
		30	20	18.9	48.7	202.3	153.4	5.34	4.05	5.06	3.84	24.2
N-line segment	30	17.4	40	18.4	56.2	211.4	144.4	5.74	3.92	2.64	1.81	31.7
		30	40	18.4	66.1	227.2	159.1	6.17	4.32	2.84	1.99	30.0
	45	17.4	40	18.4	54.4	258.4	167.0	7.02	4.45	3.23	2.09	35.4
		30	40	18.4	62.1	264.8	172.4	7.20	4.68	3.31	2.16	34.9

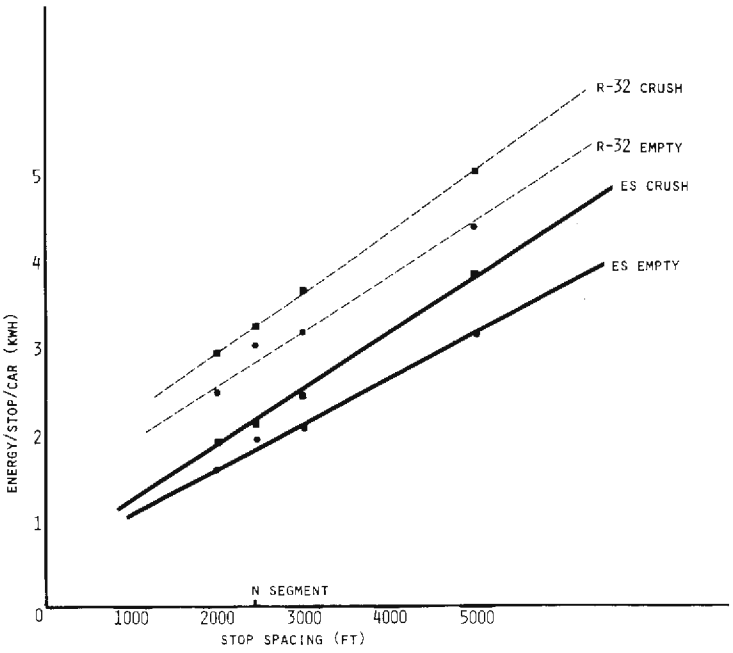

Figure 9. Duty Cycle Test: Energy per Stop vs. Stop Spacing (maximum speed)

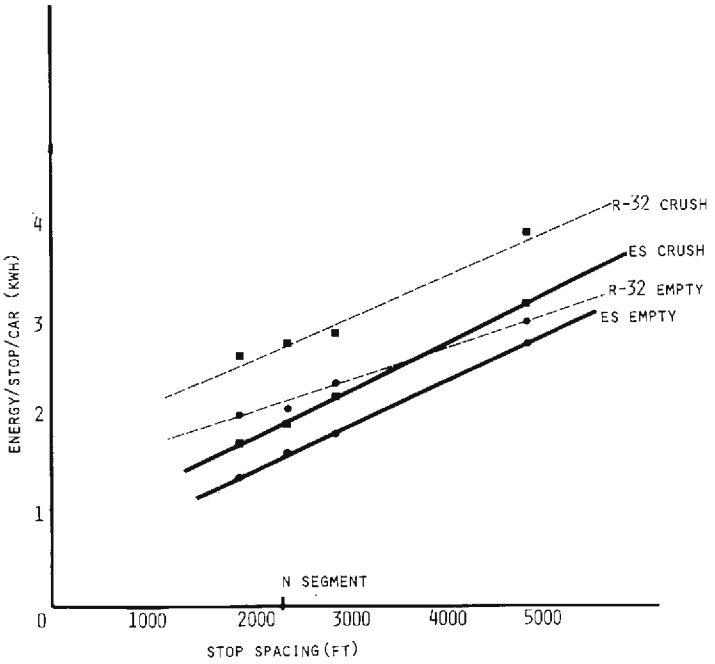

Figure 10. Duty Cycle Test: Energy per Stop vs. Stop Spacing (30 MPH)

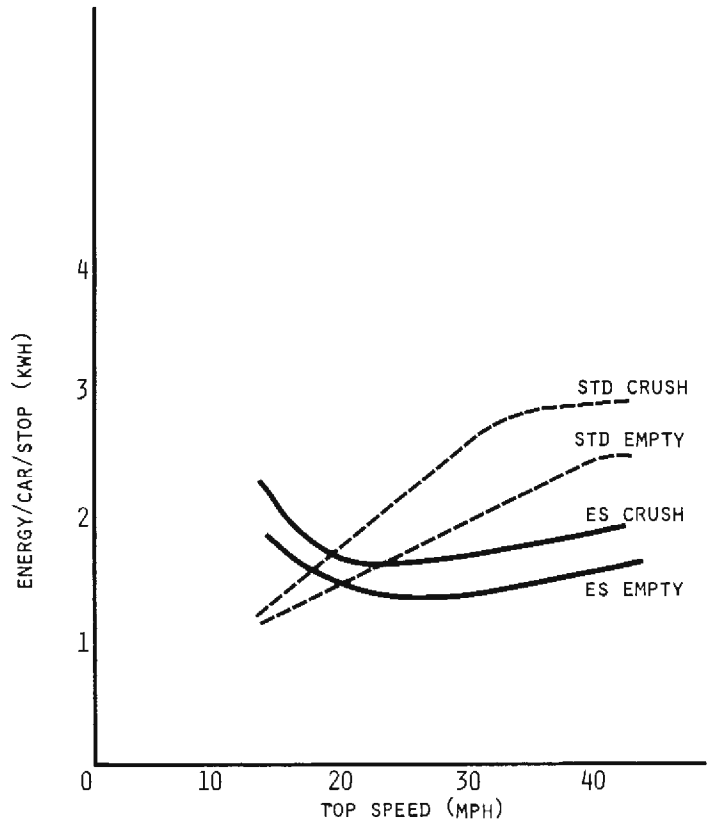

Figure 11. Energy per Stop vs. Top Speed (2000 ft. interval)

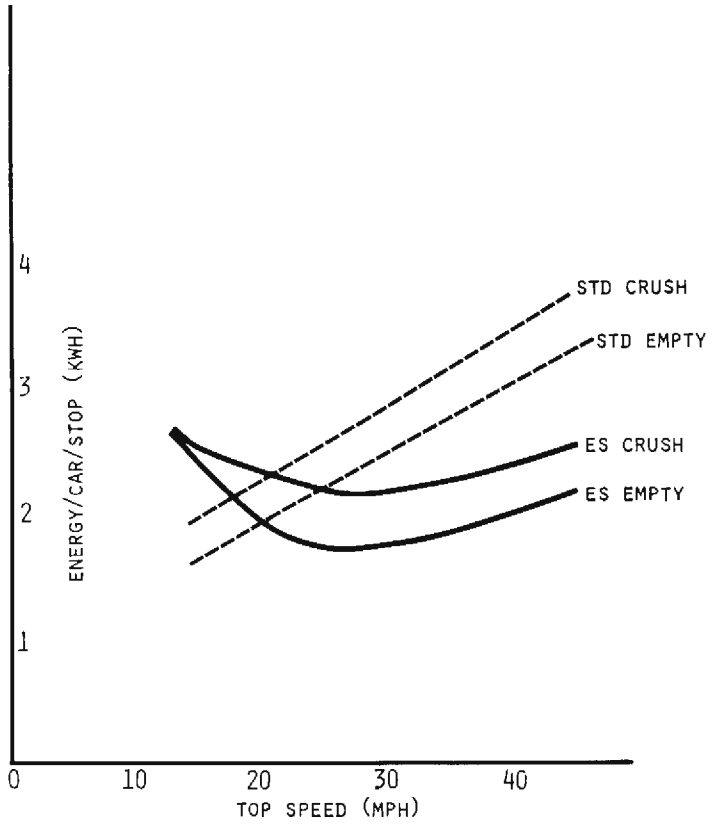

Figure 12. Energy per Stop vs. Top Speed (3000 ft. interval)

TABLE 17
Calculations of propulsion energy using duty cycle data

	One-way propulsion energy/car (kwh)								
	Duty cycle calculation			Simulated Service			Revenue Service		
Line	St'd	ES	%	St'd	ES	%	St'd	ES	%
A (Local)	125.7	86.5	31.2	109.5	76.9	29.8	103.2	66.4	35.7
AA (45 MPH)	61.3	38.9	36.5	57.3	35.4	38.1	51.8	31.0	27.9
(30 MPH)	46.2	31.7	31.4						
N (45 MPH)	71.5	51.9	27.4	68.6	51.0	25.6	59.2	47.6	19.8
(30 MPH)	47.5	42.6	10.3						

Parasitic loads on propulsion system

1. Layover energy use

The ES cars' controls were configured such that when the cars reach a terminal there would be only two possible modes of operation for the flywheels. The usual mode is one in which the flywheel speed is maintained at a constant speed of 70% of maximum. The alternative to speed maintaining is to cause the unit to shutdown by generating electrical energy which is dissipated in resistors (as in the conventional "dynamic" braking). This mode is called a quick shutdown (QSD) and reduces the flywheel speed from 82% of maximum to 10% in 6.6 minutes (an average discharge rate of 19.3 Kw/unit). The QSD circuitry was built-in to the control system as a part of the protective systems to shut down the ESU's as rapidly as possible in the event of a fault signal (See Figures 33 and 34).

It will be noted immediately that there was no provision made for a free coasting mode for the ESU's. As a result, the normal operation of the system had the flywheel speed maintained at 70% of full speed during all terminal lay-overs. This caused an unnecessary usage of energy during these periods, as has been discussed above and as detailed in Table 18. By the time in the test program that the magnitude of the effect of the ESU losses was established, it was no longer feasible to make the modifications to the controls to provide an ESU coasting mode.

In an effort to make detailed quantitative evaluations of these losses, the steady-state energy consumption of the ESU's was measured directly as a function of flywheel speed by forcing the units to maintain a set of fixed speeds for 10-minute periods and recording the input energy from the third rail. These data are plotted in Figure 15.

The alternative to this control configuration would have been to allow the ESU's to coast freely as soon as the train arrived at a terminal and to accelerate the units back up to train start-up speed (82% of maximum) just prior to departure for the next trip. In order to evaluate the energy-effectiveness of such a configuration, measurements were made for the free coast-down speed-time relationship for each ESU (Figure 16) and of the energy required to accelerate the ESU up to speed (Figure 17). The information on these curves can be combined to determine the amount of energy which would be used under that configuration for different layover periods, by finding the speed to which the ESU's RPM falls in a given time on Figure 16 and then determining the energy required to restore the speed on Figure 17. The result of this determination is shown on Figure 18, where the energy consumed in the 70% speed maintaining configuration is portrayed for comparison. The difference between the curves in Figure 18 is plotted in Figure 19, to show directly the energy savings resulting from the automatic coast mode configuration, for varing layover durations.The slight energy penalty of the coasting mode for short layovers (less than 8-min) indicates that for short periods the electrical conversion losses in the re-acceleration of the ESU are greater than the steady state losses.

In order to make the estimated effect of this modification more explicit, an analysis of the operations of the test cars in revenue service on the A and the B & AA lines was performed, determining, with the use of Figure 19, for each terminal layover period how much additional energy would have been saved (or lost) by the incorporation of a coasting mode. It was found that the coasting mode would have reduced layover energy usage by 30% on the A line and by 34% on the B & AA lines. This prediction of the effect of the coasting modification is incorporated into Table 19. Note, as well, that the reconfiguring of the controls to allow coasting when not moving would reduce energy consumption during extended yard moves, for a further benefit.

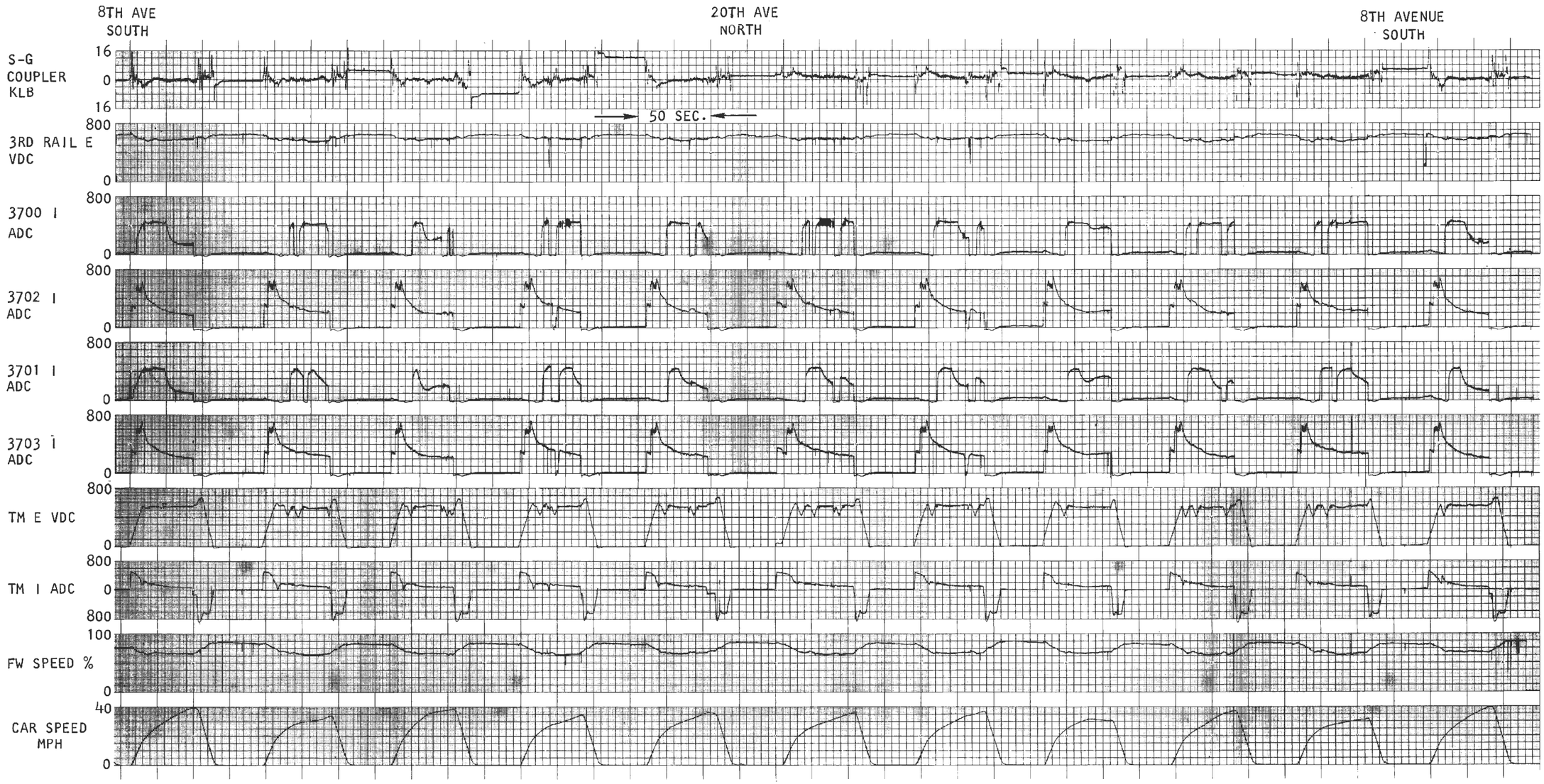

Figure 13A. 2000-ft Duty Cycle Tests (empty weight)

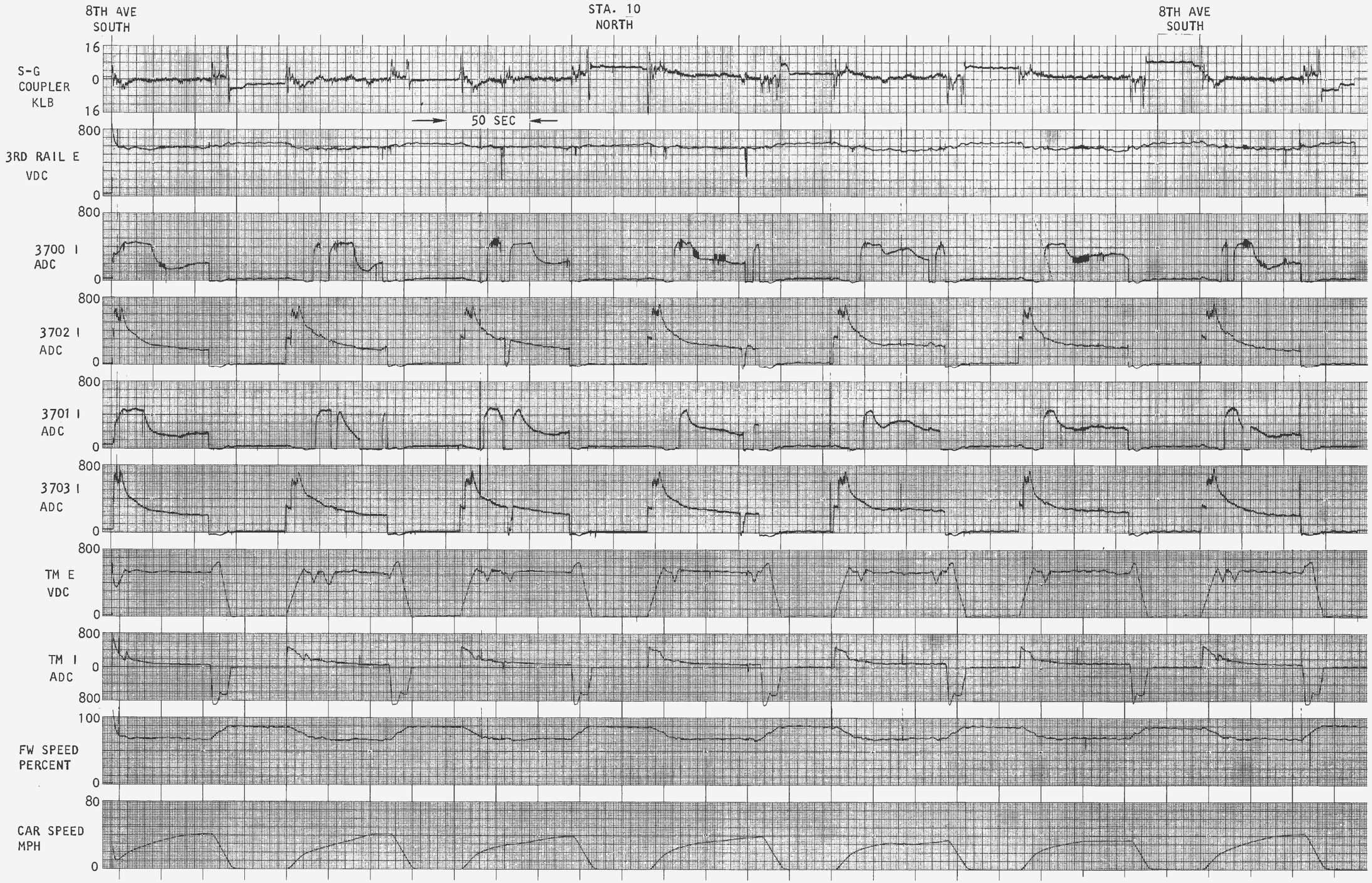

Figure 13B. 3000-ft Duty Cycle Tests (empty weight)

Figure 14A. 2000-ft Duty Cycle Tests (crush load)

S-11750

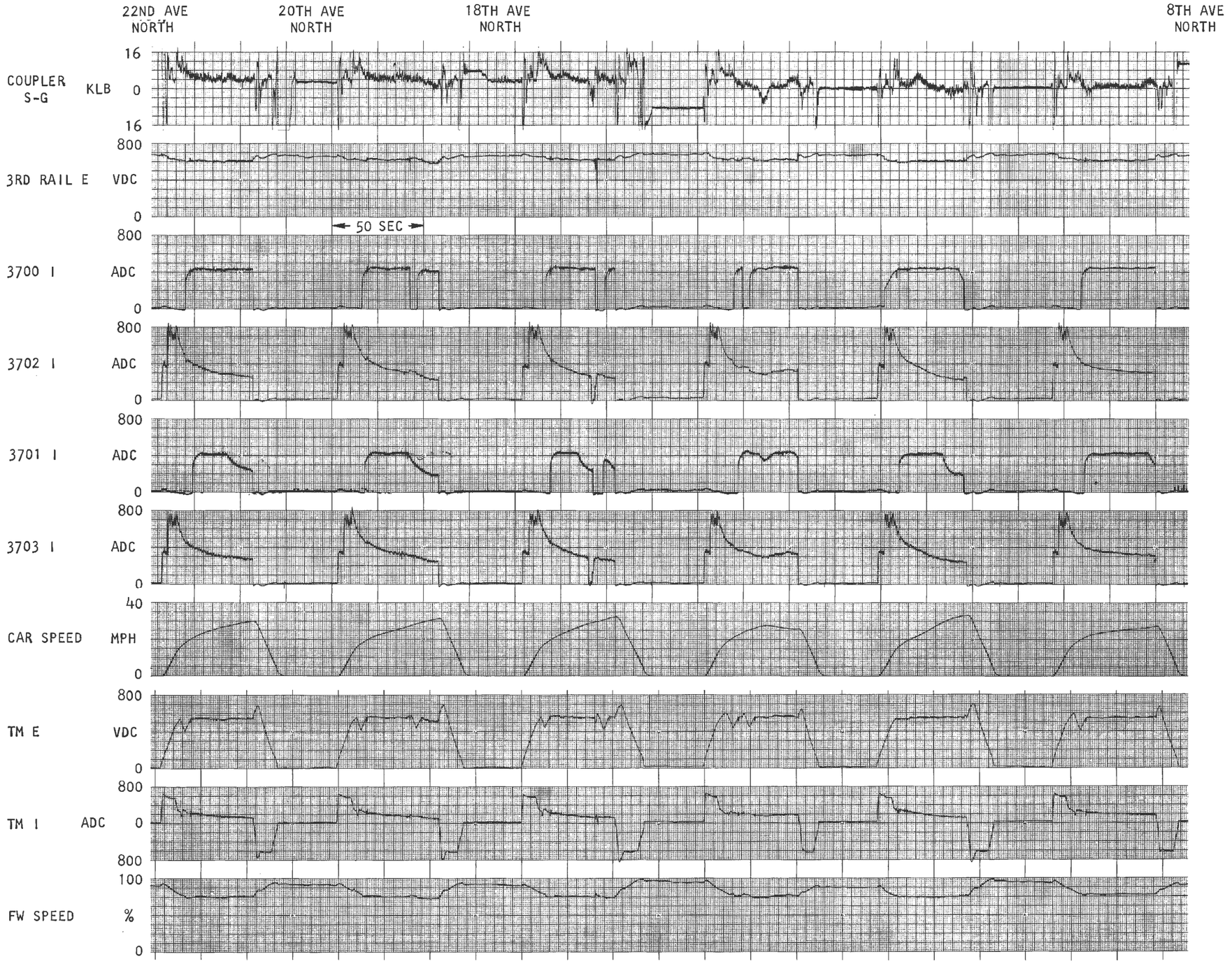

Figure 14A. Continued

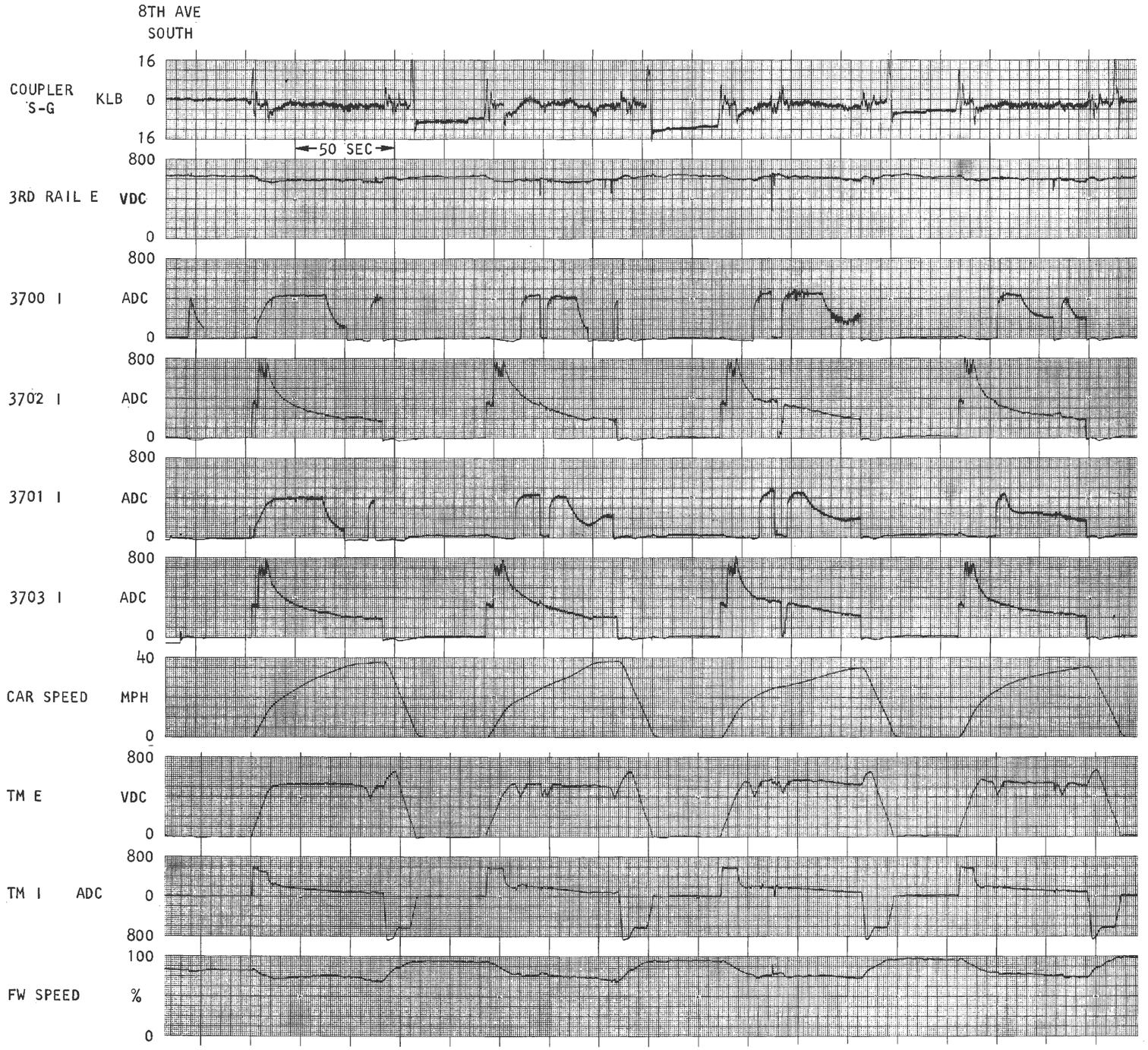

Figure 14B. 3000-ft Duty Cycle Tests (crush load)

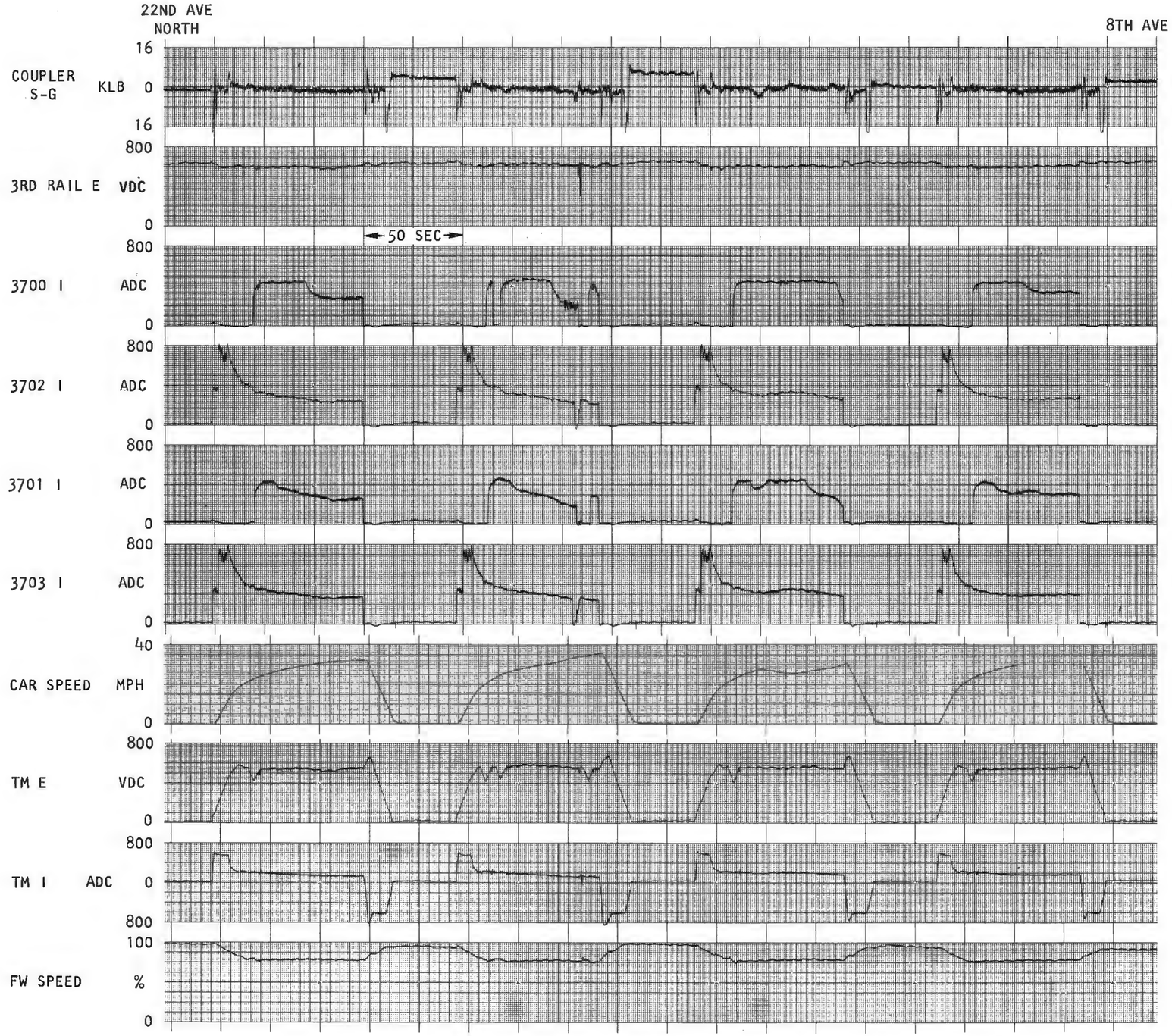

Figure 14B. Continued

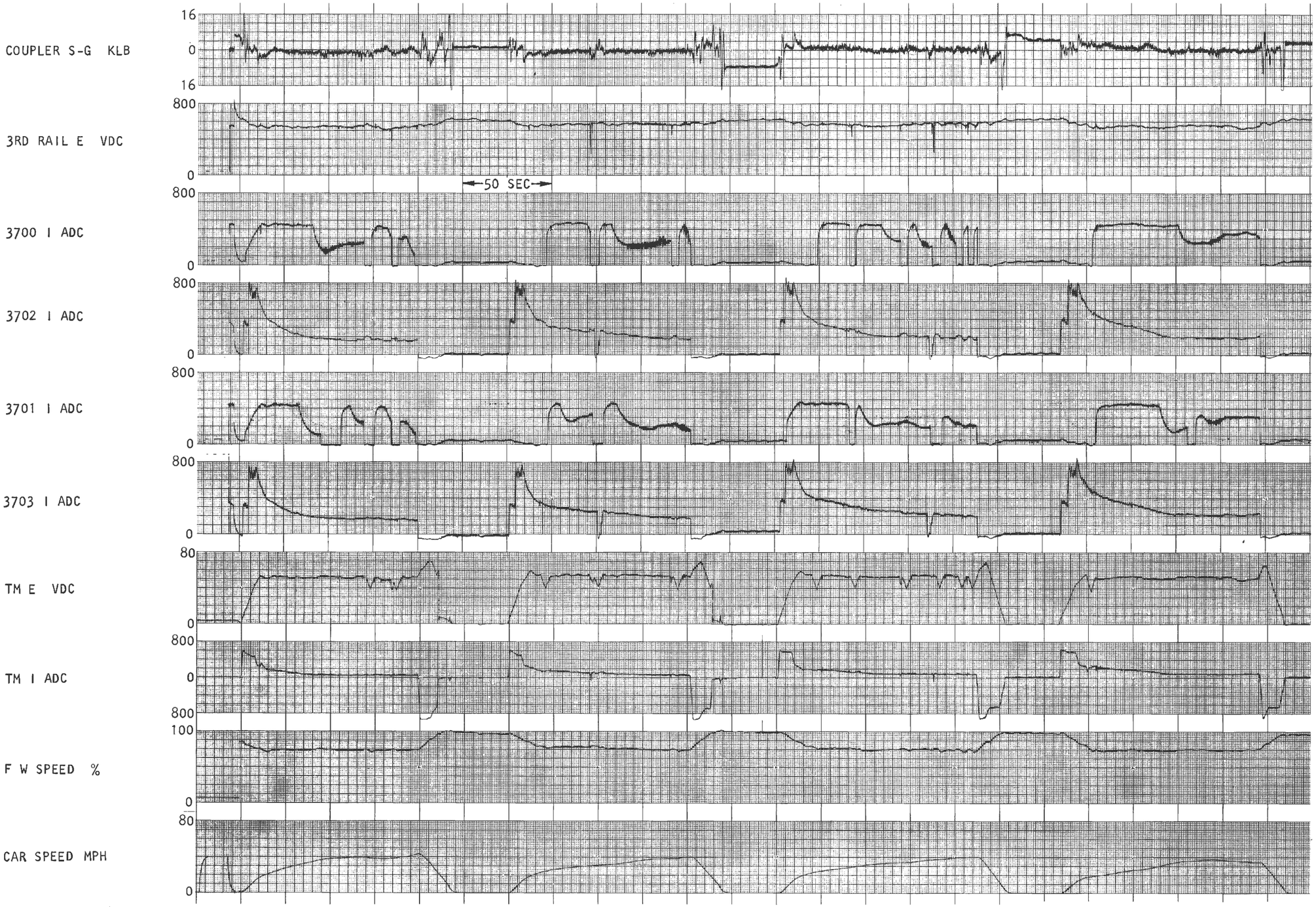

Figure 14C. 5000-ft Duty Cycle Tests (crush load)

Figure 14C. Continued

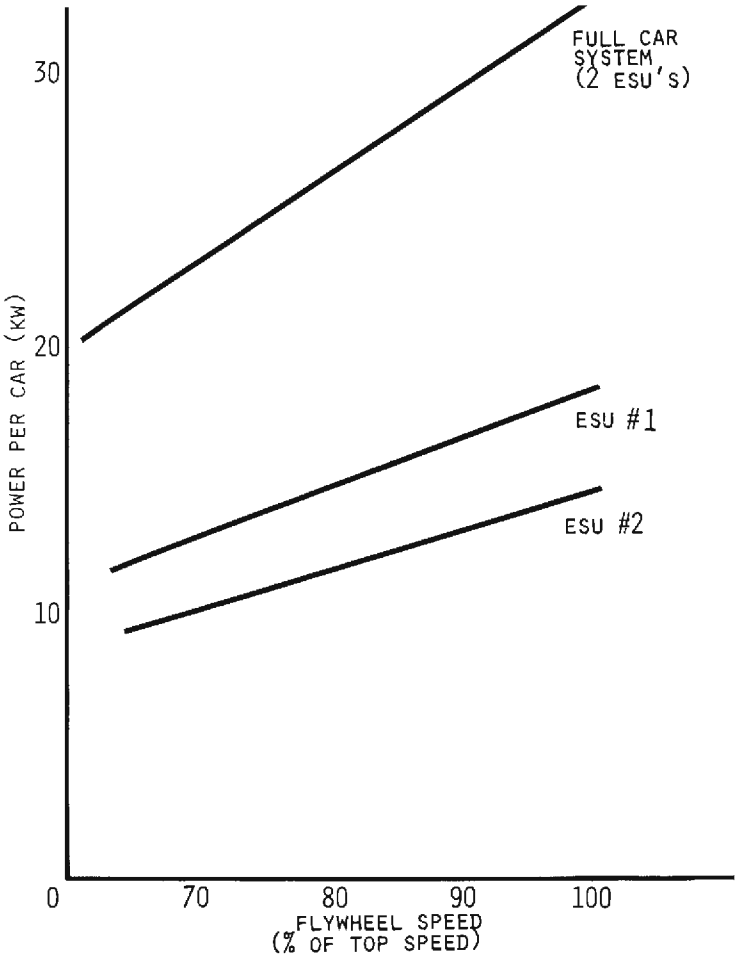

Figure 15. Steady-State ESU Losses at Constant Speed

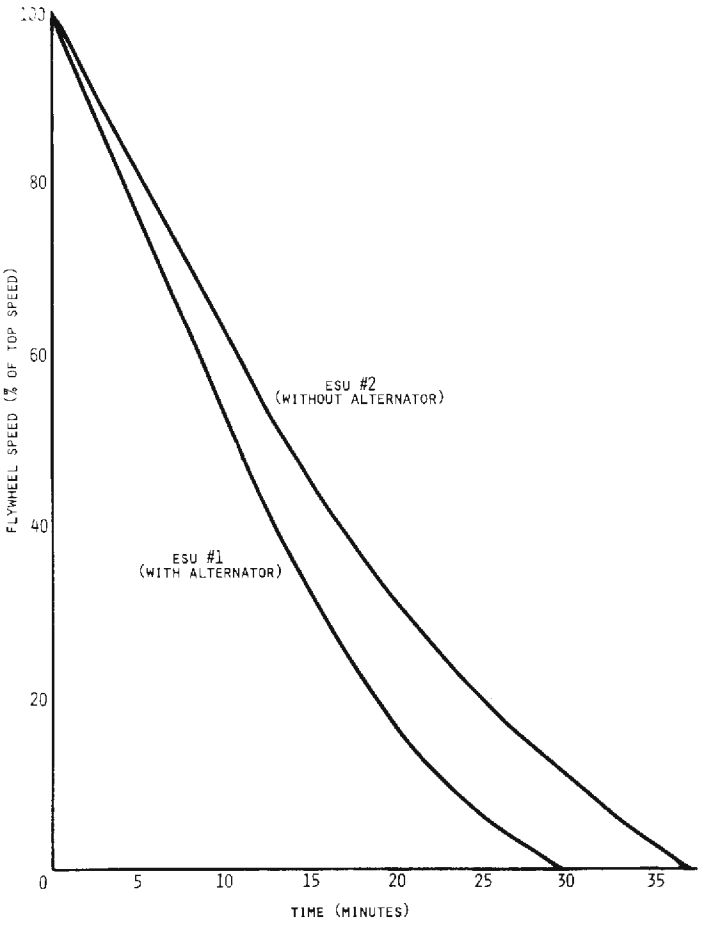

Figure 16. Free Coastdown of Energy Storage Units

TABLE 18
Layover energy consumption in revenue service (per car)

Line	Energy per car (kwh) ES	St'd	Difference	Total layover Minutes	Kwh/min	Average kw
A	508.8	1.7	507.1	1137	.45	26.8
B-AA	812.6	106.9	705.7	1697	.42	25.0
D	516.0	80.9	435.1	1173	.37	22.3
E	89.9	18.5	71.4	196	.36	21.7
N	718.6	4.8	713.8	1751	.41	28.1
RR	345.9	7.1	338.8	724	.47	28.1
			2771.9	6678	.42 AVG	24.9 AVG

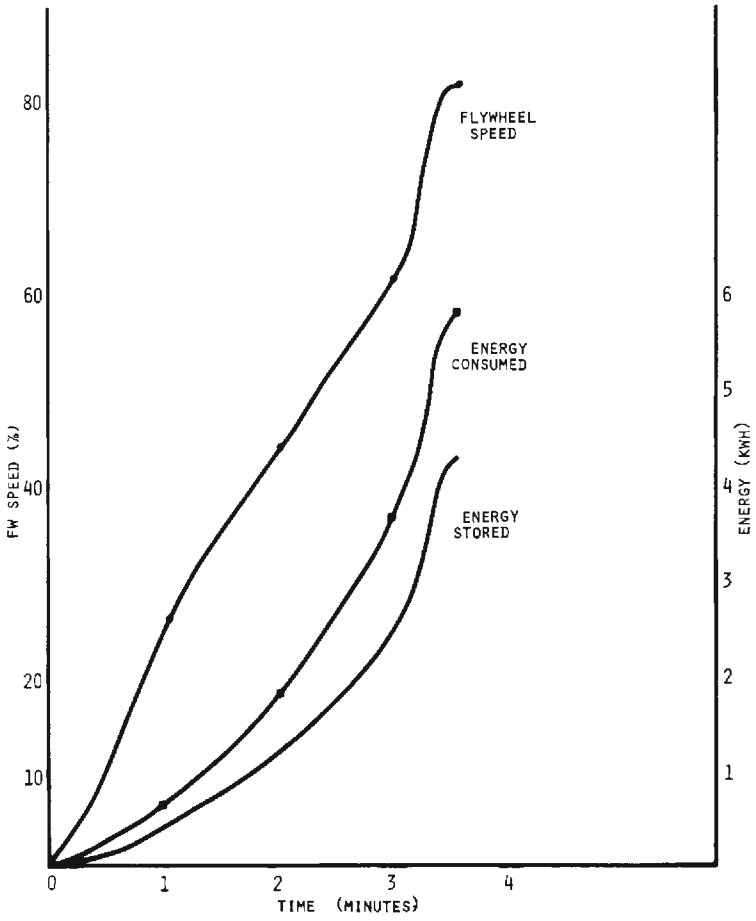

Figure 17. Start-Up of two ESU's (one carset)

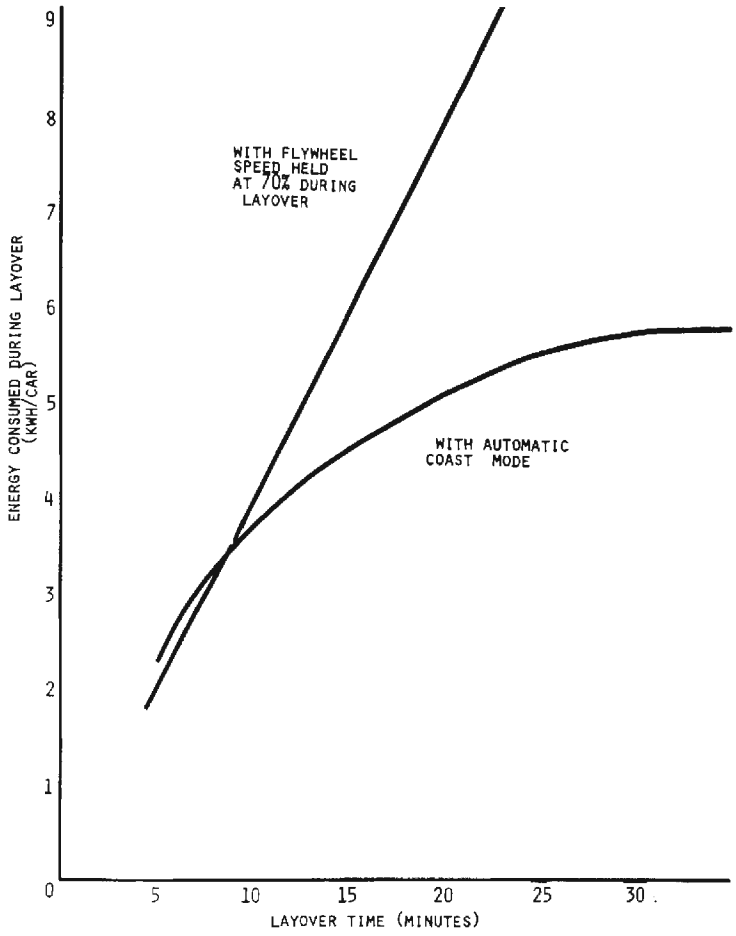

Figure 18. Comparison of Layovers in Coasting Mode vs. Speed Maintaining Mode

TABLE 19
Predicted effect of modifications to ES system to allow flywheel coasting during layover and to reduce ESU losses by 10%.

	Line	Measured overall energy saving per pair*	Added saving for coasting in layover	Further saving for 10% reduction of ESU losses	Total predicted saving
Energy saving expressed in Kwh per pair	A	3232.6	303.0	619.1	4154.7
	B & AA	2420.1	556.8	513.8	3490.7
Energy saving expressed as percentage of standard car propulsion energy	A	22.8	2.1	4.4	29.3
	B & AA	18.6	4.3	3.9	26.8

*from Table 5

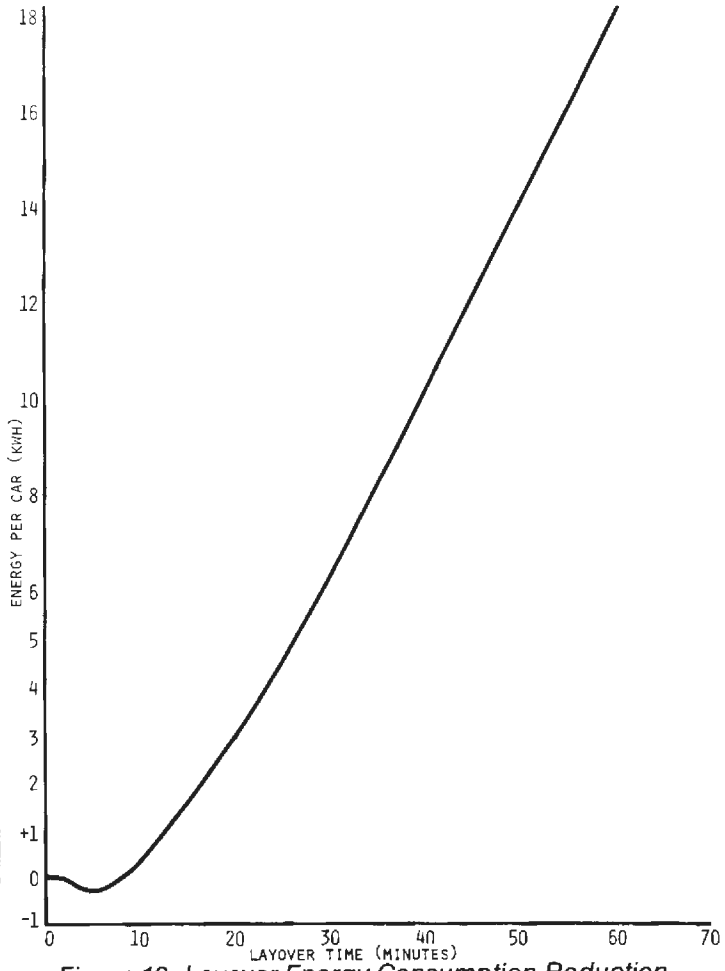

Figure 19. Layover Energy Consumption Reduction by Automatic Coast Mode

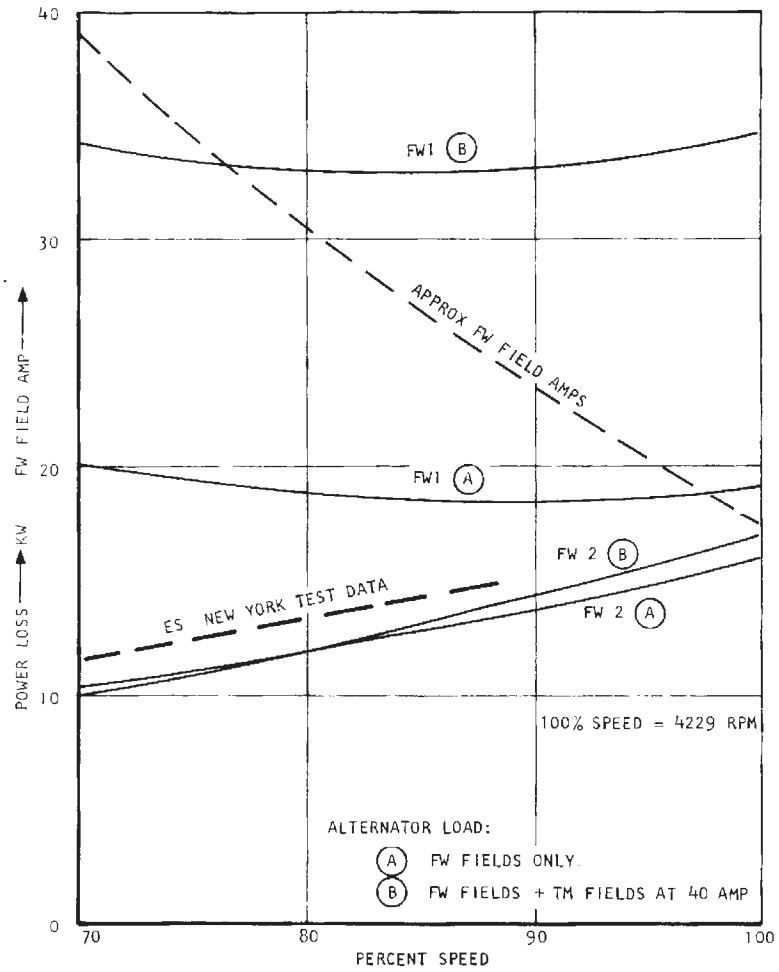

Figure 20. Steady-State Electrical Loads on ESU's

2. Operating losses in the ESU

As has been noted above, the unanticipated high level of losses in the ESU degraded the ES system's ability to produce net energy savings because the losses subtracted constantly from the savings while they were being obtained in service. An approximate breakdown of the losses within the ESU, as computed by Garrett in a simulation of A-line service, is given in Table 20. The range of losses and electrical loads on the ESU's throughout the 70-100% speed regime is shown in Figure 20.

An estimate of the impact of these losses on the measured energy effectiveness of the ES cars can be obtained by determining what would have been the reduction in ES car propulsion energy consumption if the ESU's had been redesigned to decrease the steady state losses by 10%. (In view of the very conservative nature of the design of the original ESU's, a 10% reduction in losses on future designs should be achievable with relative assurance.)

The potential significance of such an improvement can be approximated by taking 10% of the product of the number of hours in service by the average loss rate and by conservatively assuming the average loss rate to be equal to the energy consumption rate observed during terminal layover. (This is an underestimate of the losses since the actual losses in service would have been higher when the cars were in motion, with the average flywheel speeds generally greater than 70%.)

The predicted effects of the 10% ESU loss reduction for the 121.1 hrs of A-line operation and the 113.9 hrs of B & AA lines operation are shown in Table 19. It should be noted that the 10% loss reduction prediction has been adjusted downward appropriately so as to not count it twice, when it is combined with the flywheel coast modification.

Note in Table 19 that the combined effect of these two improvements would be to raise the energy savings on the B & AA service by 44% in magnitude.

3. Propulsion auxiliary loads

In addition to the normal auxiliaries on an R-32 car, including lights, heat, air compressor, M/G set and overhead fans, the ES cars had auxiliary loads associated with the propulsion equipment. These loads consisted of the power supply for the separately-excited traction motor and flywheel motor fields, the Electronic Control Unit (ECU), and equipment cooling fans. Furthermore there was temporary test instrumentation on car 3700 and a set of energy meters which remained on car 3700 during all testing, including the revenue service test.

All of these loads were supplied by the alternator (3

phase, 230V line to line) on the #1 ESU on each ES car. Thus the power used by these auxiliaries is included in the above compilations of ESU losses.

The AC power was used directly as input to the field power supplies (Figure 20). In addition the AC fed a transformer with one output rectified to 230 VDC and another rectified to 32 VDC, nominal. The 32 VDC supplied the ECU, which in turn produced ±15 VDC control power for the field power supplies. The 230 VDC powered an M-A set to provide 115 VAC, 60 Hz single phase for the cooling fans and for the instrumentation.

A compilation of all auxiliary loads (including the standard R-32 loads) is listed in Table 21.

It has been stated already that, with the exception of the present section, all of the energy measurements included in this report refer to propulsion loads, only. However, if it is needed, the total energy requirements for each car can be estimated, using the information presented in this section.

This is done by first combining the 600V auxiliary loads that would be carried by one car on an average day (half of the M/G load plus the lights plus 1 Kw for an approximate average compressor load per car plus 2.5 Kw to represent a year-round average for heat and fan usage). In this example, the total for the car auxiliaries would be 7.9 Kw. This average power can be converted to energy per mile by dividing by the schedule speed (approximately 18 MPH) to get *0.44 Kwh/car-mile*. This final number can be added to the propulsion energy data reported previously to estimate the total energy consumption of each type of car.

TABLE 20
Estimated breakdown of losses in ESU in revenue service (A-line)

Flywheels (windage, pumps, seals, bearings)		33.9%
Gear units		7.1
Flywheel motors		
fan and windage	16.7	
brush friction	11.7	
bearings and seals	1.6	
		30.0
Electrical losses		
copper	10.1	
iron	7.1	
fields	2.6	
brush drop	2.0	
stray losses	7.1	
		29.0
		100.0%

TABLE 21
Auxiliary loads (per car)

ESU loads		
230 VAC (3 phase):	**Amps**	**Kw**
Traction motor fields (approx)	40	14.5
Flywheel motor fields (100% speed)	17	3.0
(70% speed)	40	10.0
230 VDC (converted to 115 VAC, 60 Hz by M/A set):	**Amps at 240 VDC**	**Kw**
Chopper and capacitor cooling fans	4.5	1.1
Instrumentation (temporary)	6.1	1.5
Energy meters	0.5	0.1
32 VDC:	**Amps at 35.5 VDC**	**Kw**
Electronic control unit	14	0.5
Third rail loads		
	Amps at 600 VDC	**Kw**
Air compressor (odd car)	13.0*	7.8*
M/G, battery (even car)	5.9	3.5
Lights	4.4	2.6
Car heaters	8.0	4.8
Cab heaters	2.5	1.5
Fans, high	3.0	1.8
Fans, low	1.0	0.6

*intermittent

Starting grid energy consumption

When a conventional (cam controlled) transit car accelerates, the current flow from the third rail into the traction motors is limited initially by a set of resistances, called the starting grids, which are inserted in series with the motor. These resistances are removed by segments as the car accelerates and as the effective impedence (back emf) of the motors builds up. When the back emf has increased to a point where it is approximately equal to the third rail voltage, there is no longer a need for the current-limiting resistance and the last resistor element is taken out of the circuit.

Needless to say, the resistances dissipate electrical power when they are in the motor circuit. The Energy Storage propulsion system performs the identical current-limitation function in a "non-dissipative" manner by adjusting either the ESU or chopper output to match the traction motors' requirements at all times during an acceleration. It must be realized, however,

that no energy conversion can be completely non-dissipative. In fact, it is estimated that a straight chopper system consumes approximately 5% of its total propulsion output in the control circuitry components.

Because the basic energy measurements reported in the earlier sections of this report already include the effect on energy consumption due to the differences in control for the two pairs of cars, no further analysis of this matter is required. However, since several claims have been made in favor of choppers due to their "non-dissipative" acceleration control, it was decided to evaluate this category of energy consumption separately.

The evaluation was performed in two manners, first as a part of the Duty Cycle Tests and second as a part of the Revenue Service Tests. For both sets of measurements, the same energy consumption meters were used as had been used for all other tests. However, the inputs were changed so that one meter read the total propulsion energy for one standard car, while the other meter recorded only the energy that was consumed in that car's starting grids. The energy metering circuits are described in detail in Appendix B.

In the Duty Cycle testing, several start-run-stop cycles for various choices of "station" spacing and car weight were run to determine the absolute and relative amounts of propulsion energy consumed in the starting grids on the R-32 cars. These measurements are summarized in part I of Table 22.

From these data, it can be seen that (1) the amount of energy consumed in these grids is only 5-6% and (2) the amount of energy dissipated in the grids during a full-rate acceleration is 0.20 kwh/car for a crush-loaded car and 0.16 kwh/car for an empty car (assuming that the acceleration continues to a speed above the base speed of the traction motors).

As was shown to have been the case in previous comparisons between Duty Cycle and Revenue Service test results, it is clear in part II of Table 22 that the general use of less-than-maximum accelerating rates in revenue service affects the test results. In particular, both the grid energy/stop/car and the percentage grid use are higher in revenue service than in the corresponding duty cycle test.

In this case, the lack of correspondence can be explained as follows. In revenue service, the cars are not, in general, accelerated at full rate. This has the effect of keeping the propulsion system in the process of notching-out resistances for an extended time, which results in the grids consuming a relatively larger portion (8-9%) of the total propulsion energy than they would in a full-rate acceleration. (Note, of course, that over-all energy consumption by the propulsion system is lower in a less-than-full-rate acceleration).

The inclusion of energy measurements during yard moves increases the grid energy consumption proportion by another 1%, approximately, to 9-10%. This fraction is to be compared with the estimated 5% consump-

TABLE 22
Conventional R-32 starting grid energy consumption

I. Duty cycle tests*

Car weight condition	Station stop interval	Energy (kwh)/car-mile Grids	Energy (kwh)/car-mile Total	Energy (kwh)/stop/car Grids	Energy (kwh)/stop/car Total	% used by grids
Crush	2000 ft	0.50	8.04	0.19	3.04	6.2%
	3000	0.35	6.90	0.20	3.92	5.1
	5000	0.21	5.52	0.20	5.23	3.8
Empty	2000	0.40	6.88	0.15	2.61	5.9
	3000	0.29	5.75	0.16	3.27	5.0

II. Revenue service tests

Line	Average station spacing	No. of one-way trips (local-express)	Energy (kwh)/stop/car Grids	Energy (kwh)/stop/car Total	% used by grids
A	3700 ft	66 (34-32)	0.27	3.4	8.0%
D	4600	40 (32-8)	0.35	4.0	8.7

*All runs at maximum acceleration

tion for the controls in a chopper system.

For completeness, it should be noted that during all of the revenue service grid energy tests, one of the two ES cars was not providing propulsion, due to an ESU failure (which will be documented in Part III). Since the test cars were part of a 10-car train during this period, the effect of one car's being unpowered was felt to have been of only minor significance.

POWER

The previous section of this report presented a range of energy measurements and evaluated the effectiveness of the Energy Storage propulsion system in reducing energy consumption under a variety of operational conditions. The present section discusses another area of potential benefit accruing from the ES system, which results from its generally lower *rate* of energy consumption (that is, its lower average *power*) when compared with the conventional propulsion system.

Propulsion *power* levels are important to transit system design and operation because:

(1) the sizing of the power supply system is determined largely by the expected power levels.

(2) The electrical energy losses in the current distribution system, itself, are dependent upon the rates of energy consumption (more specifically, upon the mean square current delivered to the car).

It might be felt that this propulsion power reduction would bring about a diminution of utility billing for "demand", as well, but the relation between the two is only an indirect one. The billing for "demand" is, in fact, a result of determining the *energy* consumed during the peak time period (15 minutes, 30 minutes or 1 hour, depending on the local utility tariffs). During this time period, there will have been hundreds of car accelerations and the "demand" meter will combine them with the non-acceleration loads. Thus the demand measurement is not sensitive to an individual acceleration or to its *rate* of drawing current. Of course, the demand billing for a fleet of ES-propelled cars would, in general, be lower than for conventional cars, but this would be a result of reduced *energy* consumption (during the peak period), and would not relate directly to *power* levels.

Effect of ES system on design of power supply

As an example of how the size of DC power supply equipment is determined, the NYCTA Design Standard for substation equipment (Reference 5) is quoted below:

> "The power rectifier shall be of the semi-conductor type using silicon cells and shall have a continuous output rating of 3000 to 4000 KW at 625 volts, DC. The rectifier units (including rectifier, transformer and switchgear) shall, after reaching a constant temperature of rated output, be capable of delivering an overload current of 150 percent of full load for two hours and interposed cyclic overload consisting of five periods of 300 percent of full load for one minute each and one period of 450 percent of full load for fifteen seconds, equally spaced throughout the two hour period. The unit shall have a regulation of five percent at the substation bus from no load to full load."

It can be seen that the overload power ratings for the 15 second and the one minute peaks are directly related to the acceleration power characteristics of individual trains.

The charts of the Simulated Service runs on the A-line (Figure 8) were reviewed, several typical segments were chosen, and sample calculations of average power were performed for 15 and 60-second intervals. The results of these calculations are summarized in Table 23, where it can be noted that the ES system reduces the average power requirement by 18% and 28% for the 15-second and 60-second periods, respectively.

It should be realized, of course, that the continuous rating and the two-hour requirement for the substation equipment would be reduced by the use of ES equipment, because of the ES system's lower energy usage.

Effect of ES system on power distribution losses

As a rule-of-thumb, the energy losses in a typical transit type third rail distribution system (including substation conversion losses) are estimated at 10-15% of overall energy usage (see, for example, Reference 4, Figure IV-2). These losses are primarily due to resistive heating in the conductors, which is dependent upon the square of the current being carried.

As can be seen from the A-line sample calculations which are summarized in Table 23, the mean square current is reduced by one-quarter to one-third by the ES system. Thus one can approximate the reduction in third rail distribution losses as amounting to approximately 3-5% of the total propulsion energy consumed.

In summary, the ES propulsion system, if implemented system-wide, would offer the additional benefits of reducing the design capacity required for substation equipment and would provide an overall 3-5% energy savings, due to reductions in distribution los-

TABLE 23
Sample comparisons of acceleration power characteristics (average of representative accelerations observed during A-line Simulated Service runs — See Figure 8)

		60-second averaging periods			15-second averaging periods		
		Standard	ES	Reduction	Standard	ES	Reduction
Peak power/car	(Kw)	153	110	28%	280	230	18%
Mean square current	(Amp^2)	95,000	70,000	26%	220,000	150,000	32%
Root mean square current	(Amp)	308	265	14%	470	390	17%
Maximum current	(Amp)	600	470	22%			

ses, alone. These power-related benefits, it should be noted, can be obtained with propulsion systems only of the energy storage type. Those propulsion systems which save energy by regenerating the braking energy back into the third rail for re-use by other trains are very different in this regard. The input power requirement for acceleration of a regenerative car is identical to that of a conventional car.

In addition, the combination of these benefits could be used to even greater advantage in a new system, by allowing an increase in the spacing between substations. In designing a new system (at such a time as an ES-type system is fully commercially available), the overall plan of power distribution and supply would have to be approached with the particular characteristics of the ES system in mind, in order to obtain the maximum benefit. Of interest in this regard is the segment of the A-line run in Simulated Service from 190th Street to 207th Street, where the train makes three accelerations with essentially no propulsion power being drawn by the ES cars (see Figure 8).

DEAD THIRD RAIL OPERATION

Unique to the ES propulsion system is its ability to move a train in the absence of third rail voltage, using the energy stored in the flywheels. It has been hoped that this ability could be of critical benefit in a blackout or other power interruption by allowing trains to proceed to the next station for the discharge of passengers.

This potentially beneficial aspect of the ES system was investigated while the two cars were undergoing tests on New York's Sea Beach test track. For the test, the third rail power was deliberately shut off while the cars were stationary, with flywheels running at approximately 85% of top speed. When the loss of third rail was noted in the car (by the disappearance of main interior lighting), the motorman accelerated the two-car train, keeping the controller handle in one specified position until the usable energy stored in the ESU was depleted. The cars were then allowed to coast and records were made of the relevant characteristics (see Table 24).

It was observed during the test that the overall length travelled was not the most illuminating indicator of dead third rail operating capabilities, since the total length was in large degree dependent upon the particular sequence of grades traversed. More pertinent was the top speed achieved, since this represents the potential ability of the cars to coast after all stored energy had been exhausted.

The tests also showed that the most effective method for using the stored energy was to accelerate at maximum rate ("parallel" mode) until the energy was expended. This characteristic can be understood by recalling the earlier section on ESU losses and noting that the full rate acceleration uses up the stored energy quickly (in 15-18 seconds, approximately), thereby minimizing the loss of energy to the parasitic loads on the ESU.

As has been mentioned already, the parasitic losses limit the potential usefulness of the ES system for moving trains in a blackout. This is because a flywheel which is spinning at 85% of top speed would lose all of its useful energy in approximately 3½ minutes (see Figure 16). In an actual emergency, it is likely that a train would stand for that length of time before clearance for movement could be assured, thereby having the ESU losses consume the potential for propulsion.

On the other hand, the data displayed in Table 24 do indicate that significant distances *can* be traversed, if the ESU losses could be reduced to the point where a suitable amount of stored energy would be available reliably for longer periods.

Traces of the relevant parameters for the parallel mode accelerations are depicted in Figure 21. In the

TABLE 24
Dead third rail tests

Run No.	Car load	Starting location (Note 1)	Direction	Accel mode (Note 2)	Max speed (MPH)	Run distance (feet)	ESU run-down time (min:sec)	Total run time (min:sec)
951	Empty	16th Ave	N	SW	17	1890	N.A.	1:55
1011	"	577+00	S	SW	22	2554	N.A.	2:14
1030	"	616+00	N	P	32	2323	:17.5	1:25
1115	Crush	Ft. Hamilton	N	SW	12.5	1395	1:30	1:50
1145	"	16th Ave	N	SW	15.0	1925	1:38	2:00
1153	"	577+00	S	SW	19.0	(Note 3)	1:55	3:30
1210	"	16th Ave	N	P	27.0	2268	:15.5	1:25
1215	"	577+00	S	P	34.0	(Note 3)	:15.0	1.53

Note 1: All tests were performed on the NYCTA Sea Beach test track. Refer to profile chart, Figure A-3, Appendix A.

Note 2: SW = Switching; P = Parallel

Note 3: Run terminated at 5000 ft, approximately

N.A. = Not available

charts one can see the drop-off of third rail voltage, the ramping up of the ESU output voltage, and the 15-second burst of current through the traction motors, which results in motion of the car (at the expense of flywheel speed).

For completeness, two points relating to this subject should be mentioned. The first is that the ES system circuitry design did not allow for the operation of full carbody lighting on flywheel power. Thus the removal of third rail power caused the main interior lights to extinguish (leaving the emergency lights and the head and rear lights, which were battery powered). To have designed otherwise would only have ensured that the useful stored energy would be depleted prior to moving the train in an emergency.

Secondly, it should be noted that since the two ES cars were unique vehicles in New York's 6000-car fleet, their ability to move on a dead third rail could have proved hazardous to unwitting employees. For instance, a trackworker, who normally could provide a certain degree of protection against train movement by deadening the third rail, would lose that protection against a moving ES train. For this reason, the dead third rail operation feature of the ES system was nullified by suitable circuitry during all operations except when tests and demonstrations specifically requiring the feature were performed.

UNDERFLOOR TEMPERATURES

Essentially all of the energy drawn by trains from the third rail is eventually turned into the form of heat, which is dissipated within the subway. This heat is formed in the friction brakes or dynamic brake grids when the car is stopping, it is generated within the rotating equipment and the propulsion controls, and it is produced within the tunnel air, itself, as the train pushes its way through. All of this is an example of the First Law of Thermodynamics, which points out that energy is never actually "consumed" it is merely transformed from one type of energy into another. Consequently, any propulsion system that reduces the net intake of energy by the train will reduce heat dissipation into the tunnels, as well.

A significant reduction in heat in the subways would be welcomed by the public. However, the most direct methods for temperature control (e.g., exhaust fans, air cooling and other heat *removal* techniques) carry with them rather substantial capital and operating costs. Any car-borne system (such as the ES propulsion system) that would reduce the heat *at the source* promises to benefit the riders without incurring such costs.

The order of magnitude of these savings can be evaluated by using the estimates contained in the *Subway Environmental Design Handbook* (Reference 6, p I-15). The Handbook states that approximately 85 to 90 percent of all of the heat in a subway system is produced by the operation of trains. It further estimates that half of the train operation heat generation can be attributed to braking. Thus, according to the Handbook's estimates, approximately 42% of a subway system's heat load results from braking and 42% results from acceleration and motoring losses plus car-borne auxiliary usage. If one divides the latter 42% equally between propulsion and auxiliaries and if one assumes that a transit-system-wide application of an improved ES-type propulsion system would reduce propulsion

and braking energy consumption by at least 28%, which is the average of the calculations listed in Table 19, then the *total system heat load* should decrease by 18% or more.

Thus one should expect that a substantial decrease in cooling requirements for stations would follow from the introduction of a vehicle propulsion system of the ES type.

An unsuccessful attempt was made during the Simulated Service testing to evaluate directly the heat reduction effect. Six thermocouples each were mounted underneath ES car 3700 and standard car 3702 during the A-line Simulated Service runs and a complete record was taken of the temperatures in these locations during a one-way trip. (This particular trip was the second half of a round-trip, so the car equipment had achieved a certain degree of thermal equilibrium.)

On ES car 3700, the thermocouples were attached to the following locations:

Smoothing reactor — top face
Chopper — inside enclosure
Chopper — outside face
Flywheel alternator cooling air exhaust
In air space within brake grid cage
In air space at random location under car

Since there were no directly comparable locations under the standard R-32 car, the thermocouples were simply placed in the undercar air space at approximately equal intervals, one-foot below the floor.

The temperature readings for the twelve thermocouples are displayed in Figures 22 and 23, along with the A-line profile, for reference. The sharp rise in the standard car temperatures between the 8th and 9th minutes coincides with the passage of the train into the subway at Grant Avenue from the outdoor elevated trackage. (Note that the test took place late on a typically-cold January night.) From this fact and from the observation that all six of the standard car thermocouples show essentially identical readings, one can conclude that the standard car thermocouples are more sensitive to the ambient temperature, which is determined by pre-existing weather and tunnel conditions, than they are to any effects due to the heat generated by the cars.

The ES car thermocouple readings in Figure 22, on the other hand, appear to be overly dependent on very localized equipment temperature effects. As a result, the highest temperatures recorded by the thermocouples on either car were those of the flywheel alternator exhaust air on the ES car!

In summary, the test results are of little meaning. Of course, this was not entirely unexpected: the heat capacity of the subway tunnels is so large that subway air temperatures are essentially unaffected by the particular characteristics of two individual cars passing through. It would have been possible only in a large-scale and long-term test to have evaluated this effect directly. Thus one has to fall back on the First Law of Thermodynamics and perform an evaluation based on the reduction in energy usage, such as outlined previously in this section.

DYNAMIC STRESSES

Measurements

An extensive set of tests was performed on the ES cars to determine the stresses induced both in the car structure and in the ESU supports under various loadings. The bulk of this testing is not reported herein, however, since it relates solely to the particular car structure and mounting design used in the program and it has no general relevance. Among that category is the series of static stress tests performed at the Transportation Test Center (Pueblo, Colorado), which was performed to verify the rework of some poorly executed welding by Garrett during the attachment of the ESU supports to the car structure. These tests are reported separately in Reference 7.

Of more universal interest is the study of the dynamic behavior of the ESU while the ES cars negotiated curves. There had been, at the outset of the project, a concern about the possibility that the ESU would tend to "steer" the car or to overstress the structure under the gyroscopic action resulting from the change in the orientation of the flywheel's spin.

It can be shown by calculation that even in extreme cases the magnitude of this effect is small in comparison to other normally-encountered forces. A sample calculation is presented at the end of this section.

On the other hand, since it was possible to do so within the ES car test program, it was decided to verify directly the smallness of the gyroscopic effect, by placing strain gauges on the most critical elements of the car structure and ESU supports, thereby measuring stresses during limiting-speed curving operations of the cars. The strain gauges were also monitored during the Simulated Service tests, to get a reference for the stresses normally encountered on revenue trackage. The locations of the strain gauges are shown on Figure 24.

Three curving tests were performed on each of two curves on the Sea Beach Test Track (N-line). "Curve No. 1" is located between stations 617+00 and 622+00 and has a radius of 1700 ft.; "Curve No. 2" is between 628+60 and 632+00 and has a radius of 975 ft. The three tests performed on each curve were: an acceleration from 0 to 20 MPH, a deceleration from 30 MPH to 0 and a constant speed run at the maximum

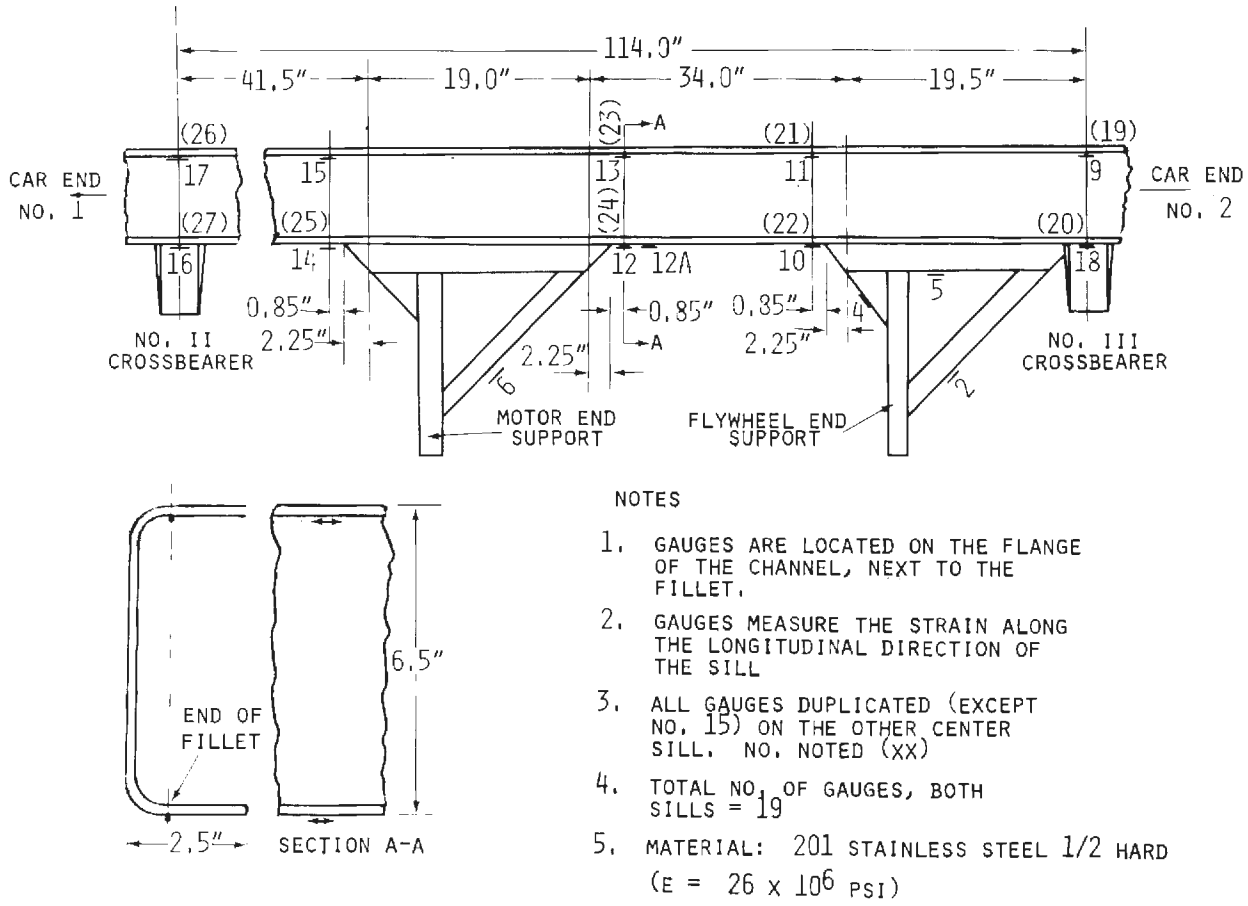

Figure 24. Strain Gauge Locations

authorized speed (46 MPH, approximately). The strain gauges were set up to measure the non-static portion of the strain (i.e., the "dynamic" strain); the strain due to the dead weight of the car and equipment, as experienced when the car was stationary, was excluded from the readings.

The strain measurements, which are reproduced in Figure 25, display both the effect of the curving — as noted by a shift in the overall level of the gauge outputs — and of the wheel-rail interaction — as seen by the vibratory nature of the signals. The most obvious conclusion from the charts is that the vibratory component is considerably larger than the level shift. Thus the carbody and equipment are more heavily stressed by the ordinary forces generated in the cars' normal motion over the tracks than they are by *any* forces due to curvature. Furthermore, the attached calculation points out that, of the curve-related forces, the common centripetal loading is comparable to any gyroscopic effects. The data in Figure 25 are summarized in Table 25.

Dynamic strain data from the Simulated Service testing are displayed in Figures 26 and 27. This information is combined with other data and is summarized in Table 26.

Discussion of maximum limit on gyroscopic force

Gyroscopic forces arise because of a change in direction of the gyro's angular momentum, which is a vector quantity. The basic relationship is Newton's Second Law (restated in rotational terms):

$$T = \frac{dL}{dt},$$

where T = torque produced
and $\frac{dL}{dt}$ = time rate of change of angular momentum

As an ES car rounds a curve, the angular momentum vector (which is always parallel to the longitudinal centerline of the car) changes direction by an angle ϕ

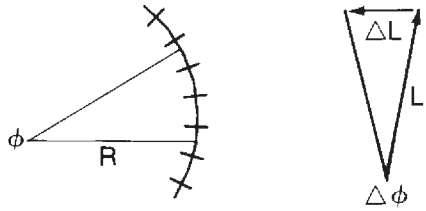

$$\text{Therefore, } T = \frac{\Delta L}{\Delta t} = L\,\frac{\Delta \phi}{\Delta t} = L\,\frac{d\phi}{dt},$$

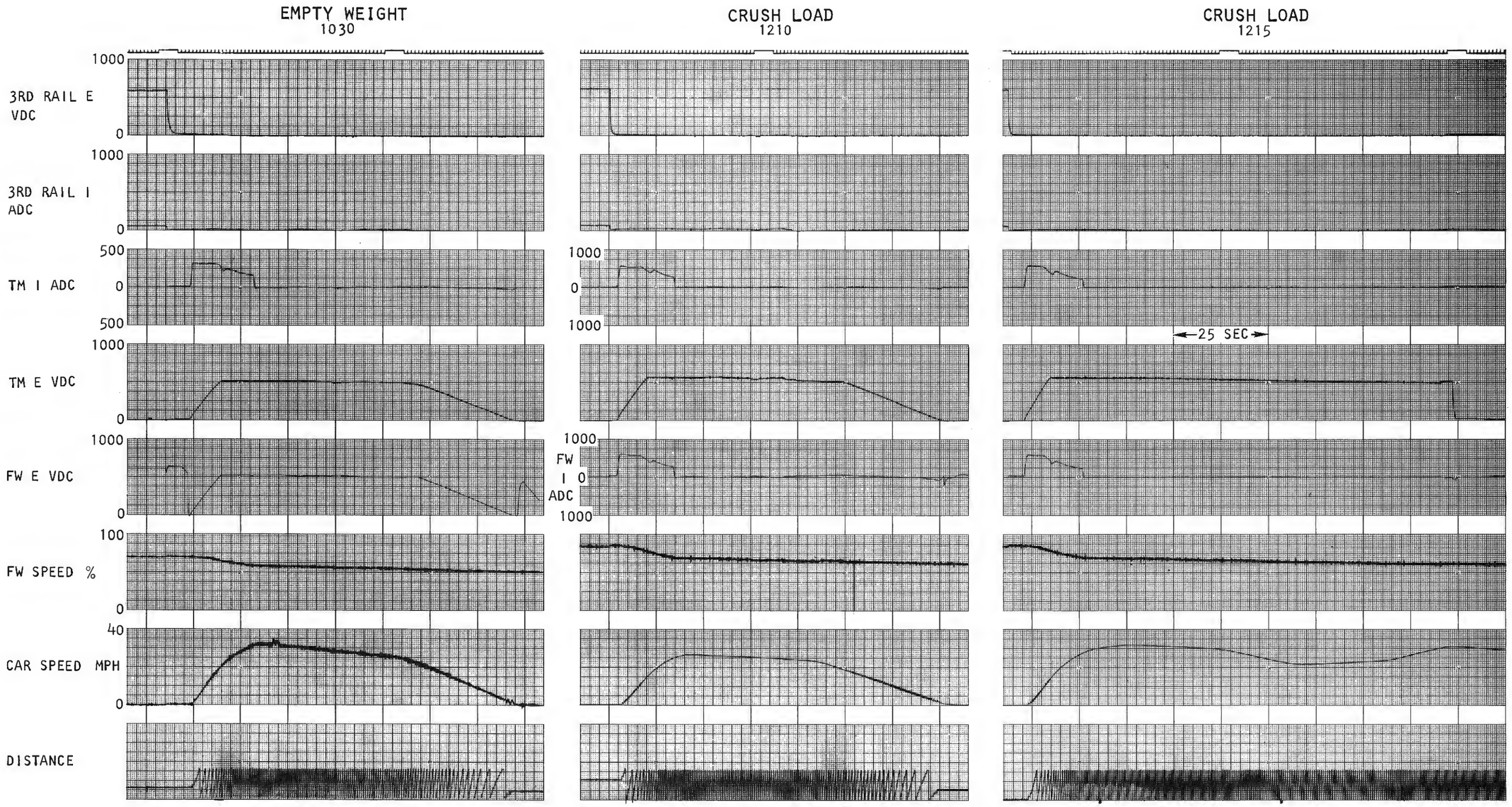

Figure 21. Dead Third Rail Evaluation

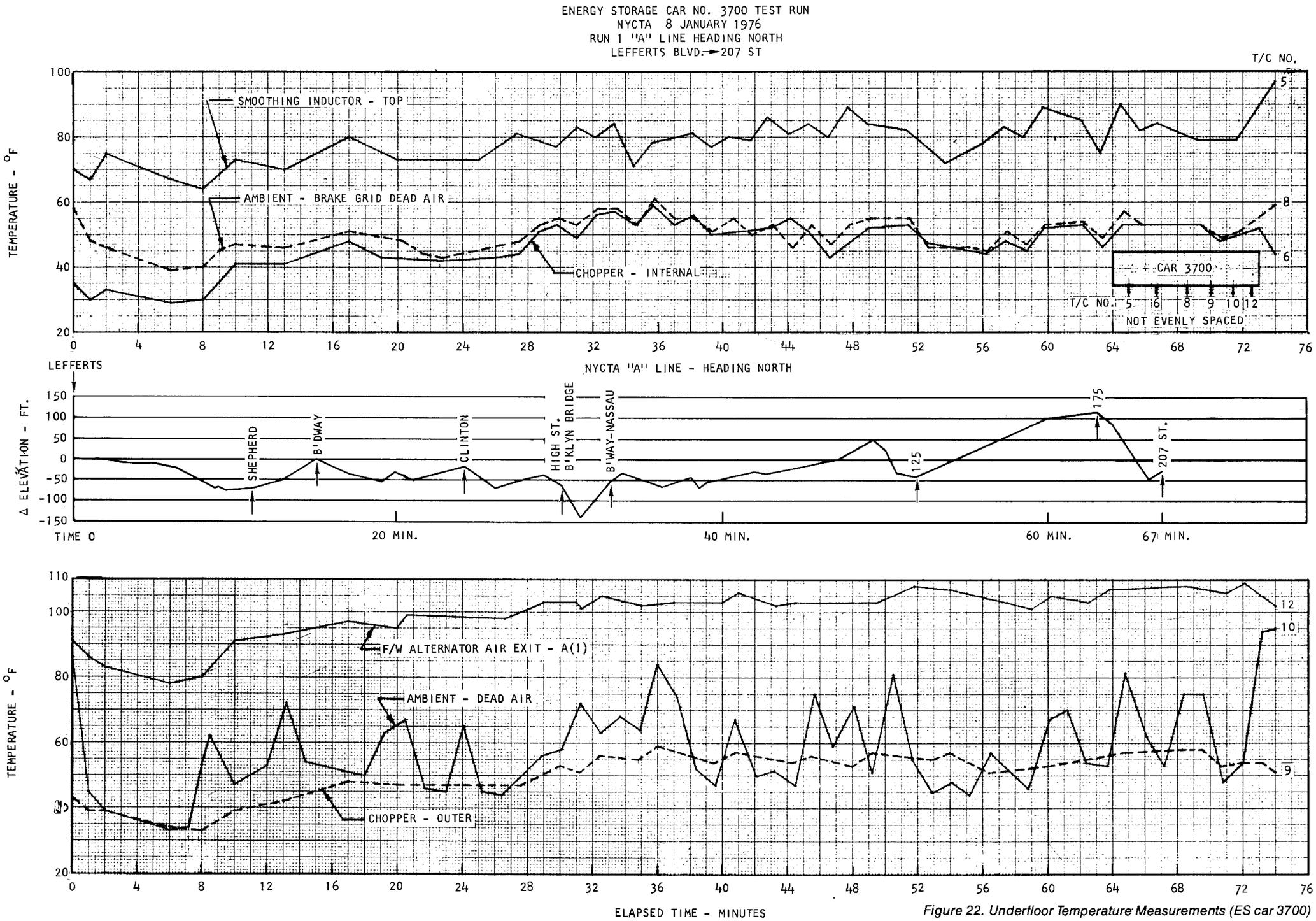

Figure 22. Underfloor Temperature Measurements (ES car 3700)

STANDARD CAR 3702 TEST RUN
8 JANUARY 1976
RUN 1 "A" LINE HEADING NORTH
LEFFERTS BLVD. → 207 ST

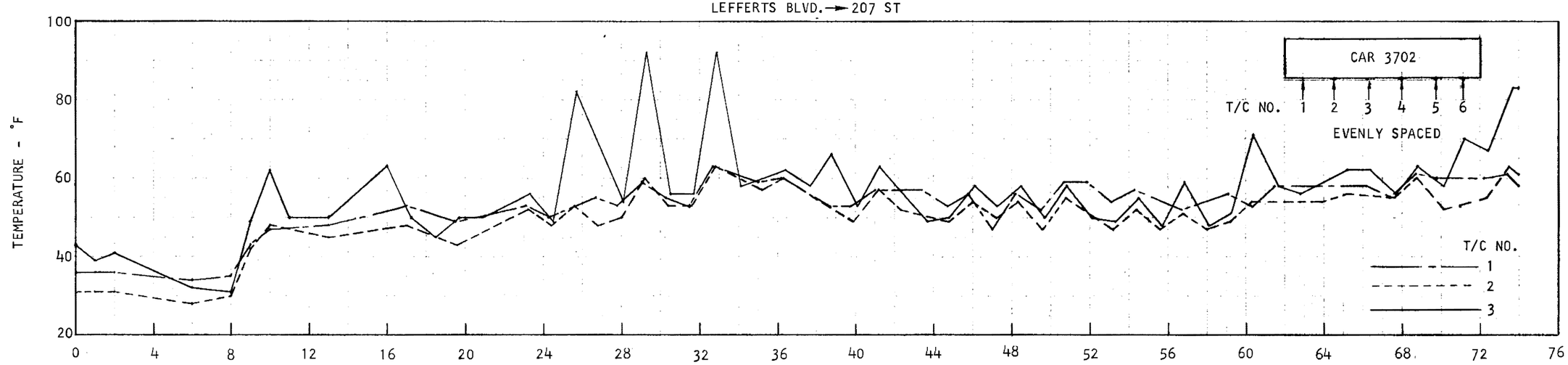

NYCTA "A" LINE - HEADING NORTH

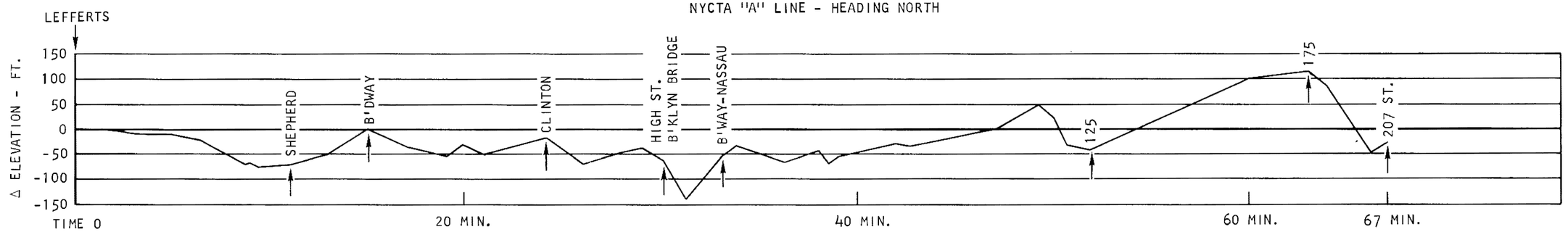

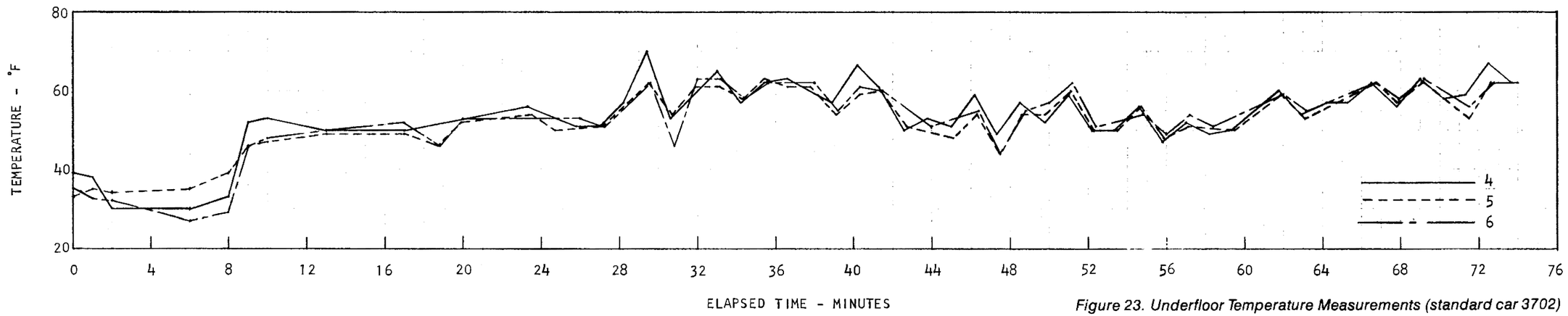

Figure 23. Underfloor Temperature Measurements (standard car 3702)

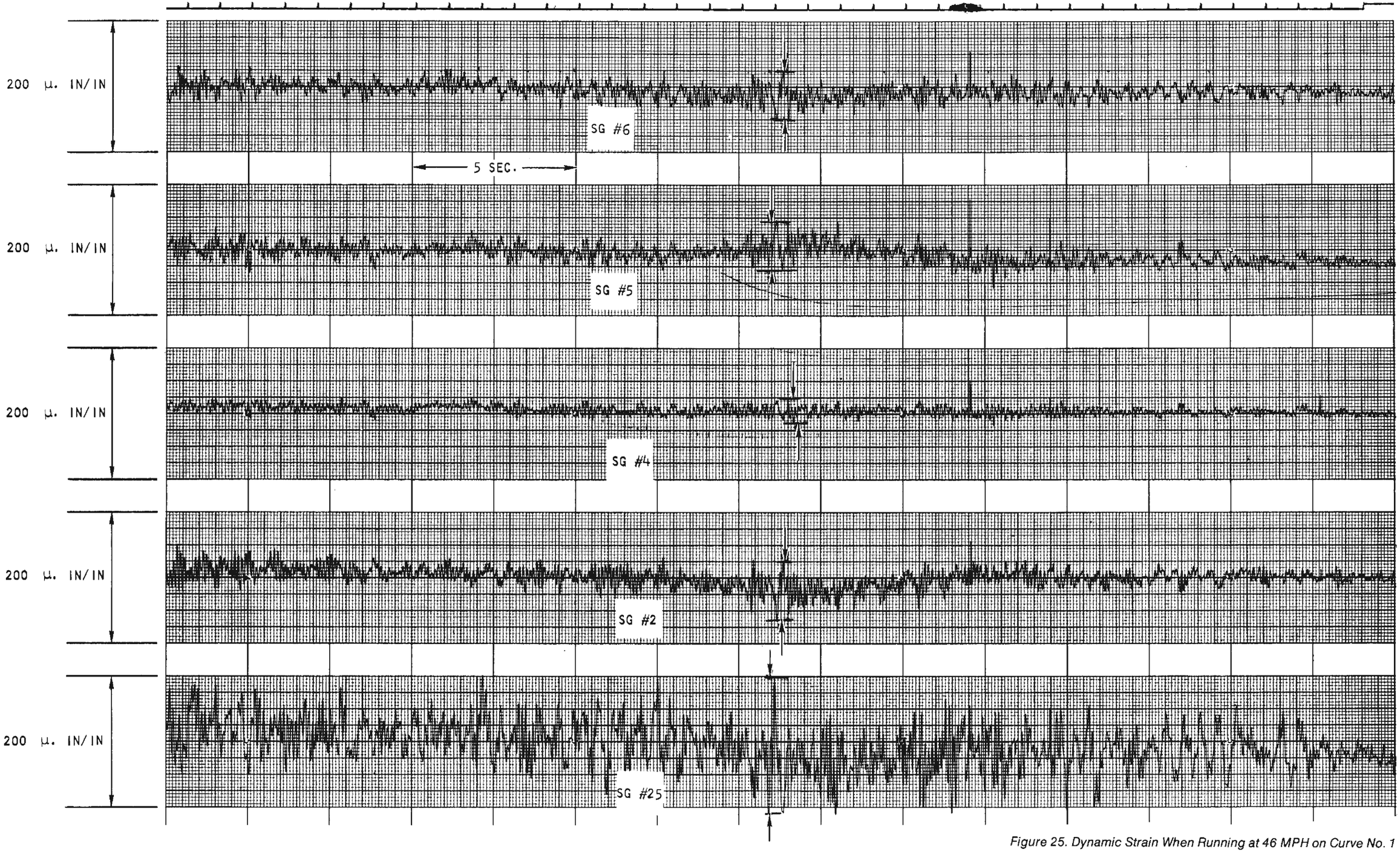

Figure 25. Dynamic Strain When Running at 46 MPH on Curve No. 1

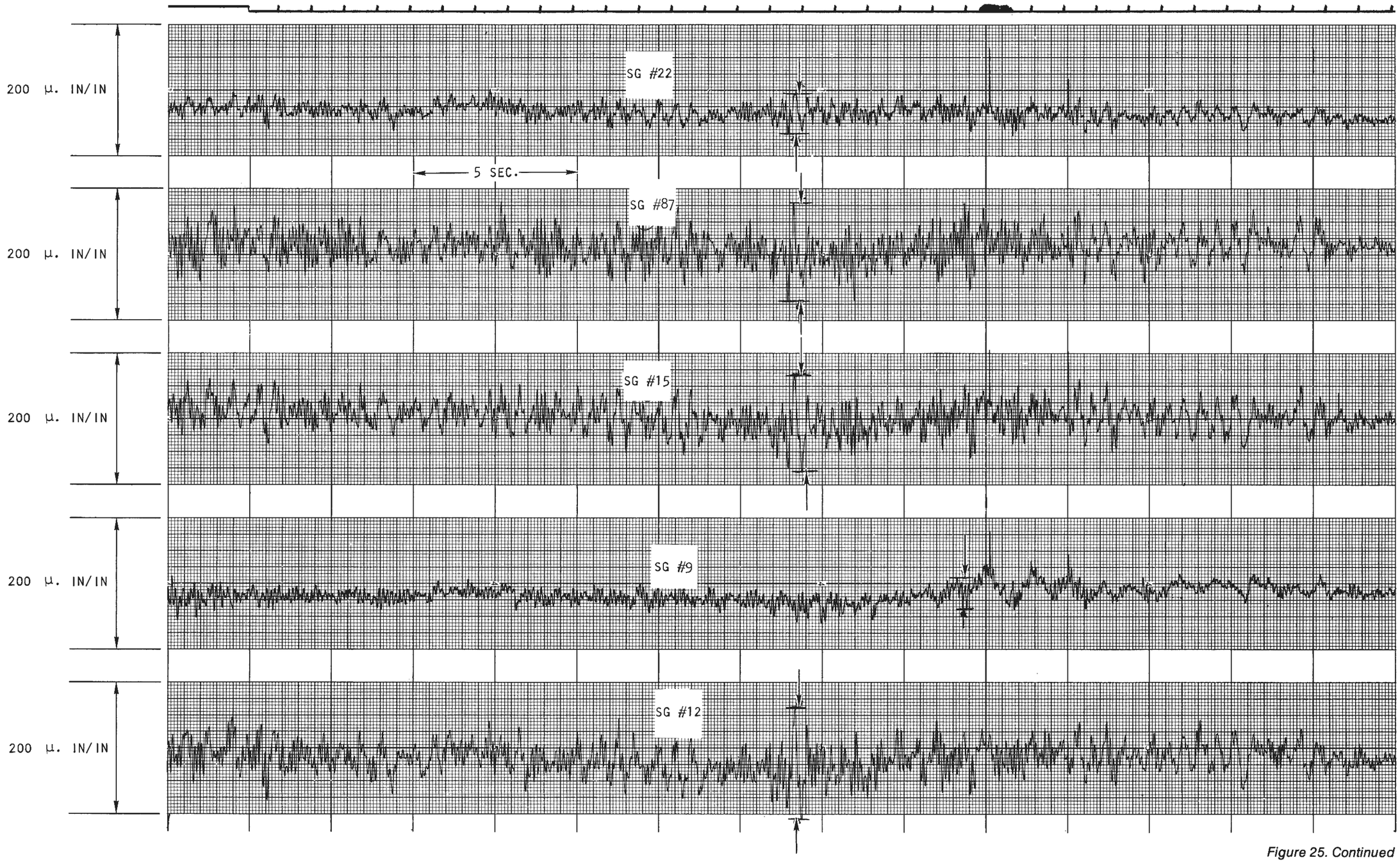

Figure 25. Continued

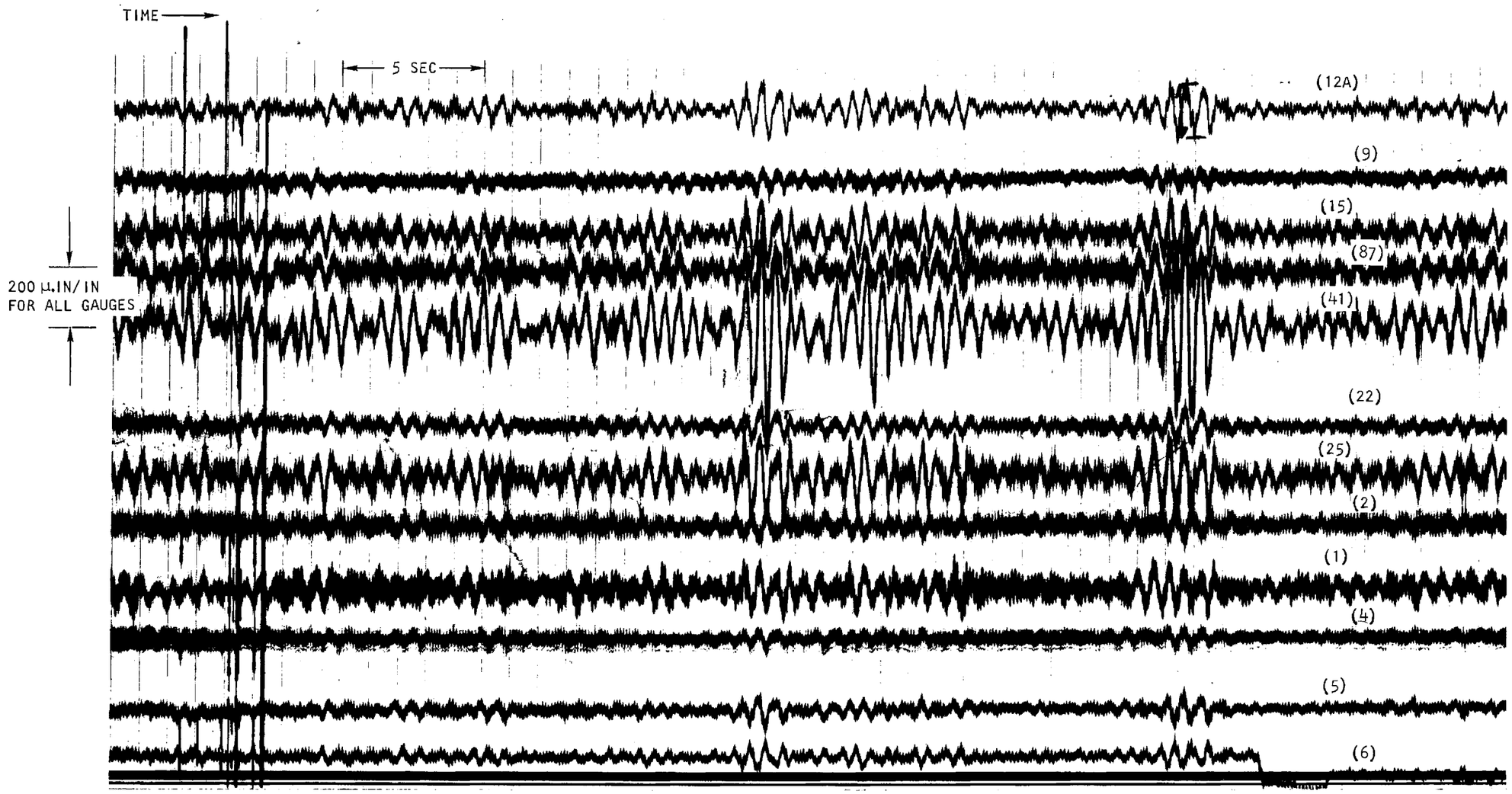

Figure 26. Dynamic Strains Between 42nd and 59th Streets on the A-Line

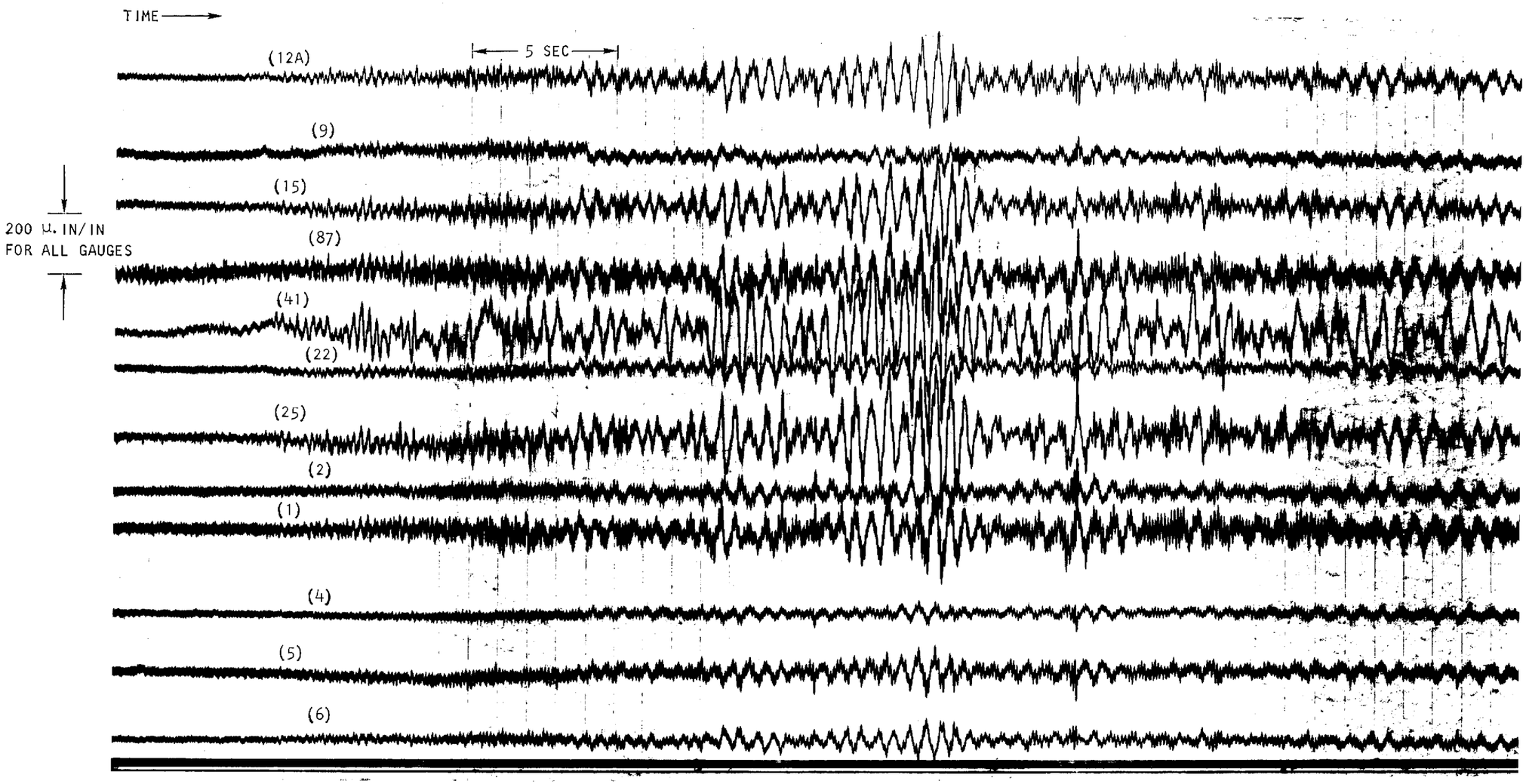

Figure 27. Dynamic Strains Between Pacific and 36th Streets on the N-Line

TABLE 25
Dynamic structural stresses on curves

Location and Gauge Number	Test Condition: Stresses on Curve 1, psi — Acceleration from 0 to 20 mph	Deceleration from 30 mph to 0	Maximum Constant speed of 46 mph	Stresses on Curve 2, psi — Acceleration from 0 to 20 mph	Deceleration from 30 mph to 0	Maximum Constant Speed of 46 mph
ESU support structure						
2	−140 ±360	140 ±560	−1120 ±1260	0 ±620	−280 ±700	−840 ±1260
4	0 ±280	280 ±340	0 ±560	0 ±280	−420 ±560	−280 ±620
5	−140 ±480	−420 ±670	+420 ±1040	−280 ±480	−840 ±1260	−280 ±1200
6	−280 ±480	280 ±560	−210 ±1040	0 ±480	−140 ±1040	−280 ±1200
Center sills						
9	−420 ±620	−280 ±620	−350 ±640	−560 ±480	0 ±1400	−1120 ±840
12a	−560 ±590	0 ±1206	−560 ±2440	−840 ±920	−560 ±1820	−1120 ±2440
15	280 ±560	560 ±1040	−630 ±2100	0 ±700	0 ±2020	0 ±2580
22	0 ±360	0 ±620	−140 ±840	−420 ±450	−280 ±1260	−840 ±920
25	560 ±1040	−560 ±1400	−1050 ±2940	560 ±980	420 ±2800	0 ±3220
Cross bearer						
87	0 ±700	280 ±1260	−3500 ±2100	0 ±840	280 ±2160	0 ±2100

NOTE: Locations of strain gauges given on Figure 24.

TABLE 26
Maximum Alternative Stresses During Simulated Service

Location and Gauge No.	Alternating Stresses, psi — A-Line (1)	D-Line (2)	E-E Line (3)	N-Line (4)
ESU Support Structure				
1	3500	2960	2690	3230
2	1940	920	1180	1180
4	970	430	538	650
5	2150	1350	1180	1620
6	1880	1290	1080	1080
Center Sills				
9	1180	1080	1350	1350
12a	4310	2800	2690	2690
15	4850	3500	2690	3020
22	3230	2580	1350	1880
25	6730	5120	4850	4310
Side Sill				
41	9690	8080	7650	9690
Crossbearer				
87	4310	3660	2690	2690

(1) Between 42nd and 59th streets
(2) Between Kings Highway and Avenue U
(3) Between Canal and Prince Streets
(4) Between Pacific and 36th streets

but $d\phi/dt$ is the angular velocity of the train as it goes through the curve, which is equal to the train velocity V divided by the curve radius R. Thus a pitching torque is generated in the ESU which equals:

$$T = \frac{LV}{R}$$

This torque generates a vertical force couple in the mounts of the ESU. If the longitudinal spacing of the mounts is *a*, then the force, which is upward at one end and downward at the other, is given at each mounting point by:

$$F_V = \frac{1}{2}\,\frac{T}{a},$$

since there are two mounts at each end.

An extreme example of this force, which should represent an upper limit on the gyroscopic force, would occur when a 145-ft radius curve is negotiated at 30 MPH (44 ft/sec). Furthermore, assume that the ESU is rotating at its maximum RPM. In this case,

$$L = \frac{2x\ (\text{stored energy})}{2\pi \times (\text{RPM})/60}$$

$$= \frac{2x\ 3.2\ \text{Kwh} \times (2.66 \times 10^6\ \text{ft-lb/Kwh})}{2\pi \times 14{,}000/60\ \text{sec}}$$

$$= 11{,}600\ \text{ft-lb sec.}$$

$$\text{and } F_V = \frac{LV}{2aR} = \frac{11{,}600 \times 44}{2x\ (53.8''/12) \times 145} = 392\ \text{lb.}$$

Thus the conservatively-estimated upper limit on the gyroscopic force on each mount is less than 400 lb. To put this number in perspective, it must be noted that the static load on each mount due to the dead weight of the ESU, alone, is 1250 lb. Since the ESU support structure must be designed for this weight under all dynamical conditions (e.g., vertical accelerations of the carbody due to rough track or switches), the addition of the gyroscopic loading is a relatively small effect.

As an additional point of reference, the centripetal forces resulting from the car's movement at 30 MPH around a 145-ft radius curve would be 500-lb per mount (0.4G's). This routinely-encountered force is greater than the maximum gyroscopic force.

For "curve No. 2" on the Sea Beach Test Track (975-foot radius) at 46 MPH (68 fps), the calculated forces on each ESU mount are:

Gyroscopic	90 lb	
Centripetal	180 lb	(0.15 G's)
Dead weight	1250 lb	

INTERIOR AND EXTERIOR SOUND LEVELS

Sound level measurements for both the ES cars and the standard R-32's were recorded on tape and analyzed by the NYCTA Environmental Staff Division, for a variety of operating conditions. These conditions included stationary tests, with each subsystem on the car being recorded individually, as well as moving tests, with each pair of cars being propelled at a series of discrete speeds.

Exterior measurements were conducted under "open field" conditions, with the microphones located 6-ft and 50-ft from the track centerline. Interior measurements were recorded simultaneously.

The results of these tests, in A-weighted decibels, are reported in Table 27. From these data, it can be observed that:

1. Stationary cars
   a. Inside, the ESU's are comparable to the fan noise.
   b. Outside, the ESU's are a few dBA higher than the compressor, although it was noted that the cycling of the compressor could be heard above the ESU noise.
2. Moving cars.
   a. Inside, the ES cars are approximately 7 dBA quieter than the standard cars.
   b. Outside, the ES cars are approximately 2 dBA quieter than the standard cars.
3. Comparison of propulsion modes
   a. Inside, switching mode is approximately 3 dBA quieter in ES cars than in standard cars.
   b. At 6-ft outside, switching mode is noisier for the ES cars than for the standard cars.
4. Service brake from maximum speed
   a. Inside, the ES cars are 12 dBA quieter than the standard cars.
   b. At 6-ft outside, the ES cars are noisier than the standard cars by 10 dBA.
5. Sound level curves for moving trains follow the equation

$$\text{dBA} = X + 22 \log V,$$

where V = car speed in MPH and

$$X = \begin{cases} 61 \text{ inside ES} \\ 68 \text{ inside standard} \\ 71 \text{ at 6' from ES} \\ 73 \text{ at 6' from standard} \\ 41 \text{ at 50' from ES} \\ 43 \text{ at 50' from standard.} \end{cases}$$

It needs to be noted that the R-32 cars are not air conditioned and, therefore, they have only minimal carbody sound insulation. From the measurements it appears that there would be little problem in reducing

the sound levels *inside the cars* to modern specified levels for an ESU-equipped new car. The *exterior* noise levels are not so easily muffled and would require more extensive work to make them acceptable for any future purchase.

INTERIOR VIBRATION

Vibration of the ESU's and of the car floors of both the ES and the standard cars were measured, in order to determine the effect of the rotating mass of the ESU.

Three-axis, low frequency accelerometers were located on the car floor, along the centerline, above the #1 ESU on car 3700 and in the same position on standard car 3702. The vibrations of the flywheel units were measured by the crystal accelerometers which were built-in during manufacture on the ESU's. Since the latter sensors are not stable below 2Hz, a filter was used to suppress these frequencies. (The filter was calibrated and found to attenuate the signal uniformly by 86% below 2Hz).

Figure 28 shows the vibration level for the ES car and for the vertical accelerometer on the floor of standard car 3702 in this series of test runs. In all these runs, vertical vibration levels recorded in the ES car were lower than in the standard car. Figure 29 shows the vibration loads in car 3702 in more detail.

The presence of the ESU modified the structural dynamics of the local area of the car floor and resulted in lower vibration response. The lateral vibration level of the carbody is generally less than ±0.1 g. The vertical vibration level of the carbody is generally below ±0.14 g, with few excursions outside this range. Maximum longitudinal acceleration of the car occurs during deceleration and is below 0.18 g.

These vibration levels are generally high, and would indicate a rough ride. However, this was true for the

TABLE 27
Interior and exterior sound levels (two-car trains)

		INSIDE (dBA)		OUTSIDE (dBA)			
Stationary Tests	**Direction**	**ES Cars**	**Standard Cars**	**6' from ES**	**6' from Standard**	**50' from ES**	**50' from Standard**
Compressor		57		65	68		
M-G		67			62		
Fans		86	87		59		
Flywheel Running		88		60 to 75			
Flywheel Rundown		87		78 to 65			
Background Noise		43		57	57		
Acceleration Mode							
Switching	South	84	87	90	88	63	63
Switching	North	82	86	88	78	66	58
Series	South	84	90	94	93	65	67
Series	North	84	87	92	88	62	60
Parallel	South	88	(95) ?	98	100	70	71
Parallel	North	87	87	97	98	68	69
500 ft, Sw/Ser/Par	South	80/88/90	85 to 92				
500 ft, Sw/Ser/Par	North	80/87/88	85 to 92				
Constant Speed Tests							
10 MPH	South	79	90	92	98	63	68
10 MPH	North	81	88	92	90	62	63
20 MPH	South	87	93	93	98	68	70
20 MPH	North	85	92	96	100	67	70
24 MPH	South	87		97		69	
24 MPH	North	87		99		71	
30 MPH	South	89	98	102	104	74	76
30 MPH	North		95		103		74
36 MPH	South	93		104		76	
40 MPH	North	99	99	105	105	80	78
40 MPH	South		99		104		78
Max. Service Brake	South	87	99	98	86	67	68
Max. Service Brake	North	90	101	108	98	68	72

standard car as well as for the ES car. It should also be noted here that the train was deliberately operated in a manner that was not typical of normal revenue service, in order to emphasize vibration response.

The vibration response of the ESU in each direction is generally less than ±0.5 g, except in a few cases where the vertical and longitudinal vibration level is about ±0.85 g, as shown in Figure 30, which is a repeat of run 1132 on an expanded time base.

One characteristic that is notable in Figure 30 (and to a lesser extent in Figure 28) is the increase in vertical acceleration in ES car 3700 when the car has come to a stop after a full brake application. This increase is due to the acceleration of the flywheel to nearly 100% speed in braking.

This observation points out the fact that the ESU has its extreme conditions of both noise and vibration at exactly those times at which they would be most noticeable — when the car comes to a halt in a station and the car doors open.

The other observation that can be made is that the same mechanism that causes the reduction in car floor vibration in the ESU car (i.e., damping by the mass of the ESU) also explains the decrease in interior noise in the moving ES car, which was noted in the previous section.

SIGNAL INTERFERENCE

Signal interference tests were conducted at various locations on the New York City Transit System, to determine the effect that the ES propulsion-equipped cars might have on the following types of track circuits:

1. Audio Frequency (2630 Hz).
2. 60 Hz Balancing Impedance type.
3. 60 Hz single rail Matching Transformer type
4. 60 Hz single rail Capacitor type
5. 25 Hz double rail.

The tests were performed by operating the ES cars over these track circuits in each direction and in each of the three acceleration modes (switching, series and parallel), in coast and braking modes, and at a standstill with the flywheel accelerated through its speed range. A tape recorder was connected across the track receiver (after the filter) and the input signal was monitored while the cars operated on the track circuit. A reference level was established by recording the input signal when the circuit was unoccupied.

The recorded signals were fed into a spectrum analyzer in order to observe that component of the input which was in the range of sensitivity of the track receiver. This frequency-selected signal (4Hz bandwidth) was compared with the reference level and the results tabulated (Table 28). The measurements show signal levels at least 5dB below those for an unoccupied block.

In one part of the 25Hz testing, however, the maximum levels increased to the range of - 3dB to -1dB. This occurred only during the southbound station stop and the southbound switching mode acceleration run. In the opinion of the NYCTA Engineer who reviewed the test data, however, this signal level should be "attributed to a momentary loss of shunt, or poor shunting rather than an interference from the Garrett system". No tests were performed to determine specifically the shunting characteristics of the cars, since the cars could not be operated without the ES propulsion system functioning.

Furthermore, no meaningful data on possible interference with car-borne cab signal speed control equipment could be obtained, since the R-32 cars are not so equipped.

Nevertheless, it *was* determined conclusively from the tests that were performed that the ES equipment

TABLE 28
Signal interference tests

Track circuit type	Manufacturer	Enclosure (Note 1)	Voltage signal at track relay (Note 2)
Audio frequency (2630 Hz)	GRS	CIH	−21.9 to −6.1 dB
60 Hz balancing impedance	GRS	UC	−34 to 12.1 dB
60 Hz matching transformers, single rail	WABCO	CIH	
60 Hz capacitor, single rail	WABCO	CIH	
25 Hz vane type, double rail	GRS	UC	−10 to 5 dB (Note 3)

Note 1: CIH = Central Instrument Housing
UC = Unit Case

Note 2: Frequency band signal at relay with track occupied, referred to signal when unoccupied.

Note 3: See text

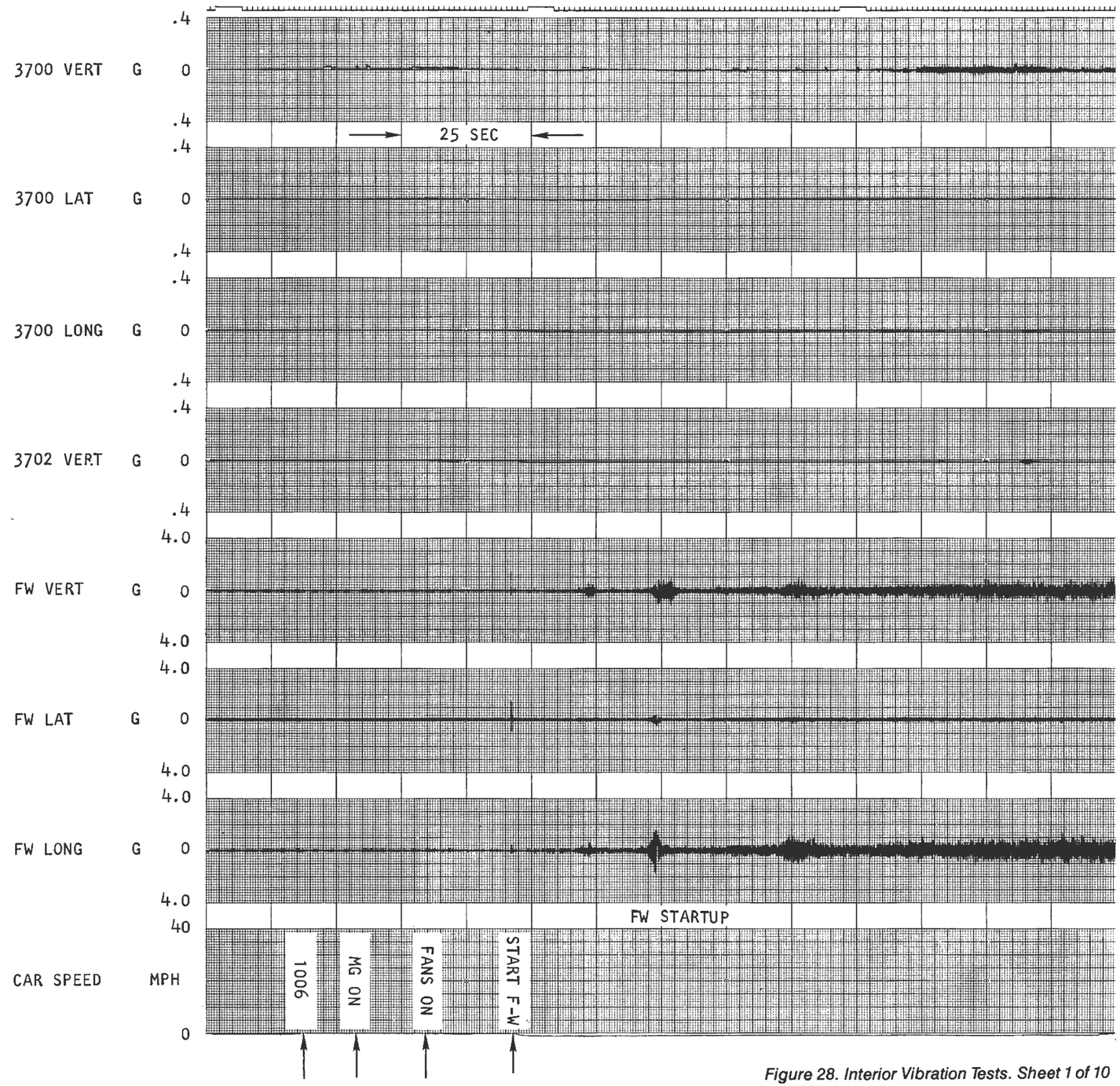

Figure 28. Interior Vibration Tests. Sheet 1 of 10

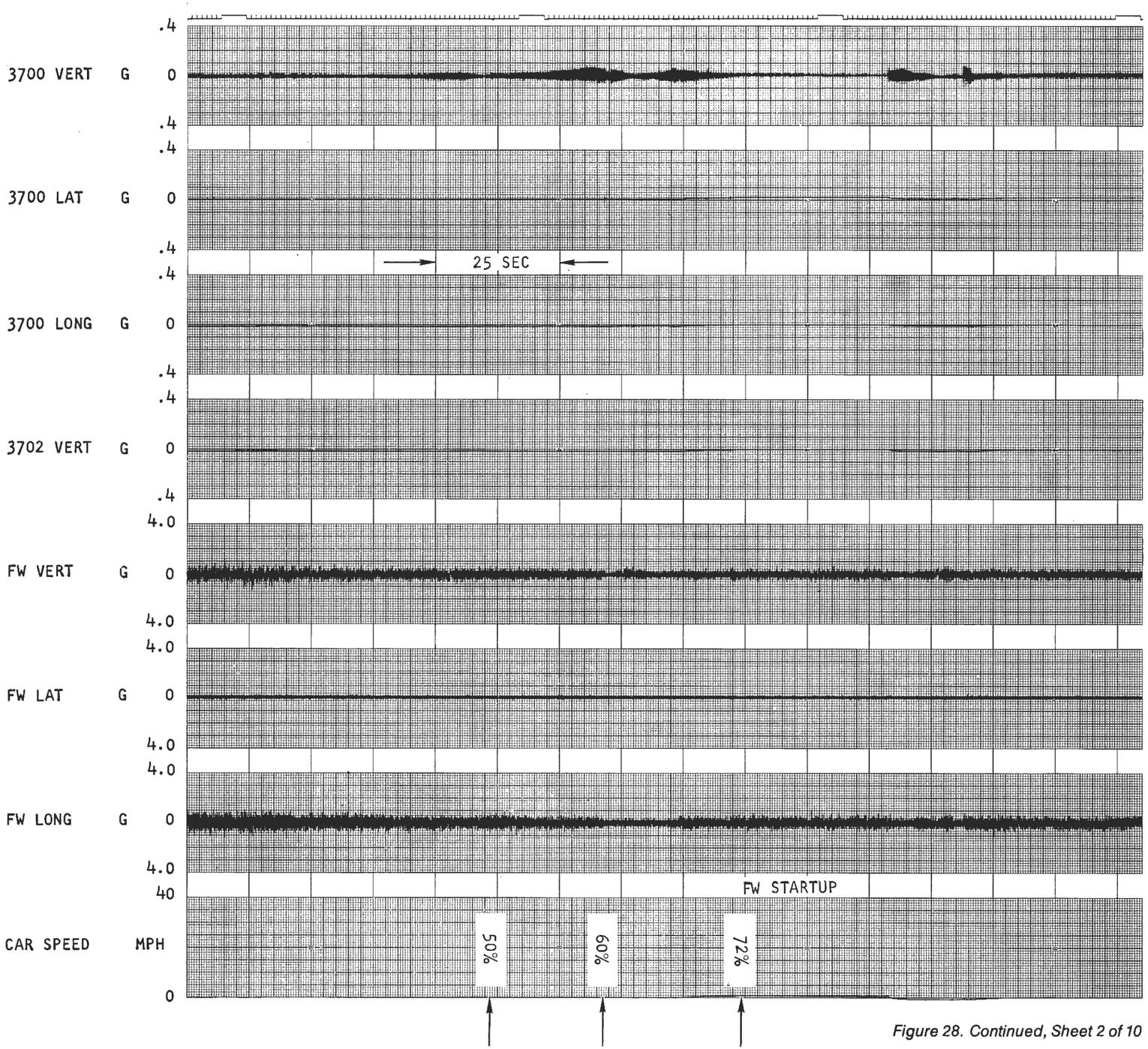

Figure 28. Continued, Sheet 2 of 10

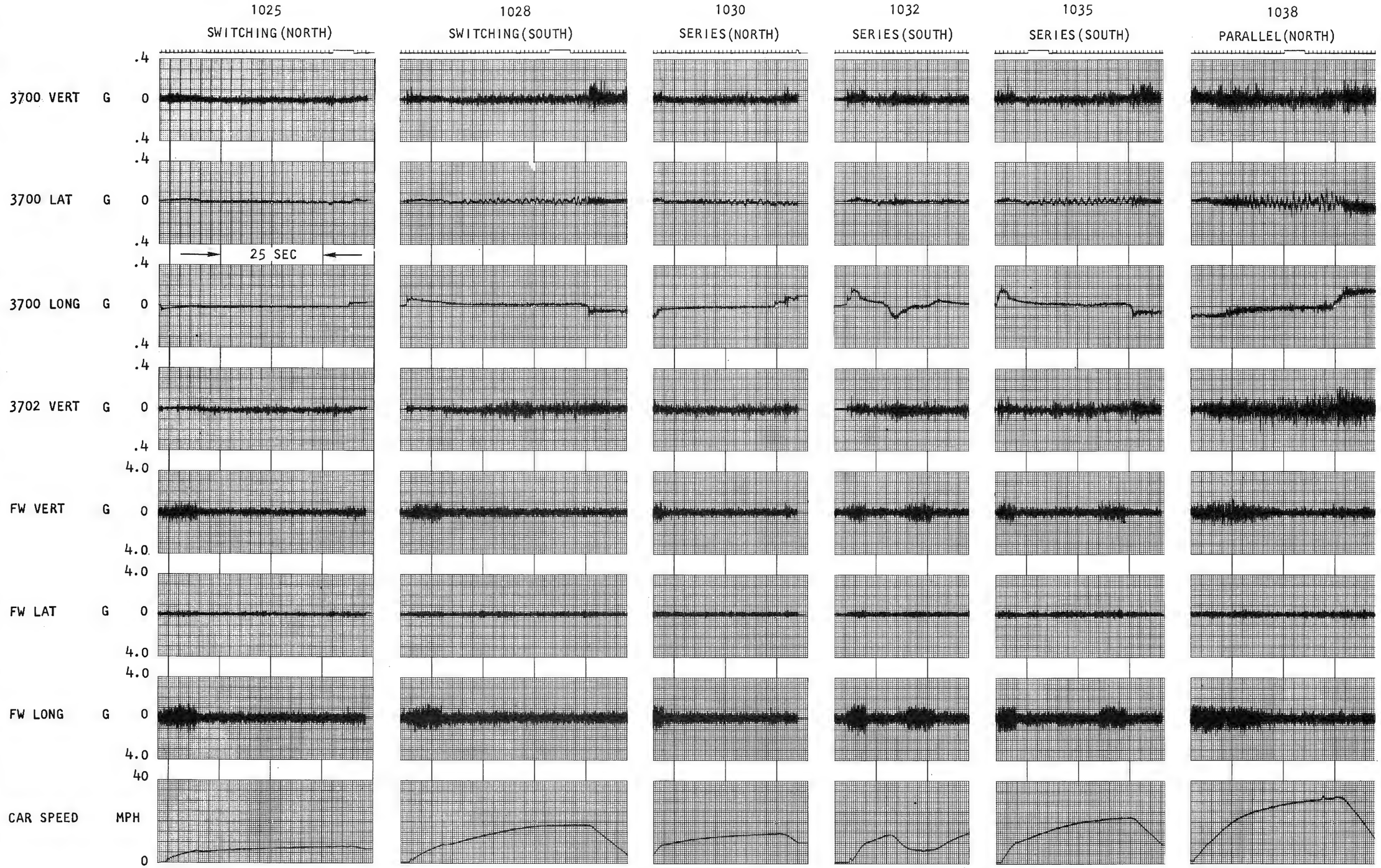

Figure 28. Continued, Sheet 3 of 10

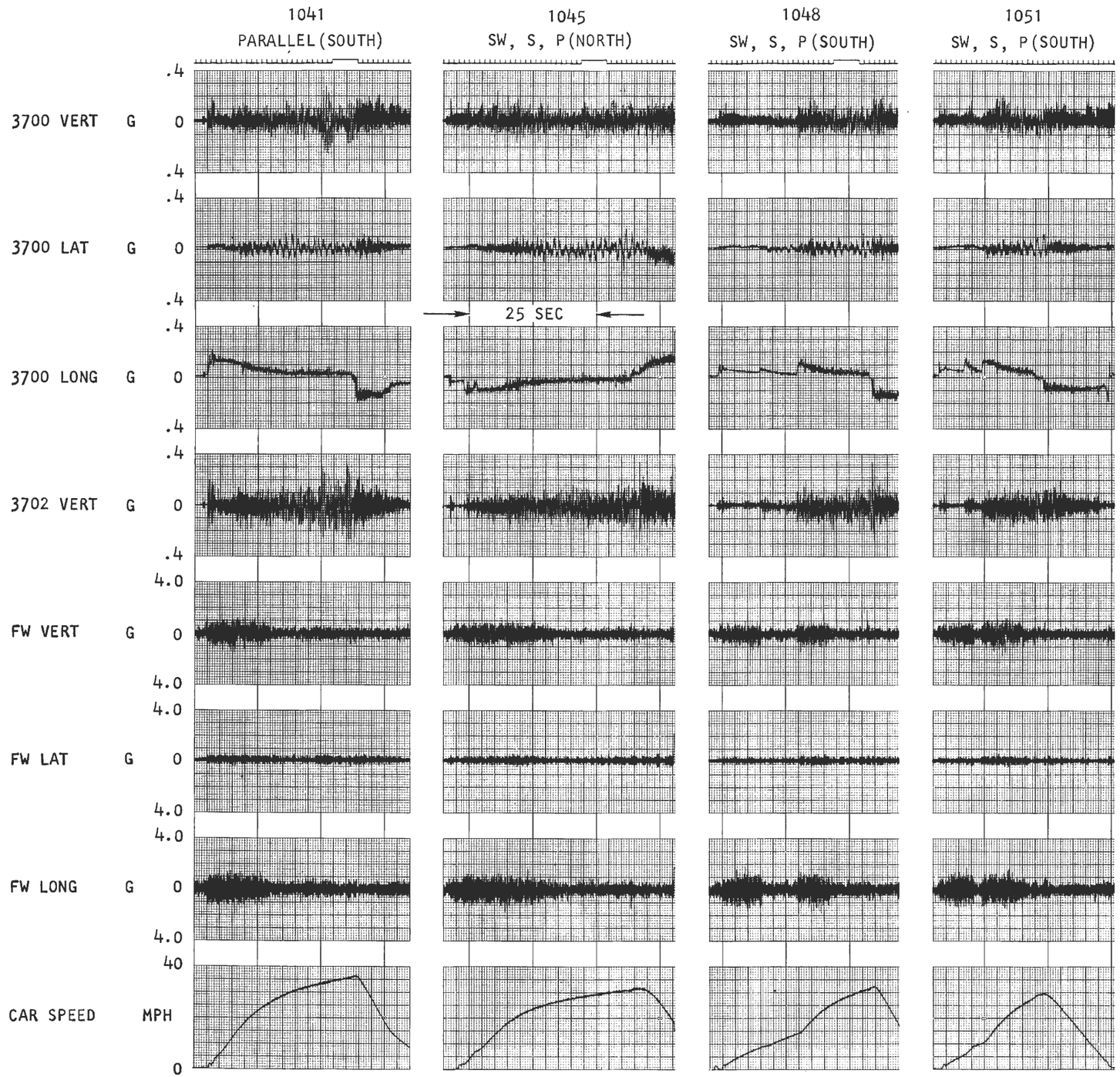

Figure 28. Continued, Sheet 4 of 10

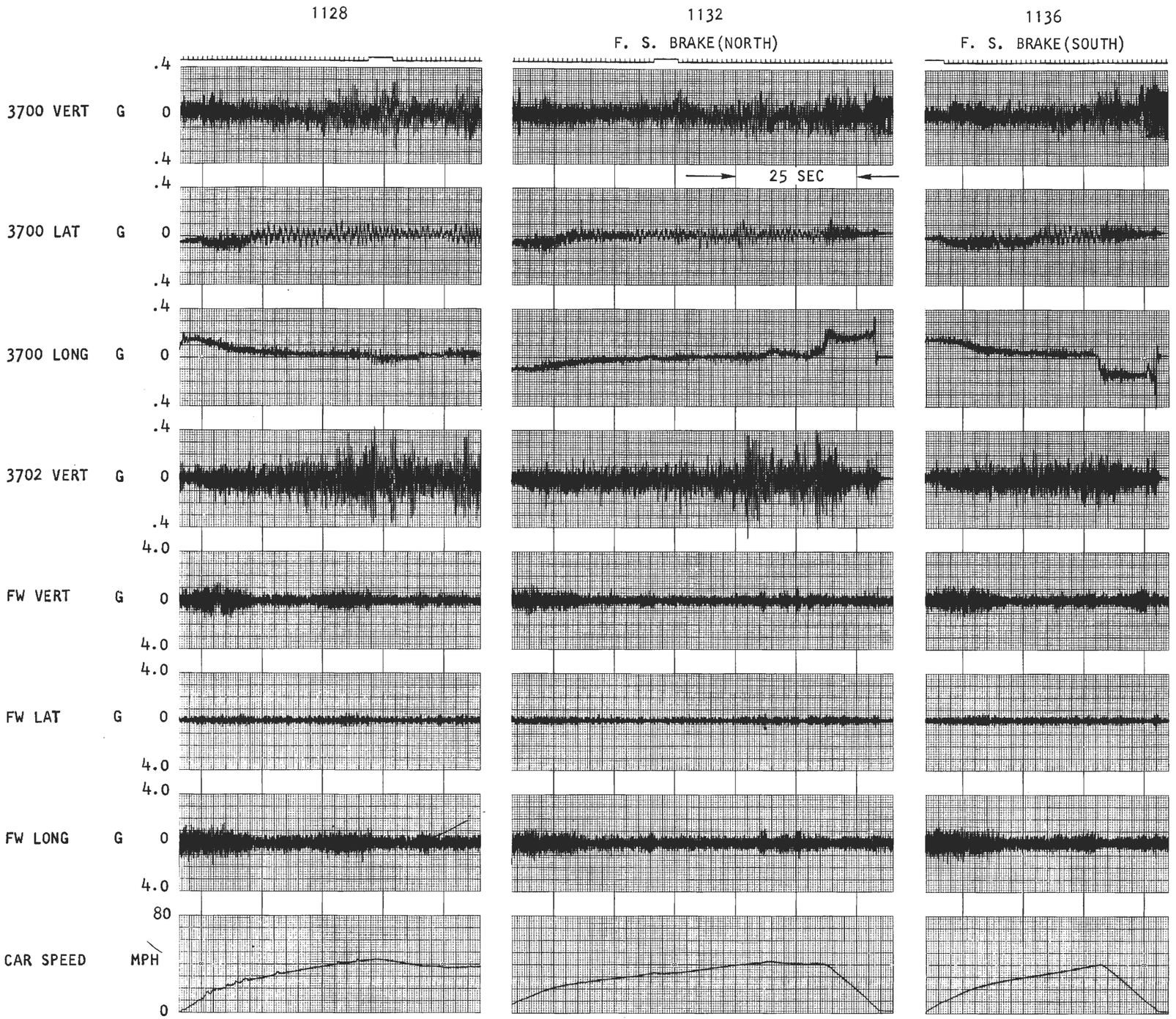

Figure 28. Continued, Sheet 5 of 10

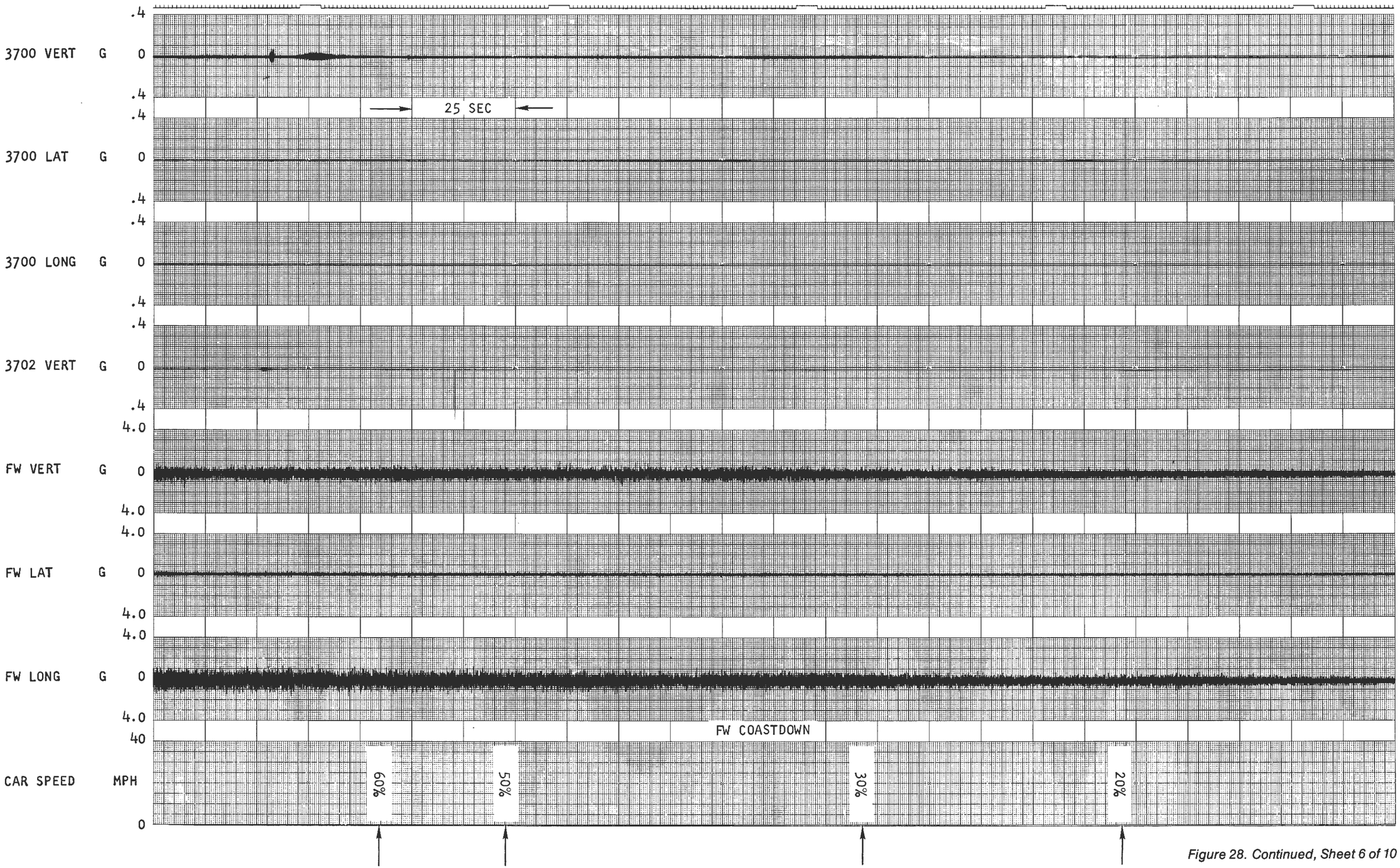

Figure 28. Continued, Sheet 6 of 10

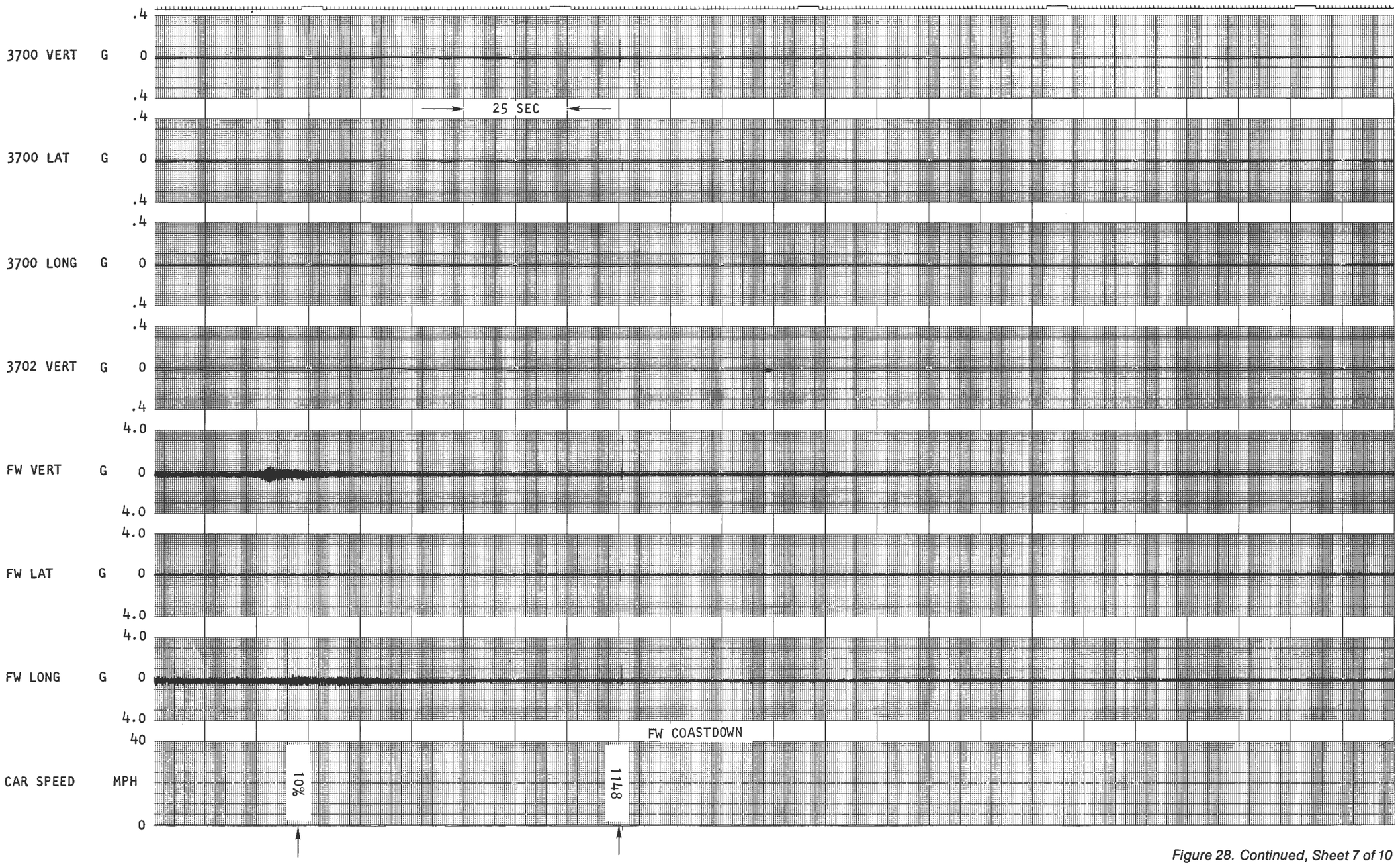

Figure 28. Continued, Sheet 7 of 10

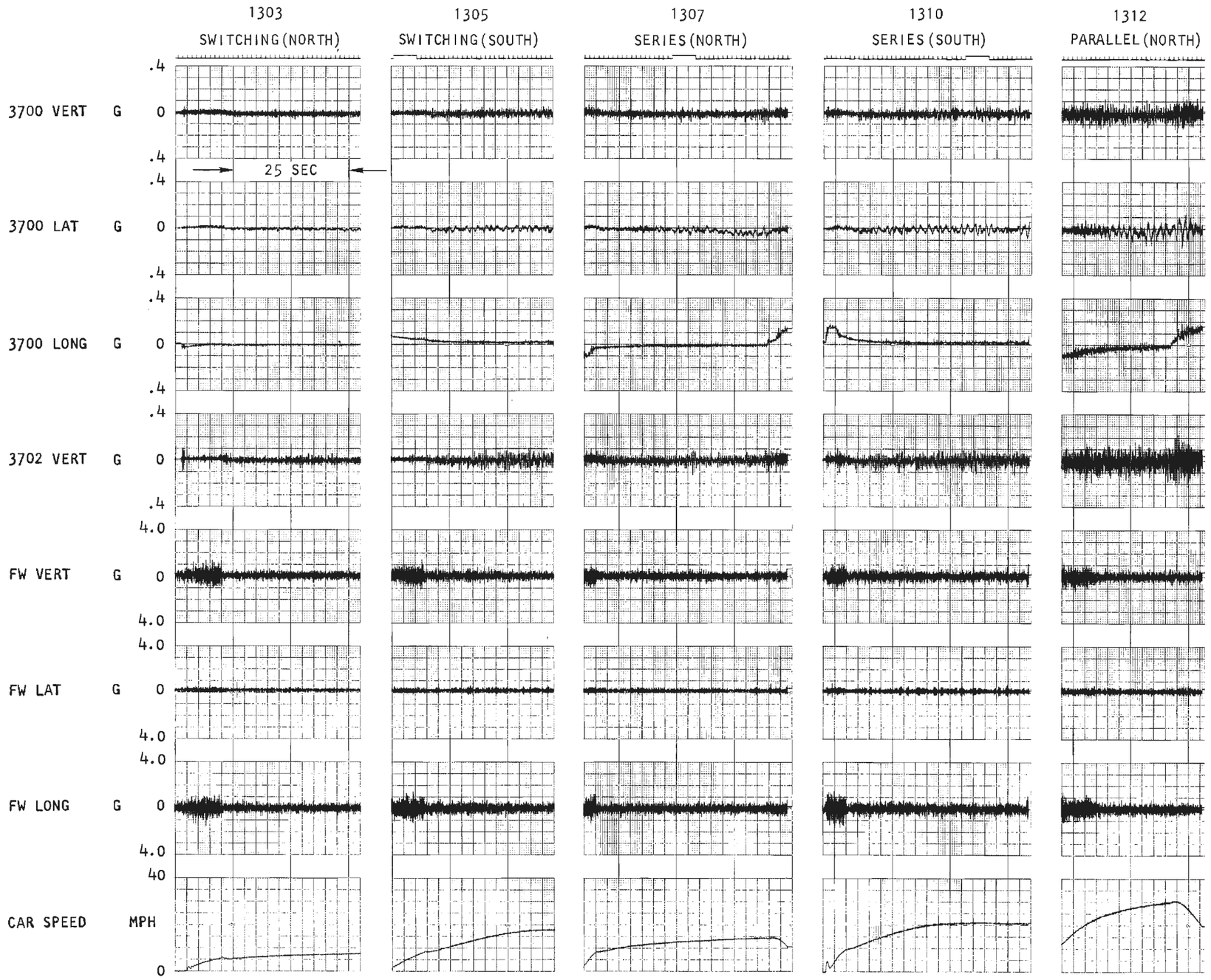

Figure 28. Continued, Sheet 8 of 10

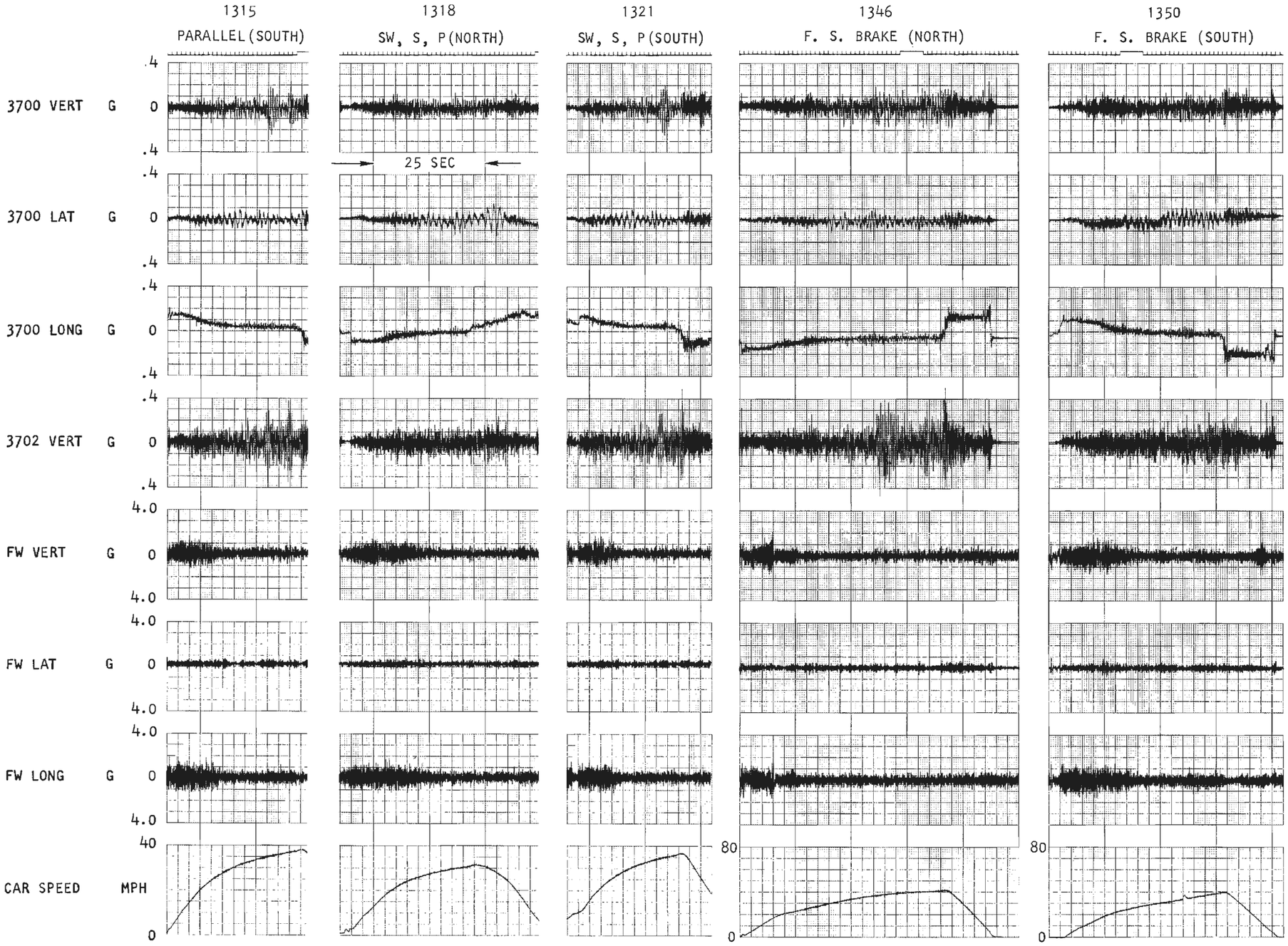

Figure 28. Continued, Sheet 9 of 10

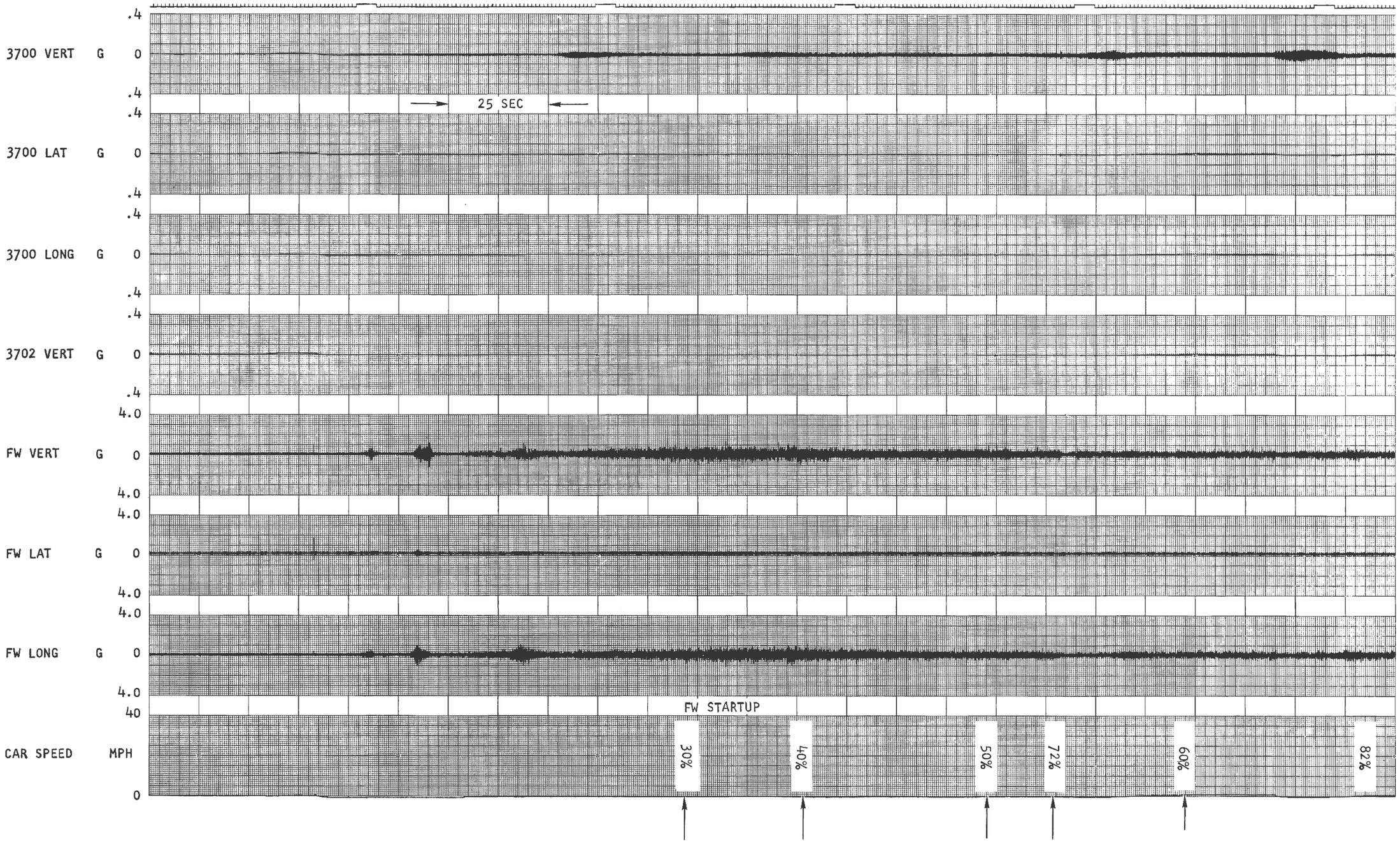

Figure 28. Continued, Sheet 10 of 10

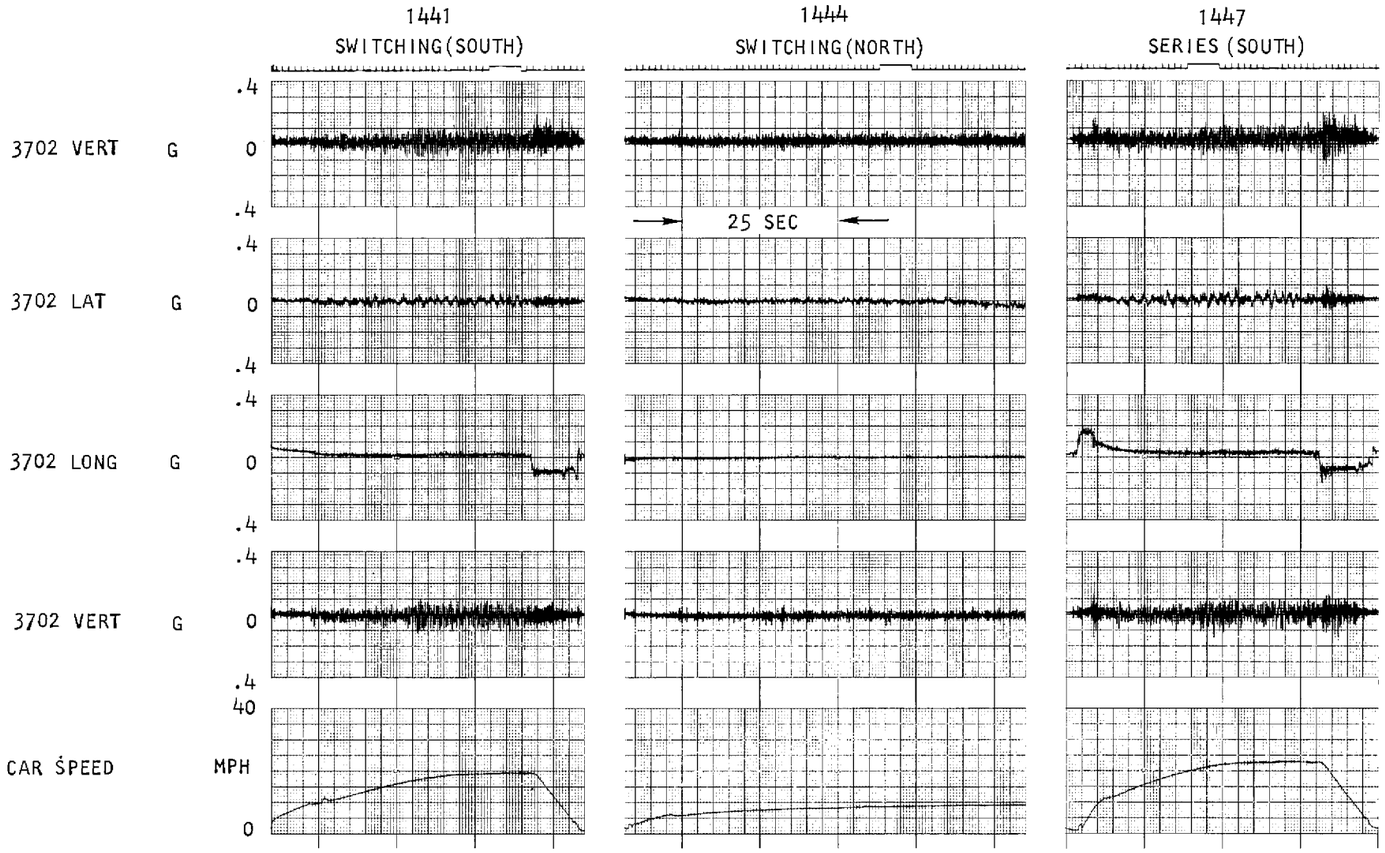

Figure 29. Interior Vibration Tests, Standard R-32 Car 3702, Sheet 1 of 3

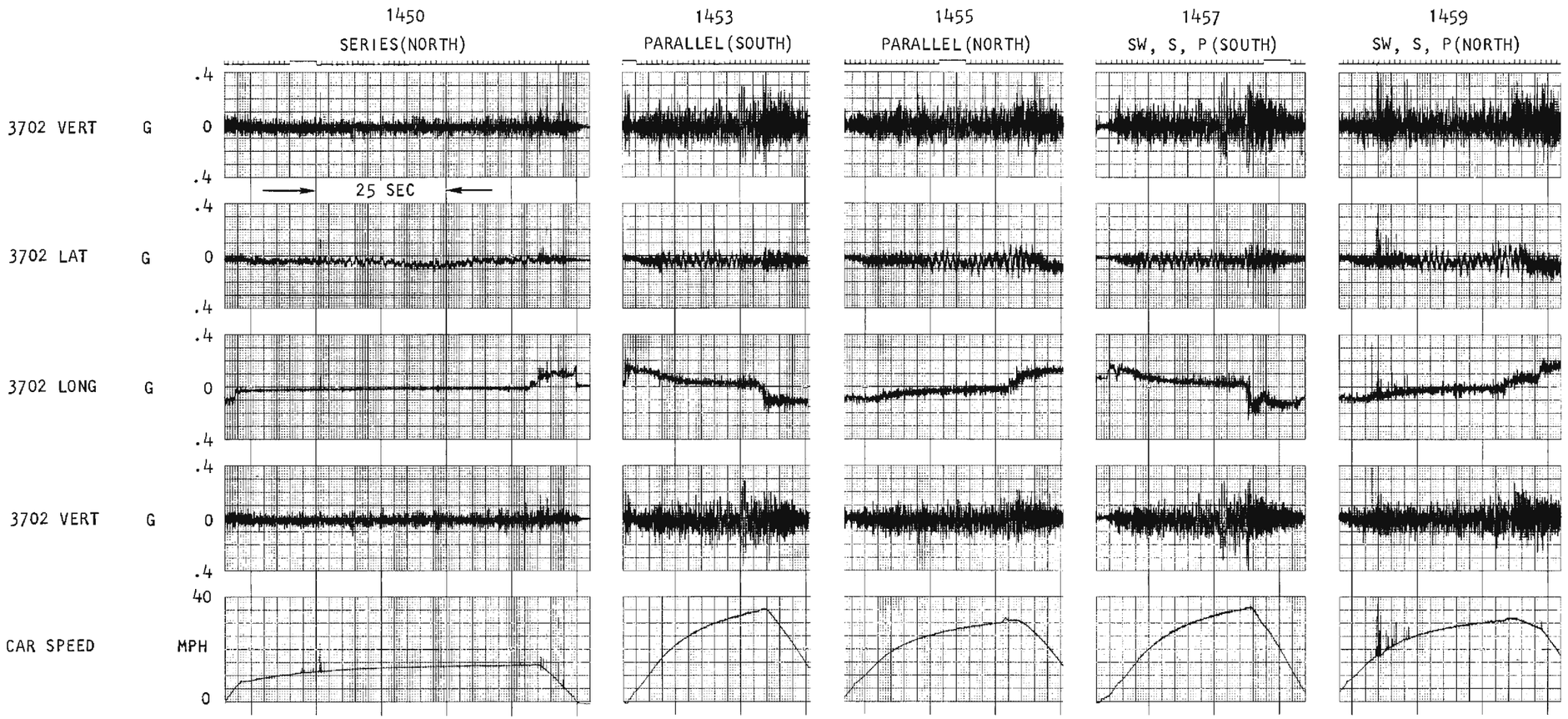

Figure 29. Continued, Sheet 2 of 3

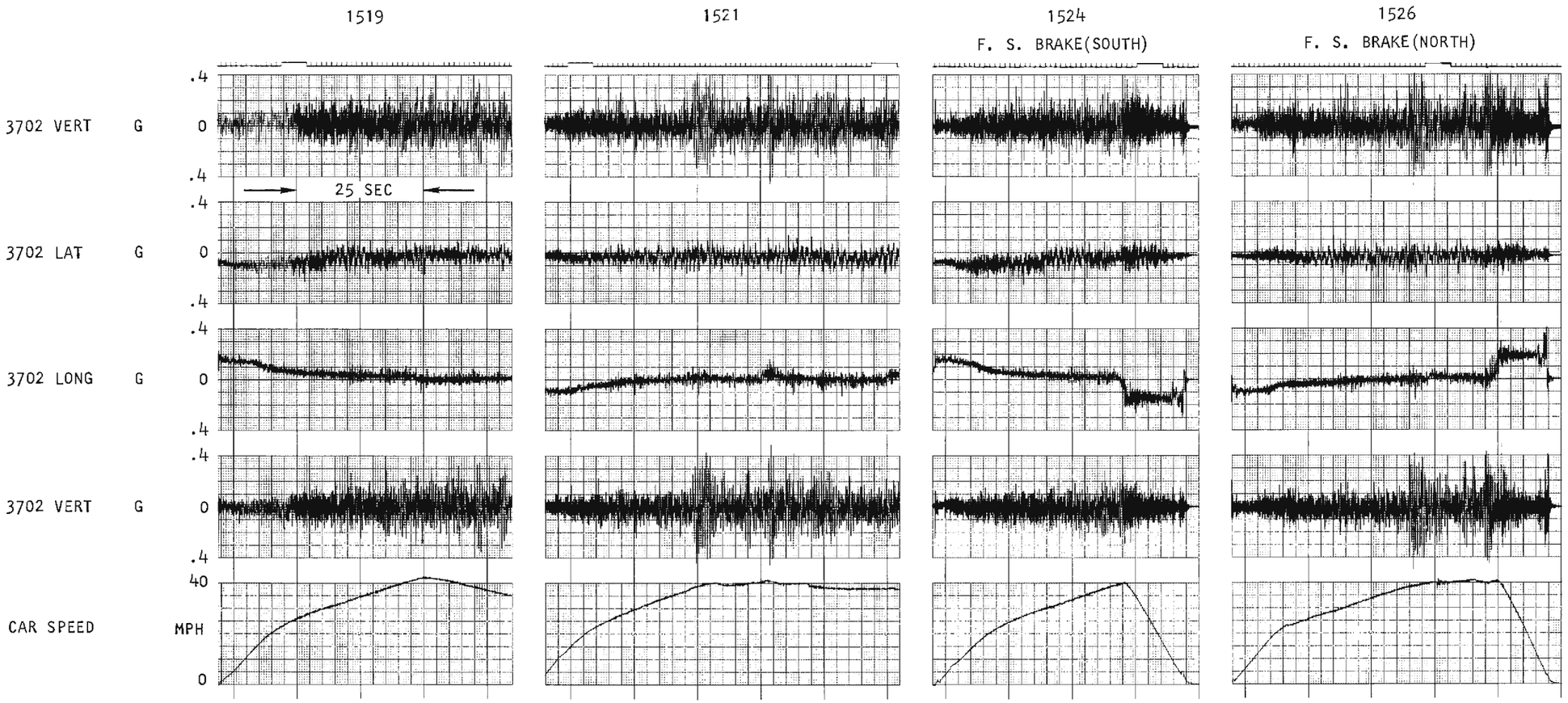

Figure 29. Continued, Sheet 3 of 3

1132

F. S. BRAKE (NORTH)

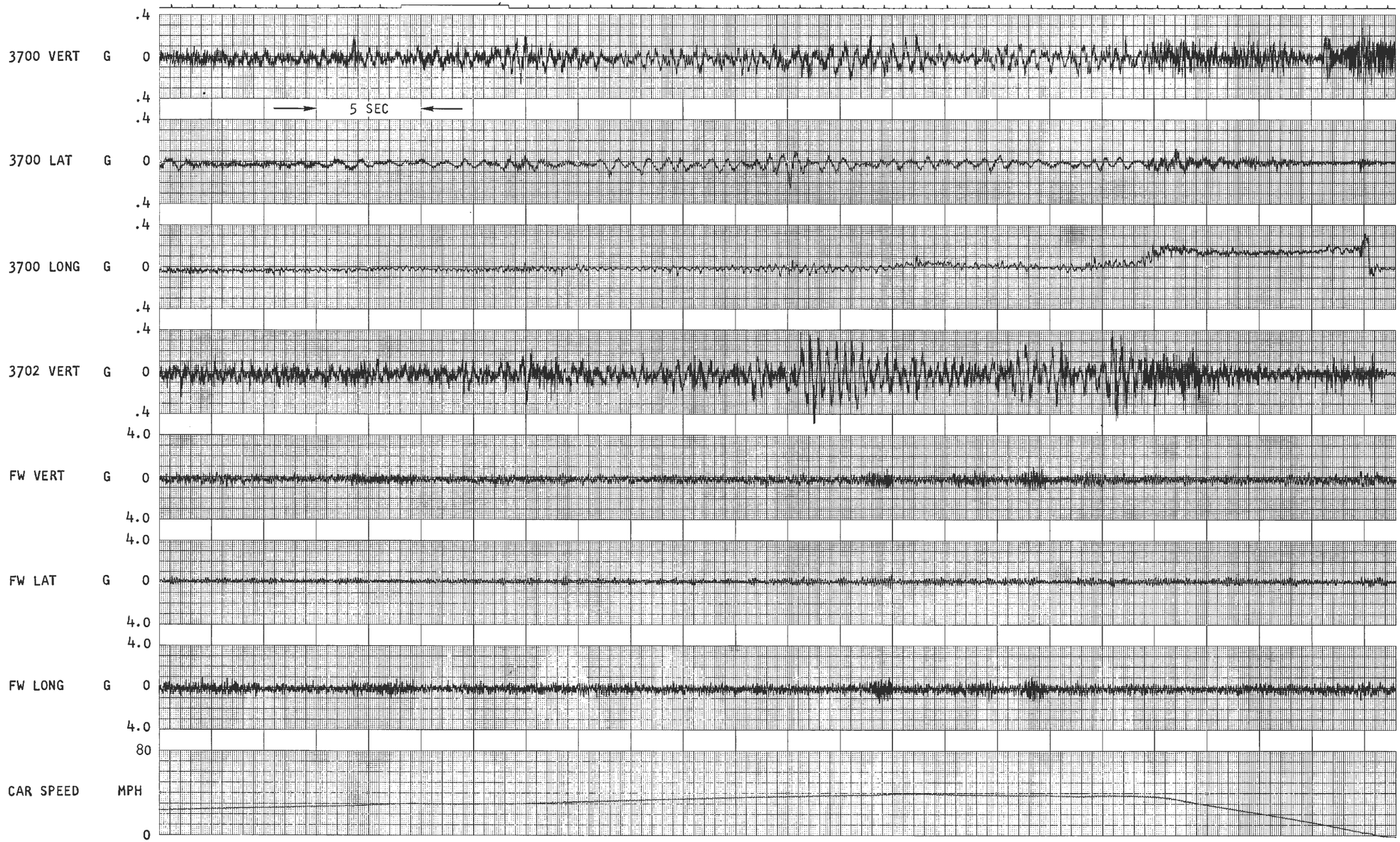

Figure 30. Interior Vibration Tests Run 1132, Expanded Time Scale

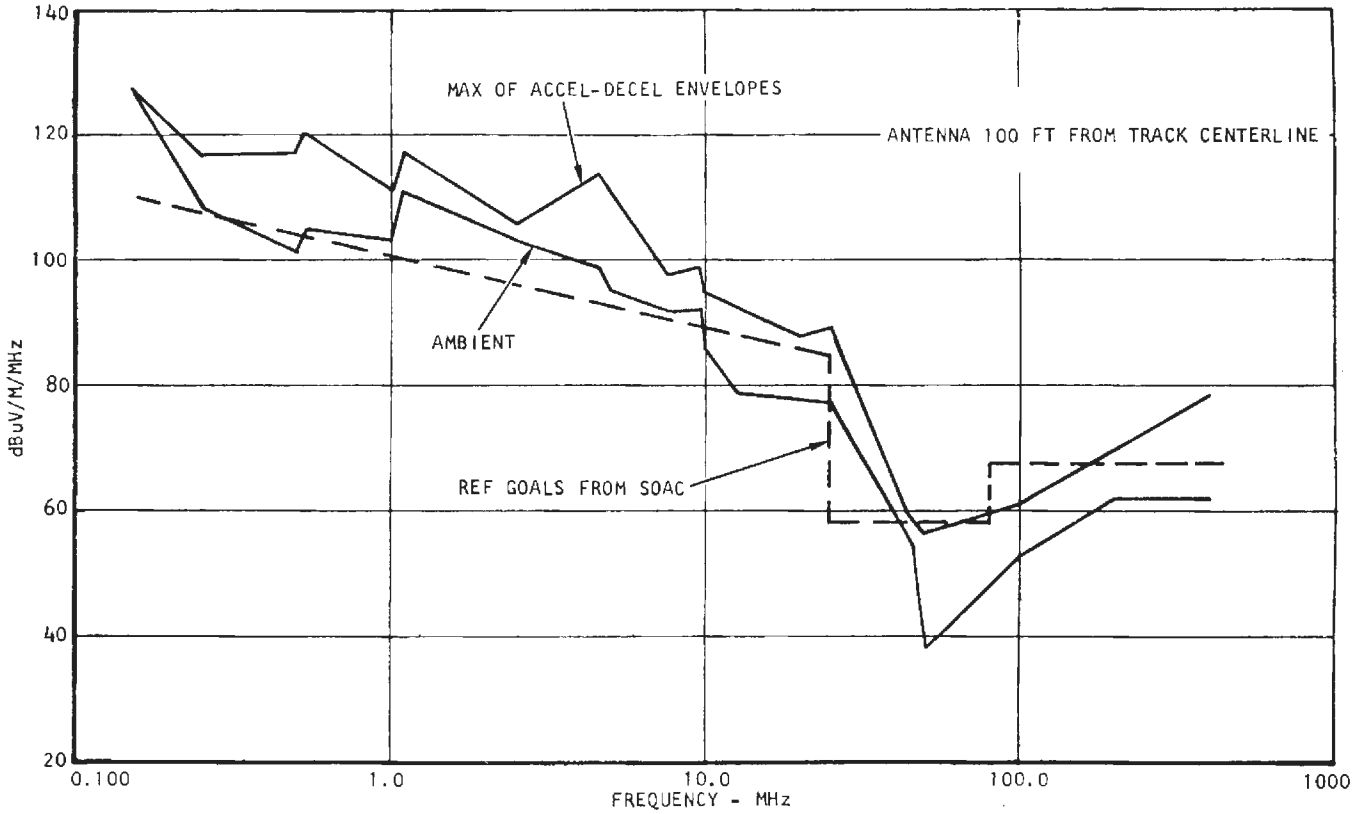

Figure 31. Broadband Radiated Emissions

installed for this test program was completely compatible with all varieties of wayside signal equipment on the New York City Transit System. As has been noted previously, the ES cars operated in revenue service during a six-month period without a safety-related incident.

While the ES cars were at Pueblo, the subject of electromagnetic interference (EMI) was investigated, as part of the Baseline Test series. The results of that testing are reported in Volume II of Reference 2, and will not be repeated herein. An analyzed sample of those measurements is included as Figure 31, which displays the maximum exterior emissions relative to ambient for an antenna located 100-ft from track centerline.

Energy storage unit (ESU) overload demonstration

The Energy Storage Unit overload test demonstrated the capability of the Energy Storage car to maintain continuous braking effort when the ESU has reached 100-percent capacity. Under conditions such as long downgrades or heavy loads, the energy generated during braking might exceed the storage capacity of the flywheels. Where this to occur, dynamic braking (using the braking resistors) would continue after a reconfiguration of the switchgear. Before the switchover, the armature currents must be reduced to a small value, and during the interim, a transition to air braking would occur to provide the commanded braking effort.

Two demonstration test runs are shown in Figure 32. Run number 1405 shows the transition described above. When the system recognizes the approach to the flywheel-full condition, it first ramps up the air brake (as shown by the brake pressure signal) and simultaneously reduces traction motor armature current. As the flywheel fills to 100 percent, flywheel fields are shut off (as evidenced by flywheel volts going to zero). After traction motor voltage is reduced to a small value, the switchgear makes the configuration change, and traction motor fields are reapplied. Simultaneously, the air brake pressure is reduced to maintain approximately constant braking effort. Finally, as the dynamic braking becomes ineffective (below 10 mph), the air brake again takes over to complete the stop.

In run 1410, the transition to dynamic braking is artificially inhibited to show the ability of the system to transition directly from energy storage to pneumatic braking. Such a situation would occur naturally if the ESU were to fill up at a car speed below approximately 10 MPH.

ESU shutdown modes and capacitor discharge

A series of tests was performed to verify:

(1) the functioning of the various protective circuits that served to cause the ESU to go into a quick

shutdown (QSD)

(2) the discharging of the chopper's capacitor bank to a safe voltage within a five-second interval after input power had been removed from the third rail shoes.

The results of a representative sample of these tests are shown in Figure 33 (stationary-car tests) and Figure 34 (moving-car tests). In each case, the arrow indicates the application of the simulated cause for shutdown.

The individual tests can be summarized as follows:

Run 1411: Third rail voltage interruption (or "gap") for 1.5 sec, approximately. Capacitor begins to discharge and then recovers.

Run 1413: Third rail voltage removed. Capacitor discharges to 50 volts within 5 seconds.

Run 1456: QSD and reset. Flywheel goes into a "dynamic brake" mode before the simulated fault is corrected and the system resets.

Run 1208: QSD during acceleration

Run 1219: QSD during coast

Run 1230: QSD during full service brake

Run 1233: QSD during emergency brake

Note in Figure 34 that the capacitor voltage takes a step increase when the chopper goes full "on" (as noted by the levelling off of the traction motor voltage). This anomalous behavior is not related to the testing.

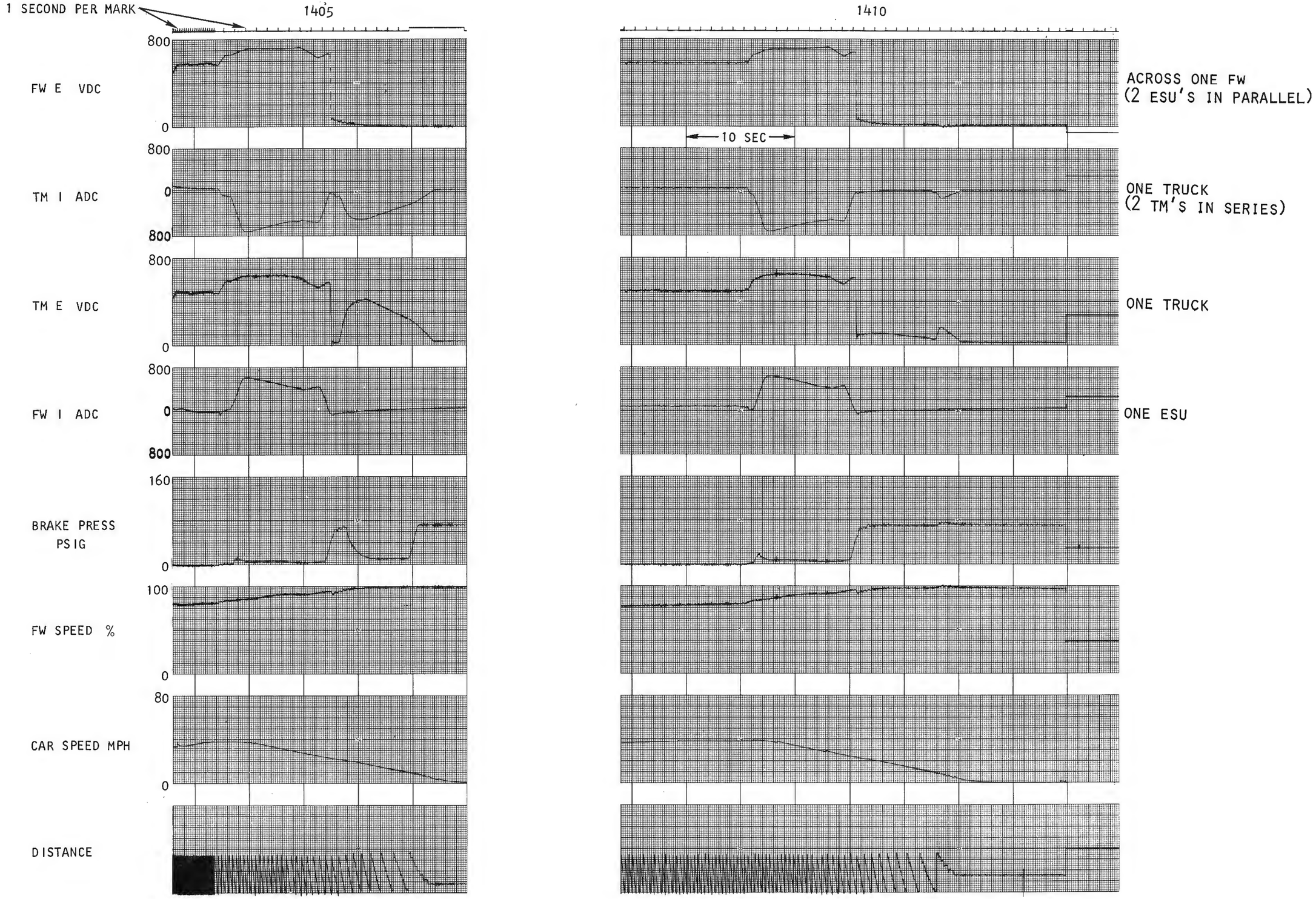

Figure 32. ESU Overload Demonstration

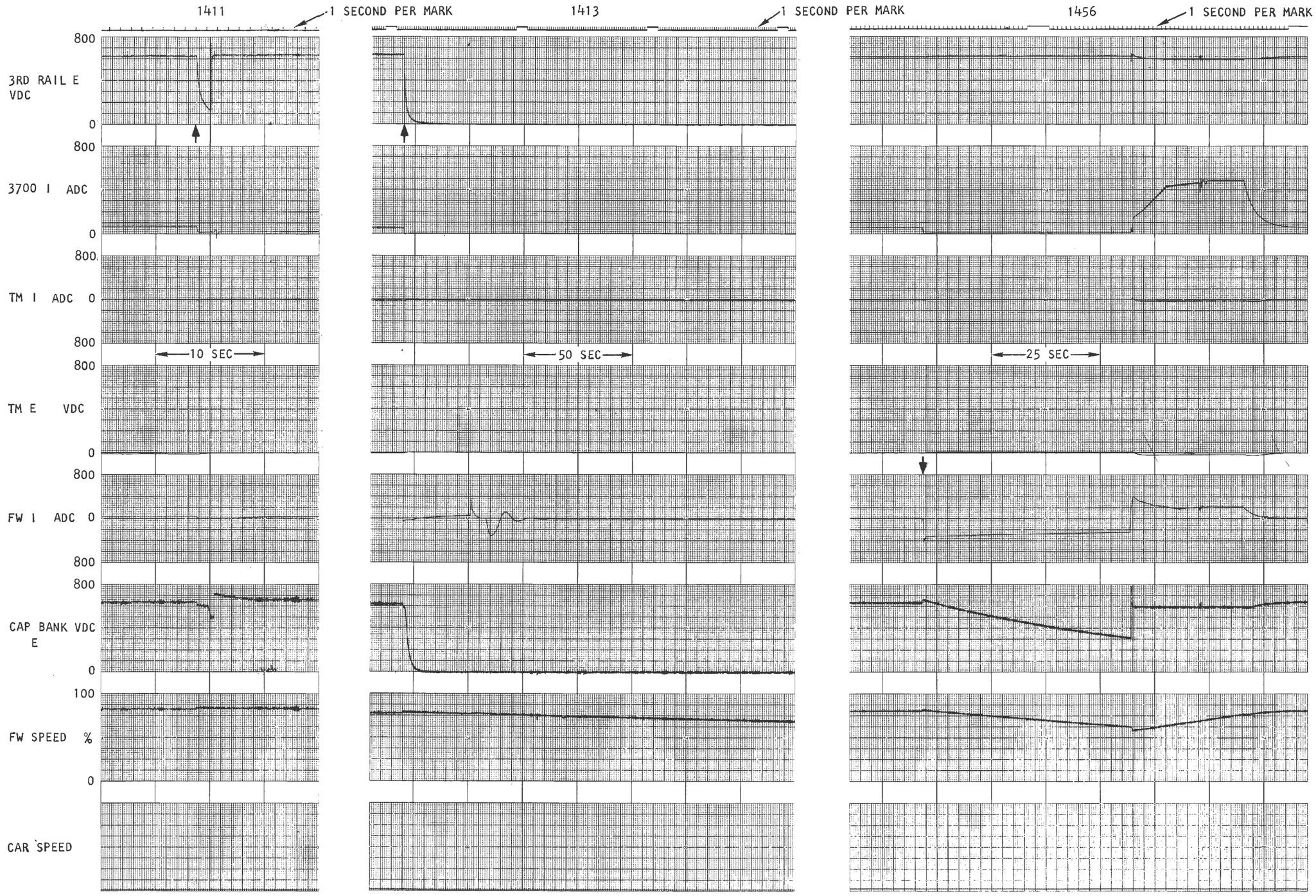

Figure 33. Shutdown Modes (stationary car)

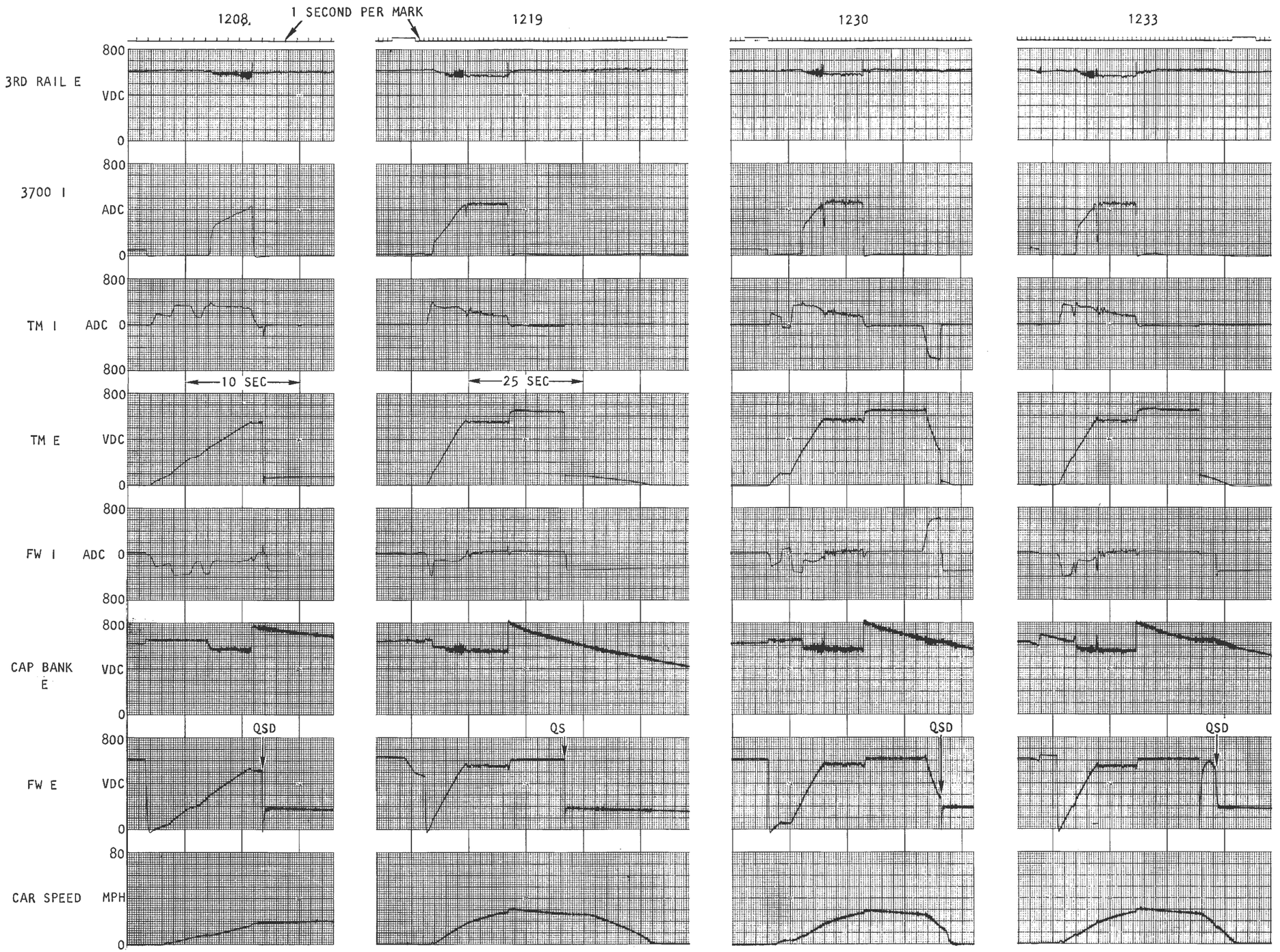

Figure 34. Shutdown Modes (moving car)

PART III — RELIABILITY AND MAINTENANCE

Revenue service experience

The Energy Storage Cars were scheduled to operate in revenue service for six months on a five-day-per-week basis, which worked out to a total of 127 days scheduled. During that period, ES Car 3700 operated for 13,900 miles and ES Car 3701 operated for 11, 400 miles (Car 3701 was hauled dead for 2,500 miles during one period, while awaiting a replacement ESU).

A daily record of the revenue service operations for the ES and Standard pairs is listed in Table 29. Three observations can be drawn from the table. First, the incidence of "resettable propulsion shutdowns" for the ES propulsion equipment decreased markedly toward the end of the test period. These random QSD's had plagued the cars throughout the development and test program and it was very gratifying to see that a true "fix" was eventually found.*

*It should be noted that a high incidence of such shutdowns in a fleet of cars would lead to a high frequency of propulsion resets by Motormen. This, in turn, would increase the chances of resetting into a shorted circuit (in a traction motor or switch group, for example), thereby escalating the degree and cost of the damage from the original fault. Thus, although the random QSD's were not considered to be "failures", they indicated a problem which very much needed to be resolved.

TABLE 29
Operations during Revenue Service Test period

			Car not available			Propulsion failure in service			Resettable propulsion shutdown		Explanation of lost run time
Date	Line	Hrs in service	ES pair	St'd pair	Other	ES pair	St'd pair	Other	ES pair	St'd pair	
Feb. 24*	B-AA	18:48							7	0	
25	B-AA	19:28							13	0	
26	B-AA	13:29				3700			5	0	ESU #2, gear shaft key
27	—	0:00	3700						—	—	ESU changeout
Mar. 1	B-AA	19:20							2	1	
2	B-AA	19:10							0	2	
3	B-AA	18:34							1	1	
4	B-AA	18:58							1	2	
5	B-AA	19:55							1	0	
8	D	16:47							0	0	Def. drum switch (doors)
9	D	19:23							0	1	
10	D	18:27							0	0	
11	D	18:14							0	0	
12	D	17:54							1	2	
15	N	12:40					3702		4	0	Cam controller
16	—	0:00		3702					—	—	In shop for above
17	N	8:22				3701			5	0	ESU #1, vac seal
18	—	0:00	3701						—	—	Awaiting drop table
19	—	0:00	"						—	—	Awaiting drop table
22	—	0:00	"						—	—	ESU reassembly problems
23	—	0:00	"						—	—	Install ESU
24	RR	17:36							0	0	
25	—	0:00		both					—	—	"B" Inspection
26+	RR	7:37						3459	0	0	
29	N	2:26				3700			1	0	TM #1, loose pole pc
30	—	0:00	3700						—	—	Diagnosis of above
31	—	0:00	"						—	—	"
April 1	—	0:00	"						—	—	"
2	—	0:00	"						—	—	"
5	—	0:00	"						—	—	"
6	—	0:00	"						—	—	Replace motor
7	—	0:00	"						—	—	"
8	N	6:02							0	0	

*20 hour operation scheduled + Changed to 12 hour operation

TABLE 29
Operations during Revenue Service Test period (continued)

Date	Line	Hrs in service	Car not available: ES pair	Car not available: St'd pair	Car not available: Other	Propulsion failure in service: ES pair	Propulsion failure in service: St'd pair	Propulsion failure in service: Other	Resettable propulsion shutdown: ES pair	Resettable propulsion shutdown: St'd pair	Explanation of lost run time
April 9	N	11:50							0	0	
12	N	9:27							2	0	Door prob's (3:16)
13	N	3:57				3701			0	0	Def. auxil. M/A
14	—	0:00	3701						—	—	Replace M/A
15	—	0:00	3701						—	—	"
16	N	11:57							2	0	
19	N	12:50							0	0	
20	N	11:31							1	1	
21	N	9:05				3701			2	0	M/A fuse blown
22	N	11:43							0	0	
23	N	11:27							2	0	
26	N	12:03							0	0	
27	N	12:10							0	0	
28	N	11:45							0	1	
29	N	11:35							0	0	
30	N	11:40							0	0	
May 3	N	12:06							0	0	
4	N	11:39							0	0	
5	N	8:26							0	0	window broken
6	N	11:52							0	0	
7	N	2:20				both			0	0	OV detector latched
10	A	1:37				"			0	0	"
11	—	0:00	3701						—	—	circuit mod for above
12	A	11:39							1	0	
13	A	7:14							0	1	vandalism clean-up
14	A	12:34							1	0	
17	—	0:00		3703					—	—	Compressor changeout
18	A	11:59				3701			0	0	TM's field short circuit
19	A	0:56				"			0	0	"
20	—	0:00	3701						—	—	Awaiting new TM's (2)
21	—	0:00	"						—	—	
24	—	0:00	"						—	—	
25	—	0:00	3701						—	—	Awaiting new TM's (2)
26	—	0:00	"						—	—	
27	—	0:00	"						—	—	Install motors
28	—	0:00	"						—	—	
June 1	A	2:00				3700			0	0	PDR failure (FW)
2	—	0:00	3700						—	—	"
3	—	0:00	"						—	—	"
4	—	0:00	"						—	—	"
7	A	1:51				3700			3	0	ECU power supply failure
8	—	0:00	3701						—	—	ESU #1, vac seal
9	—	0:00	"						—	—	Trouble shooting
10	—	0:00	"						—	—	"
11	—	0:00	"						—	—	Changeout ESU
14	—	0:00							—	—	Test circuits on Sea Beach trk
15	—	0:00							—	—	"
16	—	0:00	3700						—	—	Dyn brk grid open

TABLE 29
Operations during Revenue Service Test period (continued)

Date	Line	Hrs in service	Car not available: ES pair	Car not available: St'd pair	Car not available: Other	Propulsion failure in service: ES pair	Propulsion failure in service: St'd pair	Propulsion failure in service: Other	Resettable propulsion shutdown: ES pair	Resettable propulsion shutdown: St'd pair	Explanation of lost run time
June 17	—	0:00	3700						—	—	Test on Sea Beach track
18	A	6:19				3701			0	0	Vibration switch S/D
21	A	12:03							0	0	
22	A	12:23							0	0	
23	A	3:46							0	0	3rd rail volt surge damage to whole train
24	A	12:22				3701			0	0	Vibration switch S/D
25	A	12:10				3701			0	0	"
28	—	0:00	both						—	—	Scheduled maintenance
29	—	0:00	both						—	—	TM brush check
30	A	12:07							0	0	
July 1	A	11:55							0	1	
2	—	0:00							—	—	Change instrumentation
6	A	13:20							0	0	
7	A	12:11				3701			0	0	ESU #2, vac seal (*ran with 3701 dead 7/8 to 7/29*)
8	A	12:36	3701						0	0	
9	A	6:59	3701						0	0	
12	A	12:06	"						0	0	
13	A	12:03	"						0	0	
14	A	11:45	"						0	0	
15	A	11:17	"						0	0	
16	A	12:25	"						0	0	
19	D	11:02	"						0	0	
20	D	13:27	"						0	0	
21	D	12:20	"						0	0	
22	D	11:11	"						0	0	
23	D	12:12	"						0	0	
26	B	1:44	"			3700			0	0	ESU #1 and #2, raised bars
27	—	0:00	both						—	—	Resurface commutators
28	—	0:00	"						—	—	"
29	B	4:50	3701			3700			0	0	Control circuitry problem (3700)
30	—	0:00	both						—	—	Replaced ESU (3701)
Aug 2	B-AA	11:00							0	0	
3	D	12:10							0	0	
4	D	11:31							0	0	
5	D	9:26						X	0	0	
6	D	11:34							0	0	
9	RR	12:43							1	0	
10	RR	12:19							0	0	
11	RR	7:26				3701			1	0	ESU #2, broken brushes
12	RR	12:09							0	0	
13	RR	10:43									
16	RR	10:45							0	0	
17	RR	12:16							0	0	
18	E	0:00			X				—	—	Scheduling problems
19	E	4:15							0	0	"
20	E	12:07				3700			0	0	ESU #2, vac seal

Second, there was a significant loss of run time due to the problems of dealing with a small number of "special" cars. In particular, all shop work had to be performed at night, which meant that *two* days of potential running were lost each time that shop work was required. In addition, five days were lost while awaiting replacement parts (not including the 18 days of operation with Car 3701 in need of a replacement ESU).

Third, and most important, problems of one sort or another caused the cancellation or curtailment of 82 out of the 127 days (65%). In order to develop a better understanding of this reduction of service time, a breakdown of the 127-day test period is presented in Figure 35. The figure shows an allocation of each of the 127 days into a series of increasingly refined categories.

In summary, 45 days (35% of the 127-day period) were uneventful and an additional 13 days (11%) were marred only by the fact that Car 3701 was non-propulsive, due to an ESU needing replacement. Thus, after a full two years of on-car testing and development, only 46% of the days in revenue service could be operated in any sense of completeness.

To gain a better idea of the relative responsibility for the different components of lost time, the items in Figure 35 were re-grouped:

- The category relating directly to the ES equipment (including original failures and repairs & inspections) accounted for 25 lost or abbreviated days (20% of total service period).
- Troubleshooting time, which indicates the ability of the Garrett personnel to respond to problems, accounted for 14 days (11%).
- Items which could be ascribed to the prototype nature of the program (repeats of failures, shop scheduling time, and parts availability problems) caused the loss of 17 days (13%).
- Propulsion failures and repairs & inspections on the Standard pair accounted for 3 days (2%).
- Non-propulsion failures and repairs, along with an assortment of other irrelevant items resulted in 10 lost days (8%).

Thus the Revenue Service Test operations can be categorized as 46% successful days, 31% lost or curtailed due to Garrett equipment or technical support, 13% missed because of small-scale testing problems, and 10% lost because of conventional operational difficulties.

The failures of the propulsion equipment on the four test cars are listed in Table 30. Note that the Standard pair suffered only one propulsion failure during the

TABLE 30
Summary of propulsion system failures during Revenue Service Test period

Car	Date	Description	Operating Hrs
3700 (ES)	2/26	ESU #2, broken planetary gear shaft key	52
	3/29	TM #1, loose interpole	287
	5/7,10	Alternator overvoltage relay latched (non-resettable)	494
	6/1	FW field supply (PDR) failure	541
	6/7	Power supply for electronics failed	542
	6/16	Dynamic brake grid failed open	546
	7/26	Raised bars, both ESU motors	792
	7/29	ESU speed balance control circuit problem	797
	8/20	ESU #2, vacuum seal leakage	947
3701 (ES)	3/17	ESU #1, vacuum seal leakage	259
	4/13	Auxiliary M-A, bearing failure	318
	4/21	Auxiliary M-A, blown fuse	364
	5/7,10	Alternator overvoltage relay latched (non-resettable)	494
	5/18	TM field shorted (2 motors)	538
	6/8	ESU #1, vacuum seal leakage	543
	6/18	ESU vibration sensor failure	549
	7/7	ESU #2, vacuum seal leakage	651
	8/11	ESU #2, motor brushes broken	739
3702 (Standard)	3/15	Controller failure	251
3703 (Standard)		(None)	

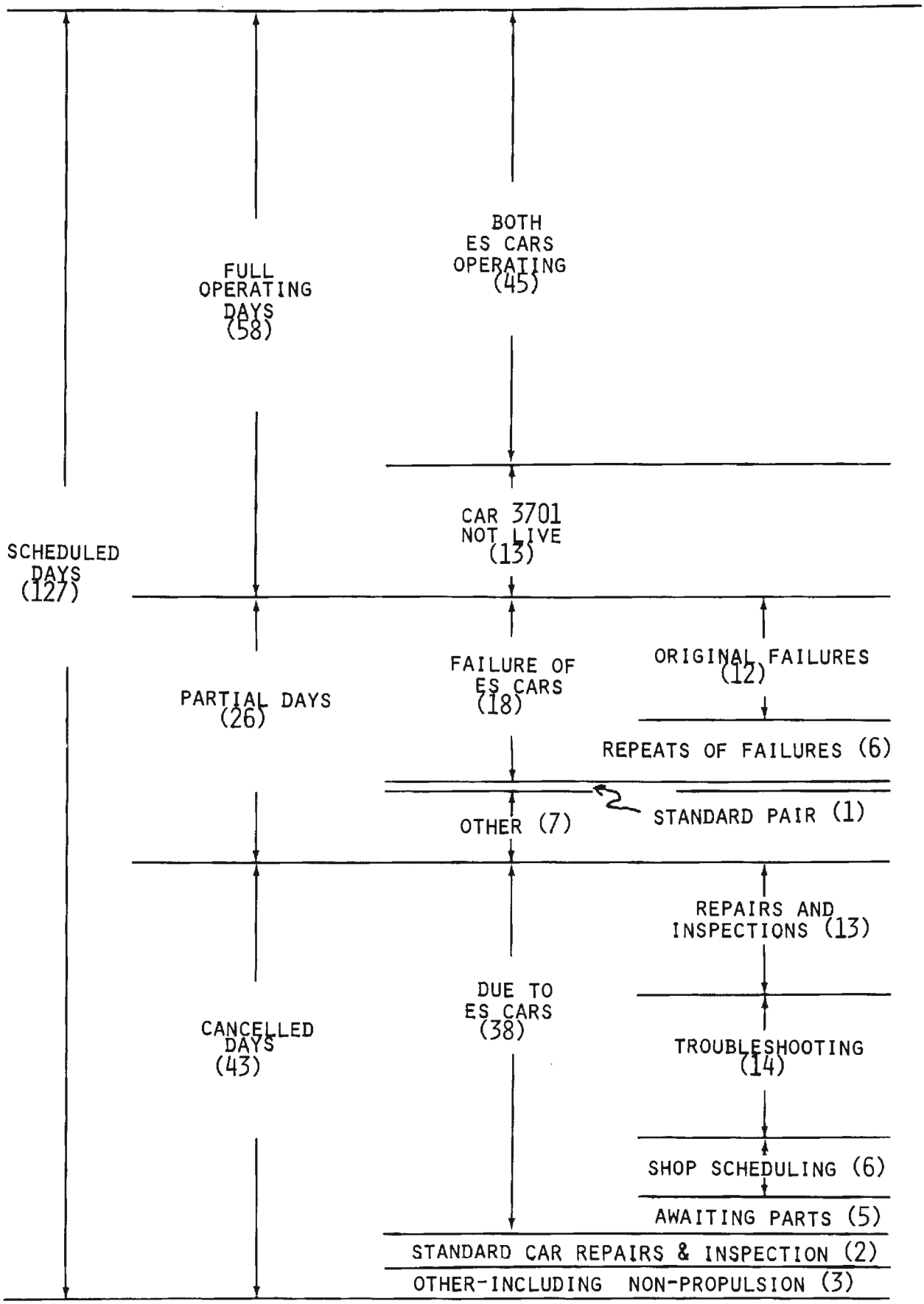

Figure 35. Analysis of Lost Run Time During Revenue Service Test Period

six-month period. This is clearly an attribute of a mature and simple equipment design. It must be realized, further, that the R-32 equipment was not newly-manufactured, which makes its relative performance that much more impressive.

As can be seen in Table 30, some the ES system failures were repetitive. It should be assumed that, if this had been a production program, the first of each failure would have led to a redesign and a product improvement. Thus it is informative to analyze the system's performance on that basis. That is, one can ask the question: what would the long-term reliability trend have been if it could be assumed that no problems would have recurred, once they had been detected the first time?

This question is addressed in the reliability progress chart ("Duane Plot" — Reference 8) shown in Figure 36 and in the tabulation of the failure rate in Table 31. In both cases, only the original failure of each kind is included. The conclusion that can be drawn from this information is that the ES equipment had "matured" to a Mean Time Between Failures of 120 hours, at the

TABLE 31
ES propulsion system failure rate analysis

Cumulative Original Failures	Car Hours	Failures / 1000 Car-hours	Cumulative MTBF
1	104	9.62	104 hr
2	518	3.86	259
3	574	5.23	191
4	636	6.29	159
5	728	6.87	146
6	988	6.07	165
7	1076	6.51	154
8	1082	7.39	135
9	1084	8.30	120
10	1092	9.16	109
11	1098	10.0	100
12	1443	8.32	120
13	1448	8.98	111
14	1624	8.62	116
14 (end of test)	1748	8.01	125

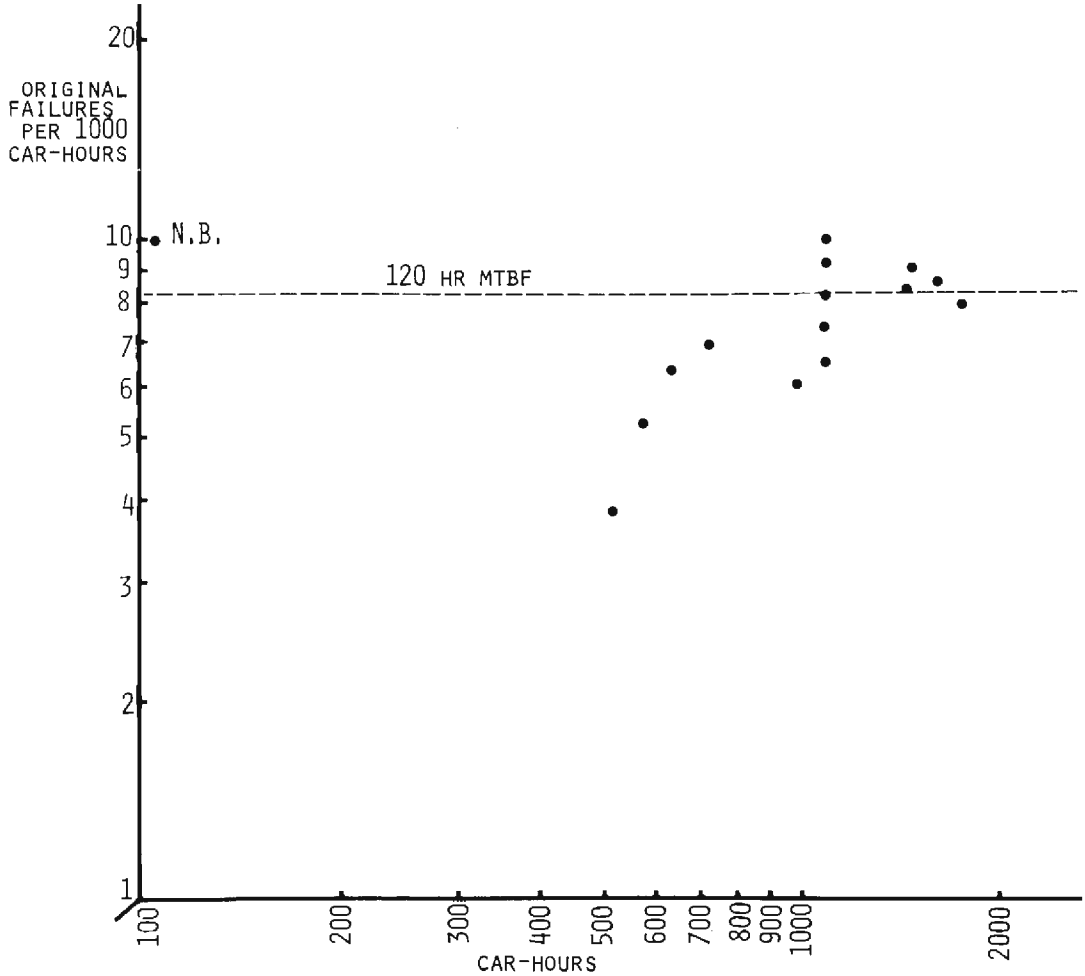

Figure 36. Reliability Progress Chart for ES Propulsion System During Revenue Service Test Period

conclusion of the Revenue Service Test. In typical service on the New York subway system, this would be equivalent to a failure interval of less than two weeks for each car, which would be unacceptable, of course.

The failure history of the Energy Storage Units throughout the entire program is given in Figure 37. It will be noted that a design problem was discovered while the cars were at Pueblo. Inadequate roller clearances and lubrication on the main flywheel bearings resulted in destruction of roller cages. Changes in the oil spray pattern and in the choice of bearing were made on all units and the problem did not recur.

Maintenance

Since it was concluded at an early point in the program that the specific ES equipment which was under test would never be put into production without major design changes, no effort was made to analyze the details of equipment maintenance costs. Nonetheless, some general conclusions relevant to maintenance and maintainability could be drawn from the test program experience.

The primary observation was, of course, that there was too great a need for maintenance, due to an extremely short MTBF. To a large degree, this high failure rate could be ascribed to (1) an overly complex system design and (2) a number of examples of weak component design.

As has been discussed earlier, the entire system could be simplified by making more complete use of the on-board energy storage devices. In a propulsion system similar to that of UMTA's ACT-1 Car (modified for a 50 MPH maximum speed) only one ESU would be required and the chopper and its associated equipment would be eliminated. This amounts to a very substantial reduction in the number of components and in the interactions between them. No longer would it be necessary, for example, to monitor and control energy balance between two sources (ESU's) on a car, nor would it be required to generate chopper firing commands.

On the subject of detailed component design, some of the experience gained in the ES program has resulted in substantial improvements in components being used on the ACT-1 Cars. In particular, the vacuum seal design has been changed from the face seal in the R-32 system, with its relatively high interface speeds, to a smaller diameter radial design for the ACT-1 ESU.

An additional lesson that was learned in the present program was that of the need for a more *maintainable* design for the ESU. In particular, twice during the program (including one instance prior to installation of equipment under the cars) there were failures of the oil-vacuum pump. Unfortunately, the ESU design resulted in this pump being incorporated internally to the ESU gear unit between the flywheel and its motor. This meant that the entire ESU had to be removed from the car and disassembled in order to gain access to the pump. The ACT-1 ESU design has the pump mounted at one end of the ESU.

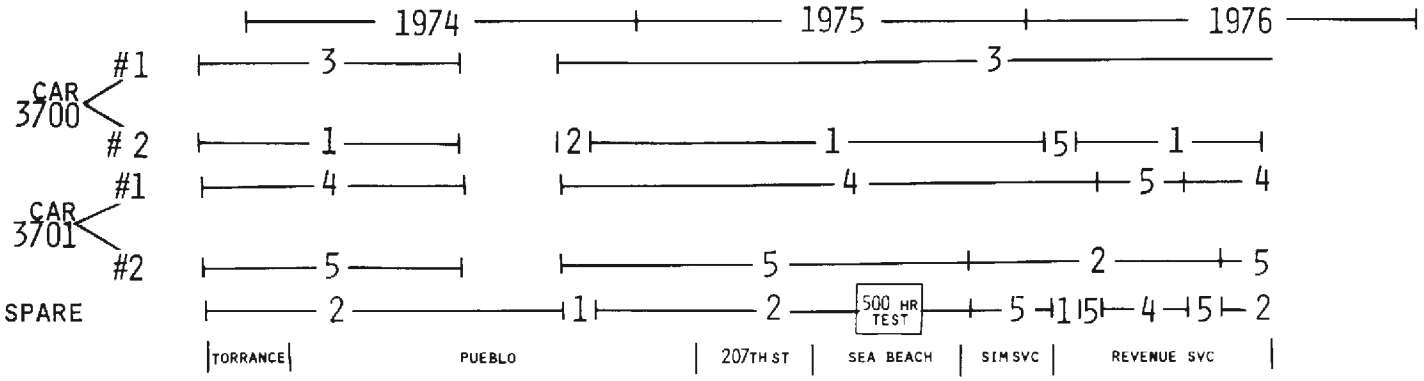

Figure 37. Energy Storage Unit Failure Chronology

7/11/74	*Main Roller Bearings (all units modified and re-installed 11/74)*
12/ 2/74	*Shorted ESU motor field*
11/12/75	*Broken Oil Pump Shaft Key*
2/ 3/76	*Leaking Main Oil Seal on Gear Unit*
2/26/76	*Rolled Planetary Gear Shaft Key*
3/17/76 *6/ 8/76* *7/ 7/76* *8/29/76*	*Leaking Vacuum Seal*

Note: Numbers on chart lines indicate the serial number of the ESU.

APPENDIX A — NYCTA ROUTE INFORMATION

This part of the report contains detailed information regarding the routes and trackage traversed by the Energy Storage Cars during all phases of the New York City testing.

Part A-1 provides information on the New York City Transit Authority routes which were covered during the Simulated Service and Revenue Service tests. The lines are listed alphabetically and for each line the stations, station spacings, and approximate running times are given. (see Table A-1)

Three comments are offered regarding these listings:

1. The B and AA lines are generally operated by the same train equipment during different times of the day. (This is why the test data for these lines were reported in combination). Under normal circumstances, a train begins the day in B-line service at Stillwell Avenue, travels to 168th St. in Manhattan, operates in AA-line service during the midday and returns to B-line service between Stillwell Avenue and 57th St. during the evening and night.

2. The R-J line, which was operated in Simulated Service, is a synthetic route not actually used in revenue operations. Information regarding the R-J route can be constructed by joining the J and RR routings at Broad Street.

3. Several routes that were in operation during the testing period were modified by the NYCTA immediately thereafter. In particular, the E-line's southern terminus is always Hudson Terminal (World Trade Center) and the E train is always local in Manhattan. The EE-line has been replaced by the extension of the N-line to Continental Avenue. (Note that the lengthening of the N train routing is favorable to the ES concept, since it increases the ratio of running time to terminal layover time). During certain off-peak hours, the A train operates locally (in place of the AA train) in Manhattan.

Part A-2 provides the basis for the designation of the A-line as most representative of the NYCTA B-Division (IND-BMT) and gives more detail on the A-line trackage.

In Figure A-2 the running speed versus average station spacing is plotted for all of the principal NYCTA routes entering Manhattan. It will be noted that the points can be associated into three groups: in the middle are the lines which enter Manhattan via bridges (F, N, D and B), the two other groupings include primarily local routes and primarily express routes. (It must be kept in mind that the routes analyzed are those which were in effect prior to September 1, 1976.)

In the effort to designate one line to be considered as typical of the entire B-Division, it was deemed inappropriate to select one of the Manhattan Bridge lines, since so much of their run was affected by the bridge crossing (which is not common to any of the other routes). Therefore, the A-line to Lefferts Boulevard was chosen, since its average station spacing is typical, even though its average speed is somewhat on the high side of the norm.

Table A-2 lists the A-line track profile parameters of grade, limiting speed, curvature and tunnel configuration versus distance from Lefferts Boulevard to 207th Street. This information was used by Garrett in their computer simulation of the A-line.

Part A-3 provides a track profile diagram of the Sea Beach test track. This trackage is on a portion of the N-line, where the two center tracks are used for testing (including performance checks of cars emerging from the Coney Island Shops as well as acceptance tests for new cars arriving on the NYCTA property) while the two outer tracks are used for revenue service. The center tracks had been used previously for express service to Coney Island at a time in New York City's history when the volume of passenger traffic warranted such service. (see Figure A-3)

TABLE A-1
Listings of NYCTA Division B routes through Manhattan

A-Line (Manhattan, Brooklyn and Queens)

Stations	Miles	Run Time (Min.) Rush Hour	Non-Rush Hour
207th Street	.00	0	0
200th Street	.42	1½	1½
190th Street	1.01	3½	3
181st Street	1.52	5	4½
175th Street	1.86	6½	6
168th Street	2.35	9	8
145th Street	3.50	12	11
125th Street	4.54	15	14
59th Street	7.89	22	21
42nd Street	8.81	25	23½
34th Street	9.16	26½	25
14th Street	10.05	29	27
West 4th Street	10.70	31	29
Canal Street	11.52	33½	31½
Chambers Street	12.05	35	33
Broadway-Nassau	12.41	36½	34½
High Street	13.63	39½	37
Jay Street-Boro Hall	14.24	41½	38½
Hoyt-Schermerhorn Sts.	14.61	43	40
*Lafayette Avenue	15.21	45	41½
*Clinton-Washington Aves.	15.69	47	43
*Franklin Ave.	16.18	48½	44½
Nostrand Ave.	16.54	49½	45½
*Kingston Ave.	17.03	51	47
Utica Avenue	17.56	52½	48½
*Ralph Avenue	18.08	54	50
*Rockaway Avenue	18.55	53	51
Broadway-East New York	18.90	56	52
*Liberty Avenue	19.51	58½	54½
*Van Siclen Ave.	19.96	60	56
*Shepherd Avenue	20.47	61½	57½
Euclid Avenue	20.91	63	59
Grant Avenue	21.35	65	61
Hudson Street	21.71	67	63
Boyd Avenue	22.11	68	64
Rockaway Blvd.	22.51	69	65
Oxford Avenue	22.84	70	66
Greenwood Avenue	23.21	71	67
Lefferts Blvd.	23.55	72	68

*Express trains do not stop at stations marked with asterisk

AA-Line (Manhattan)

Stations	Miles	Running Time
168th Street	.00	0 min
163rd Street	.33	1½
155th Street	.72	3
145th Street	1.15	5
135th Street	1.66	6½
125th Street	2.19	8
116th Street	2.64	9½
110th Street	3.00	11
103rd Street	3.35	12½
96th Street	3.70	14
86th Street	4.16	15½
81st Street	4.51	16½
72nd Street	4.97	18
59th Street (Via 8th Avenue)	5.54	20
50th Street	5.97	21½
42nd Street	6.46	23
34th Street	6.81	24½
23rd Street	7.31	26
14th Street	7.70	27½
West 4th Street	8.35	29½
Spring Street	8.81	31
Canal Street	9.19	32½
Hudson Terminal	9.82	34

TABLE A-1, Continued
Listings of NYCTA Division B routes through Manhattan
B-Line (Brooklyn and Manhattan)

Station	Miles	Run time (Minutes) Normal Local	Normal Express	Rush Hour Express
Stillwell Avenue	.00	8	6	6
Bay 50th St. (Stillwell)	.84	2½	2½	3*
25th Avenue (86th Street)	1.48	4½	4½	5
Bay Parkway (86th Street)	1.96	6	6	7*
20th Avenue (86th Street)	2.25	7	7	8½*
18th Avenue (New Utrecht)	2.57	8½	8½	9½
79th Street "	2.96	9½	9½	11
71st Street "	3.39	11	11	12½
62nd Street "	3.88	12½	12½	14
55th Street "	4.23	13½	13½	15½*
50th Street "	4.56	14½	14½	16½
Ft. Hamilton Parkway	4.88	16	16	18
9th Avenue (39th Street)	5.31	18	18	20
36th Street (4th Ave.)	6.23	21	21	23
25th Street "	6.70	22½		
Prospect Ave. "	7.14	24		
9th Street "	7.59	25		
Union Street "	8.11	26½		
Pacific Street "	8.62	28	26	28
DeKalb Avenue	9.13	31	29	30 (Bypass DeKalb)
(Via Manhattan Bridge)				
Grand Street (Chrystie Street)	11.29	38½	36½	37½
Broadway-Lafayette	11.86	41	39	40
West 4th Street (6th Ave.)	12.53	43	41	42
14th Street "	12.97	44½	42½	
23rd Street "	13.39	46	44	
34th Street "	13.87	47½	45½	45½
42nd Street "	14.23	49	47	47
50th Street "	14.58	50½	48½	48½
***To 57th Street & 6th Avenue**				
57th Street (6th Avenue)	15.01	52	50	
To Washington Heights				
7th Avenue (53rd Street)	14.95			50
59th Street (Columbus Circle)	15.44			52
72nd Street (Central Park West)	16.01			54
81st Street " " "	16.47			55½
86th Street " " "	16.82			56½
96th Street " " "	17.28			58
103rd Street " " "	17.63			59½
110th Street (8th Avenue)	17.98			61
116th Street "	18.34			62½
125th Street (St. Nicholas Ave.)	18.79			64
135th Street "	19.32			65½
145th Street "	19.83			67
155th Street "	20.26			69
163rd Street (Amsterdam Ave.)	20.65			70½
168th Street (Broadway)	20.98			72

*Non-rush hour trains terminate at 57th Street; rush hour trains do not pass through 57th Street station.

TABLE A-1, Continued
Listings of NYCTA Division B routes through Manhattan
D-Line (Bronx, Manhattan and Brooklyn)

Station	Miles	Running Time: Express Rush Hour	Running Time: Local Non Rush Hour
205th Street	.00	0	0
Bedford Park	.62	2	2
Kingsbridge Road	1.17	3½	3½
Fordham Road	1.62	5	5
182nd-183rd Streets	2.01	—	6½
Tremont Avenue	2.46	7½	8
174th-175th Street	2.87	—	9½
170th Street	3.36	—	11
167th Street	3.84	—	13
161st Street	4.48	—	15
155th Street	5.18	—	17½
145th Street	5.72	15	19
125th Street	6.76	18	22
59th Street	10.11	25	29
7th Ave. & 53rd Street	10.60	27	31
50th St. & 6th Avenue	10.97	28½	32½
42nd St. & 6th Avenue	11.32	30	34
34th St. & 6th Avenue	11.68	31½	35½
23rd St. & 6th Avenue	12.16	(Non Stop 24 Hours)	
14th St. & 6th Avenue	12.58	(Non Stop 24 Hours)	
West 4th St.-6th Ave.	13.02	35	39
Broadway Lafayette	13.69	37	41
Grand & Chrystie Sts. (Via Manhattan Bridge)	14.35	39½	43½
DeKalb Avenue	16.42	47	51
Atlantic Avenue	16.90	49½	53½
7th Avenue	17.48	51	55
Prospect Park	18.67	54	58
Parkside Avenue	19.13	—	60
Church Avenue	19.46	56½	61
Beverly Road	19.92	—	62½
Cortelyou Road	20.12	—	63½
Newkirk Avenue	20.54	59½	65
Avenue "H"	20.92	—	66½
Avenue "J"	21.24	—	67½
Avenue "M"	21.74	—	68½
Kings Highway	22.38	63	70
Avenue "U"	23.04	—	72
Neck Road	23.30	—	73
Sheepshead Bay	23.88	66	74½
Brighton Beach	24.65	68	76½
Ocean Parkway	25.06	70	78½
West 8th St.-Coney Island	25.45	72	80
Stillwell Avenue	25.81	73	81

TABLE A-1, Continued
Listings of NYCTA Division B routes through Manhattan

E-Line (Queens, Manhattan and Brooklyn)

Stations	Miles	Manhattan 8th Ave. Exp.	8th Ave. & Bklyn Exp.
179th Street	.00	0	0
169th Street	.54	1½	1½
Parsons Blvd.	1.09	3½	3½
Sutphin Blvd.	1.50	5	5
Van Wyck Blvd.	2.20	7	7
Union Turnpike	2.90	9	9
75th Avenue	3.33	10	10
Continental Avenue	3.78	11½	11½
Roosevelt Avenue	6.85	18	18
Queens Plaza	9.49	24	24
Ely Avenue	9.96	26	26
Lexington Avenue	11.38	29½	29½
5th Avenue	11.75	31	31
7th Avenue	12.14	32	32
50th St. & 8th Avenue	12.48	33½	33½
42nd St. & 8th Avenue	12.94	35	35
34th St. & 8th Avenue	13.29	36½	36½
23rd St. & 8th Avenue	13.79	38	
14th St. & 8th Avenue	14.18	39½	39
West 4th Street	14.83	41½	41
Spring Street	15.29	43	
Canal Street	15.67	44½	43½
Hudson Terminal	16.20	46	
Chambers Street	16.18		45
Broadway-Nassau	16.54		46½
High Street	17.76		49½
Jay Street	18.37		51½
Hoyt Street	18.74		53
Nostrand Avenue	20.67		57½
Utica Avenue	21.69		60
Broadway-East New York	23.03		63
Euclid Avenue	25.04		68

EE-Line (Manhattan and Queens)

Stations	Miles	Running Time Non Rush Hours	Rush Hours
Whitehall Street	.00	0	0
Rector Street	.33	2	2
Cortlandt Street	.57	3½	3½
City Hall	.90	5½	5½
Canal Street	1.40	7	7
Prince Street	1.79	8½	8½
8th Street	2.30	10	10
14th Street	2.68	11	11
23rd Street	3.08	12½	12½
28th Street	3.38	13½	13½
34th Street	3.64	14½	15
42nd Street	4.01	16	17
49th Street	4.38	17½	18½
57th Street	4.78	19	20
5th Avenue	5.27	21	22
Lexington Avenue	5.63	22½	23½
Queens Plaza (IND)	7.63	28	29
36th Street	8.16	29½	31
Steinway Street	8.76	31	33
46th Street	9.24	32½	34½
Northern Blvd.	9.69	34	36
65th Street	10.14	35½	37½
Roosevelt Avenue	10.57	37	39
Elmhurst Avenue	11.13	38½	40½
Grand Avenue	11.60	40	42
Woodhaven Blvd.	12.12	41½	43½
63rd Drive	12.58	43	45
67th Avenue	13.10	44½	46½
Continental Avenue	13.64	46	48

TABLE A-1, Continued
Listings of NYCTA Division B routes through
Manhattan
F-Line
(Queens, Manhattan and Brooklyn)

Stations	Miles	Daytime Hours		
179th Street	.00	0	0	0
169th Street	.54			
Parsons Blvd.	1.09	3	3	3
Sutphin Blvd.	1.50			
Van Wyck Blvd.	2.20			
Union Turnpike	2.90	7	7	7
75th Avenue	3.33			
Continental Avenue	3.78	9	9	9
Roosevelt Avenue	6.85	15½	15½	15½
Queens Plaza	9.49	21	21	21
Ely Avenue	9.96	23	23	23
VIA 53rd STREET TUNNEL				
Lexington Avenue	11.38	27	27	27
5th Avenue	11.75	28½	28½	28½
50th Street & 6th Avenue	12.16	30½	30½	30½
42nd Street & 6th Avenue	12.51	32	32	32
34th Street & 6th Avenue	12.87	33½	33½	33½
23rd Street & 6th Avenue	13.35	35	35	35
14th Street & 6th Avenue	13.77	36½	36½	36½
West 4th Street	14.21	38	38	38
Broadway-Lafayette	14.88	40	40	40
2nd Avenue	15.24	41½	41½	41½
Delancey Street	15.68	43	43	43
East Broadway	16.04	44	44	44
VIA RUTGERS STREET TUNNEL				
York Street	17.03	46½	46½	46½
Jay Street	17.53	48	48	48
Bergen Street	18.02	50	50	50
Carroll Street	18.49	51½		
Smith—9th Street	19.00	53		
4th Avenue	19.40	54½		
7th Avenue-Brooklyn	19.97	56	54½	54½
Prospect Park	20.51	58		
Ft. Hamilton Parkway	21.27	60½		
Church Avenue	21.81	62	59	59
Ditmas Avenue	22.36	64	61	
18th Avenue	22.82	65½	62½	61½
Avenue "I"	23.13	66½	63½	
22nd Avenue	23.43	67½	64½	
Avenue "N"	23.83	69	66	
Avenue "P"	24.27	70½	67½	
Kings Highway	24.67	72	69	66
Avenue "U"	25.17	73½	70½	67½
Avenue "X"	25.61	75	72	69
Van Sicklen	26.20	77	74	71
West 8th Street	26.58	78½	75½	72½
Stillwell Avenue	26.94	80	77	74

TABLE A-1, Continued
Listings of NYCTA Division B routes through Manhattan
N-Line (Brooklyn and Manhattan)

Stations	Miles	Rush Hours	Non-Rush Hours	Local in Brooklyn
Stillwell Avenue	.00	0	0	0
86th Street	1.09	3	3	3
Avenue "U"	1.41	5	4½	4½
Kings Highway	1.86	7	6½	6½
22nd Avenue	2.41	8½	8	8
20th Avenue	2.85	10	9½	9½
18th Avenue	3.21	11½	11	10½
New Utrecht Avenue	3.63	13	12½	12
Ft. Hamilton Parkway	4.30	15	14½	14
8th Avenue	4.71	17	16	15½
59th Street	5.53	19	18	17
53rd Street	5.87	—	—	18½
45th Street	6.20	—	—	19½
36th Street	6.73	22	21	21
25th Street	7.20	—	—	22½
Prospect Avenue	7.64	—	—	24
9th Street	8.09	—	—	25
Union Street	8.61	—	—	26½
Pacific Street	9.12	27	26	28
DeKalb Avenue	9.63	29	29	31
Canal Street	11.89	37	37	39
14th Street	13.26	41	40½	42
34th Street	14.22	44	43½	44½
42nd Street	14.59	46	45	46
57th Street	15.36	48	47	48

TABLE A-1, Continued
Listings of NYCTA Division B routes through Manhattan

"RJ-Line" (Queens, Manhattan and Brooklyn)

Stations	Miles	Run time (minutes)
168th Street	.00	0
160th Street	.36	1½
Sutphin Boulevard	.74	3
Queens Boulevard	1.07	4
Metropolitan Avenue	1.41	5
121st Street	1.89	6½
111th Street	2.37	8
102nd Street	2.83	9½
Woodhaven Boulevard	3.23	10½
Forest Parkway	3.69	12
Elderts Lane	4.07	13½
Cypress Hills	4.37	14½
Crescent Street	4.84	17
Norwood Avenue	5.29	18½
Cleveland Street	5.56	19½
Van Siclen Avenue	5.95	21
Alabama Avenue	6.32	22½
Eastern Parkway	6.69	24
Chauncey Street	7.08	25½
Halsey Street	7.49	27
Gates Avenue	7.86	28
Kosciusko Street	8.29	29½
Myrtle Avenue	8.74	31
Flushing Avenue	9.09	32½
Lorimer Street	9.51	34
Hewes Street	9.88	35
Marcy Avenue	10.14	36
Via Williamsburg Bridge		
Essex Street	11.85	41
Bowery	12.21	42½
Canal Street	12.65	44½
Chambers Street	13.03	46
Fulton Street	13.34	47½
Broad Street	13.66	49
Via Montague Street Tunnel		
Court Street	15.18	52
Lawrence Street	15.55	54
DeKalb Avenue	15.86	56
Pacific Street	16.37	59
Union Street	16.88	60½
9th Street	17.40	62
Prospect Avenue	17.85	63½
25th Street	18.29	65
36th Street	18.76	67
45th Street	19.29	69
53rd Street	19.62	70
59th Street	19.96	71
Bay Ridge Avenue	20.49	72½
77th Street	20.87	74
86th Street	21.37	75½
95th Street	21.81	77

RR-Line (Brooklyn, Manhattan and Queens)

Stations	Miles	Rush Hours	Non-Rush Hours
95th Street	.00	0	0
86th Street	.44	1½	1½
77th Street	.94	3	3
Bay Ridge	1.32	5	4½
59th Street	1.85	7	6
53rd Street	2.19	8	7
45th Street	2.52	9	8
36th Street	3.05	11	10
25th Street	3.52	13	11½
Prospect Avenue	3.96	14½	13
9th Street	4.41	16	14
Union Street	4.93	17½	15½
Pacific Street	5.44	19	17
DeKalb Avenue	5.95	22	20
Lawrence Street	6.26	23½	21½
Court Street	6.63	25½	23½
Whitehall Street	7.96	29½	27
Rector Street	8.29	31	28½
Cortlandt Street	8.53	32½	30
City Hall	8.86	34½	31½
Canal Street	9.36	36	33
Prince Street	9.75	37½	34½
8th Street	10.26	39	36
14th Street	10.64	40½	37½
23rd Street	11.04	42	39
28th Street	11.34	43	40
34th Street	11.60	44	41
42nd Street	11.97	46	42
49th Street	12.34	47½	43½
57th Street	12.74	49	45
5th Avenue	13.23	51	47
Lexington Avenue	13.59	52½	40½
Queens Plaza (IRT)	15.24	58	54
Beebe Avenue	15.75	60	56
Washington Avenue	16.06	61	57
Broadway	16.50	62	58
Grand Avenue	16.90	64	60
Hoyt Avenue	17.21	65½	61½
Ditmars Blvd.	17.64	67	63

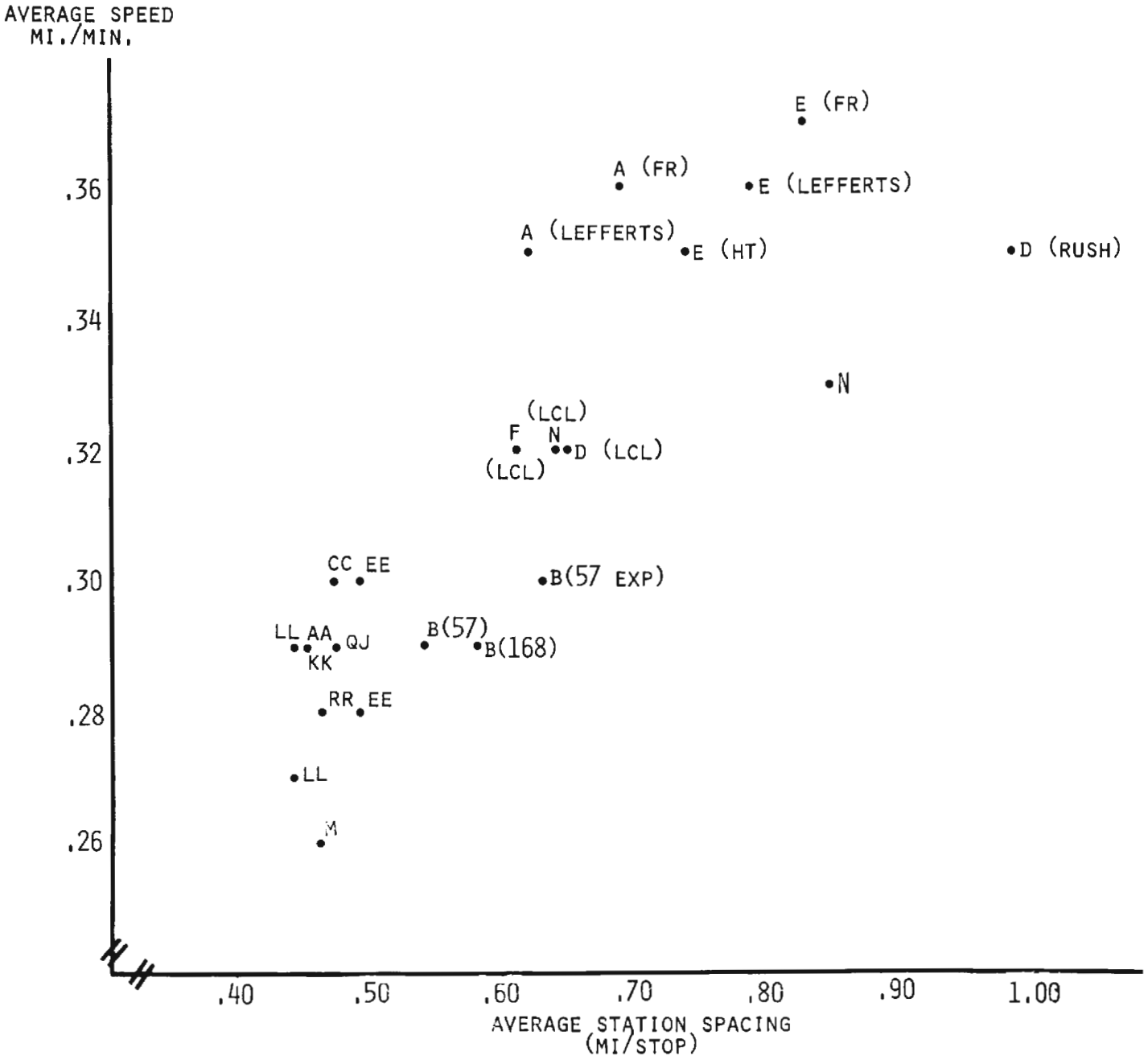

Figure A-2. Analysis of Principal NYCTA Division B Routes Through Manhattan

TABLE A-2
A-Line listing

Incremental Distance, ft	Grade, Percent	Speed Limit, mph	Curvature, deg/100 ft	Tunnel* Ident.	Cumulative Distance, ft	Relative Elevation ft
LEFFERTS						
845.	0.0	15.00	0.0	0.0	845.	0.0
127.	0.0	15.00	10.90	0.0	972.	0.0
456.	0.0	15.00	0.0	0.0	1428.	0.0
457.	0.0	55.00	0.0	0.0	1885.	0.0
111TH ST						
307.	0.0	35.00	0.0	0.0	2192.	0.0
153.	−0.55	35.00	0.0	0.0	2345.	−0.8
212.	−0.55	35.00	3.80	0.0	2557.	−2.0
662.	−0.55	35.00	0.0	0.0	3219.	−5.6
139.	−0.55	35.00	2.50	0.0	3358.	−6.4
381.	0.0	35.00	0.0	0.0	3739.	−6.4
104TH ST						
286.	0.0	55.00	2.50	0.0	4025.	−6.4
304.	3.00	55.00	2.50	0.0	4329.	2.7
317.	0.0	55.00	0.0	0.0	4646.	2.7
410.	−2.94	55.00	0.0	0.0	5056.	−9.3
489.	0.0	55.00	0.0	0.0	5545.	−9.3
ROCKAWAY BLVD						
350.	0.0	55.00	2.90	0.0	5895.	−9.3
1423.	0.0	55.00	0.0	0.0	7318.	−9.3
267.	−0.50	55.00	0.0	0.0	7585.	−10.7
88TH ST						
503.	−0.50	55.00	0.0	0.0	8088.	−13.2
1260.	−0.66	55.00	0.0	0.0	9348.	−21.5
349.	0.0	55.00	0.0	0.0	9697.	−21.5
80TH ST						
411.	0.0	55.00	0.0	0.0	10108.	−21.5
78.	0.0	55.00	12.70	0.0	10186.	−21.5
75.	0.50	55.00	12.70	0.0	10261.	−21.1
82.	0.50	55.00	0.0	0.0	10343.	−20.7
144.	−4.13	25.00	0.0	0.0	10487.	−26.7
375.	−4.13	25.00	5.60	0.0	10862.	−42.2
285.	−4.13	25.00	0.0	0.0	11147.	−53.9
39.	−4.13	25.00	0.0	1.00	11186.	−55.5
38.	1.00	25.00	0.0	1.00	11224.	−55.2
393.	−0.10	25.00	0.0	1.00	11617.	−55.6
20.	−0.40	25.00	0.0	1.00	11637.	−55.6
GRANT AVE.						
313.	−0.40	24.00	0.0	1.00	11950.	−56.9
66.	−0.40	24.00	11.50	1.00	12016.	−57.2
199.	0.0	24.00	11.50	1.00	12215.	−57.2
163.	−3.00	24.00	0.0	1.00	12378.	−62.0
100.	−0.60	24.00	0.0	1.00	12478.	−62.6
427.	−0.60	20.00	0.0	1.00	12905.	−65.2
34.	−3.60	20.00	0.0	1.00	12939.	−66.4

TABLE A-2
A-Line listing

Incremental Distance, ft	Grade, Percent	Speed Limit, mph	Curvature, deg/100 ft	Tunnel* Ident.	Cumulative Distance, ft	Relative Elevation ft
154.	−3.60	20.00	3.00	1.00	13093.	−72.0
80.	1.00	20.00	3.00	1.00	13173.	−71.2
104.	1.00	20.00	5.70	1.00	13277.	−70.1
126.	1.00	20.00	1.40	1.00	13403.	−68.9
91.	0.30	20.00	0.0	1.00	13494.	−68.6
233.	0.30	20.00	1.90	1.00	13727.	−67.9
EUCLID AVE						
157.	0.30	20.00	0.0	1.00	13884.	−67.4
65.	0.30	20.00	11.40	1.00	13949.	−67.2
494.	0.30	20.00	0.0	1.00	14443.	−65.8
200.	−3.00	20.00	0.0	1.00	14643.	−71.8
266.	0.11	20.00	0.0	1.00	14909.	−71.5
860.	0.11	55.00	0.0	1.00	15769.	−70.5
409.	0.30	55.00	0.0	1.00	16178.	−69.3
SHEPHERD AVE						
566.	0.30	55.00	0.0	1.00	16744.	−67.6
525.	3.00	55.00	0.0	1.00	17269.	−51.8
1270.	−0.50	55.00	0.0	1.00	18539.	−58.2
333.	−0.30	55.00	0.0	1.00	18872.	−59.2
VAN SICLEN						
627.	−0.30	55.00	0.0	1.00	19499.	−61.1
160.	0.60	55.00	0.0	1.00	19659.	−60.1
196.	0.60	30.00	0.0	1.00	19855.	−58.9
247.	0.60	30.00	10.30	1.00	20102.	−57.5
552.	1.80	30.00	10.30	1.00	20654.	−47.5
119.	−0.50	30.00	10.30	1.00	20773.	−48.1
426.	−0.50	30.00	0.0	1.00	21199.	−50.2
LIBERTY AVE						
475.	−0.50	25.00	0.0	1.00	21674.	−52.6
290.	2.70	25.00	0.0	1.00	21964.	−44.8
518.	2.70	25.00	11.10	1.00	22482.	−30.8
117.	1.39	25.00	11.10	1.00	22599.	−29.2
447.	1.39	25.00	11.10	1.00	23046.	−23.0
185.	1.39	25.00	2.50	1.00	23231.	−20.4
263.	1.39	25.00	0.0	1.00	23494.	−16.7
95.	0.50	25.00	0.0	1.00	23589.	−16.3
31.	3.00	25.00	0.0	1.00	23620.	−15.3
97.	3.00	25.00	2.50	1.00	23717.	−12.4
226.	3.00	25.00	0.0	1.00	23943.	−5.6
188.	3.00	25.00	5.70	1.00	24131.	0.0
3.	3.00	25.00	0.0	1.00	24134.	0.1
100.	2.63	25.00	0.0	1.00	24234.	2.7
233.	−0.50	25.00	0.0	1.00	24467.	1.6
BROADWAY						
266.	−0.50	25.00	0.0	1.00	24733.	0.2
57.	−0.50	25.00	2.50	1.00	24790.	−0.1
278.	0.40	25.00	2.50	0.0	25068.	1.1

TABLE A-2
A-Line listing

Incremental Distance, ft	Grade, Percent	Speed Limit, mph	Curvature, deg/100 ft	Tunnel* Ident.	Cumulative Distance, ft	Relative Elevation
95.	0.40	25.00	2.50	0.0	25163.	1.4
61.	0.40	25.00	0.0	1.00	25224.	1.7
276.	1.65	25.00	0.0	1.00	25500.	6.2
109.	1.65	25.00	1.90	1.00	25609.	8.0
170.	1.65	55.00	1.90	1.00	25779.	10.8
553.	−0.50	55.00	1.90	1.00	26332.	8.1
ROCKAWAY AVE						
520.	−0.50	55.00	0.0	1.00	26852.	5.5
655.	−3.00	55.00	0.0	1.00	27507.	−14.2
860.	−2.30	35.00	0.0	1.00	28367.	−34.0
440.	−0.70	35.00	0.0	1.00	28807.	−37.0
RALPH AVE						
656.	−0.70	55.00	0.0	1.00	29463.	−41.6
326.	−0.30	55.00	0.0	1.00	29789.	−42.6
244.	−0.30	55.00	2.10	1.00	30033.	−43.3
913.	−0.30	55.00	0.0	1.00	30946.	−46.1
91.	−0.30	55.00	2.40	1.00	31037.	−46.4
240.	−1.50	55.00	2.40	1.00	31277.	−50.0
292.	−1.50	55.00	1.90	1.00	31569.	−54.3
UTICA AVE						
580.	1.50	55.00	1.40	1.00	32149.	−45.6
90.	1.50	55.00	2.40	1.00	32239.	−44.3
265.	0.75	55.00	2.40	1.00	32504.	−42.3
370.	2.25	55.00	0.0	1.00	32874.	−34.0
780.	0.66	55.00	0.0	1.00	33654.	−28.8
555.	−0.70	55.00	0.0	1.00	34209.	−32.7
KINGSTON THROPP						
480.	−0.70	55.00	0.0	1.00	34689.	−36.1
714.	−0.30	55.00	0.0	1.00	35403.	−38.2
435.	−1.57	55.00	0.0	1.00	35838.	−45.0
739.	−0.58	55.00	0.0	1.00	36577.	−49.3
377.	0.70	55.00	0.0	1.00	36954.	−46.7
NOSTRAND AVE						
537.	0.70	55.00	0.0	1.00	37491.	−42.9
180.	0.70	55.00	3.20	1.00	37671.	−41.7
149.	−0.40	55.00	3.20	1.00	37820.	−42.3
375.	2.88	55.00	3.20	1.00	38195.	−31.5
105.	2.88	55.00	1.10	1.00	38300.	−28.4
127.	2.88	55.00	0.0	1.00	38427.	−24.8
402.	0.40	55.00	0.0	1.00	38829.	−23.2
FRANKLIN AVE						
300.	0.40	55.00	0.0	1.00	39129.	−22.0
1073.	−0.56	55.00	0.0	1.00	40202.	−28.0
251.	2.15	55.00	0.0	1.00	40453.	−22.6
981.	0.70	55.00	0.0	1.00	41434.	−15.7

TABLE A-2
A-Line listing

Incremental Distance, ft	Grade, Percent	Speed Limit, mph	Curvature, deg/100 ft	Tunnel* Ident.	Cumulative Distance, ft	Relative Elevation
CLINTON AVE						
389.	0.70	55.00	0.0	1.00	41823.	−13.0
54.	−1.20	55.00	0.0	1.00	41877.	−13.6
291.	−1.20	55.00	4.80	1.00	42168.	−17.1
257.	−1.20	55.00	0.0	1.00	42425.	−20.2
109.	−1.20	55.00	1.10	1.00	42534.	−21.5
675.	−0.70	55.00	1.10	1.00	43209.	−26.3
435.	−1.20	55.00	1.10	1.00	43644.	−31.5
230.	−1.00	55.00	0.0	1.00	43874.	−33.8
LAFAYETTE						
150.	−1.00	55.00	0.0	1.00	44024.	−35.3
318.	−0.30	55.00	0.0	1.00	44342.	−36.2
69.	−0.30	55.00	7.30	1.00	44411.	−36.4
248.	−2.18	55.00	7.30	1.00	44659.	−41.8
60.	−2.18	25.00	7.30	1.00	44719.	−43.1
106.	−1.00	25.00	7.30	1.00	44825.	−44.2
284.	−3.00	25.00	0.0	1.00	45109.	−52.7
134.	−3.50	25.00	0.0	1.00	45243.	−57.4
273.	−3.50	25.00	8.40	1.00	45516.	−67.0
36.	−3.50	25.00	0.0	1.00	45552.	−68.2
215.	3.00	25.00	0.0	1.00	45767.	−61.8
96.	3.00	25.00	4.80	1.00	45863.	−58.9
574.	2.00	25.00	4.80	1.00	46437.	−47.4
169.	−1.50	25.00	0.0	1.00	46606.	−50.0
353.	−1.50	15.00	0.0	1.00	46959.	−55.3
100.	−0.55	15.00	1.70	1.00	47059.	−55.8
200.	−0.55	15.00	0.0	1.00	47259.	−56.9
HOYT						
368.	0.0	20.00	0.0	1.00	47627.	−56.9
382.	3.08	20.00	0.0	1.00	48009.	−45.1
131.	3.08	20.00	20.00	1.00	48140.	−41.1
303.	−0.91	20.00	20.00	1.00	48443.	−43.9
90.	0.30	20.00	20.00	1.00	48533.	−43.6
91.	0.30	20.00	0.0	1.00	48624.	−43.3
50.	−3.05	20.00	0.0	1.00	48674.	−44.8
185.	−3.05	20.00	8.80	1.00	48859.	−50.5
207.	2.10	20.00	5.70	1.00	49066.	−46.1
90.	2.10	20.00	0.0	1.00	49156.	−44.2
77.	−0.30	20.00	0.0	1.00	49233.	−44.5
JAY ST						
283.	0.0	55.00	0.0	1.00	49516.	−44.5
140.	−0.30	55.00	2.50	1.00	49656.	−44.9
683.	0.0	55.00	2.50	1.00	50339.	−44.9
294.	0.0	55.00	1.70	1.00	50633.	−44.9
356.	1.50	55.00	0.0	1.00	50989.	−39.6
60.	1.50	31.00	0.0	1.00	51049.	−38.7
96.	−1.50	31.00	8.80	1.00	51145.	−40.1
214.	−2.50	31.00	8.80	1.00	51359.	−45.4

TABLE A-2
A-Line listing

Incremental Distance, ft	Grade, Percent	Speed Limit, mph	Curvature, deg/100 ft	Tunnel* Ident.	Cumulative Distance, ft	Relative Elevation ft
696.	−2.35	31.00	8.80	2.00	52055.	−61.8
39.	−2.35	31.00	0.0	2.00	52094.	−62.7
362.	−0.60	31.00	0.0	2.00	52456.	−64.9
HIGH ST (BB)						
57.	0.0	55.00	0.0	2.00	52513.	−64.9
326.	−0.60	55.00	1.70	2.00	52839.	−66.8
31.	−0.60	55.00	2.90	2.00	52870.	−67.0
607.	−3.00	55.00	2.90	2.00	53477.	−85.2
122.	−3.00	55.00	1.70	2.00	53599.	−88.9
158.	−3.00	35.00	0.0	2.00	53757.	−93.6
373.	−3.30	35.00	0.0	2.00	54130.	−106.0
689.	−3.30	35.00	3.50	2.00	54819.	−128.7
292.	−3.30	55.00	3.50	2.00	55111.	−138.3
222.	3.40	55.00	3.50	2.00	55333.	−130.8
163.	3.40	55.00	4.60	2.00	55496.	−125.2
133.	3.40	55.00	3.50	2.00	55629.	−120.7
326.	0.60	55.00	0.0	2.00	55955.	−118.8
1540.	3.00	55.00	0.0	2.00	57495.	−72.6
515.	1.50	55.00	0.0	2.00	58010.	−64.8
265.	1.50	55.00	9.20	2.00	58275.	−60.9
200.	1.50	55.00	0.0	2.00	58475.	−57.9
184.	1.50	55.00	1.70	2.00	58659.	−55.1
279.	0.30	55.00	0.0	2.00	58938.	−54.3
BROADWAY NASSAU						
401.	0.0	24.00	0.0	2.00	59339.	−54.3
236.	−3.00	24.00	0.0	2.00	59575.	−61.3
146.	−3.00	24.00	17.00	2.00	59721.	−65.7
374.	4.21	24.00	17.00	1.00	60095.	−50.0
341.	4.21	24.00	0.0	1.00	60436.	−35.6
378.	−0.60	24.00	0.0	1.00	60814.	−37.9
CHAMBERS ST						
360.	−0.60	24.00	0.0	1.00	61174.	−40.0
394.	1.00	24.00	0.0	1.00	61568.	−36.1
708.	−0.35	24.00	0.0	1.00	62276.	−38.6
229.	−3.00	24.00	0.0	1.00	62505.	−45.5
342.	−3.00	24.00	9.50	1.00	62847.	−55.7
116.	−3.00	24.00	0.0	1.00	62963.	−59.2
366.	−1.00	24.00	0.0	1.00	63329.	−62.9
50.	−0.17	24.00	0.0	1.00	63379.	−62.9
CANAL ST						
174.	−0.17	55.00	0.0	1.00	63553.	−63.2
176.	−0.17	55.00	1.50	1.00	63729.	−63.5
280.	−0.17	55.00	0.0	1.00	64009.	−64.0
248.	2.00	55.00	7.20	1.00	64257.	−59.1
1512.	0.32	55.00	0.0	1.00	65769.	−54.2
690.	0.48	55.00	0.0	1.00	66459.	−50.9
321.	0.48	30.00	2.20	1.00	66780.	−49.4

TABLE A-2
A-Line listing

Incremental Distance, ft	Grade, Percent	Speed Limit, mph	Curvature, feg/100 ft	Tunnel* Ident.	Cumulative Distance, ft	Relative Elevation
97.	−3.00	30.00	2.20	1.00	66877.	−52.3
291.	−3.00	30.00	0.0	1.00	67168.	−61.0
173.	2.20	30.00	0.0	1.00	67341.	−57.2
84.	2.50	30.00	0.0	1.00	67425.	−55.1
219.	2.50	30.00	1.50	1.00	67644.	−49.6
270.	−0.60	30.00	0.0	1.00	67914.	−51.2
W 4TH ST						
414.	−0.60	25.00	0.0	1.00	68328.	−53.7
331.	3.0	25.00	11.70	1.00	68659.	−43.8
210.	−2.40	25.00	0.0	1.00	68869.	−48.8
565.	−2.00	25.00	0.0	1.00	69434.	−60.1
230.	−2.00	55.00	0.0	1.00	69664.	−64.7
499.	3.00	55.00	0.0	1.00	70163.	−49.8
1.6.	−0.55	55.00	0.0	1.00	70359.	−50.8
505.	−0.55	25.00	11.50	1.00	70864.	−53.6
107.	0.0	25.00	11.50	1.00	70971.	−53.6
373.	0.0	25.00	0.0	1.00	71344.	−53.6
14TH ST						
424.	0.0	55.00	0.0	1.00	71768.	−53.6
159.	−2.40	55.00	0.0	1.00	71927.	−57.4
372.	3.00	30.00	0.0	1.00	72299.	−46.3
735.	0.0	30.00	0.0	1.00	73034.	−46.3
705.	0.0	25.00	0.0	1.00	73739.	−46.3
235.	1.50	25.00	2.50	1.00	73974.	−42.7
410.	0.50	25.00	0.0	1.00	74384.	−40.7
275.	0.50	55.00	0.0	1.00	74659.	−39.3
388.	1.50	55.00	0.0	1.00	75047.	−33.5
208.	0.55	55.090	0.0	1.00	75255.	−32.4
324.	0.39	55.00	0.0	1.00	75579.	−33.1
191.	0.39	55.00	2.50	1.00	75770.	−30.4
404.	−0.17	55.00	0.0	1.00	76174.	−31.0
34TH ST						
148.	−0.17	55.00	0.0	1.00	76322.	−31.3
232.	−0.67	55.00	0.0	1.00	76554.	−32.8
255.	−0.67	55.00	2.50	1.00	76809.	−34.6
420.	0.75	55.00	0.0	1.00	77229.	−31.4
110.	0.75	35.00	2.50	1.00	77339.	−30.6
106.	−2.50	35.00	0.0	1.009	77445.	−33.2
71.	−2.50	35.00	2.50	1.00	77516.	−35.0
358.	0.70	35.00	0.0	1.00	77847.	−32.5
525.	0.70	35.00	2.50	1.00	78399.	−28.8
35.	−0.20	35.00	0.0	1.00	78434.	−28.9
42 ND ST						
346.	−0.20	55.00	0.0	1.00	78780.	−29.6
299.	2.00	55.00	2.50	1.00	79079.	−23.6
128.	2.00	55.00	0.0	1.00	79207.	−21.0
412.	0.70	55.00	0.0	1.00	79619.	−18.2
304.	3.00	55.00	0.0	1.00	79923.	−9.0

TABLE A-2
A-Line listing

Incremental Distance, ft	Grade, Percent	Speed Limit, mph	Curvature, deg/100 ft	Tunnel* Ident.	Cumulative Distance, ft	Relative Elevation
251.	1.75	55.00	0.0	1.00	80174.	−4.6
675.	0.70	55.00	0.0	1.00	80849.	0.1
523.	1.65	55.00	0.0	1.00	81372.	8.7
609.	−3.00	55.00	0.0	1.00	81981.	−9.6
253.	1.50	55.00	0.0	1.00	82234.	−5.8
186.	1.50	55.00	1.40	1.00	82420.	−3.0
145.	1.50	55.00	0.0	1.00	82565.	−0.8
219.	0.50	55.00	1.40	1.00	82784.	0.3
59TH ST						
122.	0.50	55.00	1.40	1.00	82906.	0.9
208.	0.50	55.00	0.0	1.00	83114.	1.9
310.	1.00	55.00	1.70	1.00	83424.	5.0
372.	−2.50	55.00	1.70	1.00	83796.	−4.3
248.	3.00	55.00	1.70	1.00	84044.	3.2
469.	3.00	55.00	0.0	1.00	84513.	17.3
47.	2.00	55.00	0.0	1.00	84560.	18.2
684.	1.50	55.00	0.0	1.00	85244.	28.5
2133.	0.0	55.00	0.0	1.00	87377.	28.5
339.	−1.00	55.00	0.0	1.00	87716.	25.1
173.	1.96	55.00	0.0	1.00	87889.	28.5
295.	0.0	55.00	0.0	1.00	88184.	28.5
490.	0.70	55.00	0.0	1.00	88674.	31.9
875.	1.45	55.00	0.0	1.00	89549.	44.6
150.	0.50	55.00	0.0	1.00	89699.	45.3
765.	0.50	45.00	0.0	1.00	90464.	49.1
197.	−1.50	45.00	0.0	1.00	90661.	46.2
574.	0.0	45.00	0.0	1.00	91235.	46.2
500.	−0.83	45.00	2.50	1.00	91735.	42.0
72.	−1.43	45.00	1.70	1.00	91807.	41.0
248.	−1.43	45.00	0.0	1.00	92055.	37.5
810.	−0.70	45.00	0.0	1.00	92865.	31.8
439.	−1.62	45.00	0.0	1.00	93304.	24.7
129.	−1.62	40.00	0.0	1.00	93433.	22.6
226.	−0.30	40.00	0.0	1.00	93659.	21.9
500.	0.0	40.00	2.50	1.00	94159.	21.9
1639.	−3.00	40.00	0.0	1.00	95798.	−27.3
102.	3.00	40.00	2.50	1.00	95900.	−24.2
326.	3.00	40.00	0.0	1.00	96226.	−14.4
350.	−0.50	40.00	0.0	1.00	96576.	−16.2
112.	−0.76	40.00	2.50	1.00	96688.	−17.0
1113.	−0.76	40.00	0.0	1.00	97801.	−25.5
660.	−0.50	40.00	0.0	1.00	98461.	−28.8
258.	−0.88	40.00	0.0	1.00	98719.	−31.0
250.	−0.88	35.00	0.0	1.00	98969.	−33.2
514.	−0.88	35.00	7.60	1.00	99483.	−37.8
266.	−0.88	35.00	0.0	1.00	99749.	−40.1
104.	−0.88	25.00	0.0	1.00	99853.	−41.0
196.	−0.88	25.00	14.30	1.00	100049.	−42.8
74.	0.0	25.00	14.30	1.00	100123.	−42.8

TABLE A-2
A-Line listing

Incremental Distance, ft	Grade, Percent	Speed Limit, mph	Curvature, deg/100 ft	Tunnel* Ident.	Cumulative Distance, ft	Relative Elevation
206.	0.0	25.00	0.0	1.00	100329.	−42.8
51.	0.66	25.00	0.0	1.00	100380.	−42.4
124.	0.66	25.00	2.10	1.00	100504.	−41.6
125TH ST						
268.	0.66	55.00	2.10	1.00	100772.	−39.8
299.	0.66	55.00	0.0	1.00	101071.	−37.9
203.	2.53	55.00	0.0	1.00	101274.	−32.7
251.	2.53	55.00	2.10	1.00	101525.	−26.4
539.	0.07	55.00	2.10	1.00	102064.	−26.0
1926.	0.07	55.00	0.0	1.00	103990.	−24.6
113.	1.00	55.00	2.50	1.00	104103.	−23.5
160.	1.00	55.00	0.0	1.00	104263.	−21.9
241.	3.00	55.00	0.0	1.00	104504.	−14.7
126.	2.50	55.00	2.50	1.00	104630.	−11.5
386.	2.50	55.00	0.0	1.00	105016.	−1.9
355.	0.75	55.00	0.0	1.00	105371.	0.8
321.	0.75	55.00	2.20	1.00	105692.	3.2
114.	1.00	55.00	2.20	1.00	105806.	4.3
198.	1.00	55.00	0.0	1.00	106004.	6.3
145TH ST						
355.	1.00	55.00	0.0	1.00	106359.	9.9
200.	2.00	55.00	2.90	1.00	106559.	13.9
278.	−3.00	55.00	2.90	1.00	106837.	5.5
315.	3.10	55.00	2.20	1.00	107152.	15.3
749.	3.10	55.00	0.0	1.00	107901.	38.5
811.	0.70	55.00	0.0	1.00	108712.	44.2
283.	2.60	55.00	2.50	1.00	108995.	51.5
177.	2.60	55.00	2.20	1.00	109172.	56.1
419.	2.60	55.00	0.0	1.00	109591.	67.0
303.	2.60	55.00	5.70	1.00	109894.	74.9
84.	0.0	55.00	5.70	1.00	109978.	74.9
559.	0.0	55.00	0.0	1.00	110537.	74.9
241.	0.0	55.00	3.40	1.00	110778.	74.9
181.	1.50	55.00	3.40	1.00	110959.	77.6
180.	1.50	55.00	3.20	1.00	111139.	80.3
487.	3.00	55.00	3.20	1.00	111626.	94.9
98.	3.00	55.00	0.0	1.00	111724.	97.9
286.	0.32	55.00	0.0	1.00	112010.	98.8
168TH ST						
320.	0.32	55.00	0.0	1.00	112330.	99.8
172.	0.32	55.00	6.40	1.00	112502.	100.4
282.	0.32	55.00	0.0	1.00	112784.	101.3
5.	0.32	20.00	2.60	1.00	112789.	101.3
280.	−3.00	20.00	2.60	2.00	113069.	92.9
137.	2.37	20.00	2.60	2.00	113206.	96.1
817.	2.37	20.00	13.50	2.00	114023.	115.5
200.	2.44	20.00	13.50	2.00	114223.	120.4
382.	−0.05	20.00	0.0	2.00	114605.	120.2

TABLE A-2
A-Line listing

Incremental Distance, ft	Grade, Percent	Speed Limit, mph	Curvature, deg/100 ft	Tunnel* Ident.	Cumulative Distance, ft	Relative Elevation ft
175TH ST						
352.	−0.05	55.00	0.0	2.00	114957.	120.0
290.	−3.00	55.00	• 2.50	2.00	115247.	111.3
601.	−3.00	55.00	0.0	2.00	115848.	93.3
560.	−0.60	55.00	0.0	2.00	116408.	89.9
181ST ST						
385.	−0.60	55.00	0.0	2.00	116793.	87.6
590.	−3.00	55.00	0.0	2.00	117383.	69.9
1005.	−3.00	55.00	2.50	2.00	118388.	39.8
227.	−3.00	55.00	0.0	2.00	118615.	32.9
140.	−0.60	55.00	1.90	2.00	118755.	32.1
340.	−0.60	55.00	0.0	2.00	119095.	30.1
190TH ST						
360.	−0.60	55.00	0.0	2.00	119455.	27.9
694.	−3.00	55.00	0.0	2.00	120149.	7.1
430.	−3.00	30.00	1.90	2.00	120579.	−5.8
158.	−3.00	30.00	1.90	1.00	120737.	−10.6
472.	−3.00	30.00	2.90	1.00	121209.	−24.7
427.	−3.00	30.00	0.0	1.00	121636.	−37.5
258.	−0.50	30.00	0.0	1.00	121894.	−38.8
311.	−0.50	30.00	2.50	1.00	122205.	−40.4
200TH ST						
201.	−0.50	30.00	2.50	1.00	122406.	−41.4
259.	−0.50	30.00	0.0	1.00	122665.	−42.7
898.	1.30	30.00	0.0	1.00	123563.	−31.0
542.	1.20	15.00	0.0	1.00	124105.	−24.5
284.	−0.50	15.00	2.50	1.00	124389.	−25.9
46.	−0.50	10.00	0.0	1.00	124435.	−26.1
207TH ST						

*O = open track, 1 = subway, 2 = tube

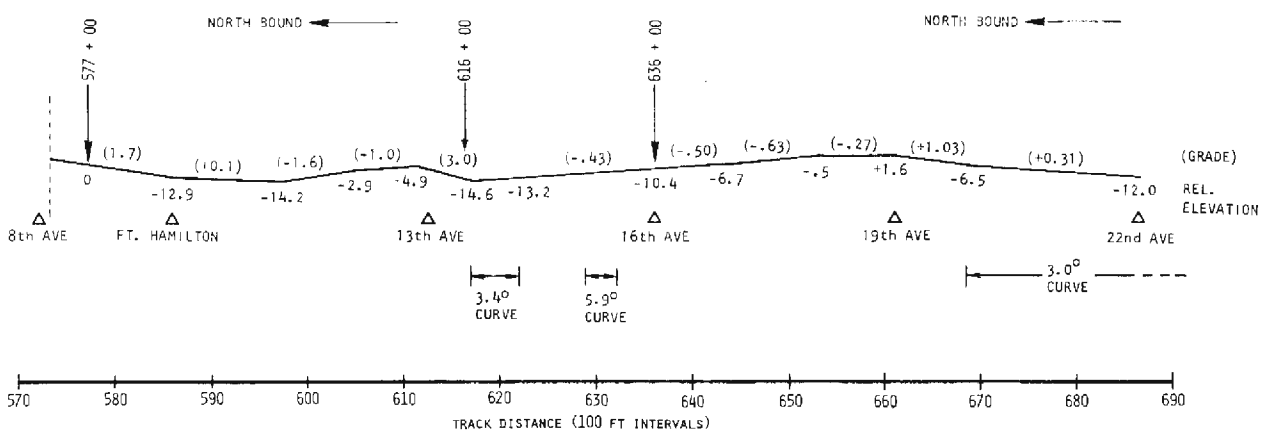

Figure A-3. Track Profile (Test Section, Sea Beach Line)

APPENDIX B — INSTRUMENTATION

INSTRUMENTATION CONFIGURATIONS

During the course of the Energy Storage Car evaluation program there were two different configurations for the test instrumentation. For all test operations prior to revenue service (i.e., Pueblo, Sea Beach and Simulated Service phases), there was a full set of instruments installed within what would normally have been the passenger space of the ES cars. For the Revenue Service Tests, of course, this exuipment had to be removed and only that which was essential to the energy measurement program was retained, being mounted within the #2 cab of ES car 3700 in such a way as to not interfere vice Tests, of course, this equipment had to be removed

Full instrumentation

The vehicle was instrumented to record data on magnetic tape for future retrieval and analysis and on an oscillograph for quick-look monitoring of selected parameters. In addition, system component temperatures were recorded on a strip chart recorder for a limited number of test operations. System input power was integrated on a digital readout to provide kilowatt-hour data for energy consumption runs. Figure B-1 is a block diagram of the onboard data acquisition system. (Refer to Table B-1 for details).

Retrieval of taped data was usually accomplished by playback on an eight-channel recorder in the same manner shown in Figure B-2. (Refer to Table B-2 for details). Data reduction was then carried out using the analog information provided from these playbacks. In some cases (e.g., energy consumption) data were manually tabulated directly from the digital records.

The measurement ranges of the recording equipment and the sensors are summarized in Table B-3. An example of the parameters recorded and the instrumentation used for the performance tests is shown in Table B-4.

ENERGY MONITORING SYSTEM

A measuring and monitoring panel (Figure B-3) was installed on-board the ES cars throughout the entire test program. This panel displayed side-by-side the energy consumed and the power drawn for each *pair* of test cars (ES and standard). The current drawn by each pair and the voltage of the third rail were displayed, as well.

The energy measurement was performed according to the functional schematic shown in Figure B-4. For each pair the third rail currents for each car were summed and the total was multiplied by the third rail voltage to get pair power. The pair power was integrated over time to get energy readings. The integration was accomplished by converting the analog power signal into a pulse train whose repetition rate (frequency) was proportional to the power. The pulses were scaled and counted to provide a digital energy readout.

This system was used for all the energy measurements which are reported herein. The components of the energy measurement system and the calibration of the system are described below.

Third rail voltage

The third rail voltage signal was first applied to the remote voltage divider. The remote voltage divider provided a differential input impedance of 760 kilohms, a division ratio of 76:1, and a single-ended output impedance less than 50 ohms. This low output impedance allowed the remote box to be located up to 500 ft away from the signal conditioning panel. The remote box was powered from the signal conditioning panel via a three-conductor cable assembly.

The buffered signal from the remote box was then routed to the multiplier card, where it was received differentially. Receiving the output of the remote box differentially provided high common-mode noise rejec-

TABLE B-1
Data Acquisition System Instrumentation

Item No.	ESC Instrumentation Description	Model No.	Mfg.	Response Range	Sensitivity	Calib.	Notes
1	Oscillograph Recorder (36 Chan.)	5-119	Bell & Howell	0 to 500 Hz	≈ 2.5 v per in.	0 to 2 in. for F.S. signal	
2	Oscillograph Recorder (12 Chan.)	5-124	Bell & Howell	0 to 500 Hz	≈ 2.5 v per in.	0 to 2 in. for F.S. signal	
3	Multipoint Temperature Recorder (12 Chan.)	Speedo-max "H"	Leeds & Northrop	N.A.	≈ 50°F per in.	0 to 1200°F (Type E Sensor)	
4	Tape Recorder	2114	Precision Instruments	0 to 10 kHz	≈ 10 mv minimum	±5 v F.S. signal	

TABLE B-1, Continued
Data Acquisition System Instrumentation

Item No.	ESC Instrumentation Description	Model No.	Mfg.	Response Range	Sensitivity	Calib.	Notes
5	Strain Gage Signal Conditioning	LSK 36398	AiResearch	0 to 10 kHz	≈ 10 $\mu\epsilon$ minimum	Depends on Sensor	
6	General Signal Conditioning	LSK 36052	AiResearch	0 to 500 Hz	N.A.	±5 v F.S. signal	Provides buffering for voltages and accels.
7	Accelerometer Charge Amplifiers	D11	Unholtz Dickie	2 to 10 kHz	lg to 1000g F.S.	5 v = 3g	
8	Speed & Distance Signal Conditioning	LSK 36220 & LSK 36054	AiResearch	0 to 1 kHz	≈ ±0.1 mph & ≈ ±1.0 ft.	0 to 50 mph —	
9	Charge Accelerometers	2272	Endevco	2 to 5 kHz	≈ .01 g minimum	AiResearch Certified	
10	Linear Accelerometers	LSBC 39-2	Schaevitz	0 to 40 Hz	≈ .001 g minimum	5 v = 2 g	
11	Current Shunts	PR1000	Quality Electric	0 to 500 Hz	≈ 0.1 mv minimum	50 mv = 1000A	
12	Current Shunt Isolators	6271A	Scientific Columbus	0 to 120 Hz	≈ 0.5% of F.S.	50 mv = 5v	
13	Voltage Dividers	—	AiResearch	0 to 1 kHz	≈ 0.5 v minimum	750 v = 9 v	0.1% Resistive Divider
14	Calibration Power Supply	LS513	Lambda	0 to 40 v	100 μv	AiResearch Certified	
15	Calibration Frequency Counter	CF601R	Anadex	1 Hz to 99,999 Hz	±1 count	AiResearch Certified	
16	Calibration Oscillator	204C	Hewlett Packard	5 Hz to 1.2 mHz	± 1%	AiResearch Certified	
17	Calibration RMS Voltmeter	427A	Hewlett Packard	0.01 v to 300 v 10 Hz to 1 mHz	≈ 0.5 mv minimum	AiResearch Certified	
18	Calibration DC Voltmeter	DS100	Doric	0 to 1000 v	0.1 mv	AiResearch Certified	
19	Inverter	1000 GCCWD	Topaz	DC to 60 Hz	N.A.	N.A.	
20	Oscilloscope	503	Tektronix	DC to 1 mHz	10 Mv minimum	AiResearch Certified	
21	Coupler Displacement	WR8	Lockheed Electronics	DC to 50 Hz	≈ 1.0 v per in.	5 in. F.S.	
22	Kilowatt Hour Meter	LSK 36129	AiResearch	0 to 99,999.9 KWHR	0.1 KWHR	1.5 MW F.S.	

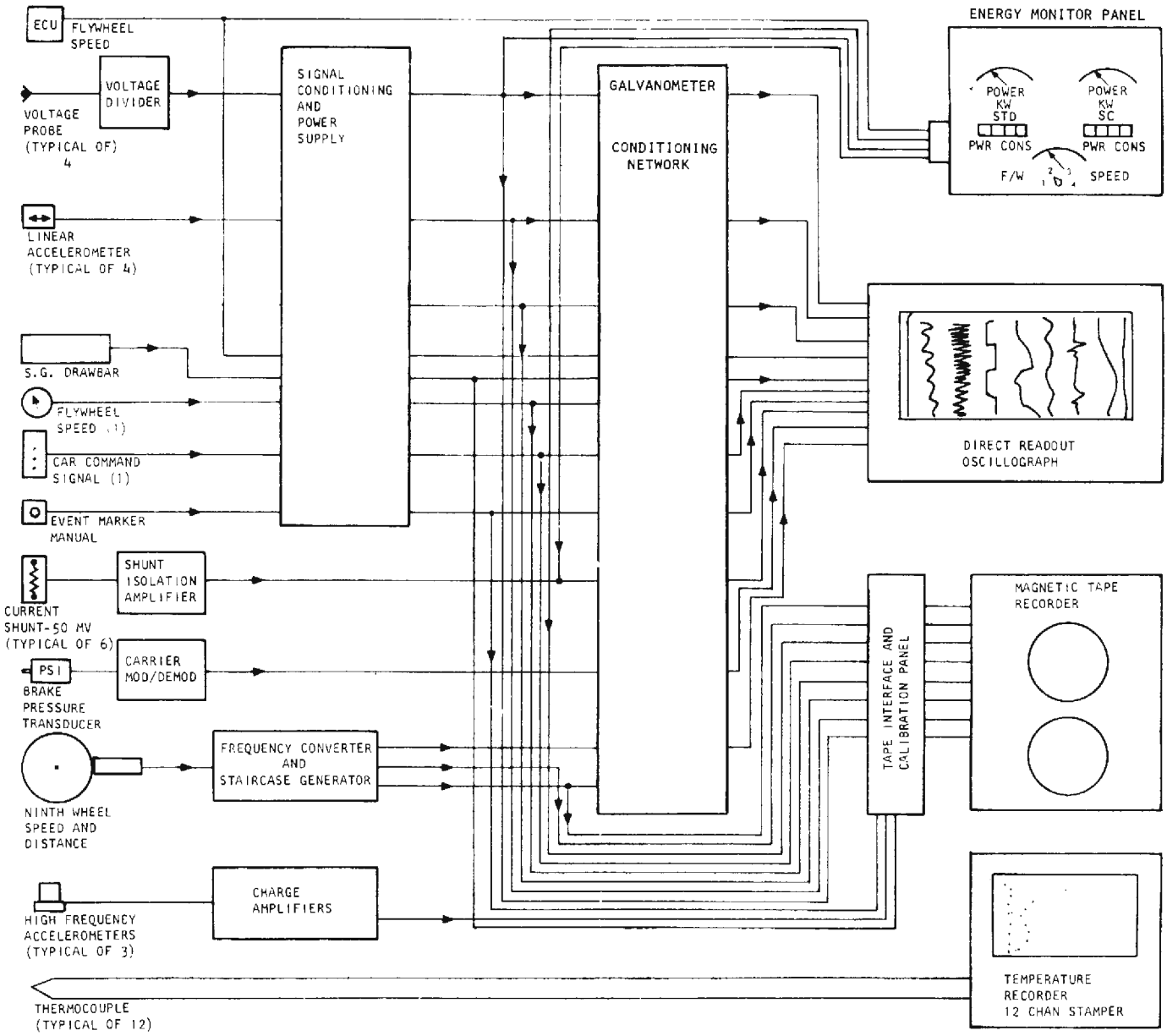

Figure B-1. Data Acquisition System

tion and ground-loop prevention.

The output of this differential amplifier was routed to three places: (a) the X input of the ES car power circuit; (b) the X input of the standard car power circuit; and (c) the input of the dual buffer amplifier. The A output of the dual buffer amplifier drove the third rail voltmeter. The range indicated on that meter was zero to 750 vdc.

Total current

The total current subsystem provided a readout of the current drawn by a "car pair". The current was sensed by two current shunts placed in the main power busbar of each car. The shunts provided a zero to ±50 mvdc output signal for an input current of zero to ± 1000 amp dc. This output signal was then applied to an isolation amplifier, which provided a gain of 100 and also isolated the high common-mode voltage (750 vdc) of the bus from the instrumentation system. The output of these isolators was then zero to ±5 vdc, referenced to instrumentation ground. The two output signals were then applied to a summing amplifier. The current signals were summed with a gain of 1.0 giving a full scale output signal of ±10 vdc for two input signals of ±5.0 vdc each.

The output of the summing amplifier was applied to a buffer amplifier which in turn drove the total current meter. The output of the summing amplifier was also applied to the Y input of the power multiplier card.

TABLE B-2
Data Recovery System Instrumentation

Item	Instrument	Model	Sensitivity	Range	Description
1	Magnetic Tape Recorder/Reproducer	Honeywell No. 7600	0.5 to 10 v peak for full deviation	3¾ ips—0 to 625 Hz 7½ ips—0 to 1250 Hz 15 ips—0 to 2500 Hz	14-channel FM reproduce medium band system.
2	Strip Chart Recorder	Beckman-Offner Typer Dynograph	1.0 mv/mm max.	0-200 Hz ±20%	8-channel direct writing oscillo-graph
3	Digital Volt Meter	Doric-DS 100	0.1 mv to 1000v	—	Dc voltmeter
4	DC Power Supply	Lambda LS 513	100 μv to 40v	—	Precision, programmable, digital adjust
5	Frequency Counter	Anadex CF601R	±1 count	1 Hz to 99.999 kHz	Digital Counter
6	Oscillator	Hewlett-Packard 204B	±1% of scale	5 Hz to 560 kHz	Solid state, battery-operated
7	Frequency Converter	Anadex P1-408R	0.01v RMS threshold voltage	5 Hz to 51.2 kHz	Frequency to analog converter with zero suppression

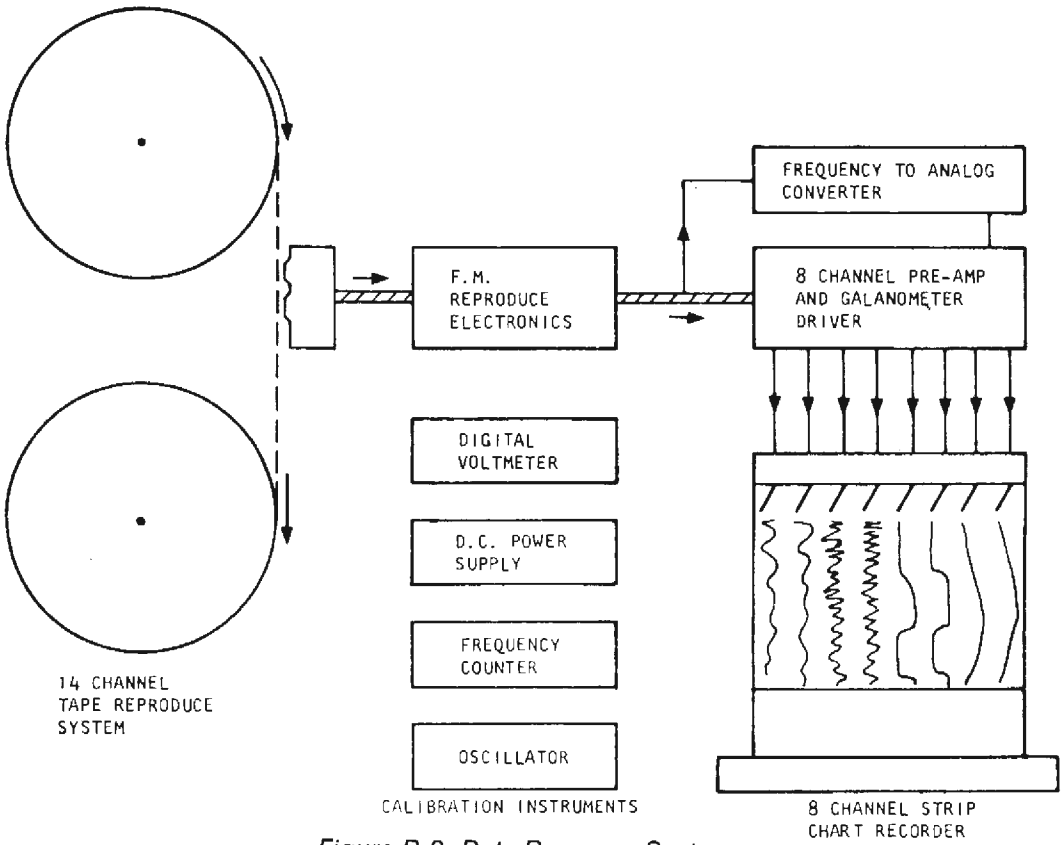

Figure B-2. Data Recovery System

TABLE B-3
Parameter Calibration Ranges

Parameter	Calibration Range	Calibration
Voltages	1000 v = F.S. (750 v = 9.000 v)	Resistive Divider (0.01% Resistors) Lambda Power Supply and Doric Voltmeter
Currents	1000 A = 50 mv	Certified Current Shunt Lambda Power Supply and Doric Voltmeter
Linear Accelerometers	±0.5 g = ±5 v	Calibrated Accelerometer Lambda Power Supply and Doric Voltmeter
Speed	0 to 50 mph	H.P. Oscillator and Anadex Counter
Charge Accelerometers	± 3 g	Calibrated Accelerometer H.P. Oscillator and H.P. RMS Voltmeter
Temperature Recorder	0 to 1200°F Type E Thermocouple	Ice Bath Reference Lambda Power Supply and Doric Voltmeter
Oscillograph Recorders	5 v = 2 in.	H.P. Oscillator & H.P. RMS Voltmeter or Lambda Power Supply and Doric Voltmeter
Tape Recorder	±5 v = F.S. (±40% deviation on FM)	Lambda Power Supply and Doric Voltmeter

Pair power

The car pair power subsystem consisted of a multiplier card and a meter readout calibrated to read zero to 1.5 Mw full scale. The multiplier card received a total current signal and a third-rail voltage signal, multiplied these two signals and buffered the resultant output for driving a meter readout located on the monitor's front panel. The current signal was applied to the Y input of the multiplier and the voltage signal to the X input. The multiplier had a transfer function of E (out) = XY/10, giving a ±10 volt dc output signal for two ± 10 volt dc input signals. The output signal was then applied to a unity-gain, non-inverting amplifier stage. This stage provided the drive current necessary for the meter readout (zero to one ma). A 10-kilohm potentiometer placed between the output amplifier and the meter was used to provide variable gain for calibration. The output signal of the multiplier was also applied to the input of the kilowatt-hour subsystem.

Kilowatt-hour subsystem

The system for computing kilowatt-hours consisted of two printed circuit cards (a dc-to-frequency converter card and a divider/driver card) and an electromechanical pulse totalizer (Haydon 44M101). The input signal, a zero to +10 vdc level corresponding to zero to 1.5 Mw, was applied to a buffer amplifier. This amplifier provided a gain of 1.0. The zero to 10-v signal from this stage drove a dc-to-frequency converter stage. This converter used an input of zero to ± 10 vdc to generate a pulse output frequency of zero to 416.667 Hz. The output level was zero to +12 vdc.

These zero to +12 vdc pulses were then applied to a series of two decade counters. Each decade counter divided the input frequency by ten, thus two counters provided a division of 100. The zero to +12v transitions of the divided pulse train fired a one-shot circuit which provided an 80-msec output pulse for each positive-going input transition. The 80-msec output pulse drove a Darlington-connected transistor pair, which provided a zero to +24 vdc pulse to the electromechanical counter. The subsystem voltage vs frequency conversion ratio was set so that the number displayed by the electromechanical counter was equal to the kilowatt-hours used by the propulsion system of the pair.

The counter displayed directly in kilowatt-hours with a resolution of 0.1 kwh. The overall accuracy of this system was ±¼ percent of full scale, between 20° and 160°F.

Current calibration

The current shunts used had a 50-mv output for 1000-amp input. They have been calibrated and certified by the AiResearch Metrology Laboratory.

Shunt signal conditioning was calibrated by inserting a precision power supply in place of the current shunt. This input signal was varied from 0 to 50 mv and the output was read on a calibrated digital voltmeter. The gain of the signal conditioning amplifiers was adjusted, if necessary, to provide the correct output.

Voltage calibration

The voltage dividers were calibrated with a precision high voltage power supply for input and a calibrated digital voltmeter for output. This provided a voltage-in/voltage-out number. Since the dividers were made up from the precision resistors, once this input to output ratio was established it should have remained constant. A two-point check was made in the field at zero voltage and line voltage inputs.

Figure B-3. Energy Metering and Monitoring Panel

TABLE B-4
Performance Test Parameters and Instrumentation

Recorded Parameter	Accel Tests	Decel Tests (Blended)	Decel Tests (Friction)	Duty Cycle Tests	Energy Consumption Tests	Misc.
Event and Time Mark	O T	O T	O T	O T	O T	
Volts, 3rd Rail	O T	O T	O T	O	O T	
Volts, Capacitor Bank				O		
Volts, Flywheel Mtr. A	O T	O T	O T	O T	O	
Volts, Trac. Mtr. A	O	O	O	O T	O T	
Current, 3rd Rail 3700	O T	O T	O T	O	O	
Current, 3rd Rail 3701	O	O	O	O	O T	
Current, Trac. Mtr. A	O(A)T	O(A)T	O(A)T	O(A)T	O T	
Current, Trac. Mtr. B				O(B)		
Current, Flywheel Mtr. A	O(A)T	O(A)T	O(A)T	O(A)T	O T	
Current, Flywheel Mtr. B				O(B)		
Vibration, Carbody Vert.				O		
Vibration, Carbody Lat.				O		
Vibration, Carbody Long.						
Vibration, Flywheel Vert.						
Vibration, Flywheel Lat.						
Vibration, Flywheel Long.						
Acceleration, Vehicle Long.	O T	O T	O T	O T	O T	
Displacement, Coupler				O	O	
Car Command Signal	O T	O T	O T	O T	O T	
Distance, Vehicle	O T	O T	O T	O T	O T	
Speed, Vehicle	O T	O T	O T	O T	O T	
Speed, Flywheel A	O T	O T	O T	O T	O T	
Lock-out Magnet	O T	O T	O T	O T		
Pressure, Brake Cylinder	O	O	O	O T		
Voice	T	T	T	T	T	
Temperature Wheel, Brake Shoe	S	S		S		
Temperature Underfloor						S

NOTE: T = Recorded on Magnetic Tape
O = Recorded on Oscillograph Paper
S = Recorded on Strip-Chart Temperature Stamper
(A) Car 3700
(B) Car 3701

Voltage signal conditioning was calibrated by inserting a precision power supply in place of the voltage divider. This input signal was varied from zero to full scale (nominally 10 vdc input) and the output was read on a calibrated-digital voltmeter. The gain of the signal conditioning amplifiers was adjusted, if necessary, to provide the correct output.

Kilowatt and kilowatt-hour calibrations

These two parameters were calibrated using a precision power supply in place of the current and voltage inputs, a frequency counter, a calibrated digital voltmeter, and a stop watch.

Scaling (full scale)

(a) Current (total): 10 v = 2000 amp
Car A: 5v = 1000 amp
Car B: 5v = 1000 amp
(b) Voltage: 10v = 750v
(c) Multiplier output: 10v = 1.5 Mw
(d) Dc to frequency converter: 416.667 Hz for 1.5 Mw
(e) Energy: 250 Kwh for 10 min at 1.5 Mw input

Data printout system

In addition to the Kwh counter on the Energy Metering and Monitoring Panel, the energy measurement circuitry was used to drive a digital printer, so that hardcopy energy records could be obtained.

The basic configuration of this system is shown in Figure B-5. A printout record could be produced either (a) manually by push-button, (b) on a timed interval basis (with interval variable by screwdriver adjustment from five to fifty minutes) or (c) by a signal generated by the opening of the car doors by the Conductor. Each record consisted of:

Time (HH.MM.SS) — generated by printer interface unit
Cumulative Kwh for ES pair
Cumulative Kwh for standard pair

For the benefit of passengers on the ES cars, the energy signals from the printer interface unit were also fed to a digital display in one of the cars. This provided a first-hand contact with the ES demonstration program (see Figure 5, in the main body of text).

R-32 car starting grid energy measurements

In order to determine the energy loss in the starting grids in conventionally-propelled cars, the energy measurement instrumentation had to be re-configured. Fortunately, the required changes were entirely external to the metering system (see Figure B-6). In effect, the normal measuring scheme required two current inputs and one voltage input; in the grid energy configuration, two voltage signals and one current signal were needed. It should be noted that the grid energy measurments related to only one car (3702), whereas the normal measurements recorded energy from each of two *pairs* of cars.

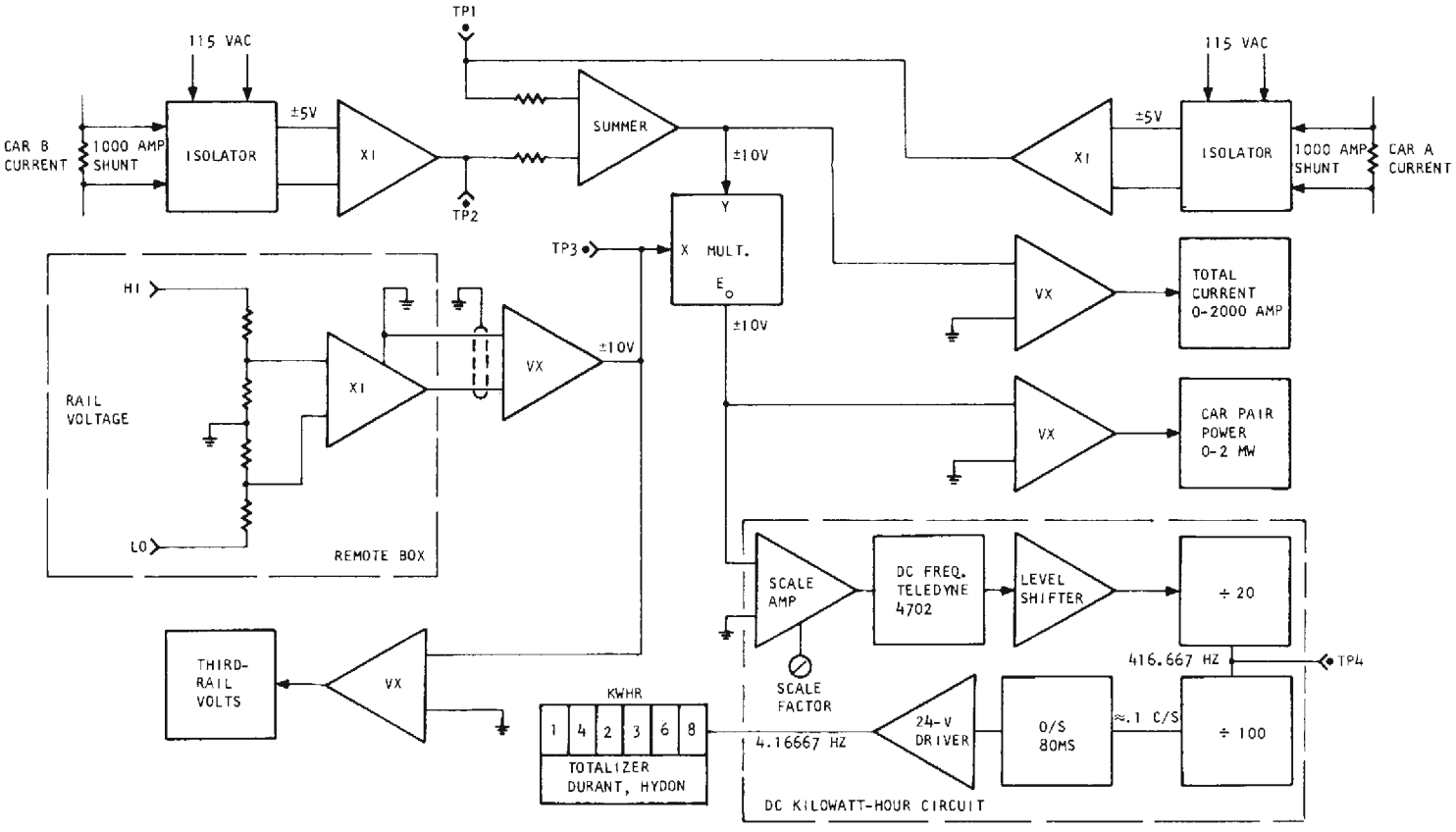

Figure B-4. Energy Metering Block Diagram

INTERCAR FORCE MONITOR

From the inception of the ES car program, it was understood that the most convincing demonstration of energy savings would be by the "side-by-side" comparison of energy consumption by the ES pair vs a standard (cam controlled) pair. However, in order to ensure a credible comparison, every effort had to be made to assure that each pair was expending an equal amount of propulsive force. Otherwise, of course, one pair could have shown lower energy consumption simply because it was being pulled by the other pair.

The conceptual basis for determining equal propulsive force was to record what was happening in the draft gear located between the two pairs. Any forces between the pairs would have to show up in the draft gear which connected them.

The initial force monitoring system involved an attempt to measure displacements of the coupler yoke. Interpair forces were assumed to be proportional to the movements of the yoke against the draft pads. Displacement was measured with a "yo-yo" style coiled spring which had its free end attached to the yoke while its housing was attached to the draft gear pocket. Motion of the yoke would then have shown up as a rotation of the coiled spring in its housing.

Unfortunately, it was found early in the testing program that the friction of the yoke against the pocket wall was great enough so that the yoke could not be assumed to return to a well-defined zero-point, when all forces on the draft gear were removed. This hysteresis made meaningful force determinations impossible.

The second method attempted was more successful. This method measured the draft and buff forces directly by monitoring stresses within a drawbar between the pairs. To perform this function, an NYCTA drawbar (such as is used between the two cars of a married pair, which are not often uncoupled from each other) was instrumented with strain gages to measure the axial force in the drawbar. The strain gages on the drawbar were electrically connected in an active four arm Wheatstone bridge. The mounting of the strain gages and the electrical hookup were made so that temperature effects and the effects of bending and torsional forces on the drawbar had negligible influence on the output of the gages.

After the drawbar was instrumented, it was calibrated in the Garrett lab for strain gage bridge output *vs* applied axial load (Table B-5). A precision, tension-compression testing machine was used to apply loads to the drawbar. Strain gage bridge outputs were measured with a precision, certified digital voltmeter.

The drawbar was installed between the standard R-32 pair and the ES pair, replacing the normal R-32 coupler. The strain gage bridge was connected to the recording equipment and a "zero load" reading was taken. Zero load was defined as that condition where the drawbar-to-car connecting pin could be turned freely by hand. This procedure for determining zero load was performed before and after each data run.

Although the strain gage drawbar performed adequately for the purpose intended, a review of the data from test runs showed that there were large axial force fluctuations during accelerating and braking of the four-car train. During quasisteady-speed operation, the axial forces on the drawbar were very small; the observed fluctuations were a result of slightly different response time and performance characteristics of the four cars. It was not practical to match the two pairs *exactly* in their acceleration and braking characteristics. Differences in response time of even a few seconds between cars resulted in momentary large relative forces between the cars. This condition was particularly apparent during initial acceleration from a completely stopped condition, where the standard R-32 cars had a 2- to 4-sec delay after a drive command was given. The ES cars had essentially no delay and as a result there was a large axial force on the drawbar during that time. A similar condition existed during braking below approximately 10 mph because of differences in dynamic braking response. In neither case, however, was the quantity of energy "transferred" between car pairs significantly high as to affect the test results.

On the surface it might appear that a better reading would have been obtained by integrating the drawbar signal vs time. In practice, this is not the case, since during station stops there were usually quite large forces locked into the drawbar as a result of slight differences in individual car stopping times. If these meaningless forces were integrated over the station stop time, the data would be grossly in error. A possible solution to this problem would be to design and build electronics that would exclude force integration during station stops or any other nondriving situation. A system of that type was beyond the scope of this program, however.

An additional source of unwanted drawbar force readings was the presence of track-induced stresses on the drawbar. These were observed during steady-speed operations, when there would have been no propulsion-induced forces.

Because of these non-propulsion forces, which were often quite large, the sensitivity of interpair force measurement system was of necessity lower than desired. However, the primary purpose of the instrumented drawbar—the verification of equal propulsive effort by each pair — *was* satisfied by the strain gage method.

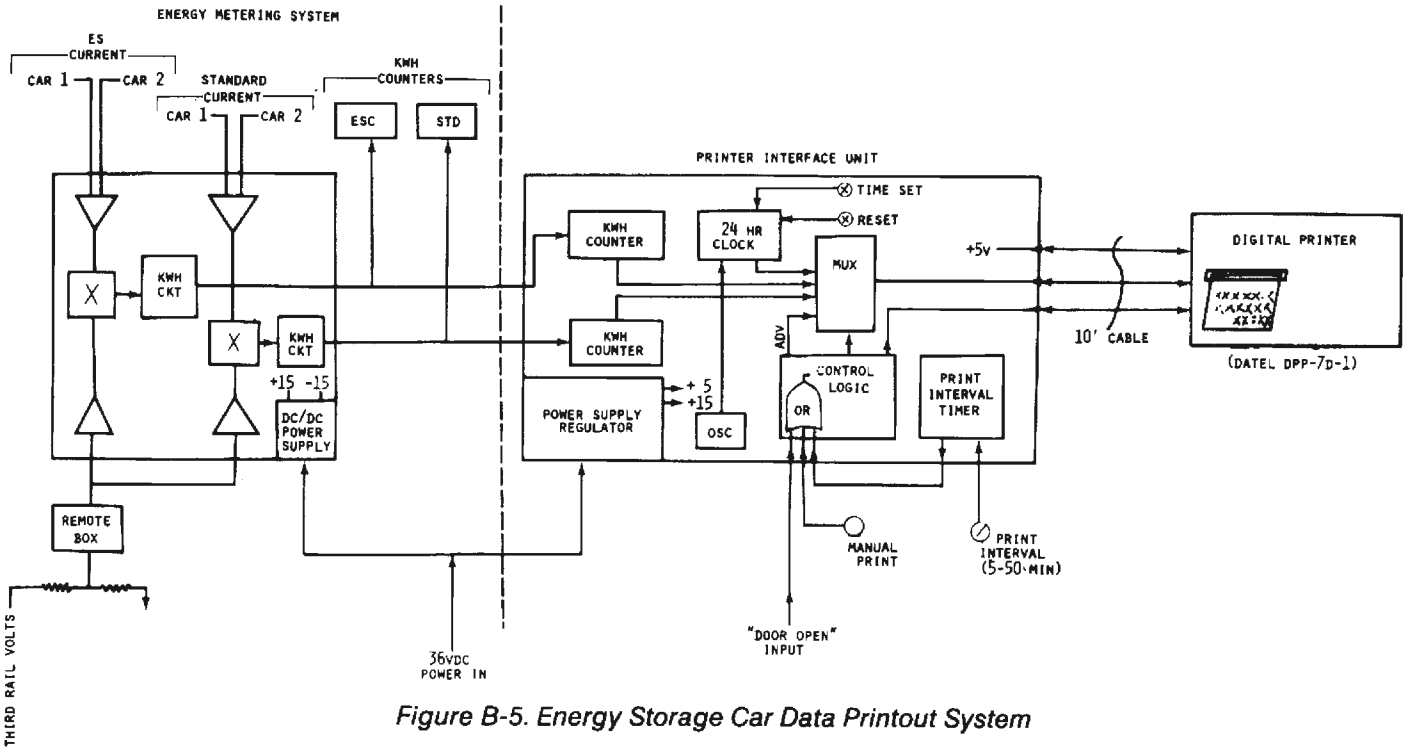

Figure B-5. Energy Storage Car Data Printout System

TABLE B-5
Strain gauge drawbar calibration

Model No. ESC-1 **Calibration Date** 08-04-75
Serial No. 1 **Excitation Voltage** 100.00 V.D.C.
Capacity 10000 Lbs **Load Step Value** 2000 Lb/Step

		Upscale			Tension			Downscale			Compression		
Load Step	Load (LB)	EO (MV)	D EO (MV)	DEV (MV)	EO (MV)	D EO (MV)	DEV (MV)	EO (MV)	D EO (MV)	DEV (MV)	EO (MV)	D EO (MV)	DEV (MV)
1	0.	−40.77	0.00	0.00	−40.74	0.00	−0.00	−40.17	0.00	0.00	−40.17	0.00	0.00
2	2000.	−39.91	0.86	0.02	−39.90	0.84	0.00	−41.00	−0.83	−0.00	−40.99	−0.81	0.00
3	4000.	−39.06	1.70	0.04	−39.08	1.66	−0.00	−41.83	−1.65	−0.00	−41.82	−1.65	0.00
4	6000.	−38.24	2.52	0.03	−38.31	2.43	−0.06	−42.66	−2.48	−0.00	−42.65	−2.47	0.00
5	8000.	−37.44	3.33	0.00	−37.42	3.32	−0.00	−43.49	−3.32	−0.01	−43.45	−3.27	0.02
6	10000.	−36.61	4.16	0.00	−36.61	4.13	−0.02	−44.31	−4.14	−0.00	−44.31	−4.14	−0.00

	Tension		Compression	
	Up	Down	Up	Down
Average D EO, MV	0.83	0.82	−0.82	−0.82
Max. Error +/− Per Cent	1.498		−0.685	
Avg. Sensitivity	0.0000041	MV/V/LB	−0.0000041	MV/V/LB

	+ Calibration			− Calibration		
RC (1/2 PC)	EO (MV)	D EO (MV)	EQ. LOAD (LB)	EO (MV)	D EO (MV)	EQ. LOAD (LB)
0.	−41.29	0.00	0.	−41.30	0.00	0.
10000002.	−36.23	5.05	12183.	−46.33	−5.03	−12163.

NORMAL ENERGY METERING CONFIGURATION

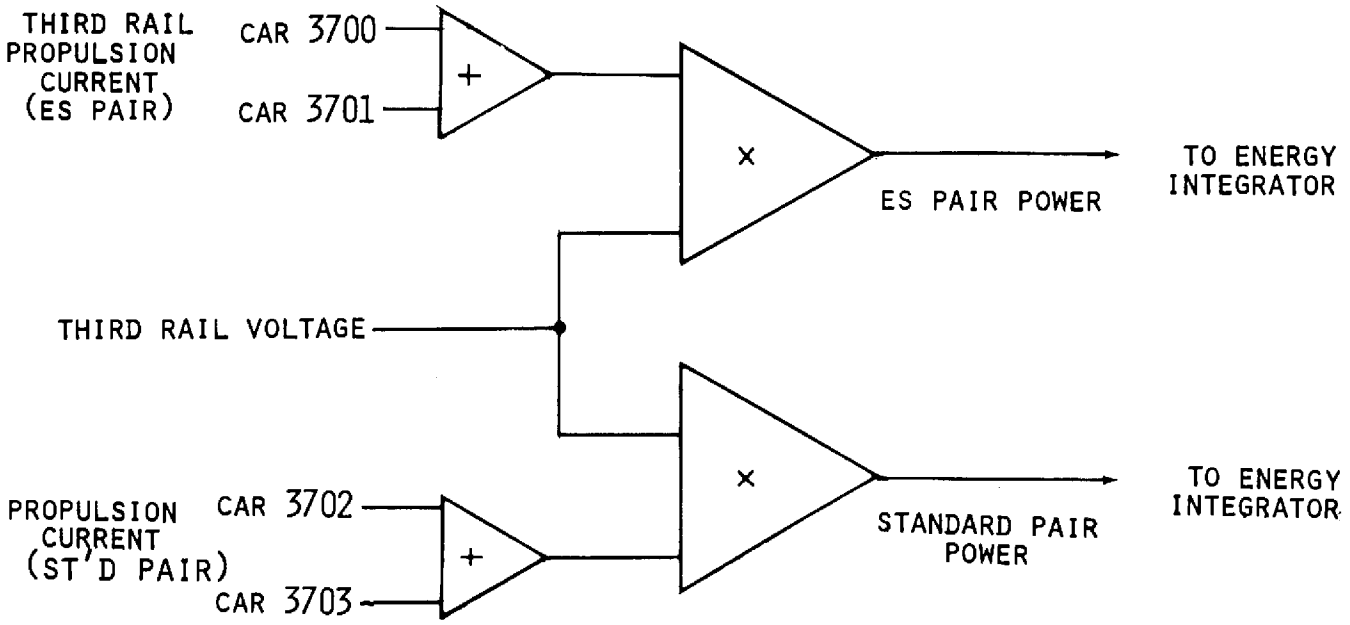

GRID ENERGY METERING CONFIGURATION

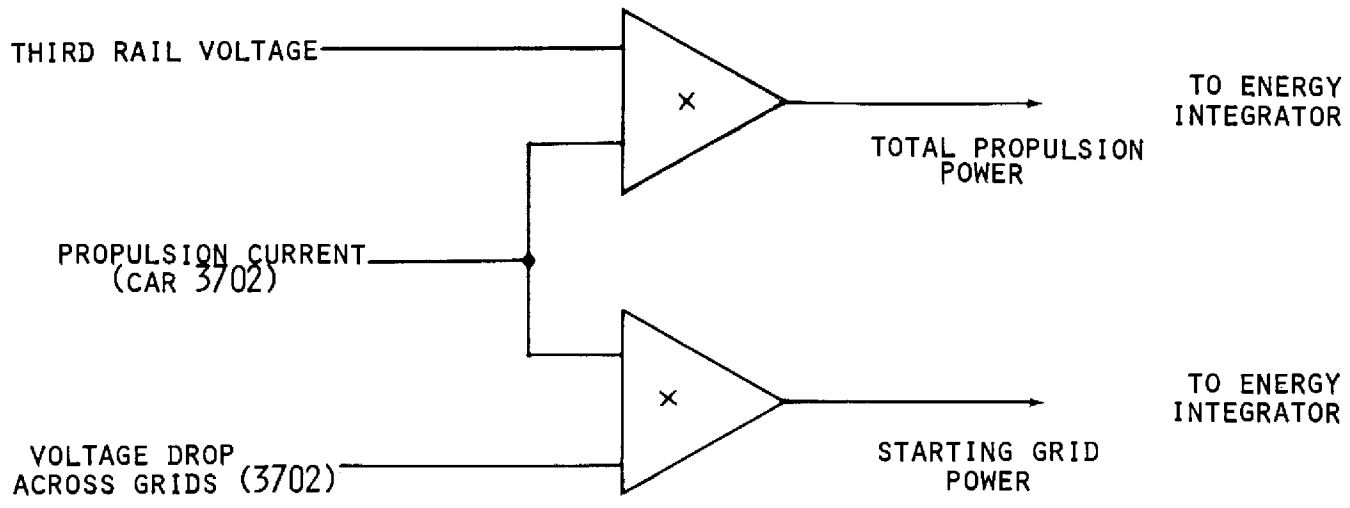

Figure B-6. Changes in Metering Inputs for Standard Car Starting Grid Energy Measurements

APPENDIX C — A-LINE REVENUE SERVICE ENERGY CONSUMPTION LISTINGS

Tables C-1 and C-2 provide samples of the operational data from the A-line Revenue Service testing. The tables give both cumulative and incremental running time (in HH:MM:SS format) and energy consumption data (in Kwh *per pair*) for each pair of cars. These data were taken directly from the on-board energy printout equipment described in Appendix B.

The particular two runs which are listed were chosen simply because the total one-way energy consumption for each was close to the overall Revenue Service average for the A-line, as indicated below:

	Kwh/car/one-way St'd	ES	Energy Saving
Brooklyn Express:			
Table C-1	91.4	65.7	28.2%
Rev. Svc. average	91.6	65.0	29.1
Brooklyn Local:			
Table C-2	102.6	63.1	38.5
Rev. Svc. average	103.2	66.4	35.7

TABLE C-1
A-Line Revenue Service Run (Express in Brooklyn)
Northbound from Lefferts Boulevard at 4:23 PM, May 12, 1976

		Cumulative			Incremental		
Station	Arr-Dep	Time	St'd pair Kwh	ES pair Kwh	Time	St'd pair Kwh	ES pair Kwh
Lefferts	D	0.00	0.0	0.0	—	—	—
Greenw'd	A	1:11	3.9	3.8	1:11	3.9	3.8
	D	1:19	3.9	3.8	:08	—	—
Oxford	A	2:17	8.1	5.4	:58	4.2	1.6
	D	2:25	8.1	5.4	:08	—	—
Rockaway	A	3:23	12.1	6.1	:58	4.0	0.7
	D	3:36	12.1	6.1	:13	—	—
Boyd	A	4:35	16.8	8.6	:59	4.7	2.5
	D	4:42	16.8	8.7	:07	—	0.1
Hudson	A	5:43	20.6	9.5	1:01	3.8	0.8
	D	5:53	20.6	9.5	:10	—	—
Grant	A	7:09	22.3	9.6	1:16	1.7	0.1
	D	7:39	22.3	9.6	:30	—	—
Euclid	A	9:03	25.0	10.2	1:24	2.7	0.6
	D	12:11	25.0	10.4	3:08	—	0.2
E.N.Y.	A	15:50	40.8	26.6	3:39	15.8	16.2
	D	16:06	40.8	26.6	:16	15.8	16.2
Utica	A	18:44	49.7	30.8	2:38	8.9	4.2
	D	19:03	49.7	30.8	:19	—	—
Nostrand	A	21:01	58.9	36.1	1:58	9.2	5.3
	D	21:15	58.9	36.1	:14	—	—
Hoyt	A	27:21	69.9	41.7	6:06	11:0	5.6
	D	27:50	69.9	41.7	:29	—	—
Jay	A	29:17	72.1	44.8	1:27	2.2	3.1
	D	29:32	72.1	44.8	:15	—	—
High	A	31:06	76.9	48.1	1:34	4.8	3.3
	D	31:24	76.9	48.1	:18	—	—
B'wy-Nass	A	33:49	85.4	53.1	2:25	8.5	5.0
	D	34:12	85.4	53.1	:23	—	—

TABLE C-1, Continued

Chambers	A	35:32	89.7	55.4	1:20	4.3	2.3
	D	36:01	89.7	55.8	:29	—	0.4
Canal	A	37:20	93.4	59.1	1:19	3.7	3.3
	D	37:43	93.4	59.2	:23	—	0.1
W. 4th	A	39:41	102.0	65.9	1:58	8.6	6.7
	D	40:02	102.0	65.9	:21	—	—
14th	A	41:41	106.2	67.1	1:39	4.2	1.2
	D	41:57	106.2	67.1	:16	—	—
34th	A	44:50	113.6	74.1	2:53	7.4	7.0
	D	45:26	113.6	74.1	:36	—	—
42nd	A	47:15	117.0	76.1	1:49	3.4	2.0
	D	47:44	117.0	76.2	:29	—	0.1
59th	A	51:42	123.9	83.4	3:58	6.9	7.2
	D	52:22	123.9	83.8	:40	—	0.4
125th	A	59:04	142.2	99.1	6:42	18.3	15.3
	D	59:36	142.2	99.1	:32	—	—
145th	A	1:01:52	152.6	108.0	2:16	10.4	8.9
	D	1:02:25	152.6	108.0	:33	—	—
168th	A	1:05:06	165.3	121.1	2:41	12.7	13.1
	D	1:06:22	165.3	121.3	1:16	—	0.2
175th	A	1:08:26	170.6	127.2	2:04	5.3	5.9
	D	1:08:51	170.6	127.4	:25	—	0.2
181st	A	1:09:46	173.2	128.6	:55	2.6	1.2
	D	1:10:22	173.2	128.7	:36	—	0.1
190th	A	1:11:35	176.8	130.8	1:13	3.6	2.1
	D	1:11:51	176.8	130.8	:16	—	—
200th	A	1:13:30	179.9	130.8	1:39	3.1	—
	D	1:13:50	179.9	130.8	:20	—	—
207th	A	1:15:55	182.8	131.3	2:05	2.9	0.5

TABLE C-2
A-Line Revenue Service Run (Local in Brooklyn)
Southbound from 207th Street at 12:06 PM, May 12, 1976

Station	Arr-Dep	Cumulative			Incremental		
		Time (H:MM:SS)	St'd pair Kwh	ES pair Kwh	Time (M:SS)	St'd pair Kwh	ES pair Kwh
207th	D	0:00	0.0	0.0	—	—	—
200th	A	1:32	4.5	4.9	1:32	4.5	4.9
	D	1:45	4.5	4.9	:13	—	—
190th	A	3:14	12.2	10.9	1:29	7.7	6.0
	D	3:24	12.2	11.0	:10	—	0.1
181st	A	4:46	19.0	17.6	1:22	6.8	6.6
	D	4:56	19.0	17.6	:10	—	—
175th	A	5:55	23.8	21.3	:59	4.8	3.7
	D	6:15	23.9	21.3	:20	0.1	—
168th	A	7:53	25.5	22.6	1:38	1.6	1.3
	D	8:11	25.5	22.6	:18	—	—
145th	A	10:38	29.0	25.1	2:27	3.5	2.5
	D	10:53	29.0	25.1	:15	—	—
125th	A	15:11	33.0	26.9	4:18	4.0	1.8
	D	16:14	33.0	27.0	1:03	—	0.1
59th	A	21:44	52.1	43.6	5:30	19.1	16.6
	D	22:27	52.1	43.6	:43	—	—
42nd	A	24.09	59.3	49.1	1:42	7.2	5.5
	D	24.26	59.3	49.1	:17	—	—
34th	A	25:24	62.1	49.1	:58	2.8	—
	D	25:54	62.1	49.2	:30	—	0.1
14th	A	27:41	68.6	53.5	1:47	6.5	4.3
	D	27:52	68.6	53.5	:11	—	—
W. 4th	A	29:20	74.0	55.1	1:28	5.4	1.6
	D	29:32	74.0	55.1	:12	—	—
Canal	A	31:11	80.8	60.0	1:39	6.8	4.9
	D	31:22	80.8	60.0	:11	—	—
Chambers	A	32:40	87.0	63.3	1:18	6.2	3.3
	D	34:24	87.0	63.3	1:44	—	—
Bwy-Nassau	A	35:36	89.3	64.5	1:12	2.3	1.2
	D	35:49	89.3	64.5	:13	—	—
High	A	38:11	97.9	71.5	2:22	8.6	7.0
	D	38:21	97.9	71.5	:10	—	—
Jay	A	39:48	105.3	76.4	1:27	7.4	4.9
	D	40:06	105.3	76.4	:18	—	—
Hoyt	A	41:09	108.9	77.6	1:03	3.6	1.2
	D	41:26	108.9	77.6	:17	—	—
Lafayette	A	43:11	114.7	82.1	1:45	5.8	4.5
	D	43:21	114.8	82.1	:10	0.1	—
Clinton	A	44:30	120.9	86.2	1:09	6.1	4.1
	D	44:40	120.9	86.2	:10	—	—

TABLE C-2, Continued

Franklin	A	45:47	125.7	88.0	1:07	4.8	1.8
	D	45:57	125.7	88.0	:10	—	—
Nostrand	A	46:50	129.5	88.0	:53	3.8	—
	D	47:01	129.5	88.0	:11	—	—
Kingston	A	48:08	135.0	90.8	1:07	5.5	2.8
	D	48:18	135.0	90.8	:10	—	—
Utica	A	49:29	140.7	93.3	1:11	5.7	2.5
	D	49:39	140.7	93.3	:10	—	—
Ralph	A	50:52	146.6	95.6	1:13	5.9	2.3
	D	51:02	146.7	96.6	:10	0.1	—
Rockaway Ave	A	52:12	153.2	100.1	1:10	6.5	4.5
	D	52:17	153.2	100.1	:05	—	—
E.N.Y.	A	53:16	157.3	102.1	:59	4.1	2.0
	D	53:29	157.3	102.1	:13	—	—
Liberty	A	55:19	160.7	102.1	1:50	3.4	—
	D	55:30	160.7	102.1	:11	—	—
V. Siclen	A	56:34	165.5	104.2	1:04	4.8	2.1
	D	56:44	165.5	104.2	:10	—	—
Shepherd	A	57:55	170.9	106.6	1:11	5.4	2.4
	D	58:05	170.9	106.6	:10	—	—
Euclid	A	59:12	175.9	108.2	1:07	5.0	1.6
	D	1:01:17	175.9	108.2	2:05	—	—
Grant	A	1:02:28	180.0	111.5	1:11	4.1	3.3
	D	1:02:38	180.0	111.5	:10	—	—
Hudson	A	1:03:37	185.5	116.5	:59	5.5	5.0
	D	1:03:46	185.6	116.5	:09	0.1	—
Boyd	A	1:04:46	190.2	119.6	1:00	4.6	3.1
	D	1:04:55	190.3	119.6	:09	0.1	—
Rockaway Blvd	A	1:05:56	194.3	121.2	1:01	4.0	1.6
	D	1:06:09	194.3	121.2	:13	—	—
Oxford	A	1:07:22	198.3	123.4	1:13	4.0	2.2
	D	1:07:32	198.3	123.4	:10	—	—
Greenwood	A	1:08:30	202.6	125.7	:58	4.3	2.3
	D	1:08:41	202.6	125.7	:11	—	—
Lefferts	A	1:10:29	205.2	126.2	1:48	2.6	0.5

ABBREVIATIONS USED IN THIS REPORT

A	Amperes
ADC	Amperes, Direct Current
AMP	Amperes
AVG	Average
dBA	A-weighted decibels
deg	Degrees
E	Voltage
ECU	Electronic Control Unit
ES	Energy Storage
ESU	Energy Storage Unit
Exp	Express
fps	Feet per second
F.S.	Full scale
ft	Feet
FW	Flywheel
g, G	Acceleration due to gravity
hr	Hour
Hz	Hertz
I	Current
kHz	Kilo-Hertz
Kw	Kilowatts
Kwh	Kilowatt-hours
LAT	Lateral (horizontal perpendicular to car centerline)
LONG	Longitudinal (parallel to car centerline)
M-A	Motor-alternator
max	Maximum
M/G	Motor/Generator
Min	Minutes
MPH	Miles per hour
MTA	Metropolitan Transportation Authority
MTBF	Mean time between failures
mv	Millivolts
MUX	Multiplex unit
N.A.	Not applicable
NYCTA	New York City Transit Authority
PDR	Phase delay rectifier
PSI	Pounds per square inch
PSIG	Pounds per square inch, gauge
RMS	Root mean square
sec	Seconds
SG, S-G	Strain gauge
St'd, STD	Standard (unmodified) car
T/C	Thermocouple
TM	Traction motor
UMTA	Urban Mass Transportation Administration of the U.S. Department of Transportation
V	Volts
VAC	Volts, alternating current
VDC	Volts, direct current
VERT	Vertical

REFERENCES

1. Energy Storage Propulsion System for Rapid Transit Cars: System Design and Equipment Description. Metropolitan Transportation Authority, New York, Report No. UMTA-NY-06-0006-75-1, September 1975. (PB 249-063).* ATTACHED TO THIS REPORT.
2. Engineering Tests for Energy Storage Cars at the Transportation Test Center, AiResearch Manufacturing Company, Torrance, California, UMTA-MA-16-0025-77-2/5, May 1977. (Set of 4, PB 269-399).*
3. General Vehicle Test Plan for Urban Rapid Transit Cars, Transportation Systems Center, Cambridge, Massachussetts, Report No. UMTA-MA-06-0025-75-14, September 1975. (PB 251-086).*
4. Optimization of Power Resources for the New York City Transit Authority, Parsons, Brinckerhoff — Gibbs & Hill, New York, Project No. IT-09-0023 (TS C 210), May 1976.
5. New York City Transit Authority Design Guidelines, New York City Transit Authority, New York, Volume IV (Power), January 1975. (PB #251-650).*
6. Subway Environmental Design Handbook, Transit Development Corporation, Washington, D.C., Volume I (2nd Edition), 1976. (PB 254-788).*
7. Strain Guage Test of R-32 Car No. 3700, AiResearch Manufacturing Co., Torrance, California, Report No. 75-11565, June 1975.
8. J. T. Duane, "Learning Curve Approach to Reliability Monitoring" *IEEE Transactions on Aerospace*, Volume 2, Number 2, April 1964, p. 563.

*Document available to the public through the National Technical Information Service, Springfield Virginia, 22161.